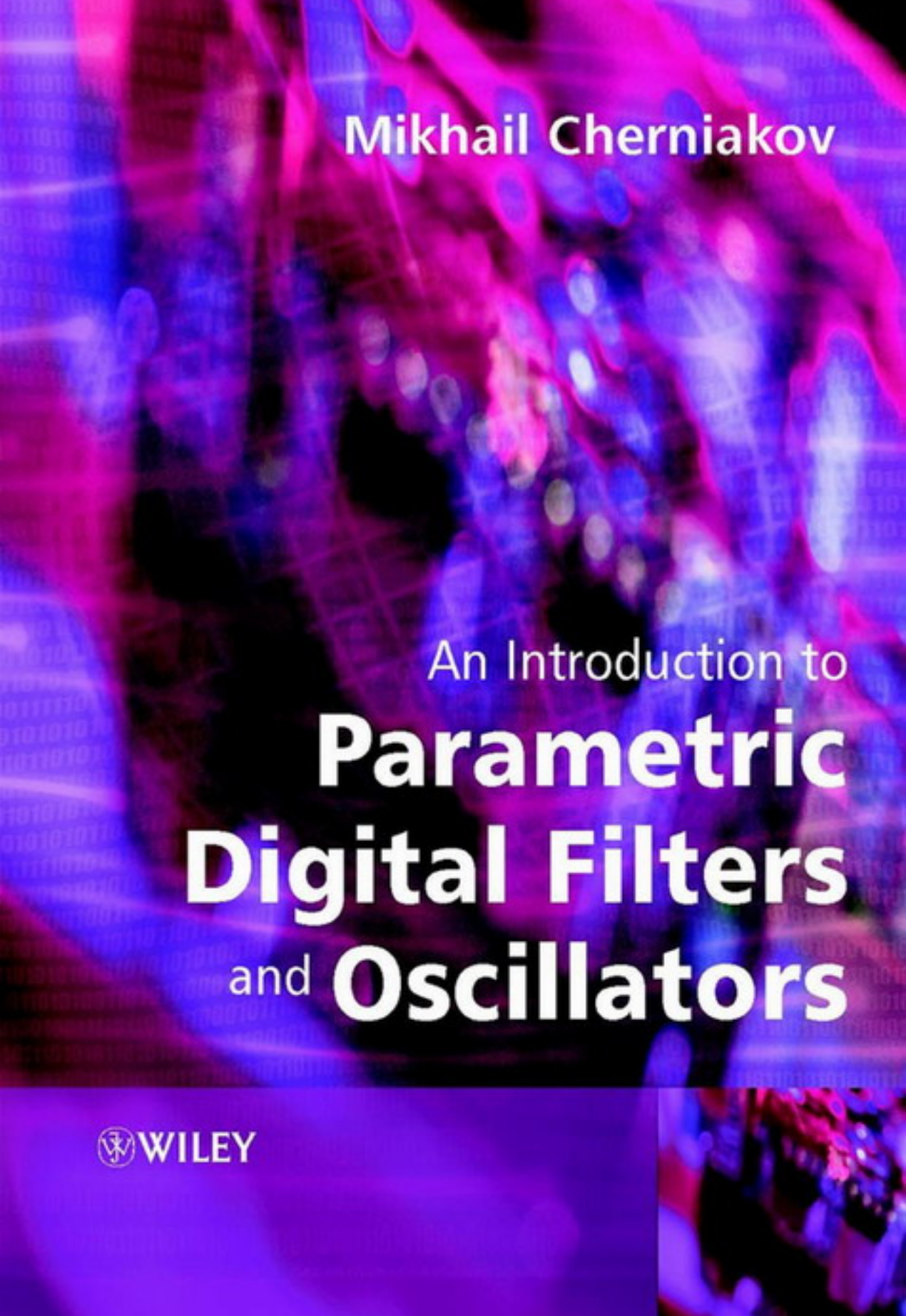
Mikhail Cherniakov
An Introduction to
Parametric
Digital Filters
and Oscillators
WILEY

An Introduction to Parametric Digital Filters and Oscillators

An Introduction to Parametric Digital Filters and Oscillators

Mikhail Cherniakov
University of Birmingham, UK

Copyright © 2003

John Wiley & Sons Ltd, The Atrium, Southern Gate, Chichester,
West Sussex PO19 8SQ, England

Telephone (+44) 1243 779777

Email (for orders and customer service enquiries): cs-books@wiley.co.uk
Visit our Home Page on www.wileyeurope.com or www.wiley.com

All Rights Reserved. No part of this publication may be reproduced, stored in a retrieval system or transmitted in any form or by any means, electronic, mechanical, photocopying, recording, scanning or otherwise, except under the terms of the Copyright, Designs and Patents Act 1988 or under the terms of a licence issued by the Copyright Licensing Agency Ltd, 90 Tottenham Court Road, London W1T 4LP, UK, without the permission in writing of the Publisher. Requests to the Publisher should be addressed to the Permissions Department, John Wiley & Sons Ltd, The Atrium, Southern Gate, Chichester, West Sussex PO19 8SQ, England, or emailed to permreq@wiley.co.uk, or faxed to (+44) 1243 770620.

This publication is designed to provide accurate and authoritative information in regard to the subject matter covered. It is sold on the understanding that the Publisher is not engaged in rendering professional services. If professional advice or other expert assistance is required, the services of a competent professional should be sought.

Other Wiley Editorial Offices

John Wiley & Sons Inc., 111 River Street, Hoboken, NJ 07030, USA

Jossey-Bass, 989 Market Street, San Francisco, CA 94103-1741, USA

Wiley-VCH Verlag GmbH, Boschstr. 12, D-69469 Weinheim, Germany

John Wiley & Sons Australia Ltd, 33 Park Road, Milton, Queensland 4064, Australia

John Wiley & Sons (Asia) Pte Ltd, 2 Clementi Loop #02-01, Jin Xing Distripark, Singapore 129809

John Wiley & Sons Canada Ltd, 22 Worcester Road, Etobicoke, Ontario, Canada M9W 1L1

Wiley also publishes its books in a variety of electronic formats. Some content that appears in print may not be available in electronic books.

British Library Cataloguing in Publication Data

A catalogue record for this book is available from the British Library

ISBN 0-470-85104-X

Typeset in 10.5/13pt Times by Laserwords Private Limited, Chennai, India
Printed and bound in Great Britain by Antony Rowe Ltd, Chippenham, Wiltshire
This book is printed on acid-free paper responsibly manufactured from sustainable forestry in which at least two trees are planted for each one used for paper production.

To my wife Irina
and our sons
Pavel, Alexei and Andrei

Contents

Preface **xi**

1 Introduction: Basis of Discrete Signals and Digital Filters **1**
1.1 Discrete Signals and Systems 1
1.2 Discrete Signals 3
1.2.1 Time-Domain Representation for Discrete Signals 3
1.2.2 Presentation of Discrete Signals by Fourier Transform 4
1.2.3 Discrete Fourier Transform 9
1.2.4 Laplace and z-Transforms 11
1.3 Time–Invariant Discrete Linear Systems 16
1.3.1 Difference Equation and Impulse Response 17
1.3.2 DLS Representation via Transfer Function 20
1.4 Stability and Causality of Discrete Systems 22
1.5 Frequency Response of a Discrete Linear System 23
1.5.1 Properties of the Frequency Response of a Discrete Linear System 25
1.5.2 Transfer Function versus Frequency Response 25
1.6 Case Study: Low-Order Filters 27
1.6.1 Purely Recursive Filters 27
1.6.2 Effects of Word Length Limitation 37
1.6.3 Transversal and Combined Filters 37
1.7 Summary 41
1.8 Abbreviations 42
1.9 Variables 42
1.10 References 43

Part One Linear Discrete Time-Variant Systems **45**

2 Main Characteristics of Time-Variant Systems **47**
2.1 Description of a Linear Time-Variant Discrete System Through Difference Equations 48
2.2 Impulse Response 49
2.3 Generalized Transfer Function 52
2.4 Signals Analysis in Frequency Domain 55

2.5 Sampling Frequency Choice for Linear Time-Variant Discrete Systems 59
2.6 Random Signals Processing in Linear Time-Variant Discrete Systems 61
2.7 Combinations of Time-Variant Systems 63
2.7.1 Parallel Connections 63
2.7.2 Cascade Connections 64
2.7.3 Systems with Feedback 66
2.7.4 Continuous and Discrete LTV Systems 68
2.8 Time-Varying Sampling 70
2.8.1 Systems with Non-Uniform Sampling 70
2.8.2 Systems with Stochastic Sampling Interval 75
2.9 Summary 77
2.10 Abbreviations 78
2.11 Variables 78
2.12 References 79

3 Periodically Time-Variant Discrete Systems 83
3.1 Difference Equation 83
3.2 Impulse Response 84
3.3 Generalized Transfer Function and Frequency Response 85
3.4 Signals in Periodically Linear Time-Variant Systems 86
3.4.1 Bifrequency Function 86
3.4.2 Deterministic Signal Processing 86
3.4.3 Random Signals Processing 89
3.5 Generalization of the Sampling Theorem 91
3.6 System Stability 95
3.6.1 General Stability Problem 95
3.6.2 Selection of Stability Criteria 96
3.6.3 Stability Evaluation 97
3.6.4 Stability of Parametric Recursive Systems 99
3.7 Stability of Second-Order Systems 100
3.8 Stability of Stochastic Systems 107
3.9 Summary 114
3.10 Abbreviations 114
3.11 Variables 115
3.12 References 116

Part Two Parametric Systems 119

4 Parametric Filters Analysis 121
4.1 Non-Recursive Parametric Filters 121
4.2 The First-Order Recursive Parametric Filter 123
4.2.1 Impulse Response 123
4.2.2 Generalized Transfer Function 126

4.3 A Recursive Parametric Filter of the Second Order 129
4.3.1 Impulse Response 129
4.3.2 Generalized Transfer Function 134
4.4 Parametric Filters of an Arbitrary Order 136
4.4.1 Direct Equation Solution 136
4.4.2 Equation Solution in a State Space 138
4.5 Approximate Method for Analysis of Periodical Linear Time-Variant Discrete Systems 142
4.6 Summary 146
4.7 Abbreviations 146
4.8 Variables 146
4.9 References 147

5 Design Studies for Parametric Filters 149
5.1 Recursive Parametric Filters 150
5.1.1 Frequency Response Correction 150
5.1.2 Multiplier-Free Filters 155
5.1.3 High-Efficiency Parametric Filters 159
5.2 Combinational Components in Parametric Filters 161
5.2.1 Evaluation of the Level of Combinational Components 162
5.2.2 Methods of Reducing Combinational Components 164
5.2.3 Comparison of the Combinational Components and Noise Levels in Digital Filters 167
5.3 Parametric Filter Design – a Case Study 168
5.4 Summary 170
5.5 Abbreviations 171
5.6 Variables 171
5.7 References 172

Part Three Digital Parametric Oscillators 175

6 Digital Parametric Oscillators 177
6.1 Regions of Parametric Oscillations 178
6.2 Parametric Resonance in Digital Resonators 183
6.3 Approximate Method of Evaluating a Region of Parametrical Generation 189
6.4 Analysis of Non-Periodic Components 193
6.5 Analysis of the Periodic Components 196
6.6 Wideband Control Signal 200
6.7 Periodic Components Spectrum 204
6.8 The Transient in Digital Parametric Oscillators 205
6.9 Summary 207
6.10 Abbreviations 208

6.11 Variables 208
6.12 References 209

7 Parametric Oscillator in Steady-State Mode 211
7.1 Limiting Mode of Parametric Oscillators 212
7.2 DPO Analysis in the Presence of Noise 222
7.3 Modelling of a Digital Parametric Oscillator Using Matlab – A Case Study 228
7.3.1 Non-Limiting Oscillation Mode 228
7.3.2 Steady-State Oscillation Mode 232
7.3.3 A Digital Parametric Oscillator with Non-Sinusoidal Control Signal 234
7.3.4 Frequency Synthesizer 236
7.4 Summary 239
7.5 Abbreviations 239
7.6 Variables 239
7.7 References 240

Index 243

Preface

Digital signal processing (DSP) does not require any special advertisements. Since the 1960s, it has become one of the most intensive fields of study in electronics-related science, and since the 1980s, owing to the extensive progress in integrated circuits technology, it has been an inseparable part of modern electronic systems. However, among the numerous DSP publications on algorithms, approaches, technical solutions, and so on, there is apparently no book on library shelves that is dedicated to linear non-adaptive time-variant digital filters. The lack of such a book is a deterrent to developing much broader engineering applications of these systems.

Different aspects of time-variant digital filters, or broader systems, have been studied for many years. Publications dedicated to this subject belong to different authors, and are spread over years and across journals. However, in spite of the many interesting and useful features of such systems, there are no systematic publications, monographs, or textbooks dedicated to filters with time-varying parameters or more complex systems based on these filters. The objective of this book is to present an appropriate introduction to theory and practice of one of the subclasses of time-varying digital systems: parametric digital filters and oscillators. The word *parametric* adopted in this book came from analog systems with periodically time-varying parameters; for example, the RLC resonator with varying capacitor [1]. This book starts with an analysis of discrete systems with parameters varying according to arbitrary laws, while the core of the book is dedicated to digital parametric filters and oscillators, which are the systems with periodically time-varying coefficients. In the general case, coefficient variation laws are arbitrary but specified beforehand, regardless of the input process. This distinguishes the discussed systems from adaptive filters [2]. This book does not cover filters with an essentially varying sampling rate $nT + \delta T(n)$ and $\delta T(n) \geq T$, which belong to the subclass of multi-rate filters [3] and also, in many instances, belong to the class of time-variant systems [4].

Thus, we will study digital systems described by the linear difference equation with time-varying parameters:

$$\sum_{k=0}^{K_1} a_k(n) \cdot y(n-k) = \sum_{k=0}^{K_2} b_k(n) \cdot x(n-k)$$

where $x(n)$ and $y(n)$ are input and output signals respectively; $n = 0, 1, \ldots$ is the time instant nT (T is the sampling interval); $a_k(n)$ and $b_k(n)$ are time-varying coefficients; and $a_0(n) \neq 0$ for any n.

Choosing an appropriate law of parameter variation in infinite impulse response (IIR) systems allows them to operate in *filtering, frequency conversion* or *parametric oscillating modes.* The latter mode has not been previously discussed in the literature except in the author's publications. In the main text, in many cases the word "filter" will describe all these systems. There will not be a focus on how to build these systems. The presented algorithms for time-variant systems will be appropriate for universal computers, microprocessors, specially developed hardware or DSP boards. For us, these will all be time-variant systems or filters.

Time-variant systems demonstrate some essential peculiarities in comparison with the traditional digital time-invariant filters. Even very small variations in parameters can change the characteristics of filters dramatically. Distinctive features of these systems are interesting from the circuit theory point of view and also have practical applications. Looking at this problem a little bit philosophically, we can regard the variation of parameters in time as offering new degrees of freedom in system design. Readers will find numerous examples within this book of how these extra degrees of freedom influence filter characteristics.

But, first let us look at an example that is very far from the field of digital systems. This example shows how it can be important to add an extra degree of freedom when attempting to solve a problem.

So, there are problems that have no solutions within $N \times D$ space, but have solutions within $(N + K) \times D$ space or have better solutions within $(N + K) \times D$ space, or have more cost-effective solutions and so on.

Comparison of the difference equation describing time-invariant filters

$$\sum_{k=0}^{K_1} a_k \cdot y(n-k) = \sum_{k=0}^{K_2} b_k \cdot x(n-k)$$

with the difference equation describing time-variant filters shows that the latter has extra degrees of freedom owing to the time dependence of coefficients. How these new degrees of freedom can be used will be discussed in the main text. The author hopes that on the basis of this information, researchers and engineers will be able to develop many new applications for time-variant digital systems.

In the book, only two algorithms of time-variant systems are discussed in detail: frequency filters that are, in some instances, equivalents of linear time-invariant (LTI) filters, and parametric oscillators. Of course, these are not the only possible types of linear time-variant (LTV) system applications. LTV systems are optimal, for example, for cyclo-stationary signals processing in communication systems [5, 6]. LTV discrete systems (DSs) can be used for spectrum [7] and image scrambling [8], image transmission [9], systems identification [10], TDM/FDM conversion [11, 12] and for many other useful applications.

The last but not the least group of LTV algorithms are two-dimensional time-variant filters for image processing, which are now the focus of much research. They include periodically time-varying filters [13] as well as more general systems and,

PUZZLE

You have six matches.

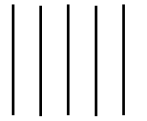

How do you build four triangles using only these six matches?

The first attempt:

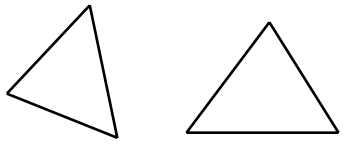

Six matches are used but only two triangles are built

The second attempt:

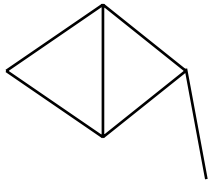

Two and a half triangles are ready but all matches have been used.

Keep going…

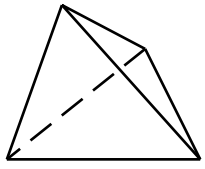

The solution is a pyramid and an extra degree of freedom is the third dimension.

in particular, time-variant filtering based on Gabor transform [14, 15]. Traditionally, one-dimensional filtering theory has generally been the basis for multidimensional signal processing. Therefore, this book can also be used as an introduction to two-dimensional LTV filtering.

As follows from the discussion above, LTV systems represent a rather broad class of systems and algorithms for signal and image processing. This book does not pretend to cover all aspects of LTV DS analysis and synthesis as well as application of time-varying algorithms in signal processing. Following the advice of the Russian folk philosopher Kozma Prutkoff that

"*. . . it is impossible to envelop the boundless . . .*"

this book is necessarily restricted in its contents. However, the author's expectation is that the book will initiate a new wave of interest in this class of systems, particularly in the engineering community.

The book contains seven chapters. There are no cross-references between the introduction and the main text, allowing the main text to be read independently of the introduction. When the first draft of the main text was ready, the author gave it to some postgraduate students to study. However, it took an unexpectedly long time for students to complete their reading of the book. After discussions with these students about how to make the book easier to read, the introduction was added. It is designed to help the reader understand the main text without requiring other special materials. The introductory chapter concisely explains the general problems of digital signals, filtering and methods of system analysis.

The introduction is not intended to substitute for numerous wonderful textbooks dedicated to digital systems and signals [16–18]. So, if readers feel confident about their knowledge of digital signals and systems they can read the book starting from the main text. Alternatively, the introduction may serve to refresh the reader's knowledge of the signals and systems basics.

This book is written, first of all, for graduate specialists in signal processing and related specialties, as well as for PhD students. Other students, for example, those engaged in final year thesis preparation, may also find it useful.

Any preface assumes some historical reference to the subject. For me, the story of this subject started when I first read the paper of reference [19]. I then started to work in this area with my PhD students. Much later I had the privilege of spending a term in Cambridge University with a world-class signal-processing group led by Prof. Peter Rayner. Some early research done by this group was also dedicated to time-variant signal processing [11, 20].

Most of the author's papers dedicated to parametric systems have been published in Russian. It is difficult to translate properly even the title of these journals. Some information regarding these papers can be found in [21].

My former postgraduate students, V. Bets, V. Sizov, I. Rogozkin, L. Donskoi, P.-J. Picot, have contributed a lot in the area covered by the book. Moreover, with the permission of V. Sizov, there are some direct adoptions from his thesis; in particular, examples of time-varying filters.

The book is also a good place to thank my former PhD supervisor and later my colleague for many years, Prof. D. Nezlin, for his contribution to my development as a scientist.

Behind any book there is a big job in manuscript preparation. I want to thank Carol Booth who helped me with this.

REFERENCES

[1] Locherer KH (1982) *Parametric Electronics: An introduction*, New York: Springer-Verlag.
[2] Haykin S (1991) *Adaptive Filter Theory*, New Jersey: Prentice Hall.
[3] Vaidyanathan P (1993) *Multirate Systems and Filter Banks*, New Jersey: Prentice Hall.
[4] Loeffler M, Burrus CS (1984) Optimal design of periodically time-varying and multi-rate digital filters. *IEEE Trans.*, **ASSP-32**(10), 991–997.
[5] Gardner WA (1994) *Cyclostationarity in Communications and Signal Processing*, IEEE Press, USA.

[6] Orozco-Lugo AG, McLernon DC (1998) An application of periodically time-varying digital filters to blind equalisation, *IEE Colloquium on Digital Filters: An Enabling Technology*, London, UK, 11/1–11/6.
[7] Ishii R, Kakishita M. (1990) A design method for periodically time varying digital filter for spectrum scrambling. *IEEE Trans.*, **ASSP-38**(7), 1219–1222.
[8] Creusere CD, Mitra SK (1994) Efficient image scrambling using polyphase filter banks, *Proc. of IEEE International Conference in Image Processing*, Austin, 81–86.
[9] Kawamata M, Mirakoshi S, Higushi T (1993) Analysis of multidimensional linear periodically shift-variant digital filters and its application to secure communication of images. *IEICE Trans.*, **E76-A**(3), 326–335.
[10] Xiang-Gen Xia (1997) System identification using chirp signals and time-variant filters in the joint time-frequency domain. *IEEE Trans.*, **SP-45**(8), 2072–2084.
[11] Critchley J, Rayner PJW (1998) Design methods for periodically time varying digital filters. *IEEE Trans.*, **ASSP-36**(5), 661–673.
[12] Yang X, Kawamata M, Higuchi T (1995) Approximations of IIR periodically time-varying digital filters. *IEE Proc. Circuits Devices Syst.*, **142**(6), 387–393.
[13] Joo KS, Bose T (1996) Two-dimensional periodically shift variant digital filters. *IEEE Trans.*, **Cas VT-6**(1), 97–107.
[14] Farckash S, Raz S (1990) Time-variant filtering via the Gabor expansion, *Signal Processing*, Vol. Theories and Applications, New York: Elsevier, 509–512.
[15] Shidong Li A (1994) Generalized non-separable 2-D discrete Gabor expansion for image representation and compression, *IEEE International Conference ICIP-94*, Vol. 1, 810–814.
[16] Oppenheim AV, Schafer RW (1989) *Discrete-Time signal processing*, New Jersey: Prentice Hall.
[17] Ifeachor EC, Jervis BW (2002) *Digital Signal Processing: A Practical Approach*, UK: Prentice Hall.
[18] Haykin S, Van Veen B (1999) *Signals and Systems*, New York: Wiley & Sons, 1999.
[19] Huang NC, Aggarwal JK (1982) Time-varying digital signal processing: a review, *Proc. IEEE Int. Symp. Cas*, Rome, Italy, 659–662.
[20] Macleod MD (1979) *The Design of Digital Signal Processing Systems with Discrete Parameters*, Ph.D. Thesis, University of Cambridge, Cambridge.
[21] Scoular S, Cherniakov M, Rogozkin I (1993) Review of Soviet research on linear time-variant discrete systems. *Signal Process.*, **30**(1), 85–101.

1

Introduction: Basis of Discrete Signals and Digital Filters

The theory and practice of digital signal processing (DSP) are currently in a mature stage. It is difficult to imagine any modern electronic system without wide application of DSP and, in particular, linear time-invariant algorithms for filtering, equalization, characteristic correction and so on.

The major goal of this chapter is to introduce the theoretical basis of discrete signals and time-invariant digital systems to help readers more easily understand the main text dedicated to time-variant systems and to minimize the necessity to consult other texts while reading this book. This introduction provides a superficial overview of DSP concepts: sampling and quantization; impulse and frequency responses; Fourier, Laplace and z-transforms; system stability and causality and finite and infinite impulse response (IIR) digital filters (DFs). For those familiar with DSP and related subjects, this introduction will help refresh their knowledge. For those who are unfamiliar, this chapter can be used as the first stage of study of discrete signals and systems. Of course, this introduction does not and cannot replace special literature and textbooks dedicated to DSP problems. Among the latest textbooks in this area, the author recommends Reference [1].

1.1 DISCRETE SIGNALS AND SYSTEMS

Most signals used in information systems are similar to analog processes. In the general case they are functions of continuous time. Digital filters belong to the group of discrete systems of signal processing, which operate with discrete input processes. Thus, an analog input signal is represented by discrete samples obtained in time moments proportional to the sampling interval T. An analog waveform can be transformed into an appropriate discrete signal without information losses if sampling frequency f_s is determined as

$$f_s = \frac{\omega_s}{2\pi} = \frac{1}{T} \geq 2 f_{o\max} \tag{1.1}$$

An Introduction to Parametric Digital Filters and Oscillators Mikhail Cherniakov
© 2003 John Wiley & Sons, Ltd ISBN: 0-470-85104-X

This corresponds to the Nyquist criteria, that is, the sampling frequency is at least two times higher than the highest frequency in the signal spectrum $f_{o\max}$ [2]. In discrete signal analysis, frequency, as a rule, is represented as a normalized frequency $\omega = \omega_a T = \omega_a / f_s$, where $\omega_a = 2\pi f_a$ is a frequency of an analog (continuous) signal.

To form a digital signal from a discrete signal, the amplitude is represented as a binary code. The device that quantizes the signal is called an *analog–digital converter* (ADC). The number of bits in signal representation depends on the system's applications and in practice, varies in a band from 1 to 16. The most widely used ADCs have 8 to 12 bits.

The analysis of digital systems is similar to the analysis of analog systems and is based on the comparison of signals at the system's input and output. In this chapter, digital signals and systems will be considered with the assumption that the number of bits in ADCs is large enough and that quantization effects are negligible. In other words, we make digital signals and systems equivalent to discrete signals and systems. If necessary, a quantization effect can be taken into account by adding some quantization noise to signal. In conventional ADCs, in the first approximation, this noise has uniformly distributed amplitude with zero mean value and its power can be calculated by [1] $\sigma_{qn}^2 = \Delta^2/12$, where Δ is the quantization level. This noise also has near uniform power spectral density over the band $|f| \le f_s/2$.

Signal-to-quantization noise ratio (S/N_{qn}) can be evaluated as $S/N_{qn} \approx 6.02B_{its} + 4.77 - 20\log(A_p/\sigma_S)$ (dB), where B_{its} is the number of bits representing an input signal, σ_S is the rms value of the input waveform and A_p is the ADC peak design level of the quantizer. For example, if an input signal is a sinusoidal waveform $(S/N_{qn}) \approx 6.02B_{its} + 1.7$ (dB). Continuous linear systems are fully characterized by their impulse response $h(t)$. The impulse response is an output system reaction to the input signal, described by the δ-function

$$\delta(t) = \begin{cases} \infty, & t = 0 \\ 0, & t \neq 0 \end{cases} \tag{1.2}$$

and

$$y(t) = \int_0^t x(t-\lambda)h(\lambda)\,\mathrm{d}\lambda \tag{1.3}$$

where $x(t)$ and $y(t)$ are input and output signals of the system respectively, and $x(t) = 0$ for $t < 0$.

For a discrete system, continuous time t should be replaced by discrete time $t = nT$ and $\lambda = mT$, and integration is replaced by summation

$$y(nT) = \sum_{m=0}^{n} x(nT - mT) \cdot h(mT) \cdot T \tag{1.4}$$

Thus, the first step of digital system analysis is the representation of an analog signal $x(t)$ by a discrete equivalent $x(nT)$. The second step is the representation of $h(t)$ by its discrete equivalent $h(mT)$.

1.2 DISCRETE SIGNALS

1.2.1 Time-Domain Representation for Discrete Signals

In the general case, discrete signals can be described in discrete time moment nT as well as in continuous time. For the analysis of discrete systems, signals description in discrete time is most popular, namely, nT. The sampling period T is often omitted and the signal at the moment nT is described as $x(n) = x(nT)$.

Some examples of discrete signal descriptions and their plots are given below.

1. Sinusoidal sequence: $x(nT) \equiv x(n) = \sin(\omega nT) \equiv \sin(\omega n)$ (Fig. 1.1)
2. Linear sequence: $x(nT) \equiv x(n) = n$ (Fig. 1.2)
3. Unit sample sequence (impulse): $x_i(n-m) = \begin{cases} 1 & \text{for } n = m \\ 0 & \text{for } n \neq m \end{cases}$ (Fig. 1.3)
4. Unit step sequence: $x_s(n-m) = \begin{cases} 1 & \text{for } n \geq m \\ 0 & \text{for } n < m \end{cases}$ (Fig. 1.4)

Unit steps and unit impulses are widely used as test signals to analyse discrete systems. It is sometimes convenient to represent function $x_s(n)$ as a function $x_i(n)$: $x_s(n-k) = \sum_{m=0}^{\infty} x_i(n-k-m)$.

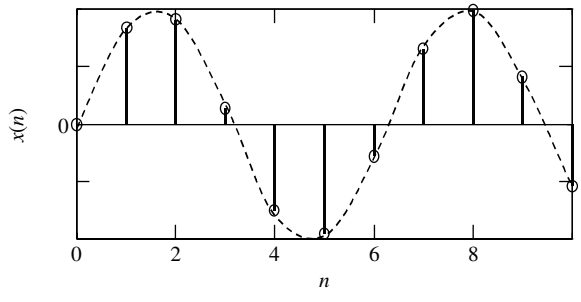

Figure 1.1 Discrete function $x(n) = \sin(\omega n)$

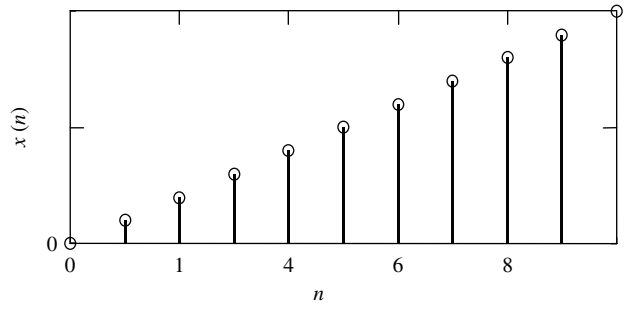

Figure 1.2 Discrete function $x(n) = n$

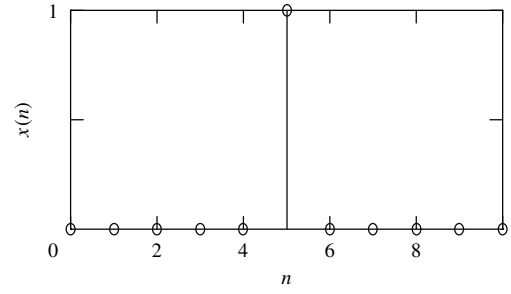

Figure 1.3 Unit sample, $m = 5$

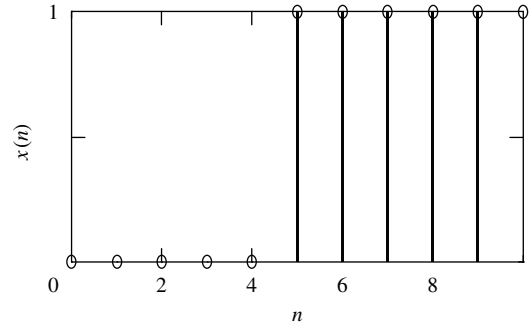

Figure 1.4 Unit step, $m = 5$

1.2.2 Presentation of Discrete Signals by Fourier Transform

Like analog signals, discrete signals can be represented and analysed in frequency domain. Spectral analysis is based on Fourier transform [2]. To apply Fourier transform to discrete signals, they have to be represented in continuous time

$$x(n) = x(nT) = x_d(t) = x(t) \cdot v(t) \tag{1.5}$$

where $x_d(t)$ is a discrete function represented in continuous time, $x(t)$ is the initial analog function (e.g., $x(n) = \sin(\omega n) \Leftrightarrow x(t) = \sin(\omega_a t)$) and $v(t)$ is a periodical sequence of δ-functions (see Fig. 1.5a) with period T

$$v(t) = \sum_{n=-\infty}^{\infty} \delta\left(\frac{t}{T} - n\right), \quad n = 0, 1, 2, \ldots \tag{1.6}$$

Note that the δ-function possesses some properties that will be used later

$$\int_{-\infty}^{\infty} \delta(t)\,\mathrm{d}t = 1 \tag{1.7}$$

$$\int_{-\infty}^{\infty} F(t)\delta(t - t_0)\,\mathrm{d}t = F(t_0) \tag{1.8}$$

where $F(t)$ is an arbitrary function. Thus, discrete function $x(n)$ in continuous time can be represented by

$$x(n) = x(t) \cdot \sum_{n=-\infty}^{\infty} \delta\left(\frac{t}{T} - n\right) \tag{1.9}$$

As was discussed earlier, a discrete function can be obtained from an appropriate analog function by discretization. But, from a practical point of view, δ-function is an abstract notion. So, for practical applications, it is more useful to consider an impulse sequence with a unit amplitude and limited duration τ (Fig. 1.5b) as a periodical sampling function:

$$v_\tau(t) = \begin{cases} 1 & \text{for } |t - nT| \le \dfrac{\tau}{2} \\ 0 & \text{for } |t - nT| > \dfrac{\tau}{2} \end{cases} \tag{1.10}$$

Then the discrete signal takes the form

$$x(n) = x(t) \cdot v_\tau(t) \tag{1.11}$$

To evaluate a spectrum of this discrete function, let us consider known expressions for a continuous waveform s(t) spectrum [2]

$$\overline{S}(\omega_a) = \int_{-\infty}^{\infty} s(t) \exp(-\mathrm{j}\omega_a t)\, \mathrm{d}t \tag{1.12}$$

where $\overline{(*)}$ denotes a complex function. We use equation (1.9) to calculate the spectrum of the discrete signal $x(n)$. Assume that $x(n) = 0$ for $n < 0$ and introduce $x(n)$ via its continuous time equivalent

$$\overline{X}_d(\omega_a) = \int_0^{\infty} x(t) \sum_{n=-\infty}^{\infty} \delta\left(\frac{t}{T} - n\right) \exp(-\mathrm{j}\omega_a t)\, \mathrm{d}t$$

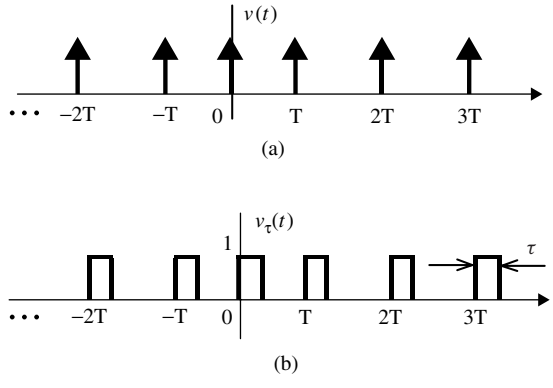

Figure 1.5 Sample functions: (a) ideal and (b) real

$$= \sum_{n=-\infty}^{\infty} \int_0^{\infty} x(t)\delta\left(\frac{t}{T} - n\right) \exp(-\mathrm{j}\omega_a t)\, \mathrm{d}t$$

$$= T \sum_{n=-\infty}^{\infty} x(nT) \exp(-\mathrm{j}\omega_a nt) \tag{1.13}$$

As seen from equation (1.13), the sampling period T is a scale factor, and in some literature, it is omitted. So, the spectrum of a discrete signal is generally a complex value and is a function of the analog frequency ω_a. However, in many cases, it is more convenient to represent this spectrum as a function of normalized frequency $\omega = \omega_a T$ or

$$\overline{X}_d(\omega) \equiv X(\omega) = \sum_{n=0}^{\infty} x(n) \exp(-\mathrm{j}\omega n) \tag{1.14}$$

for the case $x(n) = 0$ when $n < 0$. In spectrum descriptions, complexity notation $\overline{(*)}$ is also often omitted, taking into account that the spectrum, in general, is a complex value.

From expression (1.13), it follows that the discrete signal spectrum is periodical with period ω_s. This important property can be described more accurately

$$\overline{X}_d(\omega_a + k\omega_s) = T \sum_{n=0}^{\infty} x(nT) \exp[-\mathrm{j}(\omega_a + k\omega_s)nT]$$

$$= T \sum_{n=0}^{\infty} x(nT) \exp(-\mathrm{j}\omega_a nT) \cdot \exp(-\mathrm{j}k\omega_s nT) \tag{1.15}$$

However,

$$\exp(-\mathrm{j}k\omega_s nT) = \left(-\mathrm{j}k\frac{2\pi}{T}nT\right) = 1 \tag{1.16}$$

and

$$\overline{X}_d(\omega_a + k\omega_s) = \overline{X}_d(\omega_a) \tag{1.17}$$

After similar calculations for normalized frequency ω, it can be seen that the period is equal to 2π, that is,

$$\overline{X}(\omega) = \overline{X}(\omega + k2\pi) \tag{1.18}$$

A graphic interpretation of equation (1.18) is shown in Fig. 1.6.

Another peculiarity of the discrete signal spectrum is the behaviour of its phase–frequency components. If the signal is represented by a real function of time, then the spectrum values at the symmetrical points, relative to $\omega = k\pi$ are complex conjugates:

$$\overline{X}_d(2\pi - \omega) = \overline{X}_d(\omega)^* \tag{1.19}$$

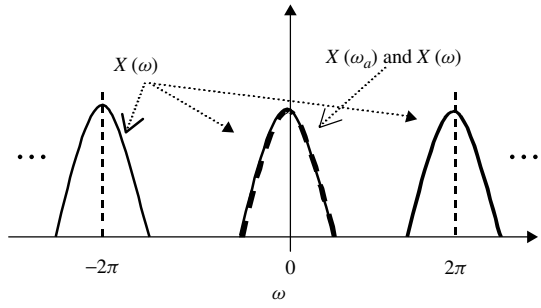

Figure 1.6 Spectrum of discrete signals

where $(\bullet)^*$ stands for a complex-conjugate value. Equation (1.19) directly follows from the simple formula

$$\overline{X}_d(2\pi - \omega) = \sum_{n=0}^{\infty} x(nT)\exp(\mathrm{j}\omega n)\cdot\exp(-\mathrm{j}2\pi n) = \sum_{n=0}^{\infty} x(nT)\exp(\mathrm{j}\omega n) \tag{1.20}$$

This peculiarity is an equivalent of the following relation between the amplitude and phase spectrum components

$$\begin{aligned} |\overline{X}_d(2\pi - \omega)| &= |\overline{X}_d(\omega)| \\ \theta_d(2\pi - \omega) &= -\theta_d(\omega) \end{aligned} \tag{1.21}$$

that correspond to the definition of the complex-conjugate function. Graphical interpretation of the equation is shown in Fig. 1.7.

It was shown earlier that the spectrum of the discrete signal is periodic. We can now determine the relations between the spectrum of an analog signal $\overline{X}(\omega_a)$ and the corresponding spectrum of a discrete signal $\overline{X}_d(\omega_a)$. In time domain, a discrete signal can be introduced via an appropriate analog signal as follows from equation (1.5)

$$x_d(t) = x(t)\cdot v(t) \tag{1.22}$$

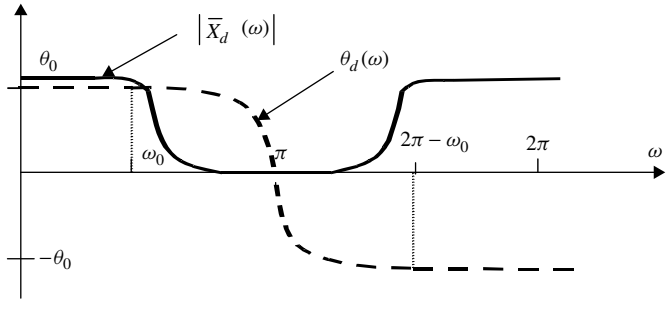

Figure 1.7 Amplitude and phase spectrum of a real discrete signal

It is known that a spectrum of the product of two functions is proportional to a convolution of these functions' spectrums [2]

$$\overline{X}_d(\omega_a) = \frac{1}{2\pi}\int_{-\infty}^{\infty} \overline{X}(\lambda)\cdot\overline{V}(\omega_a-\lambda)\,\mathrm{d}\lambda \tag{1.23}$$

where $\overline{X}(\lambda)$ is a spectrum of the initial analog signal $x(t)$ and $\overline{V}(\lambda)$ is a spectrum of the sampling signal $v(t)$. This sampling signal was specified earlier as a sequence of the δ-functions (1.6), the spectrum of which is

$$\overline{V}(\omega_a) = T\sum_{n=-\infty}^{\infty}\delta\left(\frac{\omega_a}{\omega_s}-n\right) \tag{1.24}$$

Consequently, combining (1.22) to (1.24) we obtain

$$\overline{X}_d(\omega_a) = \frac{1}{2\pi}\int_{-\infty}^{\infty}\overline{X}(\lambda)T\sum_{n=-\infty}^{\infty}\delta\left(\frac{\omega_a-\lambda}{\omega_s}-n\right) \tag{1.25}$$

After integration and taking into account equation (1.8), we finally obtain the relation between $\overline{X}_a(\omega_a)$ and $\overline{X}_d(\omega_a)$:

$$\overline{X}_d(\omega_a) = \sum_{n=-\infty}^{\infty}\overline{X}(\omega_a-k\omega_s) \tag{1.26}$$

That is, the spectrum of the discrete signal $\overline{X}_d(\omega_a)$ is a sum of the spectrums $\overline{X}(\omega_a)$ of the initial analog signal shifted along the frequency with a period equal to the sampling frequency ω_s (Fig. 1.6). In other words, the spectrum of the discrete signal is periodic, and each component of this spectrum corresponds to the spectrum of the initial analog signal.

From a practical point of view, it is useful to consider the influence of the realistic sampling function waveform on the discrete signal spectrum. In this case, the sequence of δ functions should be replaced by the sequence of unit pulses with finite duration τ (Fig. 1.5b). This corresponds to the replacement of $v(t)$ on $v_\tau(t)$:

$$\begin{aligned}\overline{X}_d(\omega_a) &= \int_0^T x(t)v_\tau(t)\exp(-\mathrm{j}\omega_a t)\,\mathrm{d}t\\ &= \sum_{n=0}^{\infty}\int_{(nT-\tau/2)}^{nT+\tau/2} x(t)\exp(-\mathrm{j}\omega_a t)\,\mathrm{d}t\end{aligned} \tag{1.27}$$

Although τ is not an infinitely small value as in the δ-function, in practice it is still considerably less than the sampling period: $\tau \ll T$. Then, the integral in

equation (1.27) can be approximately represented as

$$\int_{(nT-\tau/2)}^{nT+\tau/2} x(t)\exp(-j\omega_a t)\,dt \approx x(nT)\exp(-j\omega_a nT)\cdot\tau$$

Consequently,

$$\overline{X}_d(\omega_a) \approx \sum_{n=0}^{\infty} x(nT)\exp(-j\omega_a nT) \tag{1.28}$$

Physically, this approximation means that function $x(t)$ does not change its value in the vicinity $t = nT$. At the same time, signal (1.27) corresponds to the output signal of a real ADC.

Compare now the discrete spectrum introduced by equation (1.27) and the spectrum of the initial analog signal. The spectrum of the impulse sequence $v_\tau(t)$ is

$$\overline{V}_\tau(\omega_a) = \tau\frac{\sin\omega\tau/2}{\omega\tau/2}\cdot\sum_{n=-\infty}^{\infty}\delta\left(\frac{\omega_a}{\omega_s}-n\right) \tag{1.29}$$

Then,

$$\begin{aligned}\overline{X}_d(\omega_a) &= \frac{\tau}{2\pi}\sum_{n=-\infty}^{\infty}\int_{-\infty}^{\infty}\overline{X}(\lambda)\frac{\sin(\omega_a-\lambda)\tau/2}{(\omega_a-\lambda)\tau/2}\cdot\delta\left(\frac{\omega_a-\lambda}{\omega_s}-n\right)d\lambda \\ &= \frac{\tau}{T}\sum_{n=-\infty}^{\infty}\overline{X}(\omega_a-n\omega_s)\cdot\frac{\sin n\omega_s\tau/2}{n\omega_s\tau/2}\end{aligned} \tag{1.30}$$

From equation (1.30), it can be seen that the spectrum of the discrete signal is a sum of shifted copies of the input signal spectrum. However, the amplitude of this spectrum is modulated by the slowly decreasing function $\frac{\sin x}{x}$. Figure 1.8 shows the relations between the spectrum of the initial analog signal (Fig. 1.8a), the spectrum of the discrete signal obtained by ideal time-sampling (Fig. 1.8b) and that obtained by using impulse-sampling signal duration τ (Fig. 1.8c).

1.2.3 Discrete Fourier Transform

For spectrum analysis of discrete signals, it is convenient to use a discrete Fourier transform (DFT), which is a variation of Fourier Transform.

Let us determine the spectrum of a periodical discrete signal with period T_0. Like all periodical signals it has a discrete spectrum, which is not equal to zero at frequencies $\omega_a = k\frac{2\pi}{T_0} = k\Omega$, where $k = 0, 1, 2, \ldots$. For simplification, we choose an interval of signal sampling T in such a way that $T_0/T = N$ is an integer. This interval has

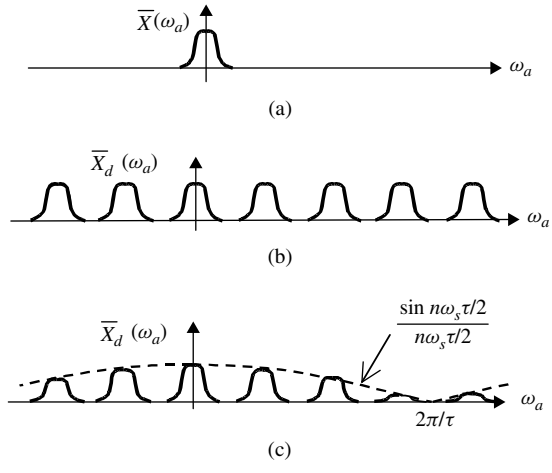

Figure 1.8 Relations between spectrums

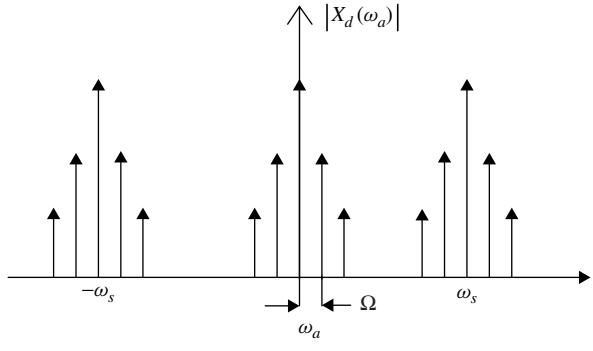

Figure 1.9 Spectrum of a periodical discrete signal

to satisfy the Nyquist criteria $\frac{\omega_s}{\Omega} = \frac{2\pi}{T} \cdot \frac{T_0}{2\pi} = N$. Components of the periodic signal spectrum are δ-functions, and this spectrum is shown in Fig. 1.9.

Then, expression (1.13) takes the form

$$\overline{X}_d(\omega_a) = \sum_{n=0}^{\infty} x(nT)\exp(-\mathrm{j}k\Omega nT) = \sum_{n=0}^{\infty} x(n)\exp\left(-\frac{\mathrm{j}kn2\pi}{N}\right) \tag{1.31}$$

Both functions $x(n)$ and $\exp(\bullet)$ in equation (1.31) are periodical with the same period N. Consequently, we can consider only the first N elements of the sum:

$$\sum_{n=0}^{N-1} x(n)\exp\left(-\frac{\mathrm{j}kn2\pi}{N}\right)$$

and

$$\overline{X}_d(\omega_a) = \sum_{l=-\infty}^{\infty} \delta(\omega_a - l\Omega) \sum_{n=0}^{N-1} x(n) \exp\left(-\frac{\mathrm{j}kn2\pi}{N}\right) \tag{1.32}$$

The first sum in equation (1.32) means that each spectrum component is a δ-function and the spectrum has a period Ω. The second sum reflects the essence of the spectrum and is the DFT:

$$\overline{X}(k) \equiv \overline{X}(k\Omega) = \sum_{n=0}^{N-1} x(n) \exp\left(-\mathrm{j}\frac{2\pi}{N}kn\right) \tag{1.33}$$

In equation (1.33), the spectrum is a function of discrete frequency $k\Omega$.

The inverse discrete Fourier transform (IDFT) is determined as

$$x(n) = \frac{1}{N} \sum_{k=0}^{N-1} \overline{X}(k) \exp\left(\mathrm{j}\frac{2\pi}{N}kn\right) \tag{1.34}$$

Thus, equations (1.33) and (1.34) are the pair of DFT that are widely used in DSP systems analysis and design [1].

1.2.4 Laplace and z-transforms

Laplace transform (LT) is an exclusively important tool used in linear systems theory. Systems described by linear differential equations can be relatively easily analysed via LT. This transform converts a differential equation into an algebraic equation [2]. A discrete signal can be represented using LT by

$$L(p) = \int_0^{\infty} x_d(t) \exp(-pt)\,\mathrm{d}t = \int_0^{\infty} x(t) \sum_{n=0}^{\infty} \delta\left(\frac{t}{T} - n\right) \exp(-pt)\,\mathrm{d}t \tag{1.35}$$

Then, using equation (1.8),

$$L(p) = T \sum_{n=0}^{\infty} x(nT) \exp(-pnT) \tag{1.36}$$

The inverse Laplace transform (ILT) is

$$x(nT) = \frac{1}{2\pi\mathrm{j}} \oint L(p) \exp(pnT)\,\mathrm{d}p \tag{1.37}$$

where the integral is taken along any contour containing all poles of the integrand function.

As known, the contour integral in equation (1.37) can be represented as a sum of residues of the integrand function at its poles p_l, that is,

$$x(nT) = \sum_{l=1}^{L} \mathrm{res}_l\{L(p)\exp(pnT)\} \tag{1.38}$$

where L is the number of poles.

For the analysis of discrete signals and systems, expressions (1.35) to (1.38) are used in different representations. Instead of p, a variable z is used:

$$z = \exp(pT) \tag{1.39}$$

and LT becomes a z-transform:

$$x(z) = \sum_{n=0}^{\infty} x(nT) \cdot z^{-n} \tag{1.40}$$

Similar to the discrete signal representation $x(nT) \equiv x(n)$, the interval of discretization is often omitted. The inverse z-transform is used to determine $x(n)$ when $x(z)$ is known, and is described as

$$\begin{aligned} x(nT) &= \frac{1}{2\pi \mathrm{j}} \oint L\left(\frac{1}{T}\ln z\right) \exp\left(\frac{1}{T}\ln z \cdot nT\right) \frac{\mathrm{d}z}{Tz} \\ &= \frac{1}{2\pi \mathrm{j}} \oint T \cdot \sum_{n=0}^{\infty} x(nT) z^{-n} \frac{\mathrm{d}z}{Tz} = \frac{1}{2\pi \mathrm{j}} \oint x(z) z^{n-1}\,\mathrm{d}z \end{aligned} \tag{1.41}$$

Equation (1.41) can be obtained directly from equation (1.37) by substituting

$$p = \frac{1}{T}\ln z \tag{1.42}$$

which follows from equation (1.39). Equation (1.41) can be evaluated using the theory of residues:

$$x(nT) = \sum_{l=1}^{L} \mathrm{res}_l(x(z) \cdot z^{n-1}) \tag{1.43}$$

Application of z-transform is very popular in the theory of discrete signals and systems, and we now consider some properties of this transform.

1.2.4.1 Properties of z-Transform

1. *Linearity*

Let $x(n) = \sum_{i=1}^{I} a_i x_i(n)$. The appropriate z-transform is

$$x(z) = \sum_{n=0}^{\infty} \sum_{i=1}^{I} a_i x_i(n) z^{-n} = \sum_{i=1}^{I} a_i x_i(z) \tag{1.44}$$

which is the sum of z-transforms of $x_i(n)$ functions.

2. *Delay*

Assume that discrete signal $x(n)$ is delayed by $T \cdot m$, that is, $x_d(n) = x(n-m)$. Evaluating z-transform, we obtain

$$x_d(z) = \sum_{n=0}^{\infty} x(n-m) z^{-n} = \sum_{n=m}^{\infty} x(n-m) z^{-n}$$

Taking into account that $x(n) = 0$ for $n < 0$, or substituting $v = n - m$, we obtain

$$x_d(z) = \sum_{v=0}^{\infty} x(v) z^{-v} z^{-m} = x(z) z^{-m} \tag{1.45}$$

3. *Multiplication by exponential function*

Assume $y(n) = a^{-n} x(n)$. The z-transform of this equation is

$$y(z) = \sum_{n=0}^{\infty} a^{-n} x(n) z^{-n} = \sum_{n=0}^{\infty} x(n) (az)^{-n}$$

or

$$y(z) = x(az) \tag{1.46}$$

4. *Differentiation*

We differentiate both sides of the equation (1.40):

$$\frac{\mathrm{d}x(z)}{\mathrm{d}z} = -\sum_{n=0}^{\infty} x(nT) n z^{-n-1} \quad \text{or} \quad -z \frac{\mathrm{d}x(z)}{\mathrm{d}z} = \sum_{n=0}^{\infty} n x(nT) z^{-n}$$

Denoting $y(n) = nx(n)$, we obtain

$$y(n) = -z \frac{\mathrm{d}x(z)}{\mathrm{d}z} \tag{1.47}$$

Some other properties can be found in [3]. The properties of the z-transform are similar to many properties of Fourier and Laplace transforms.

1.2.4.2 Examples of z-Transform

Consider some examples of z-transform for commonly used functions.

1. $x_I(n) = \begin{cases} 1 & n = 0 \\ 0 & n \neq 0 \end{cases}$

$$x_I(z) = x_I(0) \cdot z^{-0} = 1 \tag{1.48}$$

2. $x_s(n) = \begin{cases} 1 & n \geq 0 \\ 0 & n < 0 \end{cases}$

$$x_s(z) = \sum_{n=0}^{\infty} z^{-n}$$

It is important to note that this is a sum of geometrical progression z^{-1}, that is,

$$x_s(z) = \frac{1 - z^{-\infty}}{1 - z^{-1}}$$

For $|z| > 1, \lim_{N\to\infty} z^{-N} = 0$ and

$$x_s(z) = \frac{1}{1 - z^{-1}} = \frac{z}{z - 1} \tag{1.49}$$

For $|z| < 1, x_s(z) \to \infty$.

3. $x(n) = \begin{cases} a^n & n \geq 0 \\ 0 & n < 0 \end{cases}$

$$x(z) = \sum_{n=0}^{\infty} a^n \cdot z^{-n} = \sum_{n=0}^{\infty} (az^{-1})^n$$

In this case, $x(z)$ is represented by a sum of geometrical progression with denominator az^{-1}. So,

$$x(z) = \frac{1 - (az^{-1})^{\infty}}{1 - az^{-1}}$$

If $|z| > a$, then

$$x(z) = \frac{z}{z - a} = \frac{1}{1 - az^{-1}} \tag{1.50}$$

4. $x(n) = \begin{cases} \cos \omega n & n \geq 0 \\ 0 & n < 0 \end{cases}$

Taking into account that $\cos \omega n = \frac{1}{2}\{\exp(\mathrm{j}\omega n) + \exp(-\mathrm{j}\omega n)\}$ and using results from the previous section as well as assuming $\exp(\mathrm{j}\omega) = a$, we obtain

$$x(z) = \frac{1}{2}\left\{\frac{z}{z - \exp(\mathrm{j}\omega)} + \frac{z}{z - \exp(-\mathrm{j}\omega)}\right\} \tag{1.51}$$

5. $x_n(n) = \begin{cases} n & n \geq 0 \\ 0 & n < 0 \end{cases}$

This function can be represented as $x_n(n) = nx_s(n)$, where $x_s(n)$ has already been considered. Then, using a rule of differentiation

$$x_s(z) = \frac{z}{z-1} \quad \text{and} \quad \frac{\mathrm{d}x_s(z)}{\mathrm{d}z} = -\frac{1}{(z-1)^2}$$

Consequently, from equation (1.47) we obtain

$$x_n(z) = \frac{z}{(z-1)^2} \tag{1.52}$$

1.2.4.3 Calculation of the Inverse z-Transform

To calculate function $x(n)$ using inverse z-transform, it is necessary to determine the sum of residues for function $f(z) = x(z)z^{n-1}$ in its poles. There are a number of methods for residue sum calculation. We consider only two useful approaches.

1. *Determination of the residue at a prime pole*

If $f(z)$ is a rational function,

$$f(z) = \frac{P(z)}{Q(z)}$$

where $P(z)$ and $Q(z)$ are exponential polynomials. Then, residue $f(z)$ at its kth pole z_k is

$$\mathrm{res}_k = \left.\frac{P(z)}{Q'(z)}\right|_{z=z_k} \tag{1.53}$$

2. *Determination of the residue at the "m" multiple pole*

If for the same value of $z = z_k$ function $f(z)$ has "m" multiple poles, then

$$\mathrm{res}_k = \frac{1}{(m-1)!}\frac{d^{m-1}}{dz^{m-1}}\{f(z)(z - z_k)^m\}_{z=z_k} \tag{1.54}$$

1.2.4.4 Examples of Inverse z-Transform Calculations

1. $x(z) = \dfrac{z}{z-a}; f(z) = \dfrac{z^n}{z-a}$

There is one prime pole at the point $z = a$. Using equation (1.53), we obtain

$$x(n) = \left.\frac{z^n}{\dfrac{\mathrm{d}}{\mathrm{d}z}(z-a)}\right|_{z=a} = a^n \tag{1.55}$$

2. $x(z) = \dfrac{z}{(z-1)^2}; f(z) = \dfrac{z^n}{(z-1)^2}$

In this case, the pole is at the point $z = 1$ with multiplicity $m = 2$. Using equation (1.54), we obtain

$$x(n) = \frac{\mathrm{d}}{\mathrm{d}z}\left\{\frac{z^n}{(z-1)^2}(z-1)^2\right\}_{z=1} = nz^{n-1}|_{z=1} = n \tag{1.56}$$

3. $x(z) = \dfrac{a}{z-b}; f(z) = \dfrac{az^{n-1}}{z-b}$

Note that for $n = 0$, $f(z) = \frac{a}{(z-b)z}$ and, consequently, there are two primary poles $z_1 = b$ and $z_2 = 0$. For $n \geq 1$ there is only one pole $z_1 = b$. We will consider these two cases separately:

$$x(0) = \left.\frac{a}{z-b+z}\right|_{z=0} + \left.\frac{a}{z-b+z}\right|_{z=b} = 0$$

and for $n \geq 1$,

$$x(n) = az^{n-1}|_{z=b} = ab^{n-1}$$

Thus,

$$x(n) = \begin{cases} 0, & n = 0 \\ ab^{n-1}, & n \geq 1 \end{cases} \tag{1.57}$$

1.3 TIME–INVARIANT DISCRETE LINEAR SYSTEMS

For discrete linear systems (DLSs), a principle of superposition is valid, which is a criterion of system linearity. Assume that at the system input there is a signal $x_1(n)$ and that at the output there is a signal $y_1(n)$. For input signal $x_2(n)$ there will be output signal $y_2(n)$, and so on. A system is said to be time-invariant if a time shift in

the input signal leads to an identical time shift in the output signal. So, if the system is linear, then the following assumptions are true:

$$x(n) = V_1 x_1(n) + V_2 x_2(n)$$
$$y(n) = V_1 y_1(n) + V_2 y_2(n) \tag{1.58}$$

If the system is linear and time-invariant then

$$x(n-m) = V_1 x_1(n-m) + V_2 x_2(n-m)$$
$$y(n-m) = V_1 y_1(n-m) + V_2 y_2(n-m) \tag{1.59}$$

In the general case, a system can have a non-linear ADC at the LTI filter input and digital–analog converter (DAC) at its output (Fig. 1.10), for example, for speech compression.

1.3.1 Difference Equation and Impulse Response

Like the analog systems, discrete linear systems (DLSs) can be characterized by their impulse responses $h(n)$. This characteristic is a system response when the input is a unit impulse (see Fig. 1.3):

$$x_i(n) = \begin{cases} 1, & n = 0 \\ 0, & n \neq 0 \end{cases} \tag{1.60}$$

An output signal $y(n)$ in this case is represented by a discrete convolution of the signal $x(n)$ and the impulse response $h(n)$:

$$y(n) = \sum_{m=0}^{n} x(m)h(n-m) = \sum_{m=0}^{n} x(n-m)h(m) \tag{1.61}$$

where $x(n) = 0$ for $n < 0$.

As can be seen from equation (1.61), to form the output signal $y(n)$ it is necessary to undertake the following mathematical operations: summation (subtraction), multiplication and delay. It means that with a digital device that can perform these

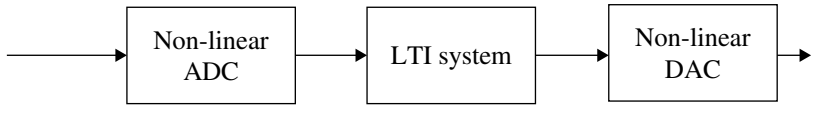

Figure 1.10 Block diagram of a digital system

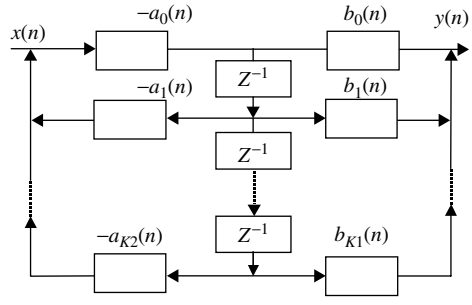

Figure 1.11 Block diagram of DF

operations, we can build a DLS and, in particular, a digital filter. In the following discussions, DLSs and DFs will be considered as equivalent systems. A block structure of a general DLS–DF is shown in Fig. 1.11.

In Fig. 1.11, the unit delay is represented by its system function z^{-1}. Note that the time delay by interval iT corresponds to the operator z^{-iT} in z-domain. By analogy with time domain, where $x(nT) \equiv x(n)$, we can denote delay as $z^{-iT} \equiv z^{-i}$. The variables a_i and b_i depict multiplication of a sequence by a constant coefficient. An input–output relation in a DLS is

$$y(n) = \sum_{i=0}^{M} b_i x(n-i) + \sum_{i=0}^{N} a_i y(n-i) \tag{1.62}$$

which is a linear difference equation.

There are many methods for the solution of difference and differential equations. For analysis of DF, z-transform is widely used, since it converts a difference equation into an algebraic one, simplifying the system analysis [4]. Applying z-transform of both sides of equation (1.62) and using its linearity property, we obtain

$$y(z) = x(z) \sum_{i=0}^{M} b_i z^{-i} + y(z) \sum_{i=0}^{N} a_i z^{-i} \tag{1.63}$$

Then,

$$y(z) = x(z) \frac{\sum_{i=0}^{M} b_i z^{-i}}{1 - \sum_{i=0}^{N} a_i z^{-i}} \tag{1.64}$$

Consider, as an example, a system described by equation (1.63) for a step input signal (Fig. 1.4) for $M = 0$ and $N = 1$, that is, a pure recursive DLS of the first order:

$$y(n) = x(n) + ay(n-1) \tag{1.65}$$

Then,

$$y(z) = \frac{x(z)}{1 - az^{-i}} = \frac{x(z)z}{z - a} \tag{1.66}$$

Taking into account that input signal $x_s(n)$ has a z-transform (1.49), $x_s(z) = \frac{z}{z-1}$, we obtain

$$y(z) = \frac{z^2}{(z - a)(z - 1)} \tag{1.67}$$

To evaluate the output sequence in time domain, it is necessary to find an inverse z-transform of the function (1.67). It is determined as a sum of residues for function $f(z) = y(z)z^{n-1}$ or

$$f(z) = \frac{z^{n+1}}{(z - a)(z - 1)} \tag{1.68}$$

This function has primary poles at the points $z_1 = 1$ and $z_2 = a$. The sum of residues of this function and, consequently, the output signal in time domain is

$$\begin{aligned} y(n) &= \sum_{i=1}^{2} \text{res}_i = \frac{P(z_1)}{Q'(z_1)} + \frac{P(z_2)}{Q'(z_2)} = \frac{z^{n+1}}{2z - a - 1}\bigg|_{z=z_1} + \frac{z^{n+1}}{2z - a - 1}\bigg|_{z=z_2} \\ &= \frac{1}{1 - a} + \frac{a^{n+1}}{a - 1} = \frac{1 - a^{n+1}}{1 - a} \end{aligned} \tag{1.69}$$

It is obvious that the output signal $y(n)$ can be found from discrete convolution (1.61). An impulse response of the system is

$$h(n) = a^n \tag{1.70}$$

Then,

$$y(n) = \sum_{m=0}^{n} x(n - m)h(m) = \sum_{m=0}^{n} a^m \tag{1.71}$$

Thus, the output signal is described by the geometric progression and after the sum evaluation, we obtain

$$y(n) = \frac{1 - a^{n+1}}{1 - a} \tag{1.72}$$

which coincides with equation (1.69).

In this example, we considered a primitive DLS, where analytical determination of the output signal using equation (1.71) was simple. In the general case, it is more convenient to use z-transform to determine $y(n)$.

1.3.2 DLS Representation via Transfer Function

A system transfer function is determined as

$$H(z) = \frac{Y(z)}{X(z)} \tag{1.73}$$

and, like the frequency response, fully describes a DLS. Equation (1.64) can be rearranged

$$H(z) = \frac{\sum_{i=0}^{M} b_i z^{-i}}{1 - \sum_{i=1}^{N} a_i z^{-i}} \tag{1.74}$$

DLSs with $N \geq 1$ are called *recursive filters* or *filters with infinite impulse response* (IIR). Value N, equal to the number of delay elements in the filter, is called the *order of the filter*.

In contrast, if all $a_i = 0$, then the filters are called *transversal filters* or *filters with finite impulse response* (FIR). The impulse responses of such filters can be simply evaluated by

$$\begin{cases} h(m) = b_m & m \leq M \\ h(m) = 0 & m > M \end{cases} \tag{1.75}$$

Although the classification of the FIR and IIR filters considered here is broad, it is possible to find systems with $N \geq 1$, but with a finite length of the impulse response. These are particular cases, but we consider one of them as an example.

Let us determine the impulse response of the system shown in Fig. 1.12 if $b = -a^k$ and k is a positive integer.

To evaluate the impulse response, assume that there is a unit impulse at the system input at the time equal to zero. The system response on this signal is $y(0) = 1$. For the time moments $0 < n < k - 1$, the impulse response is determined by the expression $h(n) = a^n, n \leq k - 1$. However, at time k there is a signal with value $-a^k$ at the summator input. Consequently, at the summator output, the signal is $y(k) = 0$. Thus,

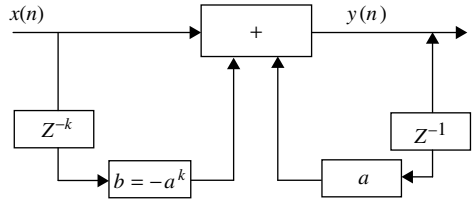

Figure 1.12 Recursive filter with finite impulse response

the impulse response of the system is

$$h(n) = \begin{cases} a^n, & 0 < n < k-1 \\ 0, & n \geq k \end{cases} \tag{1.76}$$

This example is a particular case, but it serves to warn the reader regarding the use of discussed determinations.

1.3.2.1 Canonic and Cascade Filters Structure

Equation (1.74) for the transfer functions can be expressed as

$$H(z) = \frac{1}{1 - \sum_{i=1}^{N} a_i z^{-i}} \sum_{i=0}^{N} b_i z^{-i} \tag{1.77}$$

For simplicity, assume that $M = N$. This approach does not reduce the generality of the presentation. It is always possible to make some coefficients a_i and b_i equal to zero. Equation (1.77) allows us to represent the filter as a serial connection of two sections, one of which is IIR, and the other, FIR:

$$H_R(z) = \frac{1}{1 - \sum_{i=1}^{N} a_i z^{-i}}$$

and

$$H_T(z) = \sum_{i=0}^{N} b_i z^{-i}$$

The structure of such a filter is shown in Fig. 1.13a. It shows that the signals are the same at the delay elements output in both sections. Consequently, the filter can be represented in another, so-called *canonical*, form (Fig. 1.13b).

For this purpose, we rewrite equation (1.74) as

$$H(z) = \frac{b_m}{a_n} \frac{\sum_{i=0}^{M} \frac{b_i}{b_m} z^{-i}}{\frac{1}{a_n} - \sum_{i=1}^{N} \frac{a_i}{a_n} z^{-i}} \tag{1.78}$$

or

$$H(z) = \frac{b_m}{a_n} \frac{\prod_{i=0}^{M} (z_i^{-1} - z_{iT})}{\prod_{i=1}^{N} (z_i^{-1} - z_{iR})} \tag{1.79}$$

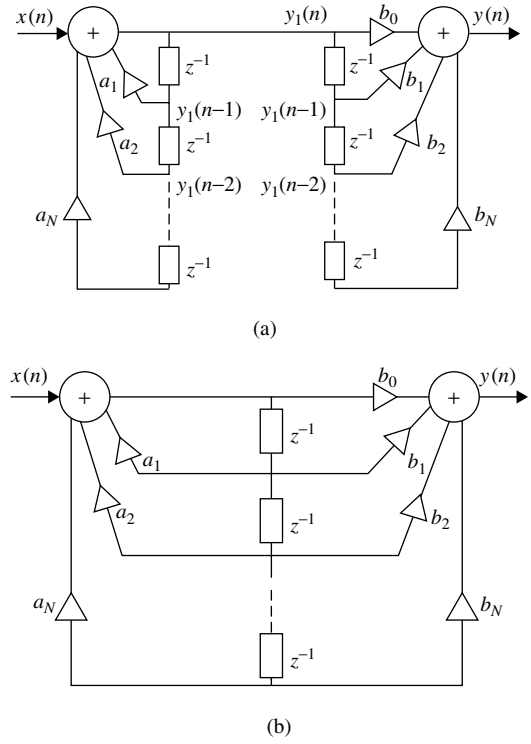

Figure 1.13 Filter transition into a canonical shape: (a) cascade connection of the filters and (b) canonic structure of the filter

where z_{iT} and z_{iR} are roots of polynomials in the nominator and denominator of equation (1.78) respectively.

In the general case, these roots can be real or complex. Note that if the roots are complex they are always complex conjugate.

1.4 STABILITY AND CAUSALITY OF DISCRETE SYSTEMS

In the previous sections, it was assumed that DLSs are causal and stable. However, it is known from the theory of differential equations that in the general case this is not obvious. In each case, the system has to be analysed from stability and causality perspectives.

A DLS is causal if its impulse response is equal to zero for the negative time values m. The meaning of this criterion is obvious: if a system is operating in real time, a signal cannot reach the system output earlier than it reaches its input. Formally, this rule is written as $h(m) = 0$ for $m < 0$.

Determination and criteria of stability are more complicated questions. From an engineering point of view, the best and most visual determination is the following [4]:

A DLS is called stable if the output signal of the system is limited for the limited input signal.

In the following chapters, problems of system stability will be studied in more detail. Here we will consider two criteria of stability:

1. A DLS is stable if the sum of all values of the impulse response is limited:

$$\sum_{m=0}^{\infty} |h(m)| < \infty \tag{1.80}$$

2. A DLS is stable if and only if all poles z_k of its transfer function at the z-plane are placed inside the unit circle with a centre at the origin of the coordinate system, that is,

$$|z_k| < 1 \tag{1.81}$$

1.5 FREQUENCY RESPONSE OF A DISCRETE LINEAR SYSTEM

Systems description via their frequency characteristics is the most popular method. In the general case, a complex frequency characteristic of a system can be determined in the following way. If there is a harmonic signal at the input of a linear system,

$$x_{\cos}(t) = \cos \omega_a t \tag{1.82}$$

then the output is

$$y_{\cos}(t) = A(\omega_a) \cos(\omega_a t + \psi(\omega_a)) \tag{1.83}$$

By analogy, for the sine signal,

$$x_{\sin}(t) = \sin \omega_a t \tag{1.84}$$

and the output signal is

$$y_{\sin}(t) = A(\omega_a) \sin(w_a t + \psi(\omega_a)) \tag{1.85}$$

Substituting the output signal as the sum

$$x_{\exp}(t) = x_{\cos}(\omega_a t) + \mathrm{j} x_{\sin}(\omega_a t) = \exp(\mathrm{j}\omega_a t) \tag{1.86}$$

the output response of the system is described as

$$y_{\exp}(t) = y_{\cos}(t) + \mathrm{j} y_{\sin}(t) = A(\omega_a) \exp \mathrm{j}(\omega_a t + \psi(\omega_a)) \tag{1.87}$$

Then the complex frequency response of the system is

$$\overline{H}(\omega_a) = \frac{y_{\mathrm{e}}(t)}{\exp(\mathrm{j}\omega_a t)} = A(\omega_a) \exp(\mathrm{j}\psi(\omega_a)) \tag{1.88}$$

Usually, $A(\omega_a)$ or $|\overline{H}(\omega_a)|$ is called an *amplitude–frequency response*, and $\psi(\omega_a)$ is called a *phase–frequency response*.

Obviously, knowing the impulse response of the system we can determine the signal at its output. If the input signal is a complex exponent, then

$$\begin{aligned} y_{\exp}(t) &= \int_0^t \exp \mathrm{j}\omega_a(t-x)h(x)\,\mathrm{d}x \\ &= \exp \mathrm{j}\omega_a t \int_0^t \exp(-\mathrm{j}\omega_a x)h(x)\,\mathrm{d}x \end{aligned} \tag{1.89}$$

Let us express $\overline{H}(\omega_a)$ through $h(t)$ of the same system:

$$\overline{H}(\omega_a) = \frac{y_{\mathrm{e}}(t)}{\exp \mathrm{j}\omega_a t} = \int_0^t h(x)\exp(-\mathrm{j}\omega_a x)\,\mathrm{d}x \tag{1.90}$$

Expression (1.90) is a Fourier transform of function $h(x)$.

By analogy with the complex frequency response of analog systems, we can find the frequency response of a DLS. In this case, the input signal is a discrete process, that is,

$$x(n) = \exp(\mathrm{j}n\omega_a T) \tag{1.91}$$

$$\overline{H}_d(\omega_a) = \frac{y(n\omega_a T)}{\exp \mathrm{j}n\omega_a T} \tag{1.92}$$

We determine the output signal $y(n\omega_a T)$ through convolution (equation (1.61)). The upper limit in this equation can be replaced by infinity as for $m > n$ all $h(n-m) = 0$ and $x(n-m) = 0$:

$$\begin{aligned} y(n\omega_a T) &= \sum_{m=0}^{\infty} \exp \mathrm{j}\omega_a(n-m)Th(m) \\ &= \exp \mathrm{j}\omega_a nT \sum_{m=0}^{\infty} h(m)\exp(-\mathrm{j}\omega_a mT) \end{aligned} \tag{1.93}$$

Equation (1.93) shows that the complex frequency response of a DLS is equal to the Fourier transform of its impulse response:

$$\overline{H}_d(\omega_a T) = \frac{y(n\omega_a T)}{\exp \mathrm{j}n\omega_a T} = \sum_{m=0}^{\infty} h(m)\exp(-\mathrm{j}\omega_a mT) \tag{1.94}$$

This coincides with the similar case for continuous systems.

1.5.1 Properties of the Frequency Response of a Discrete Linear System

1. The frequency response of a discrete system is a periodical function of discrete frequency $\omega_s = \frac{2\pi}{T}$.
2. If the impulse response of the system is a real function *h(mT)*, then for the amplitude–frequency characteristic,
3.

$$|H_d(\omega)| = |H_d(2\pi - \omega)| \tag{1.95}$$

and for the phase–frequency characteristic,

$$\psi_d(\omega) = -\psi_d(2\pi - \omega) \tag{1.96}$$

The properties described in (1.95) and (1.96) determine the main and considerable difference between frequency characteristics of analog and discrete linear systems.

Equations (1.95) and (1.96) show that for a full description of the DLS frequency characteristic it is sufficient to describe it at the frequency interval 0 to π of the normalized frequency ω. A sketch of DLS phase and frequency responses, which illustrates the properties described by (1.95) and (1.96), is shown in Fig. 1.14.

Note that a DLS impulse response can be evaluated from its frequency response via inverse Fourier transform:

$$h(n) = \frac{1}{2\pi} \int_{-\pi}^{\pi} \overline{H}_d(\omega) \exp(\mathrm{j}n\omega)\, \mathrm{d}\omega \tag{1.97}$$

Equation (1.97) contains the integral, as $\overline{H}_d(\omega)$ is a continuous function of its argument.

1.5.2 Transfer Function versus Frequency Response

As was indicated above, the most convenient analysis of a DLS is based on z-transform and the corresponding transfer function. At the same time, signals presentation and processing in frequency domain requires the use of the system's frequency

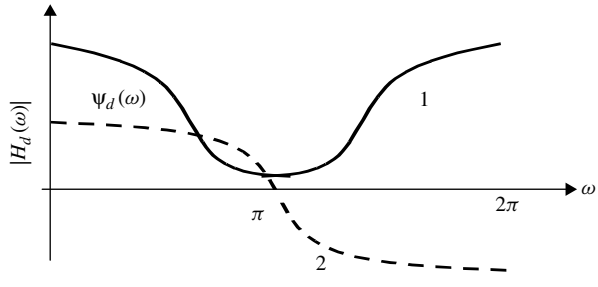

Figure 1.14 Amplitude–frequency (1) and phase–frequency (2) responses of a DLS

response. So, it is important to know the relationship between these two main characteristics. The DLS output value is

$$y(n) = \sum_{m=0}^{\infty} x(n-m)h(m) \tag{1.98}$$

Applying z-transform to the left and right parts of this expression we obtain

$$y(z) = \sum_{n=0}^{n=\infty} \sum_{m=0}^{m=\infty} x(n-m)h(m)z^{-n} \tag{1.99}$$

or

$$y(z) = \sum_{m=0}^{\infty} h(m) \sum_{n=0}^{\infty} x(n-m)z^{-n} \tag{1.100}$$

But, according to equation (1.45), the second sum is a delay operator, that is,

$$\sum_{n=0}^{\infty} x(n-m)z^{-n} = x(z)z^{-m} \tag{1.101}$$

and therefore

$$H(z) = \sum_{m=0}^{\infty} h(m)z^{-m} \tag{1.102}$$

Thus, the transfer function of the discrete system is equal to the z-transform of its impulse response. At the same time, the transfer function of a DLS can be represented by summing the residues of function $H(z)z^{m-1}$ at its poles (1.43):

$$h(m) = \sum_{k}^{m} \mathrm{res}_k(H(z)z^{m-1}) \tag{1.103}$$

To determine the relation between transfer function and frequency characteristics, we can use $H(z)$. It is not difficult to see that if the normalized frequency ω changes within the interval 0 to 2π, then variable z describes a unit circle and

$$z = \mathrm{e}^{\mathrm{j}\omega}, \quad |z| \leq 1 \tag{1.104}$$

Then,

$$H(z) = H_d(\exp \mathrm{j}\omega) = \sum_{m=0}^{\infty} h(m) \exp(-\mathrm{j}\omega m) \tag{1.105}$$

The right side of equation (1.105) is a complex frequency characteristic of the system represented by equation (1.94) and

$$\overline{H}(\omega) = H_d(\exp \mathrm{j}\omega) \tag{1.106}$$

So, equation (1.106) shows a simple way to evaluate a system frequency response via its transfer function.

1.6 CASE STUDY: LOW-ORDER FILTERS

As an example of application of the theory described above, consider DFs of the first and second order. These examples are useful for a study of the main text, since these circuits are used as the basis for more complex filter design. More detailed descriptions of these systems can be found in many books dedicated to DSP and, in particular, in [5].

1.6.1 Purely Recursive Filters

1.6.1.1 First-Order Filter

A block diagram of a first-order DF is shown in Fig. 1.15. This filter is described by the difference equation

$$y(n) = x(n) + ay(n-1) \tag{1.107}$$

An appropriate impulse response (Fig. 1.16), which is the filter reaction $y(n)$ to the unit input signal $x_i(n)$, is

$$y(n) = h(n) = \begin{cases} 0 & n < 0 \\ a^n & n \geq 0 \end{cases} \tag{1.108}$$

Hence, from equation (1.80), it follows that the system stability condition is $\sum_{n=0}^{\infty} |a|^n < \infty$. This is the sum of geometrical progression, which is limited if $|a| < 1$.

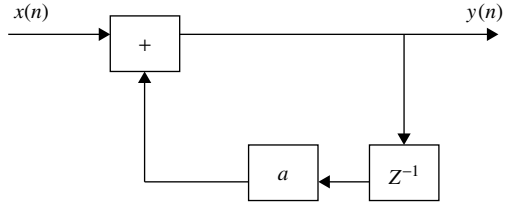

Figure 1.15 Recursive digital filter of the first order

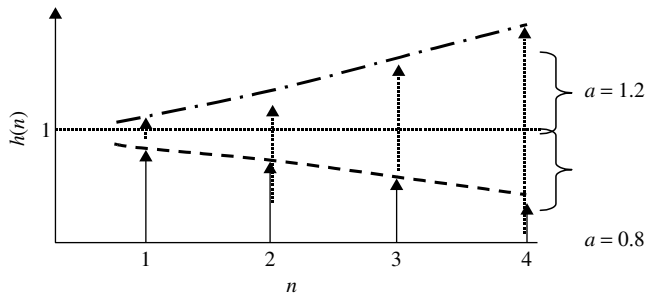

Figure 1.16 Impulse response of the first-order filter, with $a = 0.8$ (stable filter) and $a = 1.2$ (unstable filter)

The filter response on the unit step $x_s(n)$ input signal

$$x_s(n) = \begin{cases} 0 & n < 0 \\ 1 & n \geq 0 \end{cases} \tag{1.109}$$

is

$$y_s(n) = \begin{cases} 0 & n < 0 \\ (1 - a^{n+1})/(1 - a) & n \geq 0 \end{cases} \tag{1.110}$$

The graph of the function (1.110) is shown in Fig. 1.17.

By analogy with continuous systems, such as resistor–capacitor (RC) low-pass (LP) filters, we can introduce a time constant of the system, τ. The RC LP pulse response [4] is

$$h_{RC}(t) = \frac{1}{RC} \exp\left(-\frac{t}{RC}\right)$$

and the time constant is equal to RC, which specifies the time interval of the pulse response (magnitude changes in e times). This filter frequency response in the time

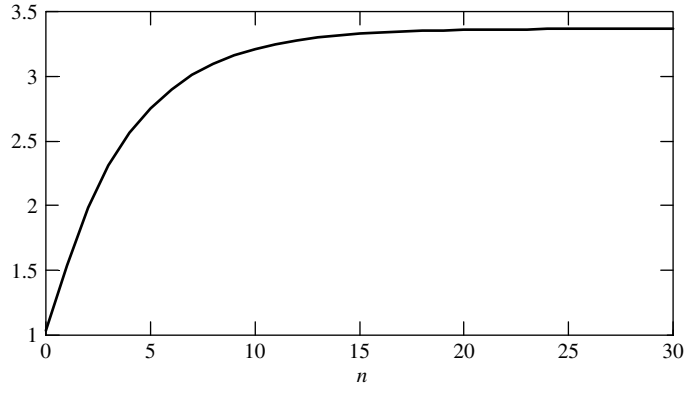

Figure 1.17 Response of the first-order filter with $a = 0.8$ to a unit step input signal

constant τ notation is

$$\overline{H}(\omega_a) = \frac{1/\tau}{\mathrm{j}\omega_a + 1/\tau}$$

In the case of DFs, this constant is normalized to the period of discretization:

$$\overline{\tau} = \tau / T \tag{1.111}$$

Then expression (1.110) can be presented as follows [4]:

$$y_s(n) = [1 - \mathrm{e}^{-(n+1)/\overline{\tau}}] \tag{1.112}$$

Consequently,

$$\mathrm{e}^{-1/\overline{\tau}} = a \tag{1.113}$$

for $a > 0$ and

$$\overline{\tau} = 1/\ln(1/a) \tag{1.114}$$

where ln is logarithm with base e. For narrowband LP DFs $a \to 1$, and it can be replaced by $a = 1 - \delta$, where $\delta \ll 1$. In this case, the normalized time constant of the DF is

$$\overline{\tau} \approx \delta^{-1} \tag{1.115}$$

Let us now study the filter reaction to harmonic signals. The sinusoidal steady-state response is the filter reaction to the complex exponential input signal $x(n) = \mathrm{e}^{\mathrm{j}n\omega}$. The signal at the output of the first-order filter is

$$y(n) = \frac{\mathrm{e}^{\mathrm{j}n\omega}}{1 - a\mathrm{e}^{-\mathrm{j}\omega}} - \frac{a^{n+1}\mathrm{e}^{-\mathrm{j}\omega}}{1 - a\mathrm{e}^{-\mathrm{j}\omega}} \tag{1.116}$$

Recalling that the stability criteria is $|a| < 1$, the steady-state ($n \to \infty$) output signal is

$$y(n) = \mathrm{e}^{\mathrm{j}n\omega}\frac{1}{1 - a\mathrm{e}^{-\mathrm{j}\omega}} \tag{1.117}$$

According to its definition, the frequency response is

$$H(\omega) = \frac{y(n)}{x(n)}$$

where $x(n)$ is a complex exponential function. Consequently, the frequency response of the first-order DF, from equation (1.117), is

$$H(\omega) = \frac{1}{1 - a\mathrm{e}^{-\mathrm{j}\omega}} \tag{1.118}$$

Amplitude- and phase–frequency responses of this system are

$$|H(\omega)| = 1/(1 - 2a\cos\omega + a^2)^{1/2} \tag{1.119}$$

and

$$\psi(\omega) = \tan^{-1}[a\sin\omega/(1 - a\cos\omega)] \tag{1.120}$$

Note that for small normalized frequencies $\omega \ll 2\pi$ and $\cos\omega \approx 1 - \frac{\omega^2}{2}$ and, thus, the amplitude–frequency characteristic of the first-order filter is

$$|H(\omega)| \approx \frac{1}{\left\{(1 - a^2)\left[1 + \dfrac{a}{(1-a)^2}\omega^2\right]\right\}^{1/2}} \tag{1.121}$$

Equation (1.121) coincides well with the frequency response of an *RC* LP filter [4]:

$$|H(\omega_a)|_{RC} = \frac{1}{(1 + R^2C^2\omega_a^2)^{1/2}} \tag{1.122}$$

Assuming that $T = 1$, we consider $\omega_a = \omega$, that is, analog and normalized frequencies are equal and we can easily compare these two functions. Figure 1.18 shows amplitude–frequency responses of the digital (curve 1) and analog (curve 2) filters for the condition that $\tau_{\mathrm{RC}} = \mathrm{RC}$ and $\overline{\tau} = 1/\ln(1/a)$ are approximately equal ($a = 0.7$ and $RC \approx 2.8$).

Analog RC LP filter gain is always 1 at DC ($\omega_a = 0$). The DF amplification gain at DC is also normalized to 1 by dividing equation (1.121) by

$$|H(0)|_{\mathrm{DC}} = \frac{1}{\sqrt{1 - a^2}}$$

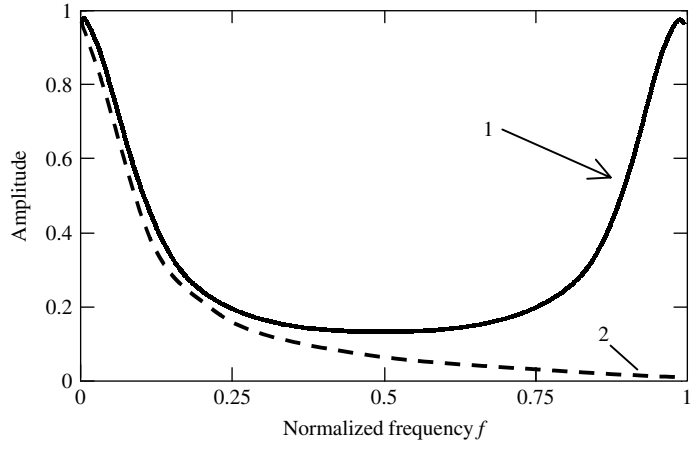

Figure 1.18 Frequency responses comparison

to equalize the filter amplitude responses:

$$|\overline{H}(\omega)| = \frac{1}{\left(1 + \dfrac{a}{(1-a)^2}\omega^2\right)^{1/2}} = \frac{1}{(1 - \delta^{-2}a\omega^2)^{1/2}} \tag{1.123}$$

Thus, when $a \to 1$, equations (1.122) and (1.123) tend to be equal to each other.

It is well known that frequency responses of first-order IIR filters and RC filters do not coincide when they have the same time constant. The general rule is if there is an analog prototype of the DF, then these two filters can have the same (with high accuracy) impulse responses or (!) frequency responses.

As indicated earlier, filters are characterized by their z-transfer function. Consider the following for a first-order DF. Let $Y(z)$ and $X(z)$ be z-transforms of the output and input signals respectively. Then,

$$Y(z) = X(z) + az^{-1}Y(z) \tag{1.124}$$

Thus, the z-transfer function is

$$H(z) = \frac{1}{(1 - az^{-1})} = \frac{z}{z - a} \tag{1.125}$$

The frequency response of this system can be found by substituting $z = \mathrm{e}^{\mathrm{j}\omega}$ (1.104) into (1.125):

$$H(\omega) = \frac{1}{1 - a\mathrm{e}^{-\mathrm{j}\omega}}$$

This equation coincides with equation (1.118).

1.6.1.2 Second-Order Filter

The second-order IIR filter is described by a difference equation:

$$y(n) = x(n) - a_1 y(n-1) - a_2 y(n-2) \tag{1.126}$$

In this expression, the signs of the coefficients have been reversed. Figure 1.19 shows a block diagram of this filter, which is referred to in literature as a pure recursive second-order filter.

The transfer function of this filter is

$$H(z) = \frac{1}{1 + a_1 z^{-1} + a_2 z^{-2}} = \frac{z^2}{z^2 + a_1 z + a_2} \tag{1.127}$$

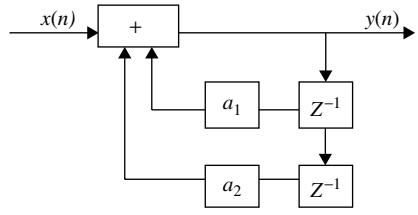

Figure 1.19 Second-order pure recursive digital filter

The denominator of function (1.127) is an equation of the second order. Consequently, in the general case it has complex-conjugate roots. Roots of the transfer function denominator are called *poles*. Then, pole values for the second-order filter are

$$p_{1,2} = -\frac{a_1}{2} \pm \frac{1}{2}\sqrt{a_1^2 - 4a_2} \tag{1.128}$$

Depending on coefficient values a_1, a_2, the poles p_1, p_2 can be either

$$\text{real } (a_1^2 \geq 4a_2) \text{ or complex } (a_1^2 < 4a_2)$$

In the first case, the filter of the second order is equivalent to the serial connection of first-order filters with real coefficients. The response of the filter on step function $x_s(n)$ is determined by the function

$$y_s(n) = \frac{1}{(1-a_1)(1-a_2)}\left[1 - a_2^{n+1} - (1-a_2)\frac{a_1^{n+1} - a_2^{n+1}}{a_1 - a_2}\right] \tag{1.129}$$

In the second case, there are two complex-conjugate poles: p and p^* with

$$p = -\frac{a_1}{2} + \mathrm{j}\frac{1}{2}\sqrt{(4a_2 - a_1^2)}$$
$$p^* = -\frac{a_1}{2} - \mathrm{j}\frac{1}{2}\sqrt{(4a_2 - a_1^2)} \tag{1.130}$$

Such a filter cannot be represented by a cascaded connection of first-order filters with real coefficients. A typical pulse response of such a filter is shown in Fig. 1.20.

The poles can be represented by polar coordinates using filter coefficients a_1 and a_2. Let

$$p = r\mathrm{e}^{\mathrm{j}\varphi} \tag{1.131}$$

Then,

$$r = a_2^{1/2} \quad \text{and} \quad \varphi = \cos^{-1}\left(-\frac{a_1}{2r}\right) = \cos^{-1}\left(-\frac{a_1}{2\sqrt{a_2}}\right)$$

or

$$a_1 = -2r\cos\varphi \quad \text{and} \quad a_2 = r^2 \tag{1.132}$$

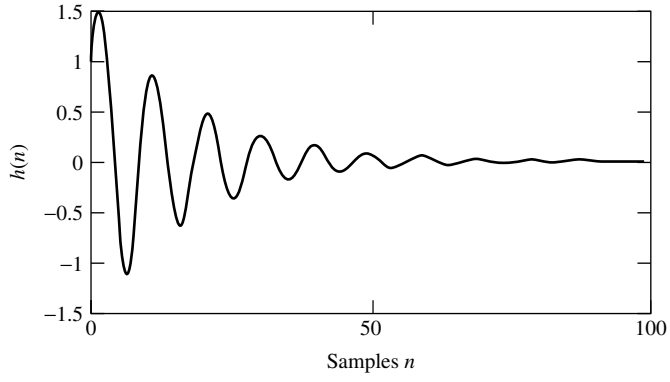

Figure 1.20 Impulse response for a second-order filter with complex poles

To evaluate the stability of the digital resonator we can use the second stability criterion, which stipulates that all poles of the transfer function should be within the unit circle $|z_k| < 1$. Introducing poles of the second-order filter via its coefficients a_1 and a_2, the criterion takes the following form:

$$\begin{aligned} 0 \le |a_2| &< 1 \\ |a_1| &\le 1 + a_2 \end{aligned} \tag{1.133}$$

A graphical interpretation of equation (1.133) is shown in Fig. 1.21. Only coefficients inside the triangle with vertex coordinates 2,1; −2, 1 and −1, −1 correspond to the stable second-order IIR digital filter.

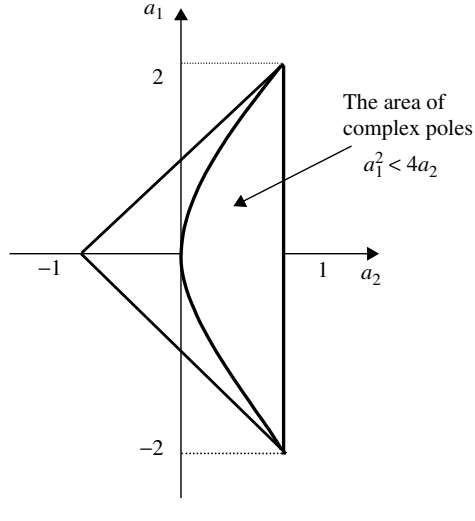

Figure 1.21 The stability area for a digital resonator

Changing z on ω in (1.127) by $e^{j\omega}$, we obtain the values of amplitude and phase characteristics of the second-order filter:

$$|H(\omega)| = [1 + a_1^2 + a_2^2 + 2a_1(1 + a_2)\cos\omega + 2a_2\cos 2\omega]^{-1/2} \tag{1.134}$$

and

$$\psi(\omega) = -\tan^{-1}\left[\frac{a_1\sin\omega + a_2\sin 2\omega}{1 + a_1\cos\omega + a_2\cos 2\omega}\right] \tag{1.135}$$

Combining equations (1.132), (1.134) and (1.135), we can obtain a more visual description of the frequency and phase characteristics of the filter:

$$|H(\omega)| = \left\{[1 + r^2 - 2r\cos(\varphi - \omega)][1 + r^2 - 2r\cos(\varphi + \omega)]\right\}^{-1/2} \tag{1.136}$$

and

$$\psi(\omega) = \tan^{-1}\left[\frac{r\sin(\varphi + \omega)}{1 - r\cos(\varphi + \omega)}\right] - \tan^{-1}\left[\frac{r\sin(\varphi - \omega)}{1 - r\cos(\varphi - \omega)}\right] \tag{1.137}$$

Analysis of the first-order system showed that in some instances, it is a digital equivalent of the RC filter. Appropriate similarities can also be found between recursive DFs of the second order (digital resonators) and resistor–inductance–capacitance (RLC) analog filters (resonators). In their frequency responses there are clear maximums or minimums. The extremes can be found by differentiating equation (1.136) by ω and evaluating frequency where the derivative is equal to 0:

$$\mathrm{d}|\overline{H}(\omega)|/\mathrm{d}\omega = \sin\omega[a_1(1 + a_2) + 4a_2\cos\omega] = 0 \tag{1.138}$$

Taking into account that ω is a normalized frequency $\omega = \omega_a T$, equation (1.138) is equal to 0 when $\omega = 0$ or $\omega = 0.5$. Another extreme can be found when the second factor in equation (1.138) is equal to 0. This is possible when

$$\left|\frac{a_1(1 + a_2)}{4a_2}\right| = 1 \tag{1.139}$$

Using polar coordinates, this corresponds to

$$\cos\varphi = \frac{2r}{1 + r^2}$$

Finally, in the coefficients domain,

$$\cos\omega_R = -\frac{a_1(1 + a_2)}{4a_2} \tag{1.140}$$

$$\omega_R = \cos^{-1}\left[-\frac{a_1(1 + a_2)}{4a_2}\right]$$

where ω_R is called the *resonance frequency*, similar to the case of analog filters. Note that in parallel RLC contours, the resonance appears at frequency

$$\omega_R = \sqrt{\frac{1}{LC} - \frac{1}{4C^2R^2}}$$

Another important characteristic of digital resonators is amplification at the resonance frequency. The system gain can be found by combining equations (1.136) and (1.140):

$$H_R = \frac{1}{1 - a_2}\left(\frac{4a_2}{4a_2 - a_1^2}\right)^{1/2} \tag{1.141}$$

Using polar coordinates,

$$H_R = \frac{1}{1 - r}\left(\frac{1}{(1 + r)\sin\varphi}\right) \tag{1.142}$$

Another useful characteristic of filters is their bandwidth. As a rule, the bandwidth of low-order filters is determined at an attenuated level -3 dB relevant to the maximum of the frequency response:

$$\Delta\omega = \omega_2 - \omega_1 \tag{1.143}$$

where

$$|H(\omega_1)|^2 = |H(\omega_2)|^2 = |H(\omega_R)|^2/2$$

Assuming that the filter is narrowband ($r \sim 1$) we can show that [5]

$$\Delta\omega \cong 2(1 - r) \cong 2(1 - \sqrt{a_2}) \tag{1.144}$$

Note that efficiency of the filter is a continually increasing function when $r \to 1$. Similar to equation (1.115) for narrowband digital resonators, the following simple formula can be used to evaluate the system bandwidth: $\Delta\omega \cong 2(1 - \sqrt{a_2}) = 2(1 - \sqrt{1 - \delta}) \approx \delta$.

Thus, equations (1.140) and (1.144) determine a resonance frequency and a bandwidth of the digital resonator. Figure 1.22 illustrates examples of amplitude–frequency responses of second-order filters for coefficient values a_1 and a_2.

If the frequency response of a filter is known, it is easy to evaluate its pulse response. For a digital resonator, the pulse response is [3]

$$h(n) = r^n \frac{\sin(n + 1)\varphi}{\sin\varphi} \tag{1.145}$$

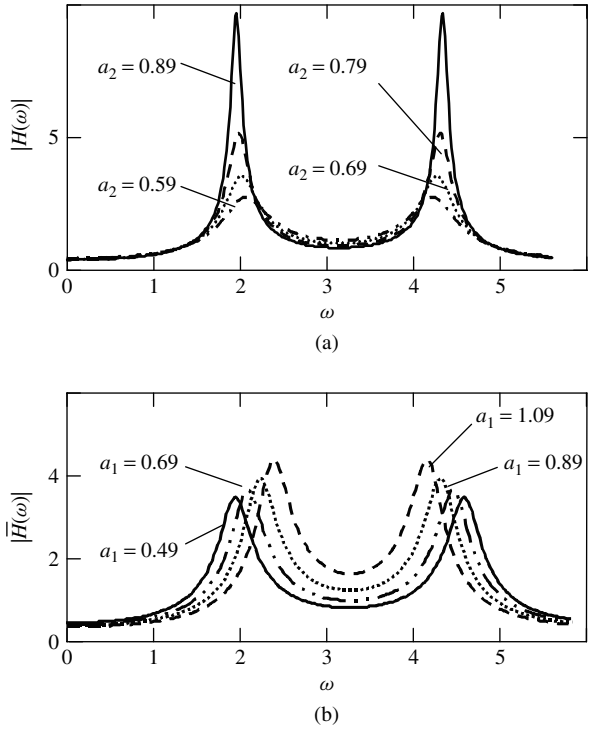

Figure 1.22 Frequency responses of a second-order filter: (a) $a_1 = 0.7$ and (b) $a_2 = 0.7$

In the general case, this corresponds to the exponentially dumped sinusoid, where r is the parameter responsible for the amplitude dumping. A normalized time constant can be defined in the following way, similar to equation (1.61):

$$\overline{\tau} = \frac{1}{\ln(1/r)} = \frac{1}{\ln(1/\sqrt{a_2})} \tag{1.146}$$

An example of the digital resonator impulse response for $r = 0.9$ and $\varphi = \pi/2$ is shown in Fig. 1.23.

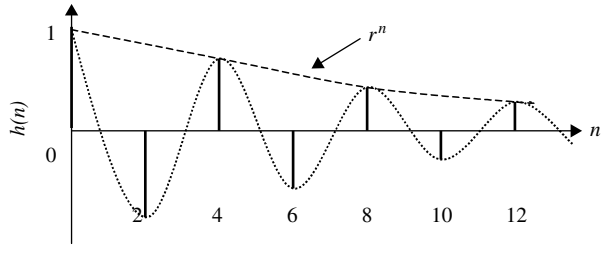

Figure 1.23 Impulse response of a digital resonator

1.6.2 Effects of Word Length Limitation

When analysing DFs, we assume that neither the coefficients' word length nor arithmetical operation processing are limited in bit number. In practice, the word length is always restricted, and investigation of the limits is an essential part of any DSP system design. Detailed analysis of this problem can be found in [1] and other sources. We will consider in brief here how the word length limitation affects parameters of digital resonators.

Restriction of the maximum bit number (L_b) in a filter's coefficients (a_1 and a_2 in this case) simply means that the coefficients can have only a limited number of discrete values. Hence, during filter design, poles can occupy only a fixed number of possible positions inside the unit circle. Consequently, we can approximate a desired frequency response with a finite accuracy that directly depends on coefficient word length.

In the relatively simple case of a digital resonator we can evaluate, for example, how the minimal filter bandwidth depends on the number of bits. Using equation (1.144) and replacing a_2 with the binary number closest to one that will be $1 - 2^{-L_b}$ we obtain the minimum resonator bandwidth:

$$\Delta\omega_{\min} = 2(1 - \sqrt{a_2}) = 2[1 - (1 - 2^{-L_b/2})] = 2^{1-L_b/2} \tag{1.147}$$

Thus, for $L_b = 8$, the minimal bandwidth is $\Delta\omega_{\min} = 0.125$ and for $L_b = 12$, the minimal bandwidth is $\Delta\omega_{\min} = 0.0312$.

For a narrowband filtering, it is important to have accurate resonance frequency adjustment. The displacement should be usually much less than the resonator bandwidth. This example clearly demonstrates that at least for a narrowband filtering, the word length is essential.

Another problem of the word length limitation follows from the rounding of arithmetical operation results to L_{ar} bits. A reasonably good approximation of the rounding noise is a process with uniform spectrum over the frequency interval $\omega = 0$ to π and power $\sigma_{RN}^2 = 2^{-2L_{ar}}/12$. In the general case, the output noise power depends on the system's frequency response. For a digital resonator, the output noise power can be evaluated through the filter noise bandwidth, which relates [6] to the -3 dB bandwidth like $\Delta\omega_{\text{noise}} \approx 1.2\Delta\omega_{-3\text{ dB}}$. Hence, the output rounding noise level for a filter with the unit gain in the first approximation is $\sigma_{RN}^2 \approx \dfrac{2^{-2L_{ar}}}{10\pi}\Delta\omega_{-3\text{ dB}}$.

1.6.3 Transversal and Combined Filters

A block diagram of a first-order FIR filter is shown in Fig. 1.24. This filter is described by the difference equation

$$y(n) = b_0 x(n) + b_1 x(n-1) \tag{1.148}$$

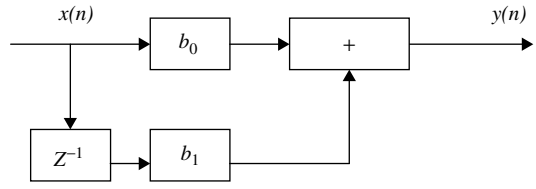

Figure 1.24 First-order FIR digital filter

An impulse response of this filter is just a pair of samples:

$$y(n) = h(n) = \begin{cases} 0 & n < 0 \\ b_0 & n = 1 \\ b_1 & n = 2 \\ 0 & n > 2 \end{cases} \tag{1.149}$$

and the filter response on the unit step input signal $x_s(n)$ is

$$y_s(n) = \begin{cases} 0 & n < 0 \\ b_0 & n = 1 \\ b_1 + b_2 & n \geq 2 \end{cases} \tag{1.150}$$

Another important test waveform is a harmonic signal. The sinusoidal steady-state response is the filter reaction on the input signal $x(n) = \mathrm{e}^{\mathrm{j}n\omega}$ and the filter output signal is

$$y(n) = b_0\mathrm{e}^{\mathrm{j}n\omega} + b_1\mathrm{e}^{\mathrm{j}(n-1)\omega} \tag{1.151}$$

According to its definition, the system frequency response is

$$\overline{H}(\omega) = \frac{y(n)}{\mathrm{e}^{in\omega}} = b_0 + b_1\mathrm{e}^{-\mathrm{j}\omega} \tag{1.152}$$

The magnitude and phase of this function are

$$|H(\omega)| = (b_0^2 + b_1^2 + 2b_0b_1\cos\omega)^{1/2} \tag{1.153}$$

and

$$\psi(\omega) = -\tan^{-1}\frac{b_0\sin\omega}{b_0 + b_1\cos\omega} \tag{1.154}$$

Examples of amplitude–frequency responses for different values b_1 when $b_0 = 1$ are shown in Fig. 1.25.

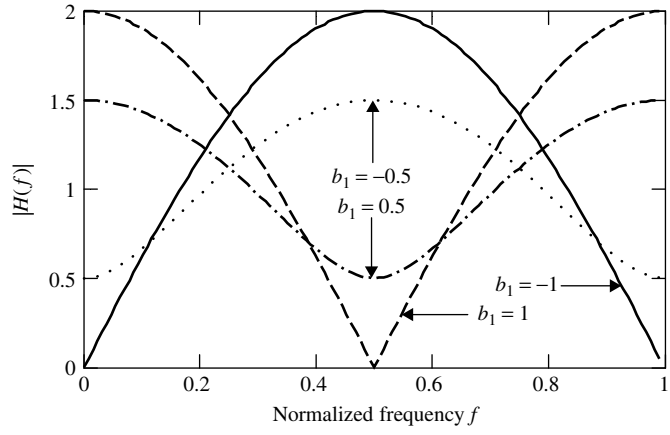

Figure 1.25 Amplitude–frequency response of a first-order transversal filter

Second-order FIR filters (see Fig. 1.26) can be considered in a way similar to that of first-order filters. The impulse response of a second-order filter is

$$h(n) = \begin{cases} 0 & n < 0 \\ b_0 & n = 1 \\ b_1 & n = 2 \\ b_2 & n = 3 \\ 0 & n > 3 \end{cases} \tag{1.155}$$

The frequency response is

$$\overline{H}(\omega) = b_0 + b_1 e^{-j\omega} + b_2 e^{-j2\omega} \tag{1.156}$$

From equation (1.156), both amplitude and phase–frequency responses can be calculated. As an example, let us consider the filter with the following coefficient values: $b_0 = b_2 = 1$ and $b_1 = -2$. The amplitude–frequency response of the filter is obtained by

$$|H(\omega)| = 2|\cos\omega - 1| \tag{1.157}$$

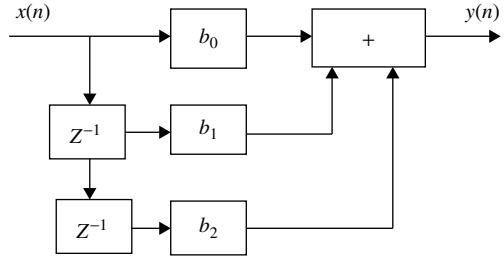

Figure 1.26 Block diagram of a second-order FIR filter

Then, for $b_0 = b_2 = 1, b_1 = -\sqrt{2}$, the frequency response is obtained by

$$|H(\omega)| = 2\left|\cos\omega - \frac{1}{\sqrt{2}}\right| \tag{1.158}$$

The appropriate functions are shown in Fig. 1.27 by curves 1 and 2 respectively.

FIR and IIR filters can be combined to form more complex filtering systems. The typical cascade realization of a combined filter assumes common delays (shift registers) in their structure (Fig. 1.28) and frequency responses of the combined filter are a product of the frequency responses of each of the constitutive filters.

For illustration purposes, Fig. 1.29 shows frequency responses of an FIR filter with $b_0 = b_2 = 1, b_1 = -2$ (curve 1), an IIR filter with $a_1 = 0.22, a_2 = 0.44$ (curve 2) and the frequency response of the cascade filter (curve 3).

It is important to note that in the literature, filters without a recursive part are usually referred to as transversal or FIR filters, and filters with both recursive and transversal parts are referred to as recursive or IIR. In the case when for some reason it is important to highlight that filters do not have transversal parts, these filters are usually referred to as purely recursive filters.

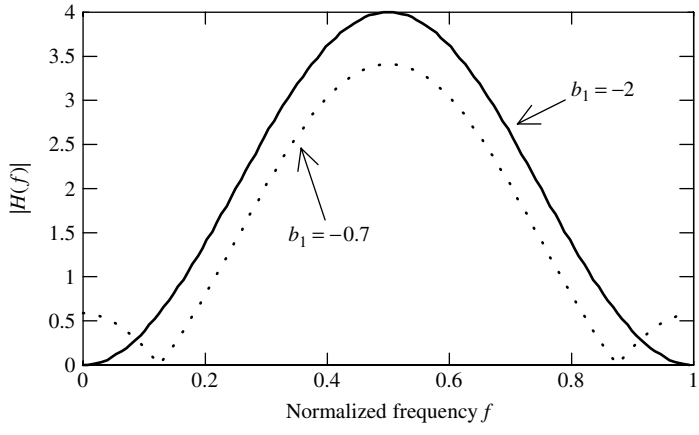

Figure 1.27 Amplitude–frequency response of a second-order transversal filter

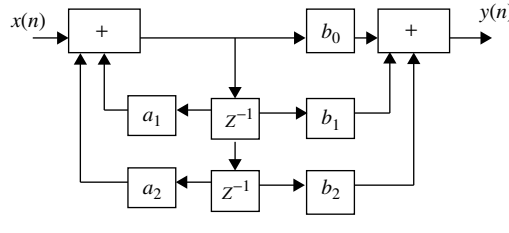

Figure 1.28 Cascade realization of the combined FIR-IIR filters

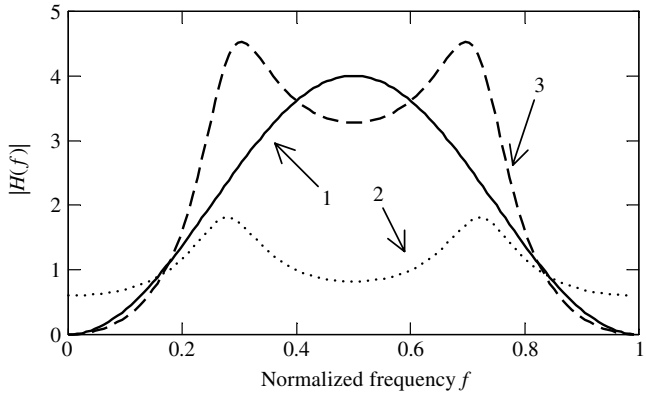

Figure 1.29 Amplitude–frequency response of the combined FIR–IIR filters

1.7 SUMMARY

In this chapter, we have developed the major parameters and characteristics of discrete signals and systems and explored their relations with continuous (analog) signals and systems. The first important issue is that analog signals can be converted into a digital domain without information losses. This requires time discretization of an analog waveform with the sampling frequency chosen according to the Nyquist theorem with further amplitude quantization via analog–digital converters. Perhaps the major difference between continuous and discrete signals is their spectrums. After analog waveform sampling, its spectrum becomes periodical with the sampling frequency period.

Like continuous signals and systems, their discrete counterparts can be described in frequency domain using the DFT, which is a modification of the Fourier transform. In many situations, it is convenient to analyse continuous systems using Laplace space. This approach is also applicable for discrete systems, but it is more convenient to use the discrete Laplace and z-transforms.

Linear time-invariant systems are the core of signal filtering algorithms. Discrete linear systems can be fully described by appropriate difference equations or their integral characteristics: impulse response in the time domain, and frequency response and transfer function in the frequency and z-domain respectively. Applying the Laplace or z-transforms, difference equations can be converted into algebraic equations, a convenient way to evaluate a system's transfer function and, eventually, all system characteristics. There is a strong similarity between digital and analog filters and, again, the core difference is that the frequency response of a DF is periodical with sampling frequency function.

A few of the problems of DSP were discussed in this introductory chapter. The topic selection follows from the chapter goal of supplying readers with knowledge essential to understand the main text. This chapter can also be viewed as a general introduction to discrete signals and systems in a wider sense than the declared goal.

1.8 ABBREVIATIONS

ADC	analog–digital converter
DF	digital filter
DC	direct current
DAC	digital–analog converter
DFT	discrete Fourier transform
DLS	discrete linear system
DSP	digital signal processing
FIR	finite impulse response
IDFT	inverse discrete Fourier transform
IIR	infinite impulse response
ILT	Inverse Laplace transform
LP	low-pass (filter)
LT	Laplace transform
RC	resistor–capacitor (filter)
RLC	resistor-inductance-capacitance (filter)

1.9 VARIABLES

$\overline{V}(\omega_a)$	spectrum of δ-function
$\lvert\overline{X}_d(\omega_a)\rvert$	amplitude spectrum of a discrete signal
$\overline{H}(\omega_a)$	complex frequency characteristic (response) of continuous system
$\theta_d(\omega_a)$	phase spectrum of discrete signal
$\overline{(\bullet)}$	complex value
$\overline{(\bullet)}^*$	complex-conjugate value
σ_{qn}^2	power of quantization noise
$A(\omega_a)$	amplitude frequency response of analog system
$H(\omega)$	system frequency response
$\delta(t)$	delta function
$\lvert H_d(\omega)\rvert$	amplitude frequency characteristic of discrete system
$\overline{H}_d(\omega_a)$	complex frequency characteristic (response) of a discrete system
$\overline{X}_d(\omega_a)$	spectrum of discrete signal
$\overline{V}_\tau(\omega_a)$	spectrum of pulse sampling function
$\overline{\tau}$	normalized time constant
σ_s	standard deviation of an input signal
$\psi(\omega_a)$	phase–frequency response
Δ	quantization level
$\overline{S}(\omega_a)$	complex spectrum of a signal
$\overline{X}(k\Omega)$	complex spectrum of periodic signal
φ	angle in polar coordinates
τ	time constant

ω	normalized frequency
Ω	main frequency of periodical signal spectrum [rad/s]
$\Delta\omega$	normalized frequency band
$\delta(n,k)$	unit sample sequence
ω_a	absolute frequency [rad/s]
ω_R	resonance frequency [rad/s]
ω_s	sampling frequency [rad/s]
a_i	coefficients of recursive filter
b_i	coefficients of transversal filter
B_{its}	number of bits in signal binary presentation
C	capacitor
$f_{o\max}$	the highest frequency in an analog signal spectrum [Hz]
f_s	sampling frequency [Hz]
$H(m)$	impulse response of a discrete system
$H(t)$	impulse response of a continuous system
$H(z)$	transfer function
$H_R(z)$	transfer function of the recursive part of a digital filter
$h_{RC}(t)$	pulse response of RC filter
$H_T(z)$	transfer function of the transverse part of a digital filter
L	inductance
$L(p)$	Laplace transform
p_i	pole of function
r	radius in polar coordinates
R	resistor
res_m	function residue
S/N_{qn}	signal-to-quantization noise ratio
T	sampling period
T_0	signal period
$v_\tau(t)$	periodical sequence of impulses with amplitude 1 and duration τ
$v(t)$	periodical sequence of δ functions
$X(\omega)$	spectrum of the discrete input signal of the normalized frequency
$x(n)$	input discrete signal
$x_d(n)$	discrete signal
$x_d(t)$	discrete signal in continuous time
$x_i(n)$	discrete pulse signal
$x_s(n)$	discrete unit step
$y(n)$	output discrete signal

1.10 REFERENCES

[1] Ifeachor EC, Jervis BW (2002) *Digital Signal Processing: A Practical Approach*, UK: Prentice Hall.

[2] Oppenheim AV (1989) *Discrete-Time Signal Processing*, New Jersey: Prentice Hall.

[3] Hsu HP (1995) *Signals and Systems*, New York: McGraw-Hill.
[4] Haykin S, Van Veen B (1999) *Signals and Systems*, New York: John Wiley & Sons.
[5] Bellanger M (1989) *Digital Processing of Signals: Theory and Practice*, New York: John Wiley & Sons.
[6] Couch II LW (1997) *Digital and Analog Communication Systems*, London: Prentice Hill.

Part One

Linear Discrete Time-Variant Systems

2

Main Characteristics of Time-Variant Systems

Traditionally, scientists and engineers have been very familiar with two types of discrete systems. The first broad group consists of linear, time-invariant systems with algorithms closely related to those used for digital filtering. The parameters for these filters do not depend on time and are specified beforehand according to various criteria. The second broad group consists of adaptive systems, whose parameters change with time, reflecting changes in input processes that cannot be fully predicted. In this book, we will consider another group of linear systems whose parameters vary with time according to previously specified laws; in other words, linear time-variant (LTV) non-adaptive systems, or time-varying systems.

These time-variant systems can be defined as follows: systems are time-variant if a time delay or time advance of the input signal leads not only to an appropriate time shift in the output signal but also to changes in other parameters of the output signals. This difference between linear time-invariant (LTI) and linear time-variant (LTV) systems is illustrated in Fig. 2.1.

Different methods for describing linear time-variant discrete systems (LTV DSs) and linear time-variant digital filters (LTV DFs) have been reported in the periodical literature, including [1–19], where the most important characteristics and relationships have been defined. These published results are systematized in this chapter in order to standardize the account of LTV systems. The aim is to present calculations and results for LTV systems in a way that is as consistent as possible with those used for linear time-invariant discrete systems (LTI DSs). Some analytical approaches to discrete systems analysis will be presented in this chapter by analogy with the theory of continuous time-invariant systems [20–26].

At this stage, we assume that amplitude quantization as well as word length limitations do not affect the major systems' parameters and that systems may not possess filtering properties. Hence, the general subject of our analysis is time-variant linear discrete systems. The notion of a "filter" will be used in the following chapters only where the LTV DS is considered as a filtering system. Similarly, the notion of

An Introduction to Parametric Digital Filters and Oscillators Mikhail Cherniakov
© 2003 John Wiley & Sons, Ltd ISBN: 0-470-85104-X

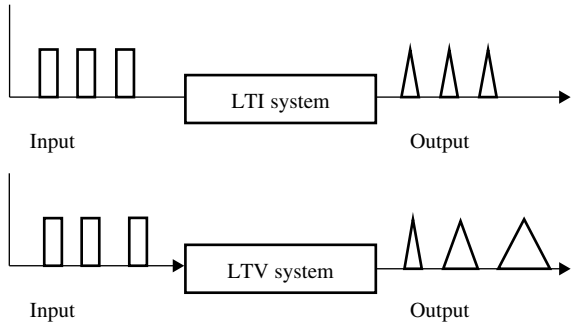

Figure 2.1 Waveforms at the input and output of LTI and LTV systems

a "digital" system or filter will be used only in those cases where quantized input signals and/or limited word lengths are specifically considered.

In summary, this chapter describes the definitions, analysis and other generic aspects of LTV DSs, which provide the basis for the next chapters.

2.1 DESCRIPTION OF A LINEAR TIME-VARIANT DISCRETE SYSTEM THROUGH DIFFERENCE EQUATIONS

An LTV DS can be described by a difference equation with time-varying coefficients:

$$\sum_{k=0}^{K_1} a_k(n) \cdot y(n-k) = \sum_{k=0}^{K_2} b_k(n) \cdot x(n-k) \tag{2.1}$$

where $x(n)$ and $y(n)$ are input and output signals respectively; $n = 0, 1, \ldots$ corresponds to the time instant nT, where T is the clock or sampling period; and $a_k(n)$ and $b_k(n)$ are time-varying coefficients and $a_0(n) \neq 0$ for any n [5, 8]. Coefficients $a_k(n)$ correspond to a recursive part of the system, and $b_k(n)$ correspond to a non-recursive (transversal) part of the system. For $K_1 > 0$, a system is called a *recursive* or *infinite impulse response* (IIR) *system* of the K_1 order, whereas for $K_1 = 0$, it is called a *non-recursive* or *finite impulse response* (FIR) *system*. So, in terms of the description, the major difference between LTI and LTV systems is in the time dependence of coefficients $a_k(n)$ and $b_k(n)$. The convenience of using difference equations follows from the transparency of the physical processes occurring in the system. The processes directly reflect the structure and the sequence of mathematical operations within the system.

Another popular method of describing LTV systems is based on state–space equations. For example, in [4, 12, 27, 28], methods employing state–space equations are used to describe LTV DSs where equation (2.1) is presented in matrix form. This makes it possible to investigate multi-variable systems and to use well-developed

mathematical matrix theory. Although we primarily apply the direct difference equation method of describing LTI systems here, the state–space method will be used later in the book for stability analysis.

Similar to the case of continuous time-varying systems, there is no general analytical solution of the difference equation (2.1) for arbitrary coefficients and system order. If the coefficients are given and an input signal $x(n)$ is known, it is possible to calculate an output signal $y(n)$ directly using the difference equation. In this case, equation (2.1) is simply used as a computer algorithm. This approach is useful in many situations but has some limitations: as it is necessary to know initial conditions, this restricts the use of the method to causal systems, and computational problems can arise when determining steady-state output signals ($n \to \infty$) that require infinitely long calculations. In spite of these limitations, the direct method of LTV systems analysis will be widely used in this book to verify analytical calculations and where no other methods can be applied.

For time-invariant systems, the most spread have linear transform (Laplace and z-transform) applications that convert differential and difference equations into algebraic equations. Using these transforms, it becomes reasonably easy to evaluate the integral system characteristics (transfer functions, frequency and pulse responses, etc.). However, it is impossible to find a suitable universal transform for time-varying systems. Such transforms have been found only for some classes of LTV DSs and, importantly, these transforms were not universal.

From the practical point of view, the most convenient approach for time-variant systems analysis is to find those integral system characteristics that do not depend on the input signal, but allow determination of output signals for known input signals. This is the major approach in time-invariant systems analysis, and the characteristics that are independent of the input signal are the impulse response and transfer function, definitions of which are given below.

2.2 IMPULSE RESPONSE

The impulse response (IR), denoted in the literature by $h(.)$, also known as *Green's function*, describes an LTV DS in the time domain. According to the definition, an IR of linear systems is the output signal measured at time moment nT in response to a unit impulse applied at time mT (m and n are integers). The unit impulse is defined thus:

$$\delta(n-m) = \begin{cases} 1 & \text{for } n = m \\ 0 & \text{for } n \neq m \end{cases} \tag{2.2}$$

The IR can be found as a solution of equation (2.1) when the input is the unit sample sequence $x(n) = \delta(n-m)$:

$$y(n) = \frac{1}{a_0(n)} \left[-\sum_{k=1}^{K_1} a_k(n) y(n-k) + \sum_{k=0}^{K_2} b_k(n) \delta(n-k-m) \right] \tag{2.3}$$

and

$$h(m,n)=\frac{1}{a_0(n)}\left[-\sum_{k=1}^{K_1}a_k(n)\cdot h(m,n-k)+\sum_{k=0}^{K_2}b_k(n)\cdot\delta(n-k-m)\right] \tag{2.4}$$

So, unlike LTI systems, the output response of the LTV system depends on the moment of the observation as well as the moment of input signal application. Therefore, in a time-variant discrete system the IR $h(m,n)$ is a function of the two time variables or time instants mT and nT.

For the known IR, a signal at the output of a time-variant DS is determined as a convolution of the IR and input sequences $x(n)$:

$$y(n)=\sum_{m=-\infty}^{\infty}x(m)\cdot h(m,n) \tag{2.5}$$

$$y(n)=\sum_{l=-\infty}^{\infty}x(n-l)\cdot h(n-l,n) \tag{2.6}$$

The latter is obtained by substitution of $n-m=l$.

The causality of LTV DSs, which means that output signals cannot appear before the input signal is applied, imposes the next limitations on the IR:

$$h(m,n)=0 \text{ for } n<0 \text{ and } m>n \tag{2.7}$$

Taking into account these limitations, we can restrict the lower limit in (2.5) to

$$y(n)=\sum_{m=0}^{\infty}x(m)\cdot h(m,n), \tag{2.8}$$

$$y(n)=\sum_{l=0}^{n}x(n-l)\cdot h(n-l,n) \tag{2.9}$$

Similar to (2.1), equations (2.3) and (2.8) do not have a solution in a closed analytical form for an arbitrary system order and coefficient values. To analyse a particular case, it is necessary to impose some restrictions or simplifications. Thus, for FIR systems, along both time coordinates nT and mT, all values of $h(m,n)$ can be directly calculated from equation (2.4). We cannot follow the same procedure in the case of systems with an IIR where there is the problem of an unlimited number of calculations. However, later we will consider systems with periodically time-varying coefficients, in which case the IR is an infinite, but periodical, function. Consequently, the IR can be calculated over a period that requires finite calculations even in the case of IIR systems.

For systems with non-recursive and recursive parts, IR calculations can be slightly simplified by first finding an IR$-g(m, n)$ – for the recursive part and, then, as shown in [5], the system impulse response will be

$$h(m, n) = \sum_{k=0}^{K_2} b_k(m + k) \cdot g(m + k, n) \tag{2.10}$$

The simplicity of equation (2.10) shows that the most complicated task is to find the IR for the recursive part of the system. One of the possible ways of solving this problem will be discussed later in detail.

Thus, in contrast to LTI systems, the IR of LTV DSs is a function of two-argument. For a better understanding of the IR of time-varying systems, let us consider the following example.

Example 2.1: Impulse Response of a Non-Recursive LTV System

Consider a system described by a third-order difference equation:

$$y(n) = \sum_{k=0}^{2} b_k(n)x(n - k) \tag{2.11}$$

The system reaction to the unit pulse $\delta(n - m)$ is the IR, and for $b_k(n) = k^{-n}$

$$h(m, n) = \sum_{k=0}^{2} k^{-n}\delta(n - k - m) \tag{2.12}$$

The calculated results for equation (2.12) are shown in Table 2.1.

Table 2.1 Impulse response of a non-recursive LTV system

n \ m	0	1	2	3	4	5
0	0	0	0	0	0	0
1	1	0	0	0	0	0
2	1/4	1	0	0	0	0
3	0	1/8	1	0	0	0
4	0	0	1/16	1	0	0
5	0	0	0	1/32	1	0
6	0	0	0	0	1/64	1
7	0	0	0	0	0	1/128

The system block diagram is shown in Fig. 2.2.

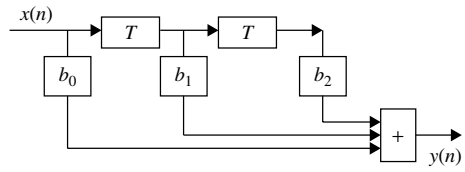

Figure 2.2 Non-recursive system

The results in Table 2.1 clearly show that the system IR depends on the time moment m of unit pulse application to the system input. A fragment of this IR is shown in Fig. 2.3

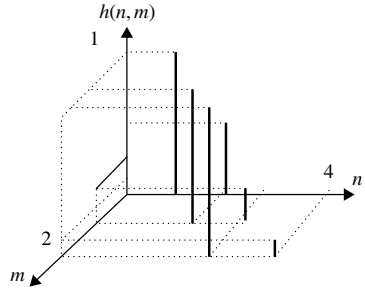

Figure 2.3 Impulse response of an LTV system

Of course, it is not an easy task to imagine this three-dimensional picture for the general case, but in terms of mathematical notation, this IR is similar to those used in descriptions of time-invariant systems.

2.3 GENERALIZED TRANSFER FUNCTION

As for LTI systems, in many cases it is more convenient to analyse LTV systems in the frequency domain. This can be achieved by describing them through the transfer function and frequency response.

The transfer function of time-varying systems binds an output and input signal in the z-domain:

$$Y(z, n) = X(z) \cdot H(z, n) \tag{2.13}$$

where $X(z) = \sum_{m=-\infty}^{m=\infty} x(m) \cdot z^{-m}$ is the z-transform of the input signal $x(m)$ and

$$H(z, n) = \sum_{m=-\infty}^{\infty} h(m, n) \cdot z^{m-n} \tag{2.14}$$

or

$$H(z, n) = \sum_{l=-\infty}^{\infty} h(n-l, n) \cdot z^{-l} \tag{2.15}$$

The transfer function of the LTV DS, unlike that of the LTI DS, depends on time, and is called a *generalized transfer function* (GTF). The definition of this GTF was first introduced in [1] for continuous parametric systems.

For causal systems, GTF is determined only for $n \geq 0$ and, taking into account equation (2.5), is

$$H(z, n) = \sum_{m=0}^{n} h(m, n) \cdot z^{m-n} \tag{2.16}$$

or

$$H(z, n) = \sum_{l=0}^{n} h(n-l, n) \cdot z^{-l} \tag{2.17}$$

An output signal in the time domain at each time moment nT can be found by inverse z-transform of $Y(z, n)$:

$$y(n) = \frac{1}{2\pi \mathrm{j}} \oint_C Y(z, n) \cdot z^{n-1} \, \mathrm{d}z = \frac{1}{2\pi \mathrm{j}} \oint_C X(z) \cdot H(z, n) \cdot z^{n-1} \, \mathrm{d}z \tag{2.18}$$

where the counter-clockwise integral contour C has to cover all poles of the integrand function. When $H(z, n)$ is known, for the input signal $x(n) = \delta(n - m)$ its z-transform is equal to $X(z) = z^{-m}$ and

$$y(n) = h(m, n) = \frac{1}{2\pi \mathrm{j}} \oint_C X(z) \cdot H(z, n) \cdot z^{n-1} \, \mathrm{d}z \tag{2.19}$$

Finally, taking into account that the $x(n) = \delta(n - m)$ unit function z-transform is equal to z^{-m}, we obtain

$$h(m, n) = \frac{1}{2\pi \mathrm{j}} \oint_C H(z, n) \cdot z^{n-m-1} \, \mathrm{d}z \tag{2.20}$$

Equation (2.16) for obtaining $H(z, n)$ describes the system response from the moment of the input signal appearance $n = 0$ that includes a transient process. For analysis of LTI signals in a steady-state mode, components of the transitional process approach zero and can be neglected. In spite of the apparent simplicity of (2.14), calculation of the GTF for LTV DSs is a complicated task. An attempt to apply z-transform to (2.4) for IR results in a recursive equation:

$$\begin{aligned} H(z, n) &= \sum_{m=-\infty}^{\infty} \frac{1}{a_0(n)} \left[-\sum_{k=1}^{K_1} a_k(n) \cdot h(m, n-k) + \sum_{k=0}^{K_2} b_k(n) \cdot \delta(n-k-m) \right] \cdot z^{m-n} \\ &= \frac{1}{a_0(n)} \left[-\sum_{k=1}^{K_1} a_k(n) \cdot H(z, n-k) \cdot z^{-k} + \sum_{k=0}^{K_2} b_k(n) \cdot z^{-k} \right] \end{aligned} \tag{2.21}$$

where in the right part of the equation there are values of $H(z, n-k)$ that correspond to previous time moments.

Equation (2.21) can be used for recursive calculations of $H(z, n)$ in a causal system for $n \geq 0$ and initial conditions $H(z, -k) = 0$. However, this is possible only for a limited time interval and does not provide an answer regarding GTF behaviour in a steady-state mode where $n \to \infty$.

The GTF of a "slowly" varying system, when $H(z, n) \approx H(z, n-k)$ for $k = 1, \ldots, K_1$, may be approximated by the LTI transfer function by freezing the LTV difference equation at the instant of consideration [5, 8, 9, 13]. For such systems, from equation (2.13), it follows that

$$H(z, n) \approx \sum_{k=0}^{K_2} b_k(n) \cdot z^{-k} \Big/ \sum_{k=0}^{K_1} a_k(n) \cdot z^{-k} \tag{2.22}$$

However, there is no exact criterion that allows determination of how "slow" the system is. Also, as has been shown in [9], use of a "frozen" GTF leads to inadmissibly large errors for many causal systems.

Another possibility for approximate evaluation of the transfer function is based on spectral analysis with a shifting time window [8], which also assumes a "slowly" varying GTF. Unfortunately, this approach has the same disadvantages and limitations as the "frozen-time" method.

Calculations of GTF can be simplified if coefficients have certain limitations. Let us consider two cases that allow GTF representation as a product of two multipliers, one of which does not depend on time.

2. *Coefficients of the recursive part are constant: $a_k(n) = a_k = const.$* In this case [5],

$$H(z, n) = F(z, n) \cdot G(z) \tag{2.23}$$

where $F(z, n)$ and $G(z)$, the GTF of the non-recursive and recursive parts respectively, equal

$$F(z, n) = \sum_{k=0}^{K_2} b_k(n) \cdot z^{-k} \tag{2.24}$$

and

$$G(z) = 1 \Big/ \sum_{k=0}^{K_1} a_k \cdot z^{-k} \tag{2.25}$$

2. *Coefficients of the non-recursive part are constant.* Substitution of $b_k(n) = b_k =$ const in equation (2.9) gives

$$H(z, n) = \sum_{m=-\infty}^{\infty} h(m, n) \cdot z^{m-n} = \sum_{m=-\infty}^{\infty} \sum_{k-0}^{K_2} b_k \cdot g(m+k, n) \cdot z^{m-n}$$

$$= \sum_{k=0}^{K_2} b_k \cdot z^{-k} \sum_{m=-\infty}^{\infty} g(m,n) \cdot z^{m-n}$$

or

$$H(z,n) = F(z) \cdot G(z,n) \tag{2.26}$$

where $F(z)$ and $G(z,n)$, the GTF of non-recursive and recursive parts respectively, equal

$$F(z) = \sum_{k=0}^{K_2} b_k \cdot z^{-k} \tag{2.27}$$

and

$$G(z,n) = \sum_{m=-\infty}^{\infty} g(m,n) \cdot z^{m-n} \tag{2.28}$$

Let us consider the following example of GTF evaluation.

Example 2.2: **Generalized Transfer Function of a Non-Recursive LTV System**

Assume a system described by the difference equation

$$y(n) = \sum_{k=0}^{2} b_k(n) x(n-k) \tag{2.29}$$

with coefficients $b_k = k^{-n}$ (similar to example 2.1). The GTF of this system binds the output and input signals in z-domain:

$$H(z,n) = \sum_{k=0}^{2} b_k \cdot z^{-k} = b_0(n) + b_1(n)z^{-1} + b_3(n)z^{-2} = z^{-1} + 2^{-n}z^{-2} = \frac{z + 2^{-n}}{z^2} \tag{2.30}$$

2.4 SIGNALS ANALYSIS IN FREQUENCY DOMAIN

Time-variant systems can be described in frequency domain, similar to LTI systems, via their frequency responses. Substitution of $z = e^{j\omega}$ in equation (2.14), where $\omega = 2\pi f T$ is a normalized frequency and allows conversion of the system description from z-domain into the frequency domain

$$H(\omega, n) = \sum_{m=-\infty}^{\infty} h(m,n) \cdot \mathrm{e}^{j\omega(m-n)} \tag{2.31}$$

By analogy with the GTF, the function $H(\omega, n)$ is called a *generalized frequency response* (GFR). Also, using an equation similar to (2.18), the output signal can be determined as

$$y(n) = \frac{1}{2\pi} \int_{-\pi}^{\pi} X(\omega) \cdot H(\omega, n) \cdot \mathrm{e}^{\mathrm{j}\omega n} \, \mathrm{d}\omega \tag{2.32}$$

where $X(\omega) = \sum_{m=-\infty}^{\infty} x(m) \cdot \mathrm{e}^{-\mathrm{j}\omega m}$ is the spectrum of the input signal.

A GFR has an explicit physical meaning. When the input signal is a harmonic waveform, represented in our case in a complex exponential form,

$$x(m) = \mathrm{e}^{\mathrm{j}\omega m} = \cos(\omega m) + \mathrm{j} \sin(\omega m) \tag{2.33}$$

the output signal is equal to

$$y(n) = \sum_{m=-\infty}^{\infty} \mathrm{e}^{-\mathrm{j}\omega m} \cdot h(m, n) = \mathrm{e}^{\mathrm{j}\omega n} \sum_{m=-\infty}^{\infty} h(m, n) \cdot \mathrm{e}^{\mathrm{j}\omega (m-n)} = \mathrm{e}^{\mathrm{j}\omega \ n} \cdot H(\omega, n) \tag{2.34}$$

That is, the GFR represents the response of LTV systems to a sampled analytical signal with frequency ω. Although equation (2.32) is an inverse spectrum transform, the product $X(\omega) \cdot H(\omega, n)$ depends on time and, unlike the LTI systems case, is no longer a spectrum of the output signal. So, the next step is to identify a function that describes an output signal in frequency domain.

The spectrum of output signals can be determined by applying a discrete Fourier transform (DFT):

$$Y(\omega) = \sum_{n=-\infty}^{\infty} y(n) \cdot \mathrm{e}^{-\mathrm{j}\omega n} \tag{2.35}$$

and after combination with (2.5) and (2.32), we obtain

$$Y(\omega) = \sum_{n=-\infty}^{\infty} \left[\sum_{m=-\infty}^{\infty} \frac{1}{2\pi} \int_{-\pi}^{\pi} X(\psi) \cdot \mathrm{e}^{\mathrm{j}\psi m} \, \mathrm{d}\psi \cdot h(m, n) \right] \cdot \mathrm{e}^{-\mathrm{j}\omega n} \tag{2.36}$$

Denoting

$$H(\psi, \omega) = \sum_{n=-\infty}^{\infty} \sum_{m=-\infty}^{\infty} h(m, n) \cdot \mathrm{e}^{\mathrm{j}(\psi m - \omega n)} \tag{2.37}$$

we finally obtain a function that depends on two frequencies but not a time:

$$Y(\omega) = \int_{-\pi}^{\pi} X(\psi) \cdot H(\psi, \omega) \, \mathrm{d}\psi \tag{2.38}$$

Function $H(\psi, \omega)$ is called a *bifrequency function* (BF) of the system, and it describes the transformation of all input spectrum components $X(\psi)$ into an output

spectrum $Y(\omega)$ with frequency ω. The first BF term was introduced in [1] for continuous systems and has been developed in [4–7] for LTV DSs.

Using (2.37), it is not difficult to obtain expressions to describe the relations between the GFR and BF

$$H(\psi, n) = \frac{1}{2\pi} \int_{-\pi}^{\pi} H(\psi, \omega) \cdot \mathrm{e}^{-\mathrm{j}n(\psi-\omega)} \, \mathrm{d}\omega \tag{2.39}$$

$$H(\psi, \omega) = \sum_{n=-\infty}^{\infty} H(\psi, n) \cdot \mathrm{e}^{\mathrm{j}n(\psi-\omega)} \tag{2.40}$$

For a better understanding of the introduced system's characteristics in frequency domain $H(\psi, n)$ and $H(\psi, \omega)$, let us compare these characteristics with the traditional frequency response of LTI systems using the next examples.

Example 2.3: Frequency and Bifrequency Responses

Let us derive an expression for the GFR and BF of an LTI DS, whose parameters do not depend on time. Substituting (2.40) into $H(\psi, n) = H(\psi)$, we obtain

$$H(\psi, \omega) = H(\psi) \cdot \sum_{n=-\infty}^{\infty} \mathrm{e}^{\mathrm{j}n(\psi-\omega)} = H(\psi) \cdot \delta(\psi - \omega) \tag{2.41}$$

The meaning of this expression is simple: LTI systems do not transform the input signal frequency, but only weight it according to the frequency response of the system. Substitution of $H(\psi, \omega)$ into equation (2.38) gives a known expression for the output spectrum of LTI systems:

$$Y(\omega) = \int_{-\pi}^{\pi} X(\psi) \cdot H(\psi) \delta(\psi - \omega) \, \mathrm{d}\psi = X(\omega) \cdot H(\omega) \tag{2.42}$$

Example 2.4: Non-Recursive System

Consider a system described by the following difference equation:

$$y(n) = \sum_{k=0}^{1} b_k(n) x(n-k) \tag{2.43}$$

where $b_k = (-1)^n$. This system has an impulse response:

$$h(m, n) = \sum_{k=0}^{1} (-1)^n \delta(n-k-m) \tag{2.44}$$

The GFR of this function is

$$H(\psi, n) = \sum_{n=-\infty}^{\infty} h(m, n)\mathrm{e}^{-\mathrm{j}\psi(n-m)} = \sum_{m=-\infty}^{\infty} \delta(n-m)\mathrm{e}^{-\mathrm{j}\psi(n-m)}$$
$$+ (-1)^n \mathrm{e}^{\mathrm{j}\psi} \sum_{m=-\infty}^{\infty} \delta(n-m)\mathrm{e}^{-\mathrm{j}\psi(n-m)} = 1 + (-1)^n \mathrm{e}^{-\mathrm{j}\psi} \qquad (2.45)$$

It has the amplitude frequency response square or power transfer function

$$|H(\psi, n)|^2 = 2[1 + (-1)^n \cos\psi] \qquad (2.46)$$

which is shown in Fig. 2.4 over one period of frequency $\psi = 2\pi$.

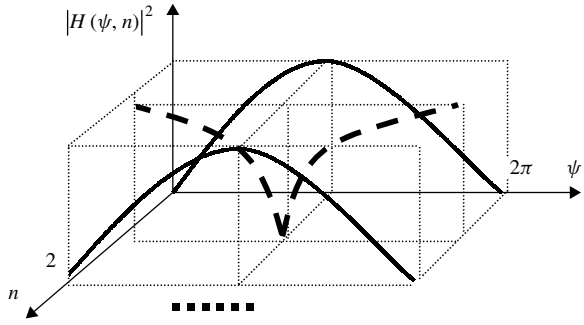

Figure 2.4 GFR modules of a non-recursive system

The BF of the system can be found by applying a DFT for the corresponding GFR, equation (2.45):

$$H(\psi, \omega) = \sum_{n=-\infty}^{\infty} \sum_{m=-\infty}^{\infty} h(m, n)\mathrm{e}^{-\mathrm{j}(n\omega - m\psi)} = \sum_{n=-\infty}^{\infty} \sum_{m=-\infty}^{\infty} \delta(n-m)\mathrm{e}^{-\mathrm{j}(n\omega - m\psi)}$$
$$+ \sum_{n=-\infty}^{\infty} \sum_{m=-\infty}^{\infty} (-1)^n \delta(n-m-1)\mathrm{e}^{-\mathrm{j}(n\omega - m\psi)} = \delta(\psi - \omega)$$
$$+ \delta(\psi - \omega \pm \pi)\mathrm{e}^{-\mathrm{j}(\psi)} \qquad (2.47)$$

So, this LTV system with an $N = 2$ periodically varying coefficient introduces at the output new frequencies $\omega = \psi \pm \pi$, which were absent in the input signal spectrum. This result is consistent with the general statement [4] that in any periodically time-varying systems with the period N an input signal with frequency ψ will appear at the output at frequencies $\psi \pm 2\pi/N$. The frequency conversion diagram for $N = 2$ is shown in Fig. 2.5. In this figure, the signals spectrums at the input and output of the LTV system are related according to the BF map $H(\psi, \omega)$.

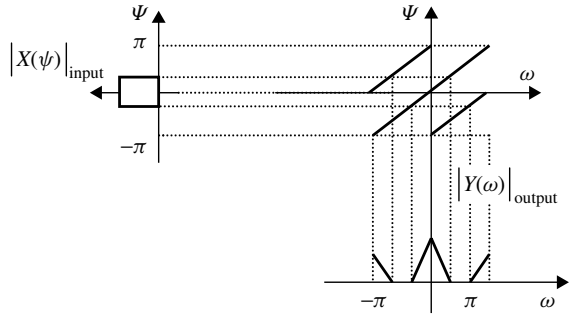

Figure 2.5 Spectrum conversions in an LTV system

2.5 SAMPLING FREQUENCY CHOICE FOR LINEAR TIME-VARIANT DISCRETE SYSTEMS

From the discussion above, it follows that in LTV systems the input signal spectrum component with frequencies ψ is transformed into a set of output frequencies ω according to the BF. This is one of the main differences between LTV discrete systems and discrete systems with constant parameters, where input signal spectrum components are only weighted by the frequency characteristic of the system. New frequency components cannot appear at the output of stable LTI systems. This conditions the common conception regarding the choice of signal sampling frequency for LTV systems. The problem of selecting suitable sampling frequencies for LTV DSs has been discussed and developed in [29–32].

For LTI systems, the sampling theorem states that the input signal must be sampled at a sampling rate that is twice greater than the highest frequency in the input signal spectrum [33]. An approach to this problem as well as the latest literature references can be found in [34].

Here, a simplified approach to this problem based on the concept of spectrum overlapping will be introduced. To avoid an aliasing effect in LTV DSs, the choice of the sampling frequency has to account for both the input and output signal spectrums. In the general case, the output signal spectrum is broader than the input signal spectrum in time-varying systems.

Let the LTV DS have a BF other than zero in the limited region of the input and output frequencies:

$$H(\omega, \psi) = 0, \text{ for } |\omega| > B \text{ and } |\psi| > C \tag{2.48}$$

and let the input signal spectrum bandwidth be limited with maximal frequency A:

$$X(\psi) = 0 \text{ for } |\psi| > A \tag{2.49}$$

where all A, B, C are normalized frequencies.

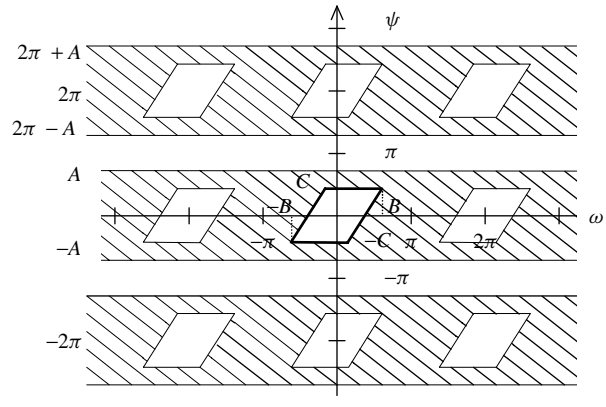

Figure 2.6 Regions of BF and input signal existence in the bifrequency plane

Areas where the BF and input signal spectrum exist are shown in Fig. 2.6, a bifrequency map, on the frequency plane $\{\omega, \psi\}$ [4, 5]. It is known that discrete signals have all spectrum components periodical with a sampling frequency $\omega_S = 2\pi$. The same applies to the characteristics of discrete systems in frequency domain: the frequency response of a discrete system is a periodical function with the same sampling frequency period (see Fig. 2.6).

Let us assume that the signal at the system output is reconstructed into the continuous waveform by an ideal analog low-pass filter (LPF) with rectangular frequency response of width $\pm\pi$. Then, from Fig. 2.6, we can derive the conditions that ensure that the aliasing effect is absent during the signal reconstruction, provided that

- the input signal spectrum $A(\psi)$ is within the frequency band $\pm\pi$ or $|A(\psi)| < \pi$, which is the traditional requirement for LTI DSs; and
- at the system output the signal frequency band $B(\omega)$ is also within the frequency band $|B(\omega)| < \pi$.

These conditions can be viewed as a generalization of Nyquist's criteria for LTV DFs [28]. This simplified geometrical approach at least guarantees an absence of frequency aliasing.

So, for any given system, the minimal sampling frequency has to satisfy the condition

$$\omega_S = \max\{2B; 2A\} \tag{2.50}$$

This generalization can be slightly modified for filtering systems when an output frequency band C is less than the frequency band of the input signals: $C < A$ [29, 31]. Let a sampling frequency be selected such that $A + C < \pi$, which potentially leads to the aliasing problem with the input signal spectrum. However, in some cases, and particularly in recursive filters, these aliasing regions are cut by the system itself (this problem will be discussed in more detail in Chapter 3) and in the first approximation does not affect the reconstructed output signal. This condition can be considered as

an expansion of the sampling theorem for systems with a frequency band narrowing from the input to the output (narrowband filtering).

So, for narrowband LTV filtering systems, the minimal sampling frequency has to satisfy the condition

$$\omega_S = \max\{2B; A + C\} \tag{2.51}$$

Thus, in equation (2.51) it is assumed that aliasing occurs, but its influence on the system performance is negligible for many applications.

In this simplified approach, we mainly demonstrate a way of selecting minimal sampling frequency and do not pretend to have presented a deep theory of sampling in LTV systems. Nevertheless, this is a descriptive way to investigate systems and will be used for analysis of periodically time-varying discrete systems.

2.6 RANDOM SIGNALS PROCESSING IN LINEAR TIME-VARIANT DISCRETE SYSTEMS

In the previous sections, we discussed LTI systems for deterministic input signals. Now we will consider the case of random signals at the system input. Let $X(n)$ be a random discrete input process with the following moments: mean value $M_X(n)$, variance $\sigma_X^2(n)$ and autocorrelation function $R_X(m, n)$, where m is a time delay. Our goal is to evaluate the same parameters for a random output process $Y(n)$, assuming that the characteristics of the system are known. To do this, we should take into account that for any particular realization of the input signal, equation (2.52) is true

$$Y(n) = \sum_{m=-\infty}^{\infty} X(m) \cdot h(m, n) \tag{2.52}$$

Then, under the condition that the input process does not depend on the law of LTV DS parameter variation, we obtain the following:

1. The mean value

$$M_Y(n) = \langle Y(n) \rangle = \left\langle \sum_{m=-\infty}^{\infty} X(m) \cdot h(m, n) \right\rangle = \sum_{m=-\infty}^{\infty} \langle X(m) \rangle \cdot h(m, n)$$

$$= \sum_{m=-\infty}^{\infty} M_X(m) \cdot h(m, n) \tag{2.53}$$

   where $\langle * \rangle$ means averaging over random process realizations,

2. The autocorrelation function

$$R_Y(m, n) = \langle Y(m) \cdot Y(n) \rangle = \left\langle \sum_{\nu=-\infty}^{\infty} X(\nu) \cdot h(\nu, m) \cdot \sum_{\xi=-\infty}^{\infty} X(\xi) \cdot h(\xi, n) \right\rangle$$

$$= \sum_{\nu=-\infty}^{\infty} h(\nu, n) \sum_{\xi=-\infty}^{\infty} h(\xi, m) \cdot \langle X(\nu) \cdot X(\xi) \rangle$$

$$= \sum_{\nu=-\infty}^{\infty} h(\nu, n) \sum_{\xi=-\infty}^{\infty} h(\xi, m) \cdot R_X(\nu, \xi) \tag{2.54}$$

and

3. The variance

$$\sigma_Y^2(n) = R_Y(n, n) = \sum_{\nu=-\infty}^{\infty} h(\nu, n) \sum_{\xi=-\infty}^{\infty} h(\xi, n) \cdot R_X(\nu, \xi) \tag{2.55}$$

If the input process $X(n)$ is a wide sense stationary, that is,

$$M_X(n) = M_X = \text{const}, R_X(m, n) = R_X(n - m), \sigma_Y^2(n) = \sigma_Y^2 = \text{const},$$

then expressions (2.53) to (2.55) take the following forms:

1. The mean value

$$M_Y(n) = M_X \sum_{m=-\infty}^{\infty} h(m, n) = M_X \cdot H(0, n) \tag{2.56}$$

where $H(0, n)$ is the GFR for direct current (DC $- \omega = 0$),

2. The correlation function

$$R_Y(m, n) = \sum_{\nu=-\infty}^{\infty} h(\nu, n) \sum_{\xi=-\infty}^{\infty} h(\xi, m) \cdot R_X(\nu - \xi) \tag{2.57}$$

and

3. The variance

$$\sigma_Y^2(n) = \sum_{\nu=-\infty}^{\infty} h(\nu, n) \sum_{\xi=-\infty}^{\infty} h(\xi, n) \cdot R_X(\nu - \xi) \tag{2.58}$$

From these equations follows a very important conclusion: *the output process of an LTV DS becomes non-stationary* even if an input signal is a stationary process. It is the consequence of the nature of time-variant systems.

The correlation function of a random time-varying discrete process is connected with its power spectral density $S_X(\omega)$ by Fourier transform, according to the Wiener–Khintchine theorem:

$$R_X(\tau) = \frac{1}{2\pi} \int_{-\pi}^{\pi} S_X(\omega) \cdot \mathrm{e}^{\mathrm{j}\omega\tau} \, \mathrm{d}\omega \tag{2.59}$$

$$S_X(\omega) = \sum_{\tau=-\infty}^{\infty} R_X(\tau) \cdot \mathrm{e}^{-\mathrm{j}\omega\tau},\ \tau = \nu - \xi \tag{2.60}$$

Using these transforms, it is possible to obtain a spectral representation of the random signals at the LTV DS output. Substituting (2.59) into (2.57), then multiplying by $\mathrm{e}^{\mathrm{j}(m-n)\omega} \cdot \mathrm{e}^{-\mathrm{j}(m-n)\omega} \equiv 1$ and conducting the relevant calculations, we obtain

$$R_Y(m,n) = \frac{1}{2\pi} \int_{-\pi}^{\pi} S_X(\omega) \cdot H(\omega, n) \cdot H(-\omega, m) \cdot \mathrm{e}^{-\mathrm{j}(m-n)\omega}\, \mathrm{d}\omega \tag{2.61}$$

as well as

$$\sigma_Y^2(n) = \frac{1}{2\pi} \int_{-\pi}^{\pi} S_X(\omega) \cdot |H(\omega, n)|^2\, \mathrm{d}\omega \tag{2.62}$$

Denoting in equation (2.61) that $n - m = \tau$, we can rewrite it as

$$R_Y(\tau, n) = \frac{1}{2\pi} \int_{-\pi}^{\pi} S_X(\omega) \cdot H(\omega, n) \cdot H(-\omega, n - \tau) \cdot \mathrm{e}^{-\mathrm{j}\omega\tau}\, \mathrm{d}\omega \tag{2.63}$$

For causal systems, in all summations it is necessary to indicate limitations for variation of the indexes, corresponding to the area of IR non-zero values as shown in equation (2.8). We will come back to these equations in the following chapters.

2.7 COMBINATIONS OF TIME-VARIANT SYSTEMS

High-order systems are often built by combining lower-order systems. Let us investigate the basic types of system combinations – parallel, cascade and with feedback connections – and obtain expressions for the IR $h(m, n)$ and GTF $H(z, n)$ of these complex M-stage systems. We denote $h_i(m, n)$ as the IR and $H_i(z, n)$ as the GTF of the *ith* stage of the systems under consideration, where $i = 1, \ldots M$.

2.7.1 Parallel Connections

A system with M parallel-connected sections is shown in Fig. 2.7. If an input signal is the unit sample sequence (2.2), then the output signal is the system's IR. In the case of parallel-connected systems, the output signal is equal to the sum of the output signals for each link between stages. The signals, themselves, are the IRs of the considered stages $h_i(m, n)$:

$$h(m,n) = \sum_{i=1}^{M} h_i(m,n) \tag{2.64}$$

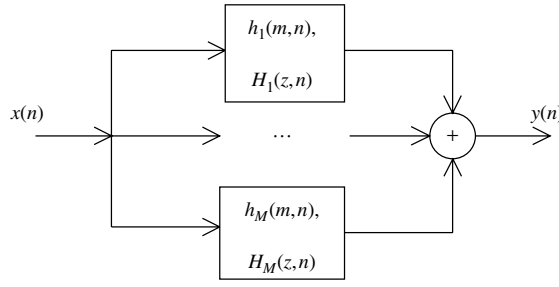

Figure 2.7 A system with parallel connections

The GTF of the system with parallel-connected stages is equal to the sum of the GTF of each stage $H_i(z, n)$. The GTF of each stage is calculated in the following way:

$$H(z,n) = \sum_{m=0}^{n} h(m,n) \cdot z^{m-n} = \sum_{m=0}^{n} \sum_{i=1}^{M} h_i(m,n) \cdot z^{m-n}$$
$$= \sum_{i=1}^{Mn} \sum_{m=0}^{n} h_i(m,n) \cdot z^{m-n} = \sum_{i=1}^{M} H_i(z,n) \tag{2.65}$$

2.7.2 Cascade Connections

Consider the two-cascade system shown in Fig. 2.8.

If the system's input signal is the unit pulse described in equation (2.2), then the first stage output signal is its IR $h_1(m, k)$. The second stage response is a convolution of the input signal and the second stage IR $h_2(m, k)$ and can be calculated using equation (2.5):

$$h(m,n) = \sum_{k=-\infty}^{\infty} h_1(m,k) \cdot h_2(k,n) \tag{2.66}$$

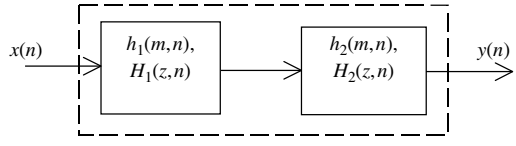

Figure 2.8 System with two cascaded sections

The GTF of the system can then be determined by applying a z-transform to (2.66):

$$H(z,n) = \sum_{m=-\infty}^{\infty} \left[\sum_{k=-\infty}^{\infty} h_1(m,k) \cdot h_2(k,n) \right] \cdot z^{m-n}$$
$$= \sum_{k=-\infty}^{\infty} \left[\sum_{m=-\infty}^{\infty} h_1(m,k) \cdot z^{m-k} \right] \cdot h_2(k,n) \cdot z^{k-n}$$

$$= \sum_{k=-\infty}^{\infty} H_1(z,k) \cdot h_2(k,n) \cdot z^{k-n} \tag{2.67}$$

Knowing $n - k = l$, this equation can be rewritten as

$$H(z,n) = \sum_{l=-\infty}^{\infty} H_1(z, n-l) \cdot h_2(n-l, n) \cdot z^{-l} \tag{2.68}$$

For causal systems, $h_1(m,k)$ and $h_2(k,n)$ in equations (2.66) and (2.67) are equal to zero, except for the case when $0 \le m \le k \le n$, in which case

$$h(m,n) = \sum_{k=0}^{n} h_1(m,k) \cdot h_2(k,n) \tag{2.69}$$

and

$$H(z,n) = \sum_{k=0}^{n} H_1(z,k) \cdot h_2(n,k) \cdot z^{k-n} \tag{2.70}$$

or

$$H(z,n) = \sum_{l=0}^{n} H_1(z, n-l) \cdot h_2(n-l, n) \cdot z^{-l} \tag{2.71}$$

Expressions (2.69) and (2.70) can be used for recurrent calculation of LTV DSs.

It is important to note that, *unlike the LTI systems case, expressions (2.64) to (2.70) are not invariant relative to the order of the connection of the stages.* This conclusion is illustrated by the following examples.

Example 2.5: Interconnected LTI–LTV Systems

The first stage of the two-cascade systems is time-invariant when the second stage is time-variant. Then $H_1(z,n) = H_1(z)$, and from equation (2.67) it follows that

$$H(z,n) = H_1(z) \cdot \sum_{k=-\infty}^{\infty} h_2(k,n) \cdot z^{k-n} = H_1(z) \cdot H_2(z,n) \tag{2.72}$$

That is, in this case the GTF of the system can be derived from the product of the GTFs for each stage.

Example 2.6: Interconnected LTV–LTI Systems

The first stage of the two-cascade systems is time-variant when the second stage is time-invariant. Applying the algorithms of the previous example, we obtain a final equation that is essentially different from equation (2.72)

$$H(z,n) = \sum_{l=-\infty}^{\infty} H_1(z, n-l) \cdot h_2(l) \cdot z^{-l} \tag{2.73}$$

Equations (2.72) and (2.73) clearly show that time-variant systems do not possess the property of invariance relative to the sequence of link combinations.

Now, let us consider a system with M cascaded stages, as shown in Fig. 2.9.

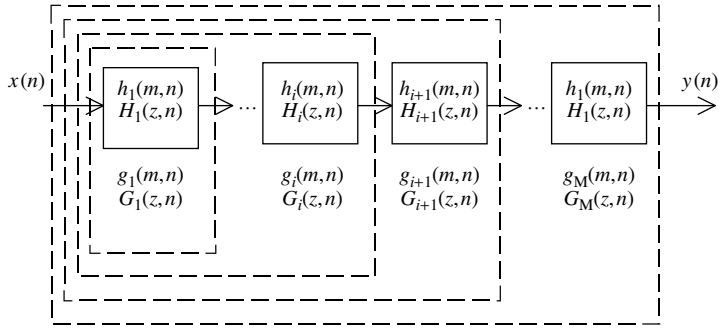

Figure 2.9 A system with M cascaded links

To calculate the characteristics of this system, it is necessary to apply formulas (2.66) and (2.67). The system can be represented as a connection of the one-stage link 'i', with IR $g_i(m, n)$ and GTF, $G_i(z, n)$, and the following '$i + 1$' link, with IR $g_{i+1}(m, n)$ and GTF $G_{i+1}(z, n)$. Figure 2.9 makes clear the principle of calculation by cascaded accumulation of links. It is obvious that for the first stage $g_1(m, n) = h_1(m, n)$ and $G_1(z, n) = H_1(z, n)$. Then, expressions (2.66) and (2.67) or (2.69) and (2.70) can be used. The final values $g_{\mathrm{M}}(m, n)$ and $G_{\mathrm{M}}(z, n)$ for $i = M$ are the desired system characteristics $h(m, n)$ and H_1(z, n).

2.7.3 Systems with Feedback

An LTV system structure with a feedback is shown in Fig. 2.10. The variables $h_1(m, n)$ and $H_1(z, n)$ represent characteristics of the direct link and $h_2(m, n)$ and $H_2(z, n)$ represent characteristics of the feedback, both of which are assumed to be known. The goal is to calculate the system's IR $h(m, n)$ and GTF $H(z, n)$. Let us denote signals at different points of the system using equation (2.5):

$$u(\xi) = \sum_{\nu=-\infty}^{\infty} y(\nu) \cdot h_2(\nu, \xi) \tag{2.74}$$

$$w(\xi) = x(\xi) + u(\xi) \tag{2.75}$$

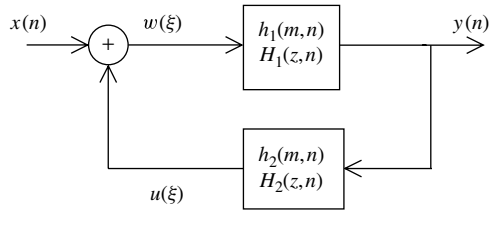

Figure 2.10 A system with a feedback

$$y(n) = \sum_{\xi=-\infty}^{\infty} w(\xi) \cdot h_1(\xi, n) \tag{2.76}$$

Then, for the output signal

$$y(n) = \sum_{\xi=-\infty}^{\infty} \left[x(\xi) + \sum_{\nu=-\infty}^{\infty} y(\nu) \cdot h_2(\nu, \xi) \right] \cdot h_1(\xi, n) \tag{2.77}$$

or, changing the summation order,

$$y(n) = \sum_{\xi=-\infty}^{\infty} x(\xi) \cdot h_1(\xi, n) + \sum_{\nu=-\infty}^{\infty} y(\nu) \cdot \sum_{\xi=-\infty}^{\infty} h_2(\nu, \xi) \cdot h_1(\xi, n) \tag{2.78}$$

If, at the system input there is the pulse signal described by equation (2.2), then the output signal of the system is its IR:

$$h(m, n) = \sum_{\xi=-\infty}^{\infty} \delta(\xi - m) \cdot h_1(\xi, n) + \sum_{\nu=-\infty}^{\infty} h(m, \nu) \cdot \sum_{\xi=-\infty}^{\infty} h_2(\nu, \xi) \cdot h_1(\xi, n) \tag{2.79}$$

The first sum of this expression represents the IR of the non-recursive part of the system $h_1(m, n)$, while the second sum in the right-hand part represents the IR of the disconnected system in the direction from output to input. Denoting this second sum as

$$g(\nu, n) = \sum_{\xi=-\infty}^{\infty} h_2(\nu, \xi) \cdot h_1(\xi, n) \tag{2.80}$$

we finally obtain a formula for the IR of the system with feedback:

$$h(m, n) = h_1(m, n) + \sum_{\nu=-\infty}^{\infty} h(m, \nu) \cdot g(\nu, n) \tag{2.81}$$

The GTF of the system with feedback can be determined using equations (2.16) and (2.81):

$$H(z, n) = \sum_{m=-\infty}^{\infty} \left[h_1(m, n) + \sum_{\nu=-\infty}^{\infty} h(m, \nu) \cdot g(\nu, n) \right] \cdot z^{m-n} = \sum_{m=-\infty}^{\infty} h_1(m, n) \cdot z^{m-n}$$
$$+ \sum_{\nu=-\infty}^{\infty} g(\nu, n) \cdot z^{\nu-n} \cdot \sum_{m=-\infty}^{\infty} h(m, \nu) \cdot z^{m-\nu} \tag{2.82}$$

or

$$H(z, n) = H_1(z \cdot n) + \sum_{\nu=-\infty}^{\infty} H(z, \nu) \cdot g(\nu, n) \cdot z^{\nu-n} \tag{2.83}$$

For causal systems, expressions (2.80) to (2.83) are represented as

$$g(\nu, n) = \sum_{\xi=0}^{\infty} h_2(\nu, \xi) \cdot h_1(\xi, n) \tag{2.84}$$

$$h(m, n) = h_1(m, n) + \sum_{\nu=0}^{\infty} h(m, \nu) \cdot g(\nu, n) \tag{2.85}$$

and

$$H(z, n) = H_1(z, n) + \sum_{\nu=0}^{\infty} H(z, \nu) \cdot g(\nu, n) \cdot z^{\nu-n} \tag{2.86}$$

The obtained recurrent relations in the case of a restricted n can be sequentially solved for all n. In the case when $n \to \infty$, the system's characteristics can be determined if some additional simplifying assumptions are made. Some of these assumptions will be discussed later in the book.

2.7.4 Continuous and Discrete LTV Systems

Mathematical expressions for the main characteristics of LTV DSs and similar expressions for continuous LTV systems are presented in publications [20–26] and, using a uniform format, are collected in Tables 2.2 to 2.4. Recall that corresponding expressions for discrete and continuous systems have the same physical meanings.

Table 2.2 The characteristics of LTV systems for deterministic input signals

	Continuous systems	Discrete systems
Difference (differential) equations	$\sum_{k=0}^{R_1} a_k(t) \cdot \frac{\mathrm{d}^k y}{\mathrm{d}t^k} = \sum_{k=0}^{K_2} b_k(t) \cdot \frac{\mathrm{d}^k x}{\mathrm{d}t^k}$	$\sum_{k=0}^{K_1} a_k(n) \cdot y(n-k) = \sum_{k=0}^{K_2} b_k(n) \cdot x(n-k)$
IR	$h(\tau, t) = y(t)$ for $x(t) = \delta(\tau - t)$	$h(m, n) = y(n)$ for $x(n) = \delta(m - n)$
GFR	$H(\mathrm{j}\omega, t) = \int_0^t h(\tau, t) \cdot \mathrm{e}^{\mathrm{j}(t-\tau)\omega}\, \mathrm{d}\tau$	$H(\omega, n) = \sum_{m=0}^{\infty} h(m, n) \cdot \mathrm{e}^{\mathrm{j}\omega(m-n)}$
BF	$H(\mathrm{j}\omega, \mathrm{j}\psi) = \int_0^{\infty} \int_0^{\infty} h(\tau, t) \cdot \mathrm{e}^{\mathrm{j}(\psi\tau - \omega t)}\, \mathrm{d}\tau\, \mathrm{d}t$	$H(\psi, \omega) = \sum_{n=0}^{\infty} \sum_{m=0}^{\infty} h(m, n) \cdot \mathrm{e}^{\mathrm{j}(\psi m - \omega n)}$
Output signal	$y(t) = \int_0^t x(\tau) \cdot h(\tau, t)\, \mathrm{d}\tau = \frac{1}{2\pi} \int_{-\infty}^{\infty} X(\mathrm{j}\omega) \cdot H(\mathrm{j}\omega, t) \cdot \mathrm{e}^{\mathrm{j}\omega t}\, \mathrm{d}\omega$	$y(n) = \sum_{m=0}^{n} x(m) \cdot h(m, n) = \frac{1}{2\pi} \int_{-\pi}^{\pi} X(\omega) \cdot H(\omega, n) \cdot \mathrm{e}^{\mathrm{j}\omega n}\, \mathrm{d}\omega$
Spectrum of the output signal	$Y(\mathrm{j}\omega) = \frac{1}{2\pi} \int_{-\infty}^{\infty} X(\mathrm{j}\psi) \cdot H(\mathrm{j}\psi, \mathrm{j}\omega) \cdot \mathrm{d}\psi$	$Y(\omega) = \frac{1}{2\pi} \int_{-\pi}^{\pi} X(\psi) \cdot H(\psi, \omega) \cdot \mathrm{d}\psi$

Table 2.3 Characteristics of LTV systems containing two stages

	Continuous systems	Discrete systems
Parallel junction	$h(\xi,t)=h_1(\xi,t)+h_2(\xi,t)$ $H(\mathrm{j}\omega,t)=H_1(\mathrm{j}\omega,t)+H_2(\mathrm{j}\omega,t)$	$h(m,n)=h_1(m,n)+h_2(m,n)$ $H(\omega,n)=H_1(\omega,n)+H_2(\omega,n)$
Cascaded junction	$h(\xi,t)=\int_{\xi}^{t} h_1(\xi,u)\cdot h_2(u,t)\cdot \mathrm{d}u$ $H(\mathrm{j}\omega,t)=\int_{0}^{t} H_1(\mathrm{j}\omega,\xi)\cdot h_2(\xi,t)\cdot \mathrm{e}^{\mathrm{j}\omega(\xi-t)}$	$h(m,n)=\sum_{k=m}^{n} h_1(m,k)\cdot h_2(k,n)$ $H(\omega,n)=\sum_{m=0}^{n} H_1(\omega,m)\cdot h_2(m,n)\cdot \mathrm{e}^{\mathrm{j}\omega(m-n)}$
Feedback connection	$h(\xi,t)=h_1(\xi,t)+\int_{\xi}^{t} h(\xi,u)\cdot g(u,t)\cdot \mathrm{d}u$ $H(\mathrm{j}\omega,t)=H_1(\mathrm{j}\omega,t)+\int_{0}^{t} H(\mathrm{j}\omega,u)\cdot g(u,t)\cdot \mathrm{e}^{\mathrm{j}\omega(u-t)}\cdot \mathrm{d}u$ $g(u,t)=\int_{\xi}^{t} h_2(u,\xi)\cdot h_1(\xi,t)\cdot \mathrm{d}\xi$	$h(m,n)=h_1(m,n)+\sum_{k=m}^{n} h(m,k)\cdot g(k,n)$ $H(\omega,n)=H_1(\omega,n)+\sum_{k=0}^{n} H(\omega,k)\cdot g(k,n)\cdot \mathrm{e}^{\mathrm{j}\omega(k-n)}$ $g(k,n)=\sum_{imk}^{n} h_2(k,m)\cdot h_1(m,n)$

Table 2.4 Output characteristics of LTV systems for random input signals

	Continuous systems	Discrete systems
Time-variant input signals		
Mean value	$M_Y(t)=\int_{0}^{t} M_X(\tau)\cdot h(\tau,t)\,\mathrm{d}\tau$	$M_Y(n)=\sum_{m=0}^{n} M_X(m)\cdot h(m,n)$
Deviation	$\sigma_Y^2(t)=\int_{0}^{t} h(\nu,t)\int_{0}^{t} h(\xi,t)\cdot R_X(\nu,\xi)\,\mathrm{d}\xi\,\mathrm{d}\nu$	$\sigma_Y^2(n)=R_Y(n,n)=\sum_{\nu=-\infty}^{\infty} h(\nu,n)\sum h(\xi,n)\cdot R_X(\nu,\xi)$
Correlation function	$R_Y(\tau,t)=\int_{0}^{\tau} h(\nu,\tau)\int_{0}^{t} h(\xi,t)\times R_X(\nu,\xi)\,\mathrm{d}\xi\,\mathrm{d}\nu$	$R_Y(m,n)=\sum_{\nu=0}^{n} h(\nu,n)\sum_{\xi=0}^{n} h(\xi,m)\cdot R_X(\nu,\xi)$
Time-invariant input signals		
Mean value	$M_Y(t)=M_X\cdot H(0,t)$	$M_Y(n)=M_X\cdot H(0,n)$
Deviation	$\sigma_Y^2(t)=\frac{1}{2\pi}\int_{-\infty}^{\infty} S_X(\mathrm{j}\omega)\cdot \lvert H(\mathrm{j}\omega,t)\rvert^2\,\mathrm{d}\omega$	$\sigma_Y^2(t)=\frac{1}{2\pi}\int_{-\pi}^{\infty\pi} S_X(\omega)\cdot \lvert H(\omega,n)\rvert^2\,\mathrm{d}\omega$
Correlation function	$R_Y(\tau,t)=\frac{1}{2\pi}\int_{-\infty}^{\infty} S_X(\mathrm{j}\omega)\cdot H(\mathrm{j}\omega,t)\times H(-\mathrm{j}\omega,t)\cdot \mathrm{e}^{\mathrm{j}(t-\tau)\omega}\,\mathrm{d}\omega$	$R_Y(m,n)=\frac{1}{2\pi}\int_{-\pi}^{\pi} S_X(\omega)\cdot H(\omega,n)\times H(-\omega,m)\cdot \mathrm{e}^{\mathrm{j}(n-m)\omega}\,\mathrm{d}\omega$

The expressions for discrete systems approach the corresponding expressions for continuous systems in the limiting case when the sampling period becomes infinitely small and the sums are converted into integrals.

2.8 TIME-VARYING SAMPLING

In the previous sections, we have considered systems with varying coefficients. The definition of these time-variant systems is based on the linear difference equation (2.1) with time-dependent coefficients. The sampling time in this equation is hidden behind the indexes "n" and "k". It is assumed that the real sampling time is uniform and follows a constant time interval T. It is also well known from digital filtering theory that this sampling time interval T specifies the scale of the frequency response for all filters. Hence, together with the coefficients, T directly influences the relations between input and output signals in discrete systems.

Now, following the analysis of linear discrete systems with time-varying coefficients, we consider linear discrete systems with constant coefficients but with a time-varying sampling interval $T = T(\mathrm{n})$. We will not discuss here a comprehensive theory of non-uniform sampling (see, for example, [35]). Here, it seems interesting to show that when variation of the sampling period is small in comparison with an average clock period, the behaviour of the discrete system is similar to the behavior of systems with time-varying coefficients. This effect has both theoretical and practical applications. Although it has been assumed that sampling or clock pulses occur regularly at interval T, in practice, pulse sequences can become non-uniform. Thus, in digital microprocessor-based filters, the clock interval is usually synchronized with the interruption procedure, which destroys the regularity of the sampling period. Another example of a non-uniform pulse sequence is in a filter in communication systems in which the clock interval is recovered from a receiving signal and is always corrupted by noise [36].

Firstly, let us recall that linear digital filters (DF), including those with time-varying coefficients, are "linear" relative to the input signal, but not to the clock signals. With respect to the clock signal, these filters are non-linear and the principle of superposition cannot be applied to these systems. Consequently, there is no characteristic similar to the bifrequency function. To resolve this problem, we can use the methods appropriate for small parameter variations. It is assumed that the deviation in the sampling period is small in comparison to the uniform sampling interval. For the practical cases described above, as well as for many other typical situations, this assumption is acceptable. Otherwise, computer modelling can be used.

2.8.1 Systems with Non-Uniform Sampling

Assume that we are analyzing linear discrete systems with constant coefficients, which can be described with a linear difference equation:

$$\sum_{k=0}^{K_1} a_k y(n-k) = \sum_{k=0}^{K_2} b_k x(n-k) \tag{2.87}$$

Note that the system can also have time-varying coefficients, but this is beyond the scope of the book. Let us try to find the relationship between the input and output signal spectrums of this system as a function of the spectrum of the sampling sequence by analogy with the bifrequency function [30]

$$Y(\omega) = \frac{1}{2\pi} \int_{-\pi}^{\pi} X(\psi) \cdot H(\psi, \omega) \cdot \mathrm{d}\psi \tag{2.88}$$

Assume that there is a sampling sequence at the system input acting at time instants $Tn + T\Delta n$. Then, the appropriate difference equation is

$$\sum_{k=0}^{K_1} a_k \cdot y'[(n-k)T + \Delta_{n-k}] = \sum_{k=0}^{K_2} b_k \cdot x'[(n-k)T + \Delta_{n-k}] \tag{2.89}$$

Introduction of the transforms $x(nT) = x'(nT + \Delta_n)$ and $y(nT) = y'(nT + \Delta_n)$ yields

$$\sum_{k=0}^{K_1} a_k \cdot y[(n-k)T] = \sum_{k=0}^{K_2} b_k \cdot x[(n-k)T] \tag{2.90}$$

which is consistent with the equation describing LTI filters [35].

Therefore, a discrete filter (system) with non-uniform sampling (DFNS) can be represented by the simplified model shown in Fig. 2.11. This model consists of three blocks: input and output time transformers *TT*1 and *TT*2, as well as an LTI discrete filter with constant sampling period T. A procedure for DFNS analysis is input signal transform in *TT*1, calculation of system characteristics at the DF output and then, again, the time-transform of the output signal in *TT*2. This procedure allows use of the well-developed methods of LTI systems analysis for DFNS investigations.

The block *TT*1 is a sampler with varying sampling time. The sampled signals arrive at the DF input at constant time interval T. Thus, the *TT*1 operates like a serial connection of a time-varying delay ($T\Delta_n$) and a uniform sampler with the sampling period T. If a continuous signal is required at the second sampler *TT*2 output, then it can be represented by a combination of a time-varying delay line ($-T\Delta_i$) and an ideal low-pass filter (LPF). These two time transformers shift the input and output signals in such a way that the filter itself could be considered as the filter with constant parameters.

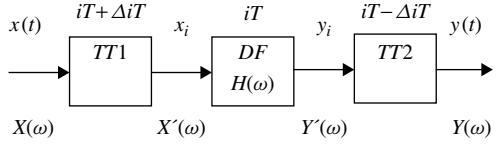

Figure 2.11 Model of discrete filter with non-uniform sampling

Assume now that there is a signal $x(t)$ with spectrum $X(\omega)$ at the $TT1$ input. This transformer's sampling period is modulated by a discrete delay Δ_i. Hence, $TT1$ selects a signal at the time moments $iT + \Delta_i$, and, according to the Nyquist theorem for non-uniform sampling [35], with a small delay modulation index (Δ_i/T),

$$x_i = \frac{1}{2\pi}\int_{-\pi}^{\pi} X(\omega)\mathrm{e}^{\mathrm{j}\omega(i+\Delta_i)}\,\mathrm{d}\omega. \tag{2.91}$$

The small delay modulation index is a requirement for applying the small parameters method, and for this case, the exponential function can be represented as

$$\mathrm{e}^{\mathrm{j}\omega(i+\Delta_i)} = \mathrm{e}^{\mathrm{j}\omega i} + \mathrm{j}\omega\Delta_i\mathrm{e}^{\mathrm{j}\omega i} \tag{2.92}$$

After substituting equation (2.92) into (2.91), equation (2.91) takes the form

$$x_i = \frac{1}{2\pi}\int_{-\pi}^{\pi} X(\omega)\mathrm{e}^{\mathrm{j}\omega i}\,\mathrm{d}\omega + \frac{1}{2\pi}\int_{-\pi}^{\pi} \mathrm{j}\omega\Delta_i X(\omega)\mathrm{e}^{\mathrm{j}\omega i}\,\mathrm{d}\omega \tag{2.93}$$

Thus, signals at the output of the time-varying sampler with a small modulation index can be represented as the sum of signals with uniform sampling (the first summand in (2.93)) and a discrete additive signal d_i (the second summand), that is,

$$x_i = x(iT) + d_i \tag{2.94}$$

where

$$d_i = \frac{1}{2\pi}\int_{-\pi}^{\pi} \mathrm{j}\psi\Delta_i X(\psi)\mathrm{e}^{\mathrm{j}\psi i}\,\mathrm{d}\psi \tag{2.95}$$

The spectrum of this signal can be represented as

$$\begin{aligned} X'(\omega) &= \sum_{i=-\infty}^{\infty}(x(iT)+d_i)\mathrm{e}^{-\mathrm{j}\omega i} = X(\omega)\sum_{i=-\infty}^{\infty}\frac{1}{2\pi}\int_{-\pi}^{\pi}\mathrm{j}\psi\Delta_i\mathrm{e}^{\mathrm{j}\psi i}X(\psi)\,\mathrm{d}\psi\,\mathrm{e}^{-\mathrm{j}\omega i} \\ &= \frac{1}{2\pi}\int_{-\pi}^{\pi} X(\psi)\left\{2\pi\delta(\omega-\psi) + \sum_{i=-\infty}^{\infty}\mathrm{j}\psi\Delta_i\mathrm{e}^{\mathrm{j}(\psi-\omega)i}\right\}\mathrm{d}\psi \end{aligned} \tag{2.96}$$

To present this spectrum in a more convenient form for analytical calculations, denote

$$L(\omega,\psi) = 2\pi\delta(\omega-\psi) + \sum_{i=-\infty}^{\infty}\mathrm{j}\psi\Delta_i\mathrm{e}^{\mathrm{j}(\psi-\omega)i} \tag{2.97}$$

Then,

$$X'(\omega) = \frac{1}{2\pi}\int_{-\pi}^{\pi} X(\psi)L(\omega,\psi)\,\mathrm{d}\psi \tag{2.98}$$

$L(\omega, \psi)$ is the BF of the first time transformer according to this equation and the definition of bifrequency function. The transformer output signal spectrum consists of input signal spectral components (SCs) and, originating within the transformers, combinational spectral components (CCs) that are a result of the signal modulation. Thus, the SCs of the BF are similar to the frequency response of the periodical (uniform) sampler with constant time interval T while the CCs determine the components of the signal's spectrum appearing because of delay modulation.

The spectrum of the discrete signal Δ_i can be specified as

$$E(\omega) = \sum_{i=-\infty}^{\infty} \Delta_i \mathrm{e}^{-\mathrm{j}\omega i} \tag{2.99}$$

and the transformer BF can be presented in the convenient form

$$L(\omega, \psi) = 2\pi\delta(\omega - \psi) + \mathrm{j}\psi E(\omega - \psi) \tag{2.100}$$

The BF for the second time transformer $TT2$ can be similarly determined with the only difference being that $\mathrm{j}\omega$ has a negative sign.

We now find the dependence between signal spectrums at the input and output of the DFNS by

$$Y'(\omega) = X'(\omega)H(\omega) \tag{2.101}$$

For $TT1$,

$$X'(\omega) = \frac{1}{2\pi}\int_{-\pi}^{\pi} X(\psi)L_1(\omega, \psi)\,\mathrm{d}\psi \tag{2.102}$$

$$Y'(\omega) = \frac{1}{2\pi}\int_{-\pi}^{\pi} Y'(\psi)L_2(\omega, \psi)\,\mathrm{d}\psi \tag{2.103}$$

where $L_1(\omega, \psi)$ and $L_2(\omega, \psi)$ are the BFs for $TT1$ and $TT2$ respectively. Finally, taking into account equations (2.100) to (2.102), the signal spectrum at the output of a DF with time-varying sampling period takes the form

$$\begin{aligned} Y(\omega) = {} & \frac{1}{2\pi}\int_{-\pi}^{\pi} X(\psi)\{H(\psi)2\pi\delta(\omega - \psi) + [H(\omega) - H(\psi)]\mathrm{j}\psi E(\omega - \psi)\}\,\mathrm{d}\psi \\ & - \frac{1}{2\pi}\int_{-\pi}^{\pi}\frac{1}{2\pi}\int_{-\pi}^{\pi} H(\psi)X(\theta)\mathrm{j}\theta E(\psi - \theta)\,\mathrm{d}\theta\mathrm{j}\psi E(\omega - \psi)\,\mathrm{d}\psi \end{aligned} \tag{2.104}$$

The double integral in (2.104) specifies the CC. This CC appears at the $TT2$ output due to the CC generated by $TT1$, passed through the filter DF (Fig. 2.11). In the general case, this value has a second order of smallness and can be neglected. So,

for the first approximation, the equation for the output spectrum can be derived with the simple and physically obvious equation

$$Y(\omega) = \frac{1}{2\pi}\int_{-\pi}^{\pi} Y(\psi)H(\omega,\psi)\,\mathrm{d}\psi \tag{2.105}$$

where $H(\omega,\psi)$ is the BF of a DF with non-uniform sampling:

$$H(\omega,\psi) = 2\pi\delta(\omega-\psi)H(\psi) + \mathrm{j}\psi|H(\omega)-H(\psi)|E(\psi-\psi)\,\mathrm{d}\psi \tag{2.106}$$

Function $H(\omega,\psi)$ also contains an SC and a CC. Substituting equation (2.62) into (2.105), we obtain

$$Y(\omega) = H(\omega)X(\omega) + \frac{1}{2\pi}\int_{-\pi}^{\pi} i\psi x(\psi)|H(\omega)-H(\psi)|E(\psi-\psi)\,\mathrm{d}\psi \tag{2.107}$$

The SC of the DFNS output spectrum for small deviations of the sampling period corresponds with the signal spectrum at the output of the corresponding LTI filter. The CC can be calculated by taking the integral from equation (2.107). The integrand components are the input signal spectrum $X(\psi)$, the modulation function of the sampling period $E(\omega)$ and the filter frequency characteristic $H(\omega)$. Consider the next example of DFNS analysis.

Example 2.7: Signal Transformation in DFNS

Consider the case when a sampling period has harmonic modulation relative to T with frequency Ω and modulation index ε, that is, the filter is clocked at the moments

$$T_i = T[1+\varepsilon(\cos\Omega i)] \tag{2.108}$$

Suppose that at the filter input there is a harmonic signal $x(t) = A\cos(\omega_c t)$. Its spectrum is

$$X(\omega) = A\pi[\delta(\omega-\omega_c)+\delta(\omega+\omega_c)] \tag{2.109}$$

The spectrum of the modulating process is

$$E(\omega) = \varepsilon\pi[\delta(\omega-\Omega)+\delta(\omega+\Omega)] \tag{2.110}$$

Substituting these equations into (2.107), we obtain

$$\begin{aligned} Y(\omega) = {} & H(\omega)X(\omega) + \mathrm{j}A\omega_c\varepsilon\frac{\pi}{2}[H(\omega_c+\Omega)-H(\omega_c)]\delta(\omega-\omega_c-\Omega) \\ & + \mathrm{j}A\omega_c\varepsilon\frac{\pi}{2}[H(\omega_c-\Omega)-H(\omega_c)]\delta(\omega-\omega_c+\Omega) \\ & - \mathrm{j}A\omega_c\varepsilon\frac{\pi}{2}[H(-\omega_c+\Omega)-H(-\omega_c)]\delta(\omega+\omega_c-\Omega) \\ & - \mathrm{j}A\omega_c\varepsilon\frac{\pi}{2}[H(-\omega_c-\Omega)-H(-\omega_c)]\delta(\omega+\omega_c+\Omega) \end{aligned} \tag{2.111}$$

The output spectrum contains SCs with frequencies ω_c and CCs with frequencies $\pm\omega_c \pm \Omega$. The amplitudes of the CCs are proportional to the product of ω_c and ε, as well as dependent on $H(\omega)$. The sharper the shape of the filter frequency response, the larger are the CC amplitudes. In the limiting case when $H(\omega) = \text{const}$, the CCs are equal to zero because the filter becomes the serially connected transformers $TT1$ and $TT2$, where the time delays are mutually compensated. In another limiting case, the filter is narrowband with high Q. This filter essentially weakens the signal CCs after $TT1$ and thus

$$\begin{aligned} Y(\omega) = {} & H(\omega)X(\omega) - \mathrm{j}A\omega_c\varepsilon\frac{\pi}{2}H(\omega_c) - H(\omega_c)\delta(\omega - \omega_c - \Omega) - \mathrm{j}A\omega_c\varepsilon\frac{\pi}{2}H(\omega_c) \\ & - H(\omega_c)\delta(\omega - \omega_c + \Omega) + \mathrm{j}A\omega_c\varepsilon\frac{\pi}{2}[H(-\omega_c)]\delta(\omega + \omega_c - \Omega) \\ & + \mathrm{j}A\omega_c\varepsilon\frac{\pi}{2}H(-\omega_c)\delta(\omega + \omega_c + \Omega) \end{aligned} \tag{2.112}$$

Figure 2.12 demonstrates the relations between $|H(\omega)|$ and $|Y(\omega)|$ for the first-order recursive low-pass DFNS. The curve numbers 1 to 3 correspond to the following conditions: 1 for $-\omega_c = \pi/8$, $a_1 = 0.99$, $\Omega = \pi/16$, $\varepsilon = 0.1$; 2 for $-\omega_c = \pi/8$, $a_1 = 0.99$, $\Omega = \pi/16$, $\varepsilon = 0.05$; and 3 for $\omega_c = \pi/8$, $a_1 = 0.5$, $\Omega = \pi/16$, $\varepsilon = 0.1$.

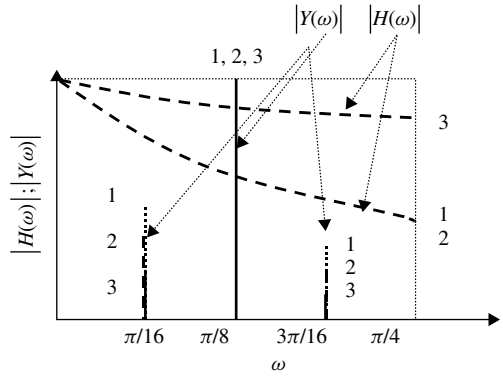

Figure 2.12 Dependence of the output signal spectrum on input frequency

The CC amplitudes of the spectrum $Y(\omega)$ are reduced when Q of the filter and the amplitude of the modulated signal (curves 3 and 2 respectively) become smaller.

2.8.2 Systems with Stochastic Sampling Interval

Consider now the case in which a random stationary discrete process η_1 modulates the periodic sampling signal. As a result, the clock pulses at the sampler occur at time instants $iT + \eta_i T$. Assume that any deviation of the random process η_1 is much less then the regular sampling interval T; this interval satisfies the Nyquist theorem and the system input signal is a random stationary continuous process $\xi(t)$ with power spectrum density (PSD) $F_\xi(\omega)$.

A signal at the system output will be a random process with realizations γ_i. As follows from equation (2.109), for zero-correlated realizations η_i and $\xi(t)$ the spectrum of an appropriate γ_i is [36]

$$\begin{aligned}\gamma(\omega) &= H(\omega)\xi(\omega) + \frac{1}{2\pi}\int_{-\pi}^{\pi} \mathrm{j}\psi\xi(\psi)[H(\omega) - H(\psi)]\eta(\omega - \psi)\,\mathrm{d}\psi \\ &= H(\omega)\xi(\omega) + Z(\omega) \end{aligned} \tag{2.113}$$

where $\xi(\omega)$ and $\eta(\omega)$ are the realizations of Fourier transforms of the random processes $\xi(t)$ and η_i respectively. Multiplying $\gamma(\omega)$ by its complex conjugated value, we obtain

$$\gamma(\omega)\gamma*(\omega) = |H(\omega)|^2\xi(\omega)\xi(\omega) + H(\omega)\xi(\omega)Z(\omega) + H(\omega)\xi(\omega)Z(\omega) + Z(\omega)Z(\omega) \tag{2.114}$$

Converting the product of integrals $Z(\omega)Z(\omega)$ into a double integral, we then obtain

$$\begin{aligned}\gamma(\omega)\gamma*(\omega) = |H(\omega)|^2\xi(\omega)\xi(\omega) + H(\omega)\xi(\omega)Z(\omega) + \frac{1}{4\pi^2}\int_{-\pi}^{\pi} \psi\theta\xi(\psi)\xi(\theta)[H(\omega) \\ - H(\psi)][H(\omega) - H(\theta)]\eta(\omega - \psi)\eta(\omega - \psi)\,\mathrm{d}\theta\,\mathrm{d}\psi \end{aligned} \tag{2.115}$$

The derived integral is a complex combination of the product of random patterns of η, ξ spectrums and their complex conjugate values. The integrating area is shown in Fig. 2.13. It has a rectangular shape with sides 2π on the frequency plane ψ, θ [32].

If an integrand's components are changed so that the inner integral is evaluated along the straight line parallel to the diagonal $\psi = \theta$, then its maximal value lies on the diagonal itself. Along this line, the integrand becomes equal to the product of the squares of the cofactor modules and the integral reaches its highest value

$$Z = \frac{1}{4\pi^2}\int_{-\pi}^{\pi} \psi^{-2}|\xi(\psi)|^2|H(\omega) - H(\psi)|^2|\eta(\omega - \psi)|^2\,\mathrm{d}\psi \tag{2.116}$$

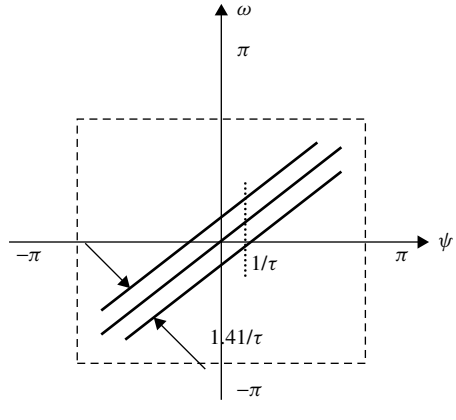

Figure 2.13 Integration area of η, ξ

The integration of the products of the spectrum components and their complex conjugated values (with shifted on ε arguments) is evaluated along the parallel lines $\psi = \theta + \varepsilon$. Such a convolution in frequency domain corresponds to the product of shifted sequences in time domain. After an averaging across the ensemble, we obtain the autocorrelation function of the output random process. If τ_k is a correlation interval of random processes introduced in a number of sampling periods T, then $1/\tau_k$ is an interval of mutual correlation for the spectrum component and its complex conjugate values. That is, for a frequency difference limited by $1/\tau_k$, the integral value along the line parallel to the diagonal can be considered equal to z. For frequency differences that are greater than $1/\tau_k$, an appropriate averaging gives small values tending towards zero. Then, the last term of equation (2.113) can be approximately calculated by multiplying the integral along the diagonal line by the width of the $1.41/\tau$ areas:

$$Z(\omega)Z(\omega)^* = 1.41z/\tau_{ko} \tag{2.117}$$

where τ_{ko} is the smallest interval of correlation for processes η and ξ. Ensemble averaging eliminates the second and third summands in equation (2.114), and the output signal spectrum can then be expressed in the following compact form:

$$F_\gamma(\omega) = |H(\omega)|^2 F_\xi(\omega) + \frac{1.41}{4\pi^2 \tau_{k0}} \int_{-\pi}^{\pi} \psi^2 F_\xi(\omega) |H(\omega) - H(\psi)|^2 F_\eta(\omega - \psi)\, \mathrm{d}\psi \tag{2.118}$$

where $F_\gamma(\omega)$, $F_\xi(\omega)$ and $F_\eta(\omega)$ are the PSDs of processes γ, ξ and η respectively, obtained by the ensemble averaging.

Thus, for a discrete system with random sampling, it is possible to estimate the PSD of the output signal using equation (2.118). Use of this equation assumes that the modulation index of the sampling interval is small, the statistical characteristics of the input and clock signals are known and these processes are non-correlated.

2.9 SUMMARY

This chapter has provided an introduction to the time and frequency analysis of linear time-variant discrete systems. The major goal was not just to present this analysis, but also to select and/or modify various approaches to this analysis in order to use methods as similar as possible to those traditional to descriptions of time-invariant systems. In particular, we examined IRs, GTFs, and GFRs for LTV systems. All these basic characteristics are similar, in some instances, to the corresponding characteristics of LTI systems. The introduction of these functions binds input and output signals in LTV systems in time, frequency and mixed time frequency or z-domains.

The major differences between time-variant and time-invariant systems follow from their parametric nature. The output signal of a time-variant system not only weights input signal spectral components but also generates new ones. Interactions of input signals and variation of the system's parameters – coefficient values and clock intervals – lead to the rather complex behavior of LTV DSs. Perhaps most disappointing

for readers is that for the general case there are no analytical methods to derive all introduced characteristics from appropriate difference equations. In contrast to LTI systems, these characteristics for time-variant systems cannot be represented in closed forms for most cases.

Both GTFs and GFRs not only exist in the transform domains (z and frequency) but also depend on the time. Consequently, new spectral harmonics appear on the system output. This essentially differentiates time-variant and time-invariant systems. Thus, for example, for complex systems that have more than one interconnected stage, this means that the sequence of stage combination becomes critical. Moreover, for LTV DSs, we have to correct the Nyquist criterion taking into account the spectral conversions.

The next chapter will be dedicated to the analysis of LTV DSs with periodically varying coefficients where the system's characteristics can be presented in analytically closed forms. LTV systems with periodically time-varying parameters are the major subject of this book and their analysis is based on the general results and definitions provided in this chapter.

2.10 ABBREVIATIONS

BF	bifrequency function
CC	combinational component
DF	digital filter
DFNS	digital filter with non-uniform sampling
DS	discrete system
GFR	generalized frequency response
GTF	generalized transfer function
IR	impulse response
LPF	low-pass filter
LTI	linear time-invariant
LTV	linear time-variant (or varying)
PSD	power spectrum density
SC	signal component

2.11 VARIABLES

$\sigma_x^2(x)$	variance of a process
ω	normalized frequency
Ω	radial frequency of a sampling period modulation
$\xi(\omega)$, $\eta(\omega)$	Fourier transforms of the random processes' realizations.
$\delta(n, k)$	unit sample sequence
$\xi(t)$, η_i	stationary random processes' realizations
γ_I	output random process realization

Δ_I	discrete process modulating sampling period
τ_k	an interval of correlation for random processes
ω_s	minimal sampling frequency
$a(n)$	time-varying coefficients of the recursive part of a difference equation
$b(n)$	time-varying coefficients of the non-recursive part of a difference equation
f	frequency
$F_\xi(\omega)$	power spectrum density
$F(z, n)$	generalized transfer function of the non-recursive part
$g(m, n)$	impulse response of the recursive part
$G(z)$	generalized transfer function of the recursive part
$H(\psi, \omega)$	bifrequency function
$h(m, n)$	impulse response
$H(z, n)$	generalized transfer function
i, l, m, n, k	integers
$M(n)$	mean value
$R(m, n)$	correlation function
$S(\omega)$	spectral density
T	sampling period
$X(\omega)$, $X(\psi)$	spectrum of the input signal
$X(n)$	input discrete random process
$x(n)$	input signal
$X(z)$	z-transform of the input signal
$Y(\omega)$	spectrum of the output signal
$Y(n)$	output discrete random process
$y(n)$	output signal
$Y(z, n)$	z-transform of the output signal

2.12 REFERENCES

[1] Zadeh LA (1950) Frequency analysis of variable networks. *IRE*, **38**, 291–299.

[2] Zadeh LA (1952) General theory of linear signal transmission. *J. Franklin Inst.*, **253**, 293–312.

[3] Liu B, Franaszec PA (1969) Class of time-varying digital filters. *IEEE Trans.*, **Ct-16**(4), 467–471.

[4] Meyer RA, Burrus CS (1975) Design and implementation of multirate and periodically time-varying filters. *IEEE Trans.*, **Cas-22**(3), 162–168.

[5] Huang NC, Aggarwal JK (1980) On linear shift-variant digital filters. *IEEE Trans.*, **Cas-27**(8), 672–678.

[6] Huang NC, Aggarwal JK (1982) Time-varying digital signal processing: a review, *IEEE Int. Symp. on Cas*, Rome, Italy, 10–12 May, 659–662.

[7] Huang NC, Aggarwal JK (1983) Synthesis and implementation of recursive linear shift-variant digital filters. *IEEE Trans.*, **Cas-30**(1), 29–36.

[8] Huang NC, Aggarwal JK (1981) Frequency-domain consideration of LSV digital filters. *IEEE Trans.*, **Cas-28**(4), 279–287.
[9] Huang NC, Aggarwal JK (1982) A comparison between time and frequency domain techniques for time-varying signal processing, *IEEE Int. Symp. on Assp*, 1, Paris, France, 7–10 May, 1341–1344.
[10] Claassen TA, Mecklenbrauker WFG (1982) On stationary linear time-varying systems. *IEEE Trans.*, **Cas-29**(2), 169–184.
[11] Park SH, Huang NC, Aggarwal JK (1983) One-dimensional time-varying digital filters using two-dimensional techniques. *IEEE Trans.*, **Cas-30**(4), 172–176.
[12] Leou T.-Y, Aggarwal JK (1984) Recursive implementation of LTV filters frozen-time transfer function versus generalized transfer function. *Proc. IEE*, **72**, 980, 981.
[13] Ferrara ER (1985) Frequency-domain implementation of periodically time-varying filters. *IEEE Trans.*, **Assp-33**(4), 883–892.
[14] Saleh BEA, Subotic NS (1985) Time-variant filtering of signals in the mixed time-frequency domain. *IEEE Trans.*, **Assp-33**(6), 1479–1485.
[15] Pei S.-C, Kiang JF (1986) Simple approach for a class of linear time-varying digital filters with generalized delay elements. *IEEE Trans.*, **Cas-33**(5), 676–679.
[16] Leou T.-Y, Aggarwal JK (1986) A structure-independent approach to the analysis of recursive linear time-variant digital filters. *IEEE Trans.*, **Cas-33**(7), 687–696.
[17] Huang NC, Aggarwal JK (1986) Spectral modifications using linear time-varying digital filters, *IEEE Int. Conf. of Assp*, Alabama, 73–76.
[18] Ishii R, Kakishita M (1988) Analysis of a time varying digital filter. *Trans. IEICE*, **J71-A**(2), 288–296.
[19] Erugin N (1988) *Linear Systems of Ordinary Differential Equations: With Periodic and Quasi-Periodic Coefficients*, New York: Academic Press.
[20] Starjinski VM, Yakubovich VA (1972) *Linear Differential Equations with Periodical Coefficients and their Applications*, Moscow: Nauka.
[21] Rozenvasser EN (1973) *Periodically Non-Stationary Systems of Control*, Moscow: Nauka.
[22] D'angelo H (1976) *Linear Time-Varying Systems: Analysis and Synthesis*, Boston: Allyn & Bacon.
[23] Cherniakov M, Rogogkin I, Sizov V (1991) Digital non-stationary filters, *Proc. Electron. Tech.*, **10**(3), 26–32.
[24] Gostev VI, Chinaev PI (1979) *Systems with Periodically Varying Parameters*, Moscow: Energia.
[25] Mihailov FA (1986) *Theory and Methods of Investigation of Non-Stationary Linear Systems*, Moscow: Nauka.
[26] Kawamata M, Yang X, Higuchi T (1992) Fundamental study on periodically time-varying state-space digital filters-statistical analysis, scaling and stability, *IEEE Int. Conf. on Systems Engineering*, New York, USA, 348–351.
[27] Leou TY, Aggarwal JK (1983) Difference equation implementation of time-variant digital filters, *IEEE Int. Conf. on Decision and Control*, 1356, 1357.
[28] Marks RJ, Walkup JF, Hagler MO (1978) A sampling theorem for linear shift-variant systems. *IEEE Trans.*, 1978, **Cas-25**(4), 229–233.
[29] Munson DC, Martin EC (1982) Sampling rate for linear shift-varying discrete-time systems, *IEEE Int. Conf. on Assp*, 1, 7–10 May, 488–491.
[30] Rogozkin IB, Cherniakov M (1991) Characteristics of digital filters with non-uniform sampling. *Radiotechnika*, (5), 35–39.
[31] Cherniakov M, Donskoi L, Sizov V (2000) Sampling theorem for time-varying digital systems, *ICSP2000: Signal Processing*, China, Beijing, 21–25 August, 95–98.
[32] Cherniakov M, Obraztsov A, Rogozkin I (1992) Effect of spectral characteristics of the clock signal on the operation of a digital filter. *Telecommun. Radio Eng.*, **47**(9), 102–105.

[33] Ifeachor EC, Jervis BW (2002) *Digital Signal Processing. A Practical Approach*, UK: Prentice Hall.
[34] Unser M (2000) Sampling – 50 years after Shannon. *Proc. IEEE*, **88**(4), 569–587.
[35] Gorelov GV (1982) *Unregular Sampling of Signals*, Moscow: Radio and Communication.
[36] Rogojkin IB, Cherniakov M (1990) Accuracy estimation of the clock generator noise influence on digital receiver channel, *Int. Conf. on TRASP in Radio-Communication Systems*, Rostov, Russia, 26–30 November, 9–14.

3

Periodically Time-Variant Discrete Systems

Chapter 2 was dedicated to a general consideration of linear time-variant discrete systems (LTV DSs). The only restrictions were that these systems should be causal and stable. In this chapter, the general analysis of LTV DS is adapted for discrete systems with periodically time varying parameters. The major characteristics and parameters of periodically linear time-variant (PLTV) systems, such as impulse response (IR), generalized transfer function (GTF) and sampling frequency, are introduced here. The vitally important problem of the instability of recursive systems is also one of the foci of this chapter. In addition, we will discuss sinusoidal and binary (rectangular) laws of coefficient variation with different on-off factors (q) in PLTV systems.

3.1 DIFFERENCE EQUATION

PLTV DSs are systems that can be described by difference equation (2.1):

$$\sum_{k=0}^{K_1} a_k(n) \cdot y(n-k) = \sum_{k=0}^{K_2} b_k(n) \cdot x(n-k) \tag{3.1}$$

with N-periodical coefficients $a_k(n)$ and $b_k(n)$, which means that

$$a_k(n) = a_k(n+N) \text{ and } b_k(n) = b_k(n+N)$$

or, for an arbitrary integer $l = 0, 1, 2 \ldots$:

$$\sum_{k=0}^{K_1} a_k(n+lN) \cdot y(n-k) = \sum_{k=0}^{K_2} b_k(n+lN) \cdot x(n-k) \tag{3.2}$$

An Introduction to Parametric Digital Filters and Oscillators Mikhail Cherniakov
© 2003 John Wiley & Sons, Ltd ISBN: 0-470-85104-X

In the general case, all or some periods of coefficient variation (N_i), where $i = 0, 1, 2 \ldots K_1 + K_2 + 1$, can be different. However, a description of periodical systems whose coefficient periods are all equal does not reduce the generality of the approach. It is always possible to find a period N that is the lowest common multiple for all N_i. For example, if all N_i are simple numbers, then $N = \prod_{i=0}^{K_1+K_2+1} N_i$. Another simplification assumed in (3.1) and (3.2) is that the periods are *integer* numbers of the sampling interval T. This restriction slightly narrows the class of considered systems. On the other hand, this approach allows us to determine the properties of general systems without solving the difference equation. As will be shown later, this approach does not essentially influence the system's parameters and, more importantly, is technically easily achievable. It also simplifies the solution of the difference equation if it is necessary to calculate this. Consequently, evaluation of the system's performance is also simplified.

3.2 IMPULSE RESPONSE

Consider equation (2.4) for the linear time-invariant (LTI) system impulse response (IR). For time moments shifted on period N of coefficient variation, the equation can be presented in the following format:

$$h(m+N, n+N) = \frac{1}{a_0(n+N)} \left[-\sum_{k=1}^{K_1} a_k(n+N) \cdot h(m+N, n+N-k) + \sum_{k=0}^{K_2} b_k(n+N) \cdot \delta(n-k-m) \right] \tag{3.3}$$

Taking into account the coefficient periodicity in equation (3.2), we obtain

$$h(m+N, n+N) = \frac{1}{a_0(n)} \times \left[-\sum_{k=1}^{K_1} a_k(n) \cdot h(m+N, n+N-k) + \sum_{k=0}^{K_2} b_k(n) \cdot \delta(n-k-m) \right] \tag{3.4}$$

which coincides with equation (2.4). Since only one IR corresponds to the difference equation [1, 2], from equations (2.4) and (3.4), it follows that

$$h(m+N, n+N) = h(m, n) \tag{3.5}$$

This equation simply states that periodically linear time-variant discrete systems (PLTV DSs) have N-periodical impulse responses. Similar relationships are also known in the theory of continuous systems with periodically time-varying coefficients and have an essential impact on systems analysis.

3.3 GENERALIZED TRANSFER FUNCTION AND FREQUENCY RESPONSE

Let us consider equation (2.14) for the generalized transfer function (GTF) at moment n and over the time interval $(n + N)$:

$$H(z, n+N) = \sum_{m=-\infty}^{\infty} h(m, n+N) \cdot z^{m-n-N} \tag{3.6}$$

Substituting equation (3.5) into (2.14) and with $\xi = m + N$, we obtain

$$H(z, n) = \sum_{m=-\infty}^{\infty} h(m+N, n+N) \cdot z^{m+N-n-N} = \sum_{\xi=-\infty}^{\infty} h(\xi, n+N) \cdot z^{\xi-n-N} \tag{3.7}$$

which coincides with equation (3.5). Thus,

$$H(z, n+N) = H(z, n) \tag{3.8}$$

Similarly, it can be easily shown that for the generalized frequency response (GFR)

$$H(\omega, n+N) = H(\omega, n) \tag{3.9}$$

The periodicity of $H(z, n)$ and $H(\omega, n)$ allows us to represent these integral characteristics using a discrete Fourier transform (DFT):

$$H(z, n) = \sum_{k=0}^{N-1} H_k(z) \cdot \mathrm{e}^{\mathrm{j}\Omega kn} \tag{3.10}$$

$$H_k(z) = \frac{1}{N} \sum_{n=0}^{N-1} H(z, n) \cdot \mathrm{e}^{-\mathrm{j}\Omega kn} \tag{3.11}$$

and

$$H(\omega, n) = \sum_{k=0}^{N-1} H_k(\omega) \cdot \mathrm{e}^{\mathrm{j}\Omega kn} \tag{3.12}$$

$$H_k(\omega) = \frac{1}{N} \sum_{n=0}^{N-1} H(\omega, n) \cdot \mathrm{e}^{-\mathrm{j}\Omega kn} \tag{3.13}$$

where $\Omega = 2\pi/N$ is the normalized radial frequency of a system's parameter variation. This frequency Ω will be widely used later in the book.

Here, readers should note that a normalizing multiplier $1/N$ in equations (3.11) and (3.13) is replaced in the equation for the DFT. This allows us to consider the DFT

harmonic at zero frequency as a mean value of the function without an additional amplification by N times, as is generally required by the DFT procedure. This replacement simplifies equations and makes physical interpretation of the results obtained below easier.

3.4 SIGNALS IN PERIODICALLY LINEAR TIME-VARIANT SYSTEMS

PLTV systems are a particular case in the broader class of time-variant systems. Nevertheless, this subclass can be more easily interpreted in mathematical descriptions than the broader class. The periodicity of parameter variation allows the use of the Fourier series, which yields some new general properties, as shown in Section 3.4.1.

3.4.1 Bifrequency Function

From equations (2.40) and (3.12), we can derive the following expression for the bifrequency function (BF) of PLTV DSs:

$$H(\psi,\omega)=\sum_{n=-\infty}^{\infty}\sum_{k=o}^{N-1}H_k(\psi)\cdot \mathrm{e}^{\mathrm{j}nk\Omega}\cdot \mathrm{e}^{\mathrm{j}(\psi-\omega)n}=\sum_{k=0}^{N-1}H_k(\psi)\sum_{n=-\infty}^{\infty}\mathrm{e}^{\mathrm{j}(\psi+k\Omega-\omega)n} \quad (3.14)$$

Let us consider the internal sum as a spectrum of the sampled harmonic signal with frequency $\psi+k\Omega$, which is equal to $2\pi\delta(\psi+k\Omega-\omega)$. We can now represent the BF as

$$H(\psi,\omega)=2\pi\sum_{k=0}^{N-1}H_k(\psi)\cdot\delta(\psi+k\Omega-\omega) \quad (3.15)$$

The physical meaning of this expression is that new spectral components appear within PLTV systems. They present in the output signal as the modulation constituents of the input signal. These new components are centred on the input signal spectrum components being shifted on frequencies $\pm k\Omega$, which are multiples of the main frequency of coefficient variation Ω. This is an *important feature* of time-variant systems. We will come back to this problem later in the chapter.

3.4.2 Deterministic Signal Processing

Let there be a discrete deterministic signal $x(n)$ with spectrum $X(\omega)$ at the input of a periodically time-variant system. The spectrum of the output signal $Y(\omega)$ is determined by equation (2.38), and taking into account equation (3.15),

$$Y(\omega)=\frac{1}{2\pi}\int_{-\pi}^{\pi}X(\psi)\cdot 2\pi\sum_{k=0}^{N-1}H_k(\psi)\cdot\delta(\psi+k\Omega-\omega)\,\mathrm{d}\psi$$

$$= \sum_{k=0}^{N-1} X(\omega - k\Omega) \cdot H_k(\omega - k\Omega) \tag{3.16}$$

For a better understanding of these important equations consider the following examples.

Example 3.1: Harmonic Input Signal

For the harmonic input signal $x(n) = e^{j\omega_0 n}$ with spectrum $X(\psi) = 2\pi\delta(\psi - \omega_0)$, the spectrum of the output signal spectrum is

$$Y(\omega) = 2\pi \sum_{k=0}^{N-1} H_k(\omega_0) \cdot \delta(\omega_0 + k\Omega - \omega) \tag{3.17}$$

The spectrum of the output signal in the general case has non-zero components with amplitude $2\pi H_k(\omega_0)$ at the frequencies $\omega = \omega_0 + k\Omega$. So, if at the input only one harmonic ω_0 presents, the output signal contains a number of harmonics concentrated around the central frequency ω_0, corresponding to the input signal. In time domain this output signal can be obtained by the inverse Fourier transform:

$$y(n) = e^{j\omega_0 n} \sum_{k=0}^{N-1} H_k(\omega_0) \cdot e^{jkn\Omega} \tag{3.18}$$

Example 3.2: Sinusoidal Input Signal

The spectrum of the sinusoidal signal $x(n) = \sin(\omega_0 n)$ has two harmonic components:

$$X(\psi) = \pi\delta(\psi - \omega_0) + \pi\delta(\psi + \omega_0) \tag{3.19}$$

The output signal spectrum for the sinusoidal input signal is

$$\begin{aligned} Y(\omega) = {} & \pi \sum_{k=0}^{N-1} H_k(\omega_0) \cdot \delta(\omega_0 + k\Omega - \omega) \\ & + \pi \sum_{k=0}^{N-1} H_k(-\omega_0) \cdot \delta(-\omega_0 + k\Omega - \omega) \end{aligned} \tag{3.20}$$

Non-zero components of the output spectrum exist for frequencies $\omega = k\Omega \pm \omega_0$. Spectrums of the input and output signals are shown in Fig. 3.1 to illustrate the example.

Let us analyse the output signal spectrum presented by equation (3.20) and the GFR of a PLTV DS described by equation (3.10) to introduce a physical sense of the different GFR components $H_k(\omega)$.

1. From equation (3.16), it can be noted that the $H_k(\omega)$ component for $k = 0$ is, in some instances, similar to the frequency response of a system with constant coefficients. $H_0(\omega)$ represents the relationships between the output spectrum components and the

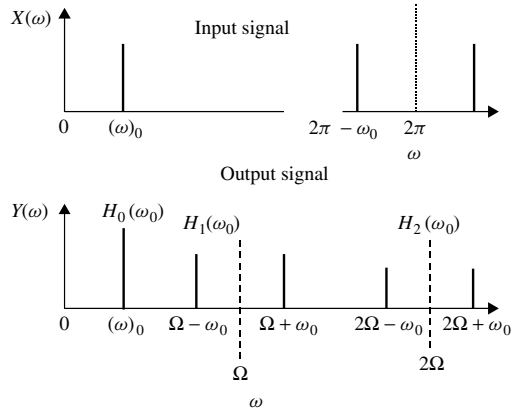

Figure 3.1 Output signal spectrum in a PLTV DS

input signal spectrum at the coinciding frequencies. This component of the GFR is not responsible for any spectrum conversion but just weights the input signal's harmonics phases and amplitudes. This GFR component ($k = 0$) is called the *signal component* (SC) and $H_0(\omega)$ is an *equivalent frequency response* (EFR) of the PLTV DS. This name reflects some similarity between time-invariant and time-variant systems.

2. The GFR $H_k(\omega)$ for $k \neq 0$ describes the conversion of input signal spectrum components into output signal spectrum combinational frequencies $\omega = \psi + k\Omega$, which are the new spectral components that originated within the time-variant system. Amplitudes and phases of these new frequency components relate to the input signal spectrum as well as $H_k(\omega)$. These output signal spectrum components as well as appropriate components of GFRs $H_k(\omega)$ are called *combinational components* (CCs). The new output signal spectrum components or CCs are multiplicative as they appear only when the input signal presents and are directly related to the input signal spectrum.

It is a property of DFTs that the spectrum shift on frequency $k\Omega$ corresponds to the multiplication of the input signal by function $e^{jkn\Omega}$ in time domain. So, equation (3.16) can be represented by an equivalent system, the block diagram of which is shown in Fig. 3.2.

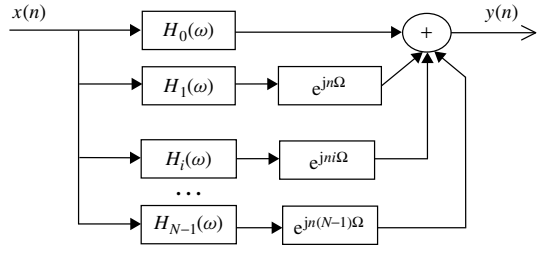

Figure 3.2 An equivalent structure for a PLTV DS

An equivalent block diagram of a PLTV DS contains N parallel channels. In each of these channels the frequency response $H_k(\omega)$ is constant, and the signal frequency is shifted (in frequency domain) on $k\Omega$. The structure is similar to the well-known representation of continuous periodical systems [3] with the exception that the number of channels is limited for N. This structure is the basis of one of the possible approaches to the synthesis of PLTV DSs using some equivalent linear time-invariant digital systems, where $H_k(\omega)$ can be calculated by equation (3.13).

3.4.3 Random Signals Processing

Consider now the response of periodically time-variant systems when an input signal is a random process $x(n)$. Assume that it is a wide sense stationary process with known mean value $M_X(n) = M_X$, variance $\sigma_X^2(n) = \sigma_X^2$, correlation function $R_X(\tau)$ and $S_X(\omega)$.

Parameters of the output random process can be determined using equations (2.56), (2.62) and (2.63) and taking into account that an appropriate GFR, described by equation (3.9), is an N-periodical function:

$$M_Y(n) = M_X \cdot H(0, n) = M_X \cdot H(0, n + N) = M_Y(n + N) \tag{3.21}$$

$$\begin{aligned}\sigma_Y^2(n) &= \frac{1}{2\pi}\int_{-\pi}^{\pi} S_X(\omega) \cdot |H(\omega, n)|^2 \,\mathrm{d}\omega \\ &= \frac{1}{2\pi}\int_{-\pi}^{\pi} S_X(\omega) \cdot |H(\omega, n + N)|^2 \,\mathrm{d}\omega = \sigma_Y^2(n + N)\end{aligned} \tag{3.22}$$

and

$$\begin{aligned}R_Y(\tau, n) &= \frac{1}{2\pi}\int_{-\pi}^{\pi} S_X(\omega) \cdot H(\omega, n) \cdot H(-\omega, n - \tau) \cdot \mathrm{e}^{-\mathrm{j}\omega\tau} \,\mathrm{d}\omega \\ &= \frac{1}{2\pi}\int_{-\pi}^{\pi} S_X(\omega) \cdot H(\omega, n + N) \cdot H(-\omega, n + N - \tau) \cdot \mathrm{e}^{-\mathrm{j}\omega\tau} \,\mathrm{d}\omega \\ &= R_Y(\tau, n + N)\end{aligned} \tag{3.23}$$

So, the output process is cyclostationary [4] or periodically non-stationary [5].

The correlation function $R_Y(\tau, n)$ of the output signal of the system depends not only on τ but also on the discrete time of observation n. To find an appropriate PSD of the output process $S_Y(\omega)$, the time mean value of the correlation function $R_{Y0}(\tau)$ can be found by averaging the correlation function over the period N:

$$R_{Y0}(\tau) = \frac{1}{N}\sum_{n=0}^{N-1} R_Y(\tau, n) \tag{3.24}$$

Combining equations (3.23), (3.24) and (3.12), we obtain

$$R_{Y0}(\tau) = \frac{1}{N}\sum_{n=0}^{N-1}\frac{1}{2\pi}\int_{-\pi}^{\pi} S_X(\psi) \cdot \sum_{i=0}^{N-1} H_i(\psi) \cdot \mathrm{e}^{\mathrm{j}\Omega i n} \cdot \sum_{k=0}^{N-1} H_k(\psi) \cdot \mathrm{e}^{\mathrm{j}\Omega k(n-\tau)} \cdot \mathrm{e}^{\mathrm{j}\psi\tau} \,\mathrm{d}\psi \tag{3.25}$$

or, changing the integration and summation order and taking into account that

$$\frac{1}{N}\sum_{n=0}^{N-1} e^{j\Omega n(k+i)} = \delta(i+k) \tag{3.26}$$

is a delayed unit sample sequence, we obtain

$$R_{Y0}(\tau) = \frac{1}{2\pi}\int_{-\pi}^{\pi} S_X(\psi)\cdot\sum_{k=0}^{N-1} H_{-k}(\psi)\cdot H_k^*(\psi)\cdot e^{j(\psi-k\Omega)\tau}\,d\psi \tag{3.27}$$

Then, substituting

$$H_{-k}(\psi)\cdot H_k^*(\psi) = |H_k(\psi)|^2 \tag{3.28}$$

into (3.27) we finally obtain

$$R_{Y0}(\tau) = \frac{1}{2\pi}\int_{-\pi}^{\pi} S_X(\psi)\cdot\sum_{k=0}^{N-1} |H_k(\psi)|^2\cdot e^{j(\psi-k\Omega)\tau}\,d\psi \tag{3.29}$$

According to the Wiener–Khintchine theorem,

$$\begin{aligned} S_Y(\omega) &= \sum_{\tau=-\infty}^{\infty} R_{Y0}(\tau)\cdot e^{-j\omega\tau} \\ &= \frac{1}{2\pi}\int_{-\pi}^{\pi} S_X(\psi)\cdot\sum_{k=0}^{N-1}|H_k(\psi)|^2\cdot\sum_{\tau=-\infty}^{\infty} e^{-j\omega\tau}\cdot e^{j(\psi-k\Omega)\tau}\,d\psi \end{aligned} \tag{3.30}$$

Considering summation along τ as the spectrum of a sampling signal with frequency $\psi - k\Omega$ equal to $2\pi\cdot\delta(\psi - k\Omega - \omega)$, we obtain

$$S_Y(\omega) = \sum_{k=0}^{N-1} S_X(\omega + k\Omega)\cdot|H_k(\omega + k\Omega)|^2 \tag{3.31}$$

So, for a wide sense stationary input signal, the output process PSD in N-periodically linear time-variant discrete systems contains N shifted by frequencies $k\Omega$ multiplicative spectrum components. The magnitudes of these new spectral components are proportional to the square of the corresponding GTF.

From equation (3.31) it follows that the representation of a PLTV DS by an equivalent block diagram, shown in Fig. 3.2 and derived initially for deterministic input processes, is also valid for wide sense stationary input random processes. In this case, the power spectrum of the output process (Fig. 3.3) is similar to that given in Fig. 3.1.

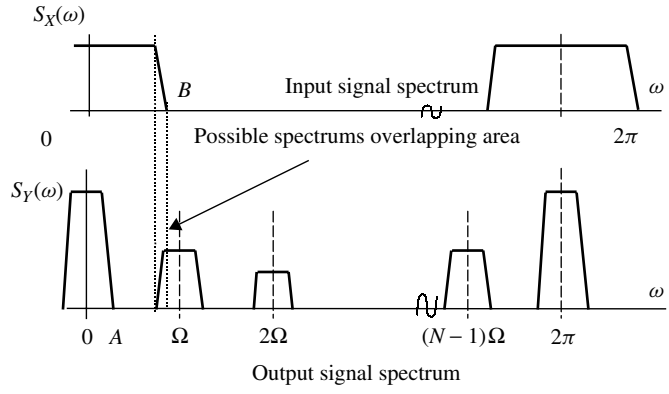

Figure 3.3 Output signal spectrums in a PLTV DS for a random input signal

3.5 GENERALIZATION OF THE SAMPLING THEOREM

From the previous section, we now know how to evaluate an output signal spectrum in PLTV DSs. Let us come back to the problem of signal sampling in these systems. We have already discussed that for time-invariant systems there is the accurate approach to the choice of sampling frequency. Because of discretization, a signal spectrum becomes periodical in frequency domain with the period equal to the sampling frequency. If there is no overlap between spectrums separated by the sampling frequency, the system output signal can be reconstructed without information losses. Ideally, a filter with a break-wall frequency response should be used for the reconstruction with the cut-off frequency equal to half the sampling rate. Using this approach PLTV DSs can be analysed [3].

In contrast to time-invariant discrete systems, in time-variant systems there is a frequency conversion of the input signal spectral components. In the general case, the output signal contains not only input signal spectral components but also new combinational components. Possible overlapping of these CCs should also be taken into account when the sampling frequency is estimated. So, we are dealing with two fundamental frequencies: B, which specifies the input signal bandwidth, and Ω, which determines the rate of parameter variation.

To analyse sampling problems in PLTV DSs, we will use the geometrical approach applied earlier. Recalling that this approach is an illustrative method at the quality level and not a mathematical proof, consider equation (3.15) and assume that a region where $H_0(\psi) \neq 0$ is limited by $\psi \in \{-A \ldots A\}$. The other GFR components, $H_k(\psi)$ and $k \neq 0$, are also limited in this case: $H_k(\psi) \neq 0$ for $\psi \in \{k\Omega - A \ldots k\Omega + A\}$. To better visualize this, consider an example of an appropriate bifrequency map.

Example 3.3: Bifrequency Map for $N = 3$

Projection of a bifrequency map on the plane $\psi - \omega$ for a PLTV DS is shown in Fig. 3.4. For the problem under consideration, the particular shape of the GFR is not

important. The only essential part of the frequency response is the region where the GFR's components are not equal to zero. In the example, the period of coefficients variation is chosen to cover three sampling periods, that is, $N = 3$ or $3T$. Bold lines correspond to the SCs or $H_0(\psi)$, while the other lines represent CCs or $H_i(\psi)$. Non-zero values of the bifrequency characteristic are placed along the line $\omega = k\Omega + \psi$.

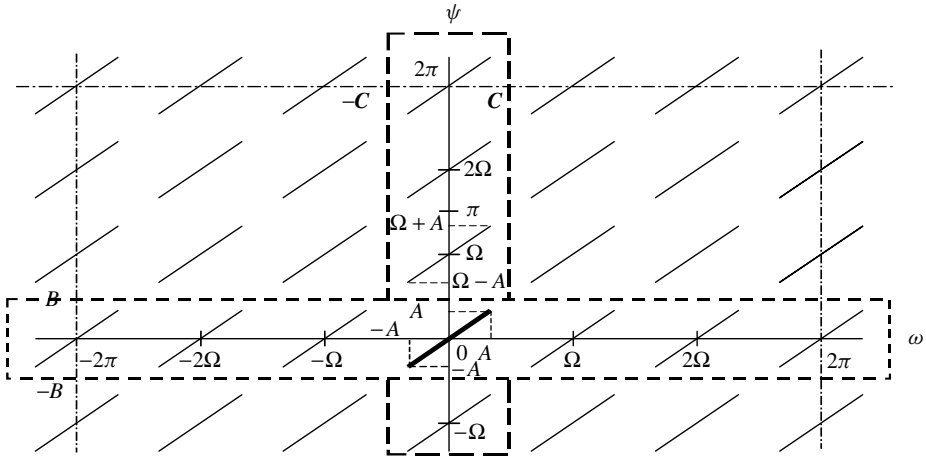

Bifrequency map for PLTV DS

(a)

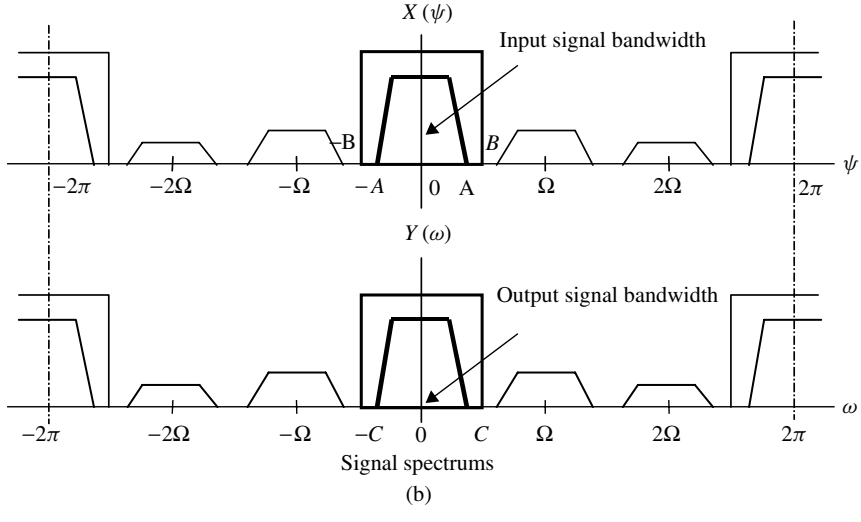

Signal spectrums

(b)

Figure 3.4 Spectrum diagram for the case with no aliasing

As mentioned above, two situations are possible: when output signal spectrums overlap or when there is no spectrum overlapping. Figure 3.4 represents a PLTV DS for which the input signal spectrum bandwidth is restricted by $B - X(\psi) \in \{-B \ldots B\}$

and satisfies the condition $B \leq \Omega/2 = \pi/N$. This condition corresponds to the case of non-overlapping output spectrums and, consequently, the output signal can be reconstructed by a filter with cut-off frequency $C - \omega \in \{-C \ldots C\}$ where $C \leq \Omega/2$.

Figure 3.4a shows a bifrequency map of this system, and Fig. 3.4b demonstrates projections of the bifrequency characteristic on the axis of the output ψ and input ω frequencies. As can be seen directly from the figure, there is no aliasing in the PLTV DS output spectrum. So, the requirements for the sampling frequency in PLTV DSs can be formulated: the sampling frequency should be at least twice higher than the frequency of parameter variation in PLTV DSs. This statement can be considered a generalization of the sampling theorem for PLTV DSs. Such systems are also known as *multi-rate digital filters* [2, 6].

This criterion of sampling frequency selection does not take into account the filtering properties of the systems under consideration. Assume now that a PLTV DS is acting as a narrowband filter. This assumption means that the $H_0(\psi)$ passband is less than the spectrum bandwidth B occupied by the input signal. In this case, the frequency band of the output signal is narrower than the frequency band of the input signal: $A < B$ (see in Fig. 3.4b). For this very practical situation, the discrete input signal spectrum components can partly overlap. These overlapping components are filtered out by the system and do not appear at the output. In this case, it is possible to reduce the sampling frequencies of the input and output signals till the normalized frequency value satisfies the condition $A = \pi/N$, where A is the PLTV filter cut-off frequency.

Let us now analyse a system with the spectrum overlapping. As has been shown, the PLTV DS output spectrum contains spectral components coinciding with the components of the corresponding spectrum of the input signal (frequency band B) as well as combinational spectral components concentrated around frequencies $k\Omega$. If the input signal bandwidth increases, its spectrum components and the CCs originating within the PLTV DS may overlap. This case is shown in Fig. 3.3, where the input signal spectrum occupies band B (upper part of the figure), which is approximately equal to Ω and partly overlaps with CCs.

A case of full spectrum aliasing is shown in Fig. 3.5, where the input signal occupies frequency band B, which is equal to one-half of the sampling frequency. This is the lowest boundary for sampling frequency, according to the Nyquist criteria, for time-invariant systems, and too low a sampling frequency for the time-variant case.

Now let us try to evaluate the consequences of the input signal spectrum overlapping with the new spectral components generated within a time-variant system. We will show that these consequences are different from those in the case of spectrums overlapping in time-invariant systems. The differences follow from the fact that the level of signal components, which is proportional to $H_0(\psi)$, is essentially different to the level of CCs, which is proportional to $H_i(\psi)$. Moreover, in many practical situations the following inequality is true: $|H_0(\psi)| > |H_i(\psi)|$, where $i \neq 0$.

Let us assume that not all newly generated spectral components at the system output are desirable parts of the output waveform. CCs of the output signal that have penetrated the frequency band of the desired signal cannot be filtered out and affect systems in a way similar to a multiplicative interference (or distortion, depending on

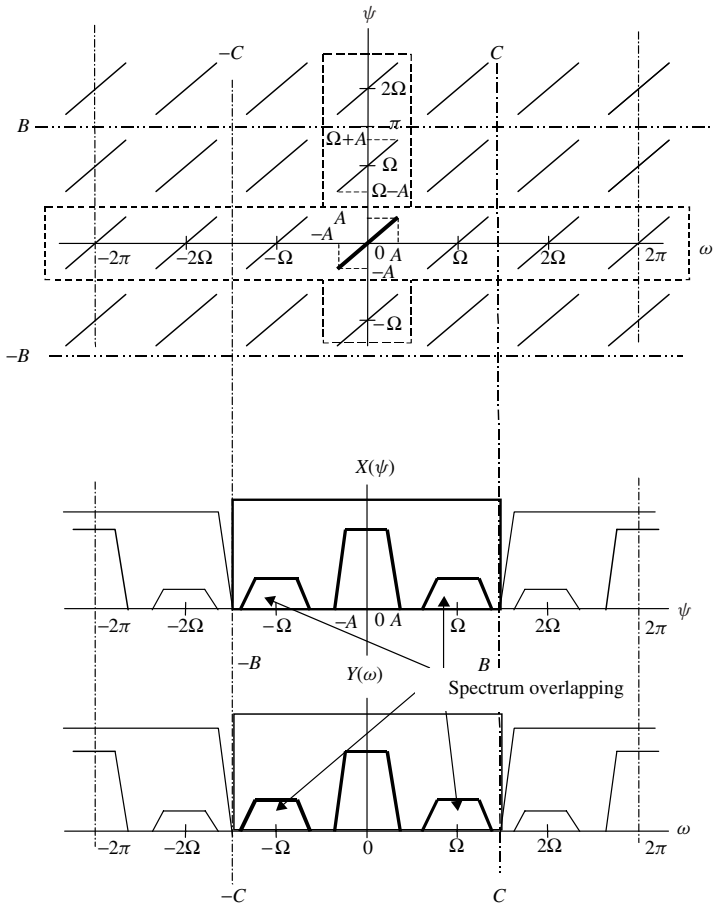

Figure 3.5 Spectrum diagram for the case with aliasing

applications). To estimate deterioration of the signal-to-interference ratio (SIR), we can calculate the ratio of the power of all CCs to the power of the useful output signal components along the whole frequency band:

$$\rho = \frac{\displaystyle\int_0^{2\pi} \sum_{k=1}^{N-1} S_X(\omega + k\Omega) \cdot |H_k(\omega + k\Omega)|^2 \cdot \mathrm{d}\omega}{\displaystyle\int_0^{2\pi} S_X(\omega) \cdot |H_0(\omega)|^2 \cdot \mathrm{d}\omega} \tag{3.32}$$

Assuming for the first approximation that the PSD of the input signal $S_X(\omega) = S$ is constant over the whole frequency band, equation (3.32) can be simplified to

$$\rho = \frac{\displaystyle\sum_{k=1}^{N-1} \int_0^{2\pi} |H_k(\omega + k\Omega)|^2 \cdot \mathrm{d}\omega}{\displaystyle\int_0^{2\pi} |H_0(\omega)|^2 \cdot \mathrm{d}\omega} \tag{3.33}$$

From this equation it follows that SIR reduction depends mainly on the characteristics of the PLTV system under consideration and, in particular, on its GFR. Let us call this coefficient ρ *the integral level of combinational components.*

3.6 SYSTEM STABILITY

The stability of systems with feedback, in general, and the stability of recursive filters, in particular, are critically important issues for system design. For practical applications, it is essential not only to obtain stability but also to have some spare stability. The reason is that even digital systems with 32 to 64 and more bits in words and the presentation of calculations cannot be considered ideal systems. They contain noise, quantization errors, round-off errors of mathematical operations and so on.

3.6.1 General Stability Problem

The stability of systems with time-varying parameters differs considerably from the stability of similar systems with constant parameters. Thus, before studying systems with time-varying coefficients it is necessary to analyse their stability. In general, this analysis is based on the classical definition of stability [7].

Of the few stability definitions, we will use the more physically descriptive definition based on the second Liapunov method [8–10]. The solution is derived from the behaviour of a system function, the state vector that manifests physically as "generalized" energy. If the system is led out of an equilibrium state and the energy of the system is constantly decreasing, then the system is stable; otherwise it is unstable.

Information about LTV digital recursive systems (DRSs) can be found in different publications, which offer methods for stability analysis that are complicated [11, 12] or have limited application [13, 14]. In contrast, a method using a discrete transient matrix to estimate the stability of continuous analog systems with periodically time-varying parameters [9, 15] is distinguished by its simplicity and easy visualization. This method has been adapted to analyse the stability of periodically linear time-variant discrete systems. It is based on eigenvalue analysis of the monodromy matrix (MM) [16], which is a transient state matrix for a given time interval and control signal (CS). The control signal is a new term introduced in this book and will be widely used in Chapters 6 and 7. Here, CS corresponds to a function describing the law of coefficient variation in the corresponding difference equation (2.1). It is introduced by analogy with a "pumping signal" used in the description of parametrical systems [17]. Introduction of this term indicates the connection between the digital systems considered here and the well-studied analog parametric systems, such as the RLC resonator with a time-varying capacitor. This representation of the law of parameter variation as an external CS will be very convenient to use later in the book when digital parametric oscillators are discussed.

3.6.2 Selection of Stability Criteria

For stability analysis, it is convenient to operate with the difference equation represented in the matrix notation. Substituting $y_1(i) = y(i)$, $y_2(i) = y_1(i-1), \ldots, y_n(i) = y_{n-1}(i-1)$, the uniform part of the difference equation of an arbitrary order

$$\sum_{k=0}^{K} a_k(n) \cdot y(n-k) = 0 \tag{3.34}$$

can be represented as a system of uniform difference equations of the first order:

$$\begin{cases} y_1(i) = -a_1(i)y_1(i-1) - a_2(i)y_2(i-1) - \cdots - a_n(i)y_n(i-1) = 0 \\ \qquad y_2(i) = y_1(i-1) \\ \qquad \cdots\cdots\cdots\cdots\cdots\cdots \\ \qquad y_n(i) = y_{n-1}(i-1) \end{cases} \tag{3.35}$$

In matrix notation, equation (3.35) can be represented as

$$\begin{bmatrix} y_1(i) \\ y_2(i) \\ \cdots\cdots\cdots \\ y_n(i) \end{bmatrix} = \begin{bmatrix} -a_1(i) & -a_2(i) & \ldots & -a_{n-1}(i) & -a_n(i) \\ 1 & 0 & \ldots\ldots & 0 & 0 \\ \cdots & \cdots & \cdots & \cdots & \cdots \\ 0 & 0 & \ldots\ldots & 1 & 0 \end{bmatrix} \cdot \begin{bmatrix} y_1(i-1) \\ y_2(i-1) \\ \ldots\ldots \\ y_n(i-1) \end{bmatrix} \tag{3.36}$$

or

$$[Y(i)] = [A(i)][Y(i-1)] \tag{3.37}$$

where, in terms of state space, $[Y(i)]$ and $[Y(i-1)]$ are n dimension state vectors of the system at moments i and $i-1$, respectively. $[A(i)]$ is a matrix of state variation for the system of n by n size, connecting system states at moments i and $i-1$ [18].

In cases of coefficient variation in LTV systems, $[A(i)]$ is a time-varying matrix, determined by coefficient values. For the known initial conditions $[Y(0)]$ and coefficients $a_{1,2}(i)$, it is possible to determine the state vector of the system at an arbitrary time moment k by the following recurrent calculations:

$$[Y(k)] = [A(k)][Y(k-1)] = [A(k)][A(k-1)][Y(k-2)] = \prod_{i=k}^{1} [A(i)][Y(0)] \tag{3.38}$$

According to the second Liapunov method, the stability of solutions of equation (3.38) can be estimated by assessing in time domain a behaviour of the state vector norm's (SVN) function:

$$\|Y(k)\| = (y_1^2(k) + y_2^2(k) + \cdots + y_n^2(k))^{1/2} \tag{3.39}$$

whose parameters will be specified later. The decrease of this function along the trajectory of movement after its displacement from the equilibrium state near the

base of the co-ordinate guarantees the similar behaviour of the SVN itself, that is, $\|Y(k)\| \to 0$ for $k \to \infty$.

When the CS is a deterministic function, each $[Y(0)]$ corresponds to only one possible trajectory. For a random CS, each given $[Y(0)]$ corresponds to a different trajectory, depending on the CS realization. For a stochastic system we can also introduce a function characterizing "generalized" energy, similar to the deterministic case. However, it is necessary to determine the function's integral behaviour along the ensemble. Then, the system described by equation (3.38) can be considered stable by stochastic means if the mean energy does not increase in time [19].

According to the definition given in [20], we can consider the solution of equation (3.38) as

1. p-stable, if for any $\varepsilon > 0$, $r > 0$ can be found such that for $k \geq k_0$, $M\|Y(0)\| < r$:

$$M\|Y(k)\|^p < \varepsilon \quad (p > 0) \tag{3.40}$$

   where $M(\cdot)$ is a mathematical mean of the pth order SVN.

2. Asymptotically p-stable, if it is p-stable and, in addition, for the small $\|Y(0)\|$

$$M(\|Y(k)\|^p) \to 0 \text{ for } k \to \infty \tag{3.41}$$

   is true.

In this book, we consider the stability in terms of the mean square ($p = 2$). We will investigate the behaviour of the SVN mean square, since this kind of Liapunov function is well matched with the "generalized" energy accumulated by the system.

3.6.3 Stability Evaluation

The problem of calculating the SVN square mean requires consideration of the mean of the Kroneker [21] square matrix $\prod_{i=k}^{1}[A(i)]$:

$$\begin{bmatrix} y_1^2(k) \\ y_1(k)y_2(k) \\ \cdots\cdots \\ y_1(k)y_n(k) \\ \cdots\cdots \\ y_n(k)y_1(k) \\ \cdots\cdots \\ y_n^2(k) \end{bmatrix} = M \left[\left[\prod_{i=k}^{1} [A(i)] \right]^{[2]} \begin{bmatrix} y_1^2(0) \\ y_1(0)y_2(0) \\ \cdots\cdots \\ y_1(0)y_n(0) \\ \cdots\cdots \\ y_n(0)y_1(0) \\ \cdots\cdots \\ y_n^2(0) \end{bmatrix} \right] \tag{3.42}$$

where $[\cdot]^{[2]}$ indicates a Kroneker square. By the definition for an arbitrary matrix $[C]$

$$[C]^{[2]} = \begin{bmatrix} C_{11} & C_{12} & \dots & C_{1/2} \\ C_{21} & C_{22} & \dots & C_{2/2} \\ \dots & \dots & \dots & \dots \\ C_{n1} & C_{n2} & \dots & C_{nn} \end{bmatrix}^{[2]} = \begin{bmatrix} C_{11}[C] & C_{12}[C] & \dots & C_{1/2}[C] \\ C_{21}[C] & C_{22}[C] & \dots & C_{2/2}[C] \\ \dots & \dots & \dots & \dots \\ C_{n1}[C] & C_{n2}[C] & \dots & C_{nn}[C] \end{bmatrix} \tag{3.43}$$

is a matrix of the order $n^2 \times n^2$.

As a result of the independency of $[Y(0)]$ and $\prod_{i=k}^{1} [A(i)]$ we can write

$$\begin{bmatrix} y_1^2(k) \\ y_1(k)y_2(k) \\ \dots\dots \\ y_1(k)y_n(k) \\ \dots\dots \\ y_n(k)y_1(k) \\ \dots\dots\dots \\ y_n^2(k) \end{bmatrix} = M \left[\left[\prod_{i=k}^{1} [A(i)] \right]^{[2]} \cdot M \begin{bmatrix} y_1^2(0) \\ y_1(0)y_2(0) \\ \dots\dots \\ y_1(0)y_n(0) \\ \dots\dots \\ y_n(0)y_1(0) \\ \dots\dots\dots \\ y_n^2(0) \end{bmatrix} \right] \tag{3.44}$$

Taking into account that

$$\left[\prod_{i=k}^{1} [A(i)] \right]^{[2]} = \prod_{i=k}^{1} [A(i)]^{[2]} \tag{3.45}$$

we obtain a mean square value of SVN:

$$\begin{bmatrix} y_1^2(k) \\ y_1(k)y_2(k) \\ \dots\dots \\ y_1(k)y_n(k) \\ \dots\dots \\ y_n(k)y_1(k) \\ \dots\dots\dots \\ y_n^2(k) \end{bmatrix} = M \left[\left[\prod_{i=k}^{1} [A(i)] \right]^{[2]} \cdot M \begin{bmatrix} y_1^2(k) \\ y_1(k)y_2(k) \\ \dots\dots \\ y_1(k)y_n(k) \\ \dots\dots \\ y_n(k)y_1(k) \\ \dots\dots\dots \\ y_n^2(k) \end{bmatrix} \right] \tag{3.46}$$

Thus, according to the criterion formulated in equations (3.40) and (3.41), a linear time-variant digital recursive system is stable in the mean square if

$$\lim_{k \to \infty} M \left[\prod_{i=k}^{1} [A(i)]^{[2]} \right] = [\varepsilon] \tag{3.47}$$

where all elements $\varepsilon_{mn} < \infty$, and are asymptotically stable in the mean square if

$$\lim_{k\to\infty} M\left[\prod_{i=k}^{1}[A(i)]^{[2]}\right] = [0] \tag{3.48}$$

Now, we can apply this method of system stability evaluation for a particular system with a known law of coefficient variation or, in other words, for a given control signal.

3.6.4 Stability of Parametric Recursive Systems

Consider a periodically linear time-variant digital recursive system. The matrix of state variation $[A(i)]$ is obviously periodical, with the period N equal to the lowest common multiple of the periods of variation of coefficients $a_{1,2}(i)$ [22, 23]. The evaluation of stability is reduced to the analysis of the following expression:

$$\lim_{k\to\infty}\left[\prod_{i=k}^{1}[A(i)]^{[2]}\right] \tag{3.49}$$

The limit calculation in the equation can be considerably simplified if we use the notion of a system monodromy matrix [24]. For a periodically linear time-variant digital recursive system (PLTV DRS) this is a matrix $[C(N,0)]$ that connects arbitrary states of the system, separated by the interval N that is the period of coefficient variation:

$$[C(N,0)] = \prod_{i=N}^{1}[A(i)] = \prod_{i=N+1}^{2}[A(i)] = \prod_{i=mN+q}^{(m-1)N+q+1}[A(i)] \tag{3.50}$$

Then equation (3.47) takes the form

$$\lim_{k\to\infty}\left[\prod_{i=k}^{1}[A(i)]^{[2]}\right] = \lim_{k\to\infty}\left[[C(N,0]^{[2]}\right]^{k/N} \tag{3.51}$$

This expression is limited (equal to 0) if all eigenvalues of matrix $[C(N,0)]^{[2]}$ satisfy the following conditions: $|\delta_1, \delta_2, \ldots, \delta_n^2| \le 1$. According to the definition given in [21], eigenvalues $[C(N,0)]^{[2]}$ are pairwise products of the form $\delta = \lambda_j\lambda_l$, where λ_j, λ_l are eigenvalues of the matrix $[C(N,0)]$. From the condition $|\delta_1, \delta_2, \ldots, \delta_n^2| \le 1$ directly follows another rather simple requirement for calculating the monodromy matrix eigenvalues: $|\lambda_1, \lambda_2, \ldots, \lambda_n| \le 1$. Thus, the stability of a discrete parametric recursive system can be determined from eigenvalues $\lambda_1, \lambda_2, \ldots, \lambda_n$ of the MM $[C(N,0)]$:

1. If all $|\lambda_1, \lambda_2, \ldots, \lambda_n| \leq 1$, then the system is stable (asymptotically), or
2. If at least one of the eigenvalues $|\lambda_1, \lambda_2, \ldots, \lambda_n| > 1$, then the system is not stable.

Eigenvalues $\lambda_1, \lambda_2, \ldots, \lambda_n$ are determined from the characteristic equation [9]

$$\det [[C(N, 0)] - \lambda[I_n]] = 0 \tag{3.52}$$

where $[I_n]$ is a unit matrix $n \times n$. From this equation we obtain

$$\lambda^n + d_1\lambda^{n-1} + \cdots + d_{n-1}\lambda + d_n = 0 \tag{3.53}$$

Coefficients $d_1, d_2, \ldots, d_n$ of the characteristic equation are expressed through the elements of the matrix $[C(N, 0)]$. Coefficient d_1 is equal to the sum of the elements of the main diagonal (trace Tr of the matrix $[C(N, 0)]$) with a negative sign:

$$d_1 = -\mathrm{Tr}_1 \tag{3.54}$$

and d_n is equal to the determinant of the matrix $[C(N, 0)]$. Other coefficients are determined using the recursive formula:

$$d_m = -\frac{1}{m}(d_m\mathrm{Tr}_1 + d_{m-1}\mathrm{Tr}_2 + \cdots + d_1\mathrm{Tr}_{m-1} + \mathrm{Tr}_m) \tag{3.55}$$

where Tr_m is a trace of the matrix $[C(N, 0)]^m$. Calculation of d_n is considerably simplified by taking into account that the determinant of the matrix $[C(N, 0)]$ (see equation (3.50)) is a product of matrixes $[A(i)]$ and is equal to the product of the determinants [25]. In our case,

$$\det[A(i)] = a_n(i) \tag{3.56}$$

Then,

$$d_n = \det[C(N, 0)] = \det \prod_{i=N}^{1} [A(i)] = \prod_{i=N}^{1} \det [A(i)] = \prod_{i=N}^{1} a_n(i) \tag{3.57}$$

and using coefficients $d_1, d_2, \ldots, d_n$ of the characteristic equation (3.43) it is easy to determine eigenvalues $\lambda_1, \lambda_2, \ldots, \lambda_n$ of the monodromy matrix.

In the discussions above, we have covered the mathematical aspects of evaluating the stability of parametric systems.

3.7 STABILITY OF SECOND-ORDER SYSTEMS

The method for stability evaluation described above can be applied for the arbitrary-order system. Let us investigate the stability of a second-order recursive system. This analysis has significant practical and methodological implications. The second-order

units are often used in digital filtering as bricks for more complex and higher order systems design. These second-order systems are also the key components for the parametric oscillator analysis introduced later in the book.

A block diagram of the second-order PLTV system is shown in Fig. 3.6a, which can be simplified to those shown in Fig. 3.6b. This system is described by the equation

$$y(i) + a_1(i)y(i-1) + a_2(i)y(i-2) = f(x(i), x(i-1), x(i-2)) \tag{3.58}$$

For stability analysis of linear systems, it is not necessary to consider the particular values of input signal $f(x(i))$. The important issue is the initial conditions (IC), that is, the values stored in the system memory (the delay registers 'Z^{-1}' in Fig. 3.6a). These ICs are shown in Fig. 3.6b as an independent input parameter.

Assume that coefficients $a_1(i)$ and $a_2(i)$ are the periodical functions $a_1(i) = a_1(i + N_1)$, $a_2(i) = a_2(i + N_2)$, with the lowest common multiple of the intervals N_1 and N_2 equal to N. For this case, the MM elements

$$[C(N,0)] = \begin{bmatrix} C_{11} & C_{12} \\ C_{21} & C_{22} \end{bmatrix} = \prod_{i=N}^{1} \begin{bmatrix} -a_1(i) & -a_2(i) \\ 1 & 0 \end{bmatrix} \tag{3.59}$$

can be determined using the recurrent procedure [22]:

$$\begin{cases} C_{11} = C_{11}(N) = -a_1(N)C_{11}(N-1) - a_2(N)C_{21}(N-1) \\ C_{12} = C_{12}(N) = -a_1(N)C_{12}(N-1) - a_2(N) \\ C_{21} = C_{21}(N) = C_{11}(N-1) \\ C_{22} = C_{22}(N) = C_{12}(N-1) \end{cases} \tag{3.60}$$

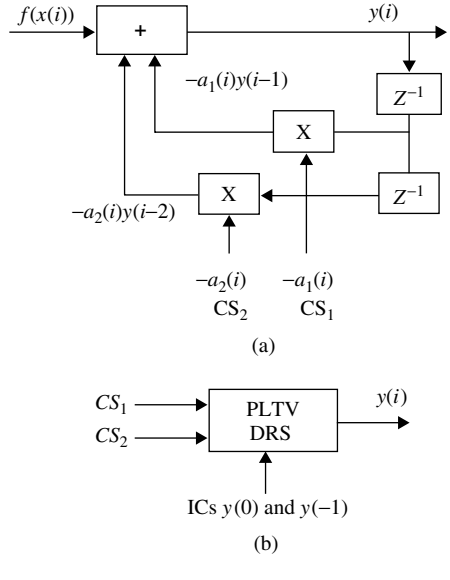

Figure 3.6 A second-order system: (a) block diagram and (b) simplified block diagram

In this expression, (N) and $(N-1)$ mean that MM elements are obtained as a result of N and $N-1$ matrix $[A(i)]$ multiplication.

For the MM, the characteristic equation is

$$\lambda^2 + d_1\lambda + d_2 = 0 \tag{3.61}$$

According to equations (3.54) and (3.57), the coefficients d_1, d_2 are

$$\begin{aligned} d_1 &= \mathrm{Tr}[C(N,0)] = -C_{11} - C_{22} \\ d_2 &= \det[C(N,0)] = \prod_{i=1}^{N} a_2(i) \end{aligned} \tag{3.62}$$

Then, equation (3.61) takes the following reasonably simple form for calculations:

$$\lambda^2 - (C_{11} + C_{22})\lambda + \det[C(N,0)] = 0 \tag{3.63}$$

The condition $|\lambda_1| \le 1, |\lambda_2| \le 1$ imposes the following limitations on the coefficient values in equation (3.63):

$$\begin{cases} 1 - C_{11} - C_{22} + \det[C(N,0)] \ge 0 \\ 1 + C_{11} + C_{22} + \det[C(N,0)] \ge 0 \\ |\det[C(N,0)]| \le 1 \end{cases} \tag{3.64}$$

Consider the stability of the second-order system when coefficients vary under the influence of two control signal waveforms: binary (square wave) and sinusoidal [22, 23]. First, let us consider the simplest case using the following example.

Example 3.4: Second-Order Filter with "Fast" Sinusoidal Control Signals

The second-order parametric DRS has the binary law of coefficient variation with periods $N_1 = N_2 = N = 2$: $a_1(i) = a_1 + \gamma_1 \cos(\pi i)$ and $a_2(i) = a_2 + \gamma_2 \cos(\pi i)$.

This case is interesting, first of all, from the methodological point of view and later we will refer to it as the "fast" sinusoidal CS. Elements of the monodromy matrix $[C(N<0)]$ can be evaluated using recurrent relations (3.60):

$$\begin{cases} C_{11} = -a_1(2)C_{11}(1) - a_2(2)C_{21}(1) = a_1(2)a_1(1) - a_2(2) \\ C_{22} = C_{12}(1) = -a_2(1) \\ |\det C(2,0)| = a_2(1)a_2(2) \end{cases} \tag{3.65}$$

Conditions (3.64) for the system stability take the form

$$\begin{cases} 1 - a_1(2)a_1(1) + a_2(2) + a_2(1) + a_2(1)a_2(2) \ge 0 \\ 1 + a_1(2)a_1(1) - a_2(2) - a_2(1) + a_2(1)a_2(2) \ge 0 \\ |a_2(1)a_2(2)| \le 1 \end{cases} \tag{3.66}$$

Whether CSs are in-phase or have opposite phases, in both cases we obtain the following stability area (SA) introduced in the plane of coefficients a_1, a_2:

$$\begin{cases} \dfrac{(1+a_2)^2}{\gamma_1^2-\gamma_2^2} - \dfrac{a^2}{\gamma_1^2-\gamma_2^2} \geq 1 \\ (1-a_2)^2 + a_1^2 \geq \gamma_1^2 + \gamma_2^2 \\ a_2 \leq 1 + \gamma_2^2 \end{cases} \tag{3.67}$$

These coincide with those specified in [14, 18, 22 and 23]. Recall that CSs in our case correspond to the law of variation for coefficients $a_1(i)$ and $a_2(i)$.

Figure 3.7a represents the boundaries of the SA for PLTV DRSs of the second order on the plane of coefficients: a_1, a_2 for $|\gamma_1| > |\gamma_2|$. Figure 3.7b represents the same for the case $|\gamma_1| < |\gamma_2|$. The dashed line is the stability area for $\gamma_1 = \gamma_2 = 0$, which coincides with known results for second-order recursive filters with constant coefficients. Data analysis from example 3.4 allows us to make some visual generalizations at the physical level.

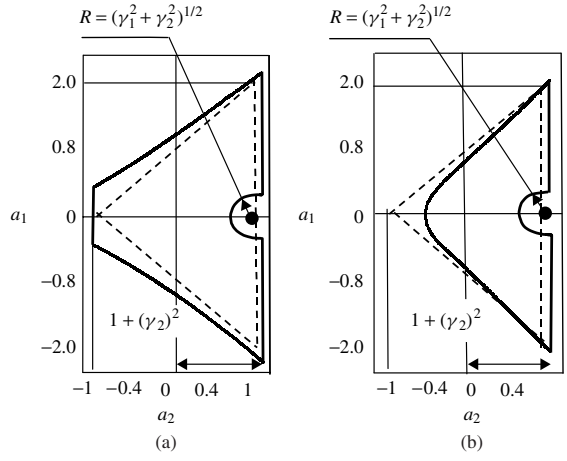

Figure 3.7 Stability area for "fast" coefficient variation

It is clear that the stability of PLTV systems is essentially different from the stability of LTI systems. There are the following deformations of the stability area due to coefficient variation:

1. In the neighbourhood of the point with coordinates $a_1 = 0, a_2 = 1$ an enclave of instability occurs, which is limited by a circle with radius $R = (\gamma_1^2 + \gamma_2^2)^{1/2}$. For $a_1 = 0$ and $a_2 \to 0$, a DRS with constant coefficients is a narrowband filter with the resonance frequency $\omega_{\text{res}} = \cos^{-1}(-a_1/2\sqrt{a_2}) = \pi/2$. This frequency corresponds to the first sub-harmonic of the control signal: $\Omega_S/2 = 2\pi/2N = \pi/2$.
2. Variation of the coefficient $a_2(i)$ expands the SA boundary to values $a_2 > 1$, that is, $a_2 = 1 + \gamma_2^2$ (instead of $a_2 = 1$ for LTI systems).
3. The bigger the amplitude of coefficient variation, the bigger is the degree of SA deformation.

It is now very important to note that relative to CSs, the system is not linear. So, for each law of coefficient variation the SA evaluation should be independently applied.

For more complex CSs ($N > 2, q > 2$), the stability conditions can also be obtained in closed analytical form using the same equations. However, these formulas become too tedious for direct analysis. So, we will introduce only the results of computer calculations for the further analysis of stability areas.

Example 3.5: Second-Order Filter with 'Slow' Sinusoidal Variation of Control Signals

Consider now a "slow" sinusoidal CS with the period $N = 16$. Let $a_1(i) = a_1$ be constant and $a_2(i) = 0.125 \cos\left(\frac{\pi}{8} i\right) + a_2$. The stability area for $-2 < a_1 < -1.6$ and $0.7 < a_2 < 1$ is shown in Fig. 3.8. It clearly shows two instability enclaves centred around values of coefficients a_1: -1.94 and -1.84, when $a_2 \approx 1$. A digital recursive second-order system with these coefficients corresponds to a narrowband filter with resonance frequencies $\omega_{res} \approx \pi/8$ and $\omega_{res} \approx \pi/4$, respectively. These two frequencies coincide with the first and second sub-harmonic of the control signal. In Fig. 3.8, the grey colour corresponds to the instability area.

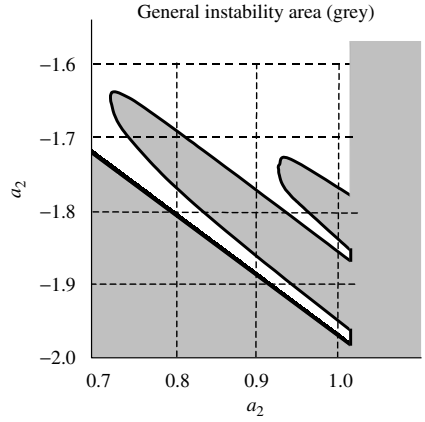

Figure 3.8 Stability area for sinusoidal CS ($N = 16$)

The analytical analysis of LTV DSs developed above is appropriate for stability evaluation of any system. Nevertheless, it seems useful to consider two more examples for better understanding of the physical processes behind this stability analysis. Of course, these results are illustrative and cannot be used as graphs for stability evaluation.

Example 3.6: Second-Order Filter with "Slow" Binary Variation of Control Signals

The results of an SA evaluation for binary (square waves) CSs with a period of $N = 16$ and the same on/off factor $q = 2$ for several values of γ_1 and γ_2 are shown in Fig. 3.9. The keys for the modelling parameters for the figure are in Table 3.1.

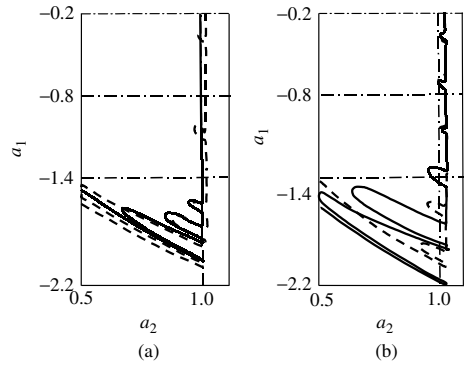

Figure 3.9 Stability areas for binary CS

Table 3.1 PLTV DRS and CS parameters

Curve nos.	γ_1	γ_2	Line	Figure nos.
1	0.125	0	Solid	3.9a
2	0	0.125	Dashed	3.9a
3	0	0.125	Solid	3.9b
4	0	0.0625	Dashed	3.9b

The SA obtained by varying only coefficients $a_1(i)$ (solid line) and $a_2(i)$ (dashed line) with equal amplitudes $\gamma_1 = \gamma_2 = 0.125$ is shown in Fig. 3.9a. A similar SA for $a_2(i)$ variation with amplitudes $\gamma_2 = 0.125$ (solid line) and $\gamma_2 = 0.0625$ (dashed line) is shown in Fig. 3.9b.

The enclaves of instability in example 3.3 occur in different positions from the enclaves for the case when $N = 2$. However, in terms of the resonance frequencies of digital resonators, these enclaves again correspond to the sub-harmonics of control signals: $\omega_{\text{res}} = \cos^{-1}(-a_1/2\sqrt{a_2}) \approx S\Omega_S/2$. This situation is typical for parametric systems [26], so let us call these enclaves parametrical instability zones (PIZs). PIZs' axes of symmetry coincide with the frequencies of CS sub-harmonics and follow the parabolas of the equal frequencies $a_2 = a_1^2/[4\cos(S\Omega_S/2)]$. The higher the resonator efficiency Q (e.g., a_2 is close to 1) and the bigger the coefficient variations γ, the wider along the axes a_2 and the deeper along the axes a_1 are these PIZs. Conversely, the higher the sub-harmonic number to which the system is matched, the smaller are the PIZs. We will come back to this problem later in the book. Qualitatively, this picture corresponds to the conclusions of Mathieu and Mysner in their stability analysis of equations [26–28].

Example 3.7: Second-Order Filter with "Slow" Sinusoidal Variations of Control Signals

Let us consider a sinusoidal CS with different periods N and amplitudes γ_1, γ_2. The influence of parameter variation on the system SA is shown in Fig. 3.10, while the keys for the figure are collected in Table 3.2

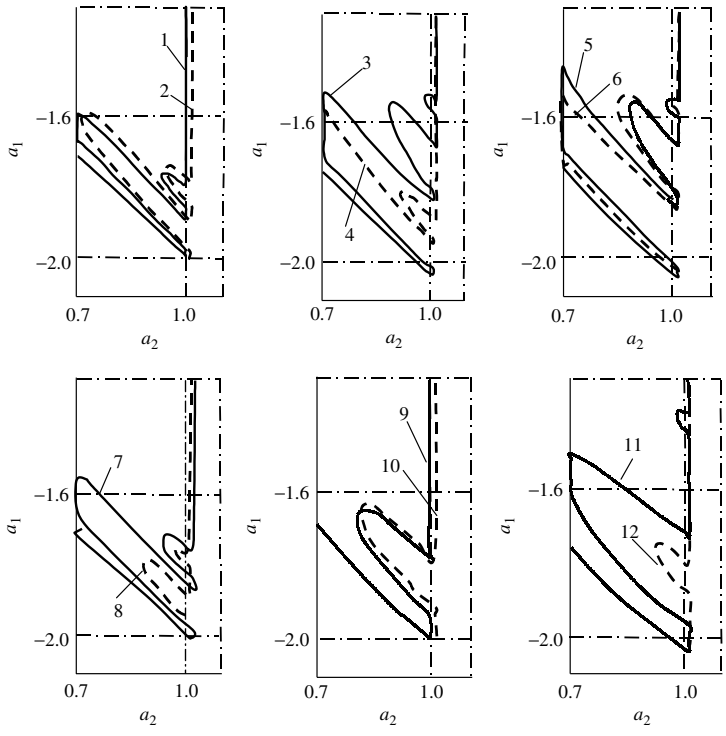

Figure 3.10 Stability areas of a second-order parametric system

Table 3.2 PLTV DRS and CS parameters

Curve nos.	N	γ_1	γ_2	Line	Figure nos.
1	16	0.125	0	Solid	3.10a
2	16	0	0.125	Dashed	
3	16	0.125	0.125	Solid	3.10b
4	16	0.125	−0.125	Dashed	
5	16	0.125	0.125	Solid	3.10c
6[a]	16	0.125	0.125	Dashed	
7	16	0	0.125	Solid	3.10d
8	16	0	0.0625	Dashed	
9	8	0.125	0	Solid	3.10e
10	8	0	0.125	Dashed	
11	8	0.125	0.125	Solid	3.10f
12	8	0.125	−0.125	Dashed	

[a]CS $a_1(i)$ and $a_2(i)$ are shifted by $N/4$

Using the method described above, the stability of arbitrary time-variant systems can be evaluated analytically. For consideration of parametric systems in this book we can draw some general conclusions regarding the stability of highly efficient second-order systems or digital resonators:

1. Because of the variation of coefficients $a_1(i)$ and/or $a_2(i)$ in high Q *systems*, specific instability enclaves occur near resonance frequencies corresponding to CS subharmonics $S\Omega_S/2$.
2. The existence, positions and shapes of these zones are determined by parameters of the resonator and CS. The width of the zones along axis a_1 (frequency) is proportional to the amplitudes of coefficient variation.

3.8 STABILITY OF STOCHASTIC SYSTEMS

From theoretical and practical points of view, it is important to consider time-variant systems with CSs containing random components. In this section, we will study the influence of these random components on the stability of periodically time-variant systems.

For stability determination in the mean square [20], first consider the general expression

$$\lim_{k\to\infty} M\left[\prod_{i=k}^{1}\left[A(i)^{[2]}\right]\right] \tag{3.68}$$

where the matrix contains random components. Determination of the mean value of an infinite number of random matrix multiplications can be considerably simplified if matrixes $[A(i)]$ are independent and equally distributed [29, 30]. For parametric system analysis, we can use this approach without essential losses in a generality. Matrix independence here means that the time intervals by which they are separated exceed correlation intervals of the random process. However, in general, the matrix elements can be cross-correlated with each other. Let us determine a monodromy matrix, introducing it at the correlation interval $\overline{\tau}_k = N$, which is equal to the lowest common multiple of coefficient correlation intervals [31]:

$$\begin{aligned}
&[C(N,0)] = \prod_{i=N}^{1}[A(i)],\\
&\cdots\cdots\cdots\cdots\\
&[C_m(N,0)] = \prod_{i=mN+q}^{(m-1)N+1+q}[A(i)]
\end{aligned} \tag{3.69}$$

Then, equation (3.53) can be rewritten as

$$\lim_{k\to\infty} M\left[\prod_{i=k}^{1}[A(i)]^{[2]}\right] = \lim_{k\to\infty} M\left[\prod_{m=k/N}^{1} C_m(N,0)^{[2]}\right] = \lim_{k\to\infty}\left[M[C_m(N,0)]^{[2]}\right]^{k/N} \tag{3.70}$$

It is limited if all absolute eigenvalues $\delta_1, \delta_2, \ldots, \delta_n$ of the matrix $M[C_m(N,0)]^{[2]}$ do not exceed 1 [23], which is the criteria for system stability. This approach can be used for the stability analysis of an arbitrary-order system.

For better understanding of this problem, let us apply the method for stability analysis of the second-order difference equation with stochastic coefficients. So, we are analysing a second-order PLTV DRS with coefficients containing stochastic components, which is described by the following equation:

$$y(i) + a_1(i)y(i-1) + a_2(i)y(i-2) = f(x(i), x(i-1), x(i-2)) \tag{3.71}$$

In the general case, the coefficients contain deterministic $a(i)$ and random η (i) components. We can specify the MM if $a_1(i)$ and $a_2(i)$ are known:

$$[C(N,0)] = \prod_{i=N}^{1} [A(i)] = \begin{bmatrix} C_{11} & C_{12} \\ C_{21} & C_{22} \end{bmatrix} \tag{3.72}$$

where elements $[C(N,0)]$ can be determined using the recurrent expression (3.65). Thus, for investigation of the Kroneker square of a matrix 2×2, it is possible to consider only the matrix with the dimensions 3×3, which is determined as

$$[C(N,0)]_{[2]} = \begin{bmatrix} C_{11}^2 & 2C_{11}C_{12} & C_{12}^2 \\ C_{11}C_{21} & C_{11}C_{22} + C_{12}C_{21} & C_{12}C_{22} \\ C_{21}^2 & 2C_{21}C_{22} & C_{22}^2 \end{bmatrix} \tag{3.73}$$

Coefficients d_1, d_2, d_3 of the characteristic equation of the third order,

$$\delta^3 + d_1\delta^2 + d_2\delta + d_3 = 0 \tag{3.74}$$

are determined according to equations (3.57) to (3.64) as

$$\begin{cases} d_1 = M(C_{11}^2) + M(C_{11}C_{22} + C_{12}C_{21}) + M(C_{22}^2) \\ d_2 = M(C_{11}^2)M(C_{11}C_{22} + C_{12}C_{21}) + M(C_{11}^2)M(C_{22}^2) \\ \quad + M(C_{11}C_{22} + C_{12}C_{21})M(C_{22}^2) - 2M(C_{11}C_{22})M(C_{11}C_{21}) \\ \quad - M(C_{12}^2)M(C_{21}^2) - 2M(C_{12}C_{21})M(C_{12}C_{22}) \\ d_3 = M(C_{11}^2)M(C_{11}C_{22} + C_{12}C_{21})M(C_{22}^2) + 2M(C_{11}^2)M(C_{21}C_{22})M(C_{12}C_{22}) \\ \quad + 2M(C_{11}C_{22})M(C_{11}C_{21})M(C_{22}^2) - 2M(C_{11}C_{12})M(C_{21}^2)M(C_{12}C_{22}) \\ \quad - 2M(C_{12}^2)M(C_{11}C_{21})M(C_{21}C_{22}) + M(C_{12}^2)M(C_{21}^2)M(C_{11}C_{22} + C_{12}C_{21}) \end{cases} \tag{3.75}$$

Thus, d_1, d_2 and d_3 are fully specified within the correlation theory. The conditions for which all absolute values of the roots λ_1, λ_2 and λ_3 of the third-order equation are less than or equal to 1 are

$$\begin{cases} -1 \le d_2 \le 3/2 \\ 1 - d_3^2 + d_1 d_3 - d_2 \ge 0 \end{cases} \tag{3.76}$$

By sequentially performing all the above-enumerated operations, we obtain stability conditions as a function of the random components' statistical first and second moments as well as autocorrelation (ACFs) and cross-correlation (CCFs) functions of the coefficients. For a simpler understanding of the stability of stochastic systems and the method of stability analysis discussed above, let us consider the following examples.

Example 3.8: Second-Order System with Non-Correlated Random Coefficients

Evaluate the stability conditions for a second-order system with coefficients $a_1(i) = a_1 + \eta_1(i)$ and $a_2(i) = a_2 + \eta_2(i)$. They have constant deterministic coefficients a_1 and a_2, and random $\eta_1(i)$ and $\eta_2(i)$ components. Assume that the stochastic components are two white noise zero-mean processes with known variance σ_1^2 and σ_2^2. According to the definition, the correlation time interval for white noise is $\tau_k = 0$ and the MM is

$$[C_i(1,0)] = \begin{bmatrix} -a_1 - \eta_1(i) & -a_2 - \eta_2(i) \\ 1 & 0 \end{bmatrix} \tag{3.77}$$

Coefficients d_1, d_2 and d_3 of the characteristic equation of the matrix $M[[C_i(1,0)]_{[2]}]$ are determined according to equation (3.76), as functions $a_1(i), a_2(i)$ of their moments and the CCF

$$\begin{cases} d_1 = M((a_1 + \eta_1(i))^2) + M(a_2 + \eta_2(i)) = -a_2 - a_1^2 - \sigma_1^2 \\ d_2 = -M((a_1 + \eta_1(i))^2) + M(a_2 + \eta_2(i)) + 2M((a_1 + \eta_1(i))M((a_1 + \eta_1(i)) \\ M((a_2 + \eta_2(i)) - M((a_2 + \eta_2(i))^2) = a_2\sigma_1^2 + a_1^2 A_2 + 2a_1 K_{12} - a_2^2 - \sigma_2^2 \\ d_3 = -M((a_2 + \eta_2(i))^2)M((a_2 + \eta_2(i)) = -a_2(a_2^2 + \sigma_2^2) \end{cases} \tag{3.78}$$

where $\sigma_1^2 = M(\eta_1^2(i))$ and $\sigma_2^2 = M(\eta_2^2(i))$ are variances of the random components and $K_{12} = M(\eta_1(i)\eta_2(i))$ is their CCF. So, the stability conditions take the following form:

$$\begin{cases} a_2\sigma_1^2 + a_1^2 a_2 + 2a_1 K_{12} - a_2^2 - \sigma_2^2 \geq -1 \\ a_2\sigma_1^2 + a_1^2 a_2 + 2a_1 K_{12} - a_2^2 - \sigma_2^2 \leq 3/2 \\ 1 - a_2^2(a_2^2 - \sigma_2^2)^2 - a_2(a_2 - a_1^2\sigma_1^2)(a_2^2 + \sigma_2^2) + a_2\sigma_1 - a_1^2 a_2 \\ -2a_1 K_{12} + a_2^2 + \sigma_2^2 \geq 0 \end{cases} \tag{3.79}$$

Using equation (3.79), it is possible to evaluate the stability of a system with known coefficients. The corresponding SA on the plane of coefficients a_1, a_2 is shown in Fig. 3.11, which can be used for SA analysis. Key parameters for the figure are collected in Table 3.3. The case of time-invariant systems or $\sigma_1^2 = \sigma_2^2 = K_1 = K_2 = K_{12} = 0$ is shown in this figure as well as in Figs. 3.12 and 3.13 by a solid line (curve 1). Thus, the presence of noise leads to uniform reduction of the SA (Fig. 3.11a). The bigger the noise variance, the smaller is the stability area. For non-correlated noise components of the coefficients $a_1(i)$ and $a_2(i)$, a uniform reduction of SA size can be observed from all directions. When the cross-correlation of coefficients does not equal zero ($K_{12} \neq 0$), the reduction in SA is not uniform (Fig. 3.11b) due to the mutual influence of coefficient variation.

Table 3.3 CS parameters

Curve nos.	σ_1^2	σ_2^2	K_{12}	Figure nos.
1	0	0	0	
2	0.1	0	0	
3	0.2	0	0	3.11a
4	0	0.1	0	
5	0	0.2	0	
1	0	0	0	
2	0.1	0.1	0	3.11b
3	0.1	0.1	0.05	
4	0.1	0.1	0.1	

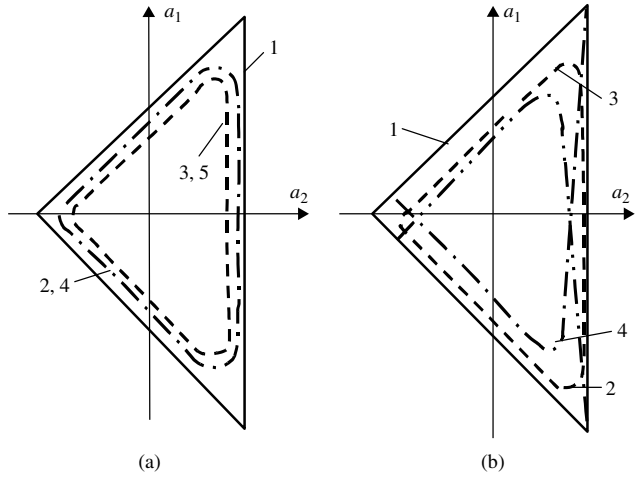

Figure 3.11 Stability areas for a second-order DRS with coefficients corrupted by correlated noise

Example 3.9: Second-Order System with Correlated Random Coefficients

Consider the case when constant coefficients $a_1(i) = a_1$ and $a_2(i) = a_2$ of the system are distorted by correlated noise $\eta_1(i), \eta_2(i)$ with the known correlation coefficients over an interval $\tau_k = 2T{:}K_1$ and K_2 [32]. To estimate the stability of such a system it is necessary to investigate eigenvalues of the matrix:

$$M\left[[c_i(2,0)]_{[2]}\right] = \left[\prod_{i}^{i-1}[A(i)]_{[2]}\right]$$

$$= \left[M\left[\begin{array}{cc}[a_1+\eta_1(i)][a_1(i-1)]-[a_2+\eta_2(i)] & -(a_1\eta_1(i))(a_2+\eta_2(i-1)) \\ -(a_1+\eta_1(i-1)) & -(a_2+\eta_2(i-1))\end{array}\right]\right]_{[2]} \tag{3.80}$$

The calculations yield conditions similar to those in equation (3.79). The results of computer analysis of these conditions are shown in Fig. 3.12 for different parameters, which are collected in Table 3.4. Two auxiliary curves in Fig. 3.12 (curve 1) and (curve 2) are shown for comparison.

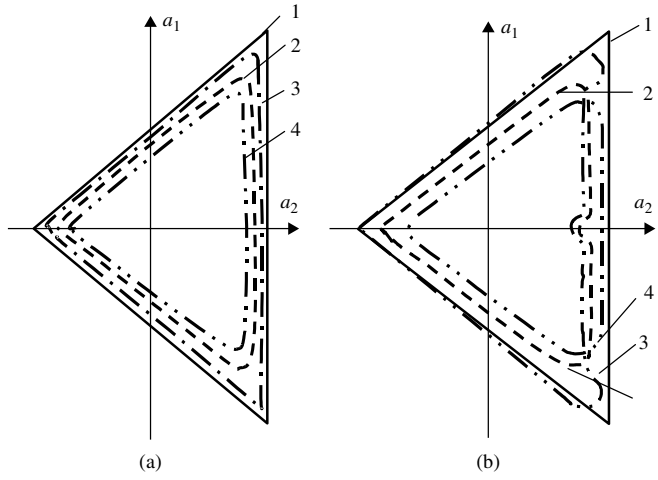

Figure 3.12 Stability areas for a second-order DRS with coefficients corrupted by correlated noise

Table 3.4 CS parameters

Curve nos.	σ_1^2	σ_2^2	K_1	K_2	Figure nos.
1	0	0	0	0	
2	0.1	0	0	0	
3	0.1	0	−0.1	0	3.12a
4	0.1	0	0.1	0	
1	0	0	0	0	
2	0	0.1	0	0	3.12b
3	0	0.1	−0.1	−0.1	
4	0	0.1	0.1	0.1	

It is interesting to note that the instability area appears near the point with coordinates $a_1 = 0, a_2 = 1$, which corresponds to resonance frequency $\omega_{\text{res}} = \pi/2$ (Fig. 3.12a). Note also that, in general, the nature of SA distortions is similar to that in the case of the "fast" sinusoidal variation of the deterministic coefficient $a_1(i)$.

Example 3.10: Second-Order Digital Recursive System with Periodically Varying Coefficients Corrupted by Noise

Consider a second-order discrete system with deterministic coefficients similar to those discussed in example 3.4, but corrupted by white noise components η_1, η_2 with variance

σ_1^2 and $\sigma_2^2 : N_1 = N_2 = N = 2; a_1(i) = a_1 + \gamma_1 \cos(\pi i) + \eta_1$ and $a_2(i) = a_2 + \gamma_2 \cos(\pi i) + \eta_2$. To estimate stability it is necessary to consider the following matrix:

$$[M[C(2,0)]]_{[2]} = \left[M \prod_{i}^{i-1} [A(i)] \right]_{[2]}$$

$$= \left[M \begin{bmatrix} [a_1 - \gamma_1 + \eta_1(i)][a_1 + \gamma_1 + \eta_1(i-1)] & -[a_2 - \gamma_2 + \eta_2(i)] \\ -[a_1 - \gamma_1 + \eta_1(i)] & \times [a_2 + \gamma_2 \eta_2(i-1)] \\ -a_1 - \gamma_1 - \eta_1(i-1) & -a_2 - \gamma_2 - \eta_2(i-1) \end{bmatrix} \right] \tag{3.81}$$

Then, using equations (3.75) and (3.76) stability conditions can be obtained. Appropriate results calculated by a computer are shown in Fig. 3.13 for different CS parameters. The key parameters for the figure are collected in Table 3.5.

Table 3.5 CS parameters

Curve nos.	γ_1	γ_2	σ_1^2	σ_2^2	Figure nos.
1	0	0	0	0	
2	0.3	0	0	0	3.13a
3	0.3	0	0.1	0	
4	0.3	0	0.2	0	
1	0	0	0	0	
2	0	0.2	0	0	3.13b
3	0	0.2	0	0.2	

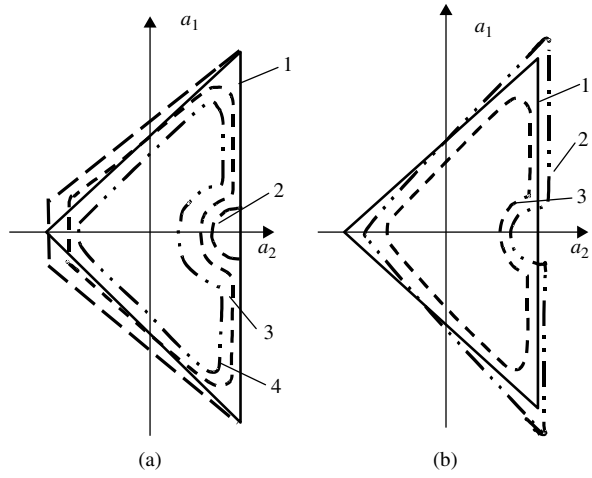

Figure 3.13 SA For a second-order DRS with binary CS distorted by white noise

Analysis of the results of stability analysis of systems with random varying coefficients allows us to draw the following conclusions:

1. Existence of a random component in the CS leads to distortions in SAs, which are mainly a reduction proportional to the deviation of the random component.
2. The particular kind of ACFs and CCFs of the CS random components influence SA shape and size.
3. Results of system stability analysis are well agreed for random and deterministic variations of coefficients.
4. Stability of stochastic PLTV DSs is fully determined by Eigen and compound moments of the random variations of coefficients, that is, solutions can be obtained within the correlation theory, which corresponds to known results [19, 20].

The stability conditions obtained above for systems with random coefficients have been verified by computer experiments. These experiments were done using direct modelling of the difference equation (3.71) for zero input signal and initial condition $\|Y(0)\| = 1$. Results of the experiments are shown in Fig. 3.14. A system of the second order with constant coefficients was used for the experiment. The coefficients $a_1(i)$ have been corrupted by noise with a variance $\sigma_1^2 = 0.1$. An appropriate solution for equation (3.71) was found. Then, mean values of the state vector norms were calculated, using results of 50 realizations of random component observations for different a_1.

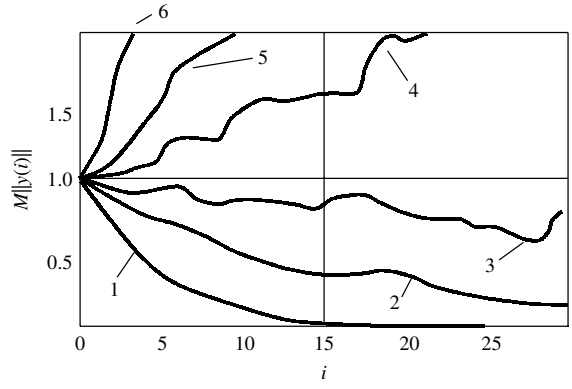

Figure 3.14 Experimental verification of conclusions derived from the theory of stability for systems with stochastic coefficients

Dependence of the SVN mean value on time moments iT is shown in Fig. 3.14. Calculations were done for coefficients $a_1 = 0.85$, 0.95 that correspond to the SA (curves 1, 2). The other values, $a_1 = 1$, 1.05, 1.1, 1.3 (curves 3–6), correspond to an instability area in the mean square determined earlier using equations (3.75) to (3.79) for the parameters being considered. Analysis of the processes shown in Fig. 3.14 allows selection of the following typical areas:

1. monotone reduction of the mean square SVN (curves 1, 2) for systems inside the SA, which corresponds to the selected earlier stability determination;
2. non-monotone reduction or expansion of parameters, located outside the SA, but close to its boundaries (curves 3 and 4);

3. monotone expansion of the mean square SVN for the big system boundary receding from the SA with noisy coefficients ($a_1^2 = 1 - \sigma_1^2$), as well as for similar receding from the SA boundary of the system with constant coefficients corrupted by noise (curves 5, 6).

The modelling results confirm the validity of the analytical approach to stochastic system stability analysis developed above.

3.9 SUMMARY

In this chapter, we studied periodically time-variant systems. These systems are a subclass of LTV DSs introduced in Chapter 2. Because of the coefficients' periodicity it became possible to introduce the major system characteristics in analytically closed forms. The important consequences of coefficient periodicity are the periodicity of such system characteristics as impulse response, generalized transfer function and frequency response. Applying Fourier transform to the GFR yielded a new and practically useful characteristic, the *bifrequency function*. This function has a clear physical sense as it tiers input and output signal spectrums. Analysis of this function permits relaxation of requirements for the sampling frequency choice in some cases.

The specifically important consequence of the coefficient periodicity is the system stability behaviour. In this chapter, the analytical method for the stability evaluation for any periodically varying systems was introduced. This study highlights that the stability of PLTV DSs derives from sophisticated behaviour, and when time-variant systems are designed the stability issues should be the focus of the system analysis. The recursive systems become extremely sensitive to the relationships between their frequency-selective properties and the spectrum of coefficient variations. Except, perhaps, for second-order systems, it is very difficult to imagine the SA of the system, and all PLTV systems should be stability tested even in the case of only small parameter variations.

Analysis of second-order systems revealed strong deformations of the SAs in the coefficient domain. PLTV systems are losing their stability when resonance frequencies of the system coincide with sub-harmonics of the CS spectrum components.

3.10 ABBREVIATIONS

ACF	autocorrelation function
CC	Combinational component
CCF	cross-correlation function
CS	control signal
DFT	discrete Fourier transform
DRS	digital recursive systems
DS-1	discrete system of the first order
DS-2	discrete system of the second order

GFR	generalized frequency response
GTF	generalized transfer function
IR	impulse response
LTI DS	linear time-invariant discrete system
MM	monodromy matrix
PIZ	parametrical instability zone
PLTV DRS	periodically linear time-variant digital recursive system
PLTV DS	periodically linear time-variant discrete system
PSD	power spectral density
SA	stability area
SVN	state vector norm

3.11 VARIABLES

$H_0(\omega)$	an equivalent frequency response
ρ	integral level of MC
γ	MC integral level of PLTV DS losses in comparison with stationary system
Ω	normalized frequency of system parameter variation
ω	normalized frequency of the signal
$\xi(\omega)$, $\eta(\omega)$	spectrums of the random processes
$\xi(t)$, η_i	stationary continuous random process
Δ_i	discrete process modulating sampling period
γ_i	output random signal
λ_i	eigenvalues of the characteristic equation
τ_k	an interval of correlation for random processes
$\sigma_X^2(n)$	deviation
$[A(i)]$	a matrix of state variation
$[Y(i)]$	n dimension state vector of the system at moment i
$\|\|Y(k)\|\|$	state vector norm
$a(n)$	time-varying coefficients of the recursive part of a difference equation
$b(n)$	time-varying coefficients of the non-recursive part of a difference equation
d_i	coefficients of the characteristic equation
f	frequency
$F_\xi(\omega)$	power spectrum density
$F(z, n)$	GTF of the non-recursive part
$g(m, n)$	impulse response of the recursive part
$G(z)$	GTF of the recursive part
$H(\psi, \omega)$	bifrequency function
$h(m, n)$	impulse response
$H(z, n)$	generalized transfer function

$M(\cdot)$	a mathematical mean of the pth order SVN
$M(n)$	mean value
$R(m, n)$	correlation function
$S(\omega)$	spectral density
Tr	trace of the matrix
$X(\omega)$, $X(\psi)$	spectrum of the input signal
$X(n)$	input discrete random process
$x(n)$	input signal
$X(z)$	z-transform of the input signal
$Y(\omega)$	spectrum of the output signal
$Y(n)$	output discrete random process
$y(n)$	output signal
$Y(z, n)$	z-transform of the output signal

3.12 REFERENCES

[1] Huang NC, Aggarwal JK (1980) On linear shift-variant digital filters. *IEEE Trans.*, **Cas-27**(8), 672–678.

[2] Meyer RA, Burrus CS (1975) Design and implementation of multirate and periodically time-varying filters. *IEEE Trans.*, **Cas-22**, 162–168.

[3] Cherniakov M, Sizov V, Donskoi L (2000) Sampling theorem for time-varying digital systems, *Int. Conf. on Signal Processing (ICSP 2000)*, Beijing, China, 21–25 August, 95–98.

[4] Gardner WA (1994) *Cyclostationarity in Communications and Signal Processing*, IEEE Press US.

[5] Iaglom AM (1987) *Correlation Theory of Stationary and Related Random Function*, New York: Springer-Verlag.

[6] Loeffler CM, Burrus CS (1984) Optimal design of periodically time varying and multirate digital filters. *IEEE Trans.*, **Assp-32**, 991–997.

[7] Merkin DR (1997) *Introduction to the Theory of Stability*, New York: Springer-Verlag.

[8] Meys RP (1990) Review and discussion of stability criteria for linear 2-ports. *IEEE Trans.*, **Cas-37**(11), 1450–1452.

[9] Derusso P, Roy R (1965) *Close C State Variables for Engineers*, New York: John Wiley & Sons.

[10] Agathoklis P (1985) Estimation of the stability margin on 2-D Liapunov equation. *Proc. Int. Symp. Cas*, **2**, 1091, 1092.

[11] Bose T, Brown DP (1987) On the stability of linear shift variant digital filters. *Proc. Int. Conf. Assp*, **2**, 880–883.

[12] Agathoklis P, Antonion A (1986) Stability of 2-D digital filters under parameter variations. *IEEE Trans.*, **Cas-33**(5), 476–482.

[13] Saleh BEA, Subotic NS (1985) Time-variant filtering of signals in the mixed time-frequency domain. *IEEE Trans.*, **Assp-33**(6), 1479–1485.

[14] Subramanyan R, Radhakrishna RK (1986) Novel high-Q narrowband/notch digital filter. *Electron. Lett.*, **22**(16), 870–872.

[15] D'Angelo H (1976) *Linear Time-Varying Systems: Analysis and Synthesis*, Boston: Allyn & Bacon.

[16] Ostrovsky MY, Chechurin SL (1989) *Stationary Models of Automatic Control Systems with Periodical Parameters*, Leningrad: Energoizdat.

[17] Decroly JC, Laurent L, Lienard J (1973) *Parametric Amplifiers*, New York: Macmillan Publishing.
[18] Premaratne K, Mansour M (1997) Robust stability of time-variant discrete-time systems with bounded parameter perturbations. *IEEE Trans.*, **Cas-1-42**(1), 40–45.
[19] Aoki M (1967) *Optimization of Stochastic Systems*, New York: Academic Press.
[20] Hasminskiy PE (1969) *System Stability of the Differential Equations for Random Perturbations of its Parameters*, Moscow: Nauka.
[21] Bellman R (1970) *Introduction to Matrix Analysis*, New York: McGraw-Hill.
[22] Bets V, Cherniakov M (1987) Application of the discrete transition matrix method for amplitudes of the digital filter stability. *Radiotechnica*, **4**, 24–26.
[23] Bets V, Mudrik D, Cherniakov M (1986) Investigation of stability of periodically nonstationary algorithms for digital filtering, *Conference Proc. "Microprocessors 85"*, MIET, Moscow, 27, 28.
[24] Ostrovski M, Chechurin S (1989) *Stationary Models of the Automatic Control Systems with Periodic Parameters*, Leningrad: Energoizdat.
[25] Kreyszig E (1993) *Advanced Engineering Mathematics*, New York: Wiley & Sons.
[26] Kharkevich AA (1962) *Nonlinear and Parametric Phenomena in Radio Engineering*, New York: John F Rider Publishing.
[27] Locherer KH (1982) *Parametric Electronics: An Introduction*, New York: Springer-Verlag.
[28] Von Tungfer H Die stabilitatsbereiche einer Erweiterten Meihnerschen Differentjalgleichung. *Frequenz*, **186**(1), 1–8.
[29] Korn G, Korn T (1968) *Mathematical Handbook*, New York: McGraw-Hill.
[30] Kats IY, Krasovsky NN (1960) On the stability of systems with random parameters. *Sov. Appl. Math.*, **24**(5), 312–321.
[31] Bets V, Cherniakov M (1987) Stability of the digital filters with random varying parameters. Izvestia Vuzov, *Radioelectronika*, **2**, 72–75.
[32] Mao X (1994) *Exponential Stability of Stochastic Differential Equations*, New York: Marcel Dekker.

Part Two
Parametric Systems

4

Parametric Filters Analysis

In Chapter 2, we discussed the general properties of linear systems with time-variant parameters, with periodically linear time-variant discrete systems (PLTV DSs) as the specific focus of our discussion. Now let us study the main characteristics of PLTV systems, which act relevant to input signals as frequency selective circuits. If these systems are stable, their behaviour and characteristics are similar in some instances to the relevant characteristics of time-invariant systems. We will call these systems parametric filters (PFs). In this chapter, we will examine how the major characteristics of PFs can be calculated.

4.1 NON-RECURSIVE PARAMETRIC FILTERS

As was discussed in previous chapters, analysis of non-recursive linear time-variant (LTV) filters is a relatively simple task. A block diagram of a non-recursive system with periodically varying coefficients is shown in Fig. 4.1. The system can be described by a difference equation:

$$y(n) = \sum_{k=0}^{K_2} b_k(n) \cdot x(n-k) \tag{4.1}$$

where

$$b_k(n) = b_k(n+N) \tag{4.2}$$

In this block diagram nT represents delay of the input signal by n periods of sampling interval. The impulse response (IR) of the system is determined from equation (4.1) for the unit pulse input signal represented by equation (1.2):

$$h(m,n) = \sum_{k=0}^{K_2} b_k(n) \cdot \delta(m-n+k) \tag{4.3}$$

An Introduction to Parametric Digital Filters and Oscillators Mikhail Cherniakov
© 2003 John Wiley & Sons, Ltd ISBN: 0-470-85104-X

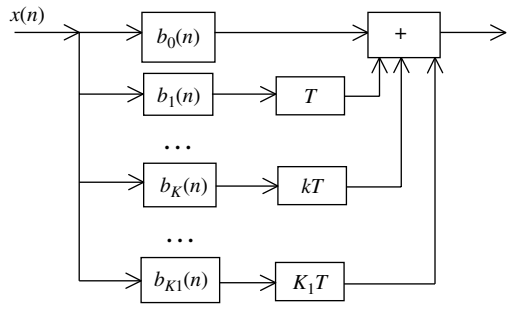

Figure 4.1 Non-recursive PF

The generalized transfer function (GTF), which is a z-transform of the IR, is determined using equation (1.14):

$$H(z,n) = \sum_{m=-\infty}^{\infty} \sum_{k=0}^{K_2} b_k(n) \cdot \delta(n-k-m) \cdot z^{m-n} = \sum_{k=0}^{K_2} b_k(n) \cdot z^{-k} \tag{4.4}$$

and the generalized frequency response (GFR) can be found by substituting $z = \mathrm{e}^{\mathrm{j}\omega}$:

$$H(\omega,n) = \sum_{k=0}^{K_2} b_k(n) \cdot \mathrm{e}^{-\mathrm{j}\omega k} \tag{4.5}$$

The periodical coefficients of the system can be represented by a discrete-time Fourier series:

$$b_k(n) = \sum_{i=0}^{N-1} b_{k,i} \cdot \mathrm{e}^{\mathrm{j}\Omega i n} \tag{4.6}$$

where $\Omega = 2\pi/N$ and

$$b_{k,i} = \frac{1}{N} \sum_{n=0}^{N-1} b_k(n) \cdot \mathrm{e}^{-\mathrm{j}\Omega i n} \tag{4.7}$$

Then,

$$H(\omega,n) = \sum_{k=0}^{K_2} \sum_{i=0}^{N-1} b_{k,i} \cdot \mathrm{e}^{\mathrm{j}\Omega i n} \cdot \mathrm{e}^{-\mathrm{j}\omega k} = \sum_{i=0}^{N-1} \left(\sum_{k=0}^{K_2} b_{k,i} \cdot \mathrm{e}^{-\mathrm{j}\omega k} \right) \cdot \mathrm{e}^{\mathrm{j}\Omega i n} \tag{4.8}$$

and

$$H_i(\omega) = \sum_{k=0}^{K_2} b_{k,i} \cdot \mathrm{e}^{-\mathrm{j}\omega k} \tag{4.9}$$

These useful expressions will be applied in the following discussions.

4.2 THE FIRST-ORDER RECURSIVE PARAMETRIC FILTER

Consider a causal recursive parametric filter of the first order, which is illustrated by the block diagram in Fig. 4.2. This system is described by the difference equation

$$y(n) = a(n) \cdot y(n-1) + x(n), n \geq 0, y(n) = 0 \text{ if } n < 0 \tag{4.10}$$

where the coefficient of the filter $a(n) = a(n+N)$ is N-periodical. Now we will study the main characteristics of this filter.

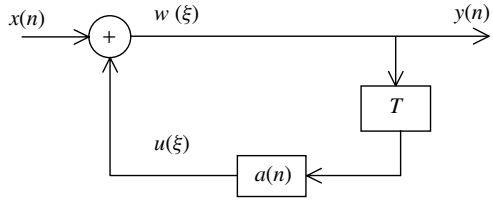

Figure 4.2 Recursive PF of the first order

4.2.1 Impulse Response

The solution of this equation represents the IR of the filter if the input signal is represented by equation (1.2):

$$h(n,m) = \begin{cases} a(n) \cdot h(m, n-1) + \delta(m,n) & \text{for } 0 \leq m \leq n \\ 0 & \text{for } n < 0 \text{ and } m > n \end{cases} \tag{4.11}$$

Let us solve the difference equation for values $n \in 0, \ldots, P; m \in 0, \ldots, R < P$ and, in particular, for $m = 0$ and different n [1, 2]:

$$\begin{aligned} n = 0 \quad & h(0,0) = \delta(0,0) = 1 \\ n = 1 \quad & h(0,1) = a(1) \cdot h(0,0) = a(1) \\ n = 2 \quad & h(0,2) = a(2) \cdot h(0,1) = a(2) \cdot a(1) \\ & \cdots \\ n = P \quad & h(0,P) = a(P) \cdot a(P-1) \cdot \ldots \cdot a(2) \cdot a(1) \end{aligned}$$

Then, for $m = 1$ and different n, we obtain

$$\begin{aligned} n = 0 \quad & h(1,0) = 0 \\ n = 1 \quad & h(1,1) = \delta(1,1) = 1 \\ n = 2 \quad & h(1,2) = a(2) \cdot h(1,1) = a(2) \end{aligned}$$

$$n = 3 \quad h(1,3) = a(3) \cdot h(1,2) = a(3) \cdot a(2)$$
$$\dots$$
$$n = P \quad h(1,P) = a(P) \cdot a(P-1) \cdot \ldots \cdot a(2)$$

and for $m = 2$ and different n, we obtain

$$n = 0 \quad h(2,0) = 0$$
$$n = 1 \quad h(2,1) = 0$$
$$n = 2 \quad h(2,2) = \delta(2,2) = 1$$
$$n = 3 \quad h(2,3) = a(3) \cdot h(2,2) = a(3)$$
$$\dots$$
$$n = P \quad h(2,P) = a(P) \cdot a(P-1) \cdot \ldots \cdot a(3)$$

Finally, for $m = R$ and different n, we obtain

$$n = 0 \quad h(R,0) = 0$$
$$n = 1 \quad h(R,1) = 0$$
$$\dots$$
$$n = R \quad h(R,R) = \delta(R,R) = 1$$
$$n = R+1 \quad h(R,R+1) = a(R+1) \cdot h(R,R) = a(R+1)$$
$$n = R+2 \quad h(R,R+2) = a(R+2) \cdot h(R,R+1) = a(R+2) \cdot a(R+1)$$
$$\dots$$
$$n = P \quad h(R,P) = a(P) \cdot a(P-1) \cdot \ldots \cdot a(R+1)$$

Comparing the obtained values for the same n and different m, note that the IR can be represented as

$$h(m,n) = \begin{cases} \prod_{i=m+l}^{n} a(i) & \text{for } 0 \le m \le n \\ 0 & \text{for } n < 0; m > n \end{cases} \tag{4.12}$$

After denoting

$$g(n) = \prod_{i=1}^{n} a(i) = h(0,n) \tag{4.13}$$

for $n \ge 1$, $g(0) = 1$, equation (4.12) takes the form

$$h(m,n) = \begin{cases} \prod_{i=m+1}^{n} a(i) = \dfrac{g(n)}{g(m)}, & 0 \le m \le n \\ 0, & m > n \\ 0 & n < 0 \end{cases} \tag{4.14}$$

We then introduce the new variable

$$n = \mu N + \nu \tag{4.15}$$

where $\mu = 0, 1, \ldots$, an integer representing the total number of periods of coefficient variation till the moment nT, and $\nu = n - \mu N$ is some addition, which can take values from the range $0, \ldots, N-1$, depending on the instant n.

For the periodic coefficient, from equations (4.13) and (4.14), it follows that

$$g(n+N) = g(N) \cdot g(n) \tag{4.16}$$

where

$$g(N) = \prod_{i=1}^{N} a(i) = \prod_{i=0}^{N-1} a(i) \tag{4.17}$$

is a multiplication of all coefficient values for the period. Continuing the calculations,

$$h(\eta N + \xi, \mu N + \nu) = g^{\mu-\eta}(N) \cdot h(\xi, \nu) \tag{4.18}$$

where m is also represented by an integer number of periods $\eta < \mu$ and by an "addition" ξ.

According to the stability criteria, the IR should decrease in time. From equation (4.14), we can see that this condition is obtained if

$$g(N) < 1 \tag{4.19}$$

Thus, an important conclusion is that the product of all instantaneous coefficient values of a stable first-order system for the whole period of coefficient variation must be less than 1. But, at any particular interval within the period, the coefficient can be bigger than 1. This characteristic represents an essential distinction between first-order time-variant systems and time-invariant discrete systems. In stable linear time-invariant (LTI) systems, the coefficient always has to be less than 1. We will come back to this problem later in the book. So, we have found an analytical equation that describes the IR of the first-order PF. Consider now a numerical example to confirm the analytical results of (4.14) and (4.17).

Example 4.1: Coefficients of a First-Order Filter

First, calculate the IR of the filter with coefficients equal $a(1) = 0.5$, $a(2) = 0.5$, $a(3) = 0.4$ and $N = 3$ directly from the appropriate difference equation. These results are presented in Table 4.1.

The results fully coincide with the calculation by equations (4.14) and (4.17). For instance, $g(3) = 0.5 \cdot 0.5 \cdot 0.4 = 0.1$ or $g(5) = 0.5 \cdot 0.5 \cdot 0.4 \cdot 0.5 \cdot 0.4 = 0.2$. Table 4.1 also shows the periodicity of the PF impulse as specified by equation (2.5) derived for

the general case. Thus, we have shown that the proposed method can be used to evaluate the first-order recursive PF impulse response.

Table 4.1 Impulse response of the filter

$a(n)$	0.5	0.5	0.4	0.5	0.5	0.4	0.5	0.5	0.4
$M\,n$	0	1	2	3	4	5	6	7	8
0	**1**	**0.5**	**0.2**	**0.1**	**0.05**	**0.02**	**0.01**	**0.005**	**0.002**
1	**0**	**1**	**0.4**	**0.2**	**0.1**	**0.04**	**0.02**	**0.01**	**0.004**
2	**0**	**0**	**1**	**0.5**	**0.25**	**0.1**	**0.05**	**0.025**	**0.01**
3	0	0	0	**1**	**0.5**	**0.2**	**0.1**	**0.05**	**0.02**
4	0	0	0	**0**	**1**	**0.4**	**0.2**	**0.1**	**0.04**
5	0	0	0	**0**	**0**	**1**	**0.5**	**0.25**	**0.1**
6	0	0	0	0	0	0	**1**	**0.5**	**0.2**
7	0	0	0	0	0	0	**0**	**1**	**0.4**
8	0	0	0	0	0	0	**0**	**0**	**1**
$G(n)$	1	0.5	0.2	0.1	0.05	0.02	0.01	0.005	0.002

4.2.2 Generalized Transfer Function

We can determine the GTF of a first-order system using equation (1.10) for z-transform and taking into account equation (4.15):

$$H(z, \mu N + \nu) = \sum_{l=0}^{\mu N-1} h(\mu N + \nu - l, \mu N + \nu) \cdot z^{-l} + \sum_{l=\mu N}^{\mu N+\nu} h(\mu N + \nu - l, \mu N + \nu) \cdot z^{-l} \tag{4.20}$$

Substituting equation (4.18) into (4.20), we obtain after calculations

$$H(z, \mu N + \nu) = \sum_{\eta=0}^{\mu-1} g^{\mu-1}(N) \cdot z^{-(\mu-1)N} \cdot \sum_{\xi=0}^{N-1} h(N + \nu - \xi, N + \nu) \cdot z^{-\xi} + g^{\mu}(N) \cdot z^{-\mu N} \cdot \sum_{\xi=0}^{\nu} h(\nu - \xi, \nu) \cdot z^{-\xi} \tag{4.21}$$

The value of the second part of this expression decreases with time in a stable system, satisfying equation (4.19). This part describes a transition process, which damps starting from the moment of arrival of an input signal. An obvious method used in the theory of continuous LTV systems is to discard the second part of equation (4.21) and

consider only the first part that corresponds to the steady-state mode. The first sum is a decreasing geometric progression, converging to $\frac{1}{1 - g(N) \cdot z^{-N}}$ for $\mu \to \infty$. Hence,

$$H(z, n) = H(z, \mu N + \nu) = H(z, \nu) = \frac{\sum_{\xi=0}^{N-1} h(N + \nu - \xi, N + \nu) \cdot z^{-\xi}}{1 - g(N) \cdot z^{-N}} \tag{4.22}$$

Note that the obtained expression for the GTF has the property of periodicity, as revealed in Chapter 3.

In equations (4.21) and (4.22), the impulse response contains period N, to overcome time values less then zero in calculations and limitations on the causality of the system. If we replace N by 1 in (4.22) or assume that coefficients are *constant*, equation (4.22) takes the form of the well-known expression [3] for the transfer function of a first-order system with constant coefficients

$$H(z) = \frac{1}{1 - a \cdot z^{-1}} \tag{4.23}$$

Comparison of equation (4.22) with (4.4) shows that a recursive discrete system of the first order (DS-1) can be represented as a cascaded non-recursive PLTV DS of the $N - 1$ order with coefficients

$$b_{\xi}(\nu) = h(N + \nu - \xi, N + \nu) \tag{4.24}$$

and as a recursive system with constant coefficients and transfer function

$$H(z) = \frac{1}{1 - g(N) \cdot z^{-N}} \tag{4.25}$$

An equivalent structure of a recursive PLTV DS-1 using this representation is shown in Fig. 4.3.

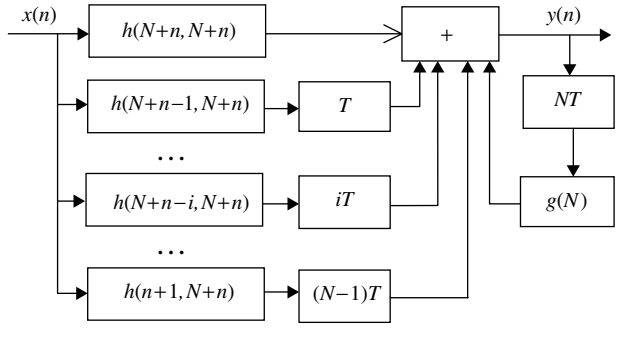

Figure 4.3 An equivalent structure of the recursive PLTV DS of the first order

The GFR of a first-order PF as well as the harmonics of the GTF and GFR can be found using equations (2.10) to (2.12). In particular, for an equivalent frequency response (EFR) characteristic of the first-order system,

$$H_0(\omega) = \frac{1}{N}\sum_{\nu=0}^{N-1} \frac{\sum_{\xi=0}^{N-1} h(N+\nu-\xi, N+\nu)\cdot \mathrm{e}^{-\mathrm{j}\xi\omega}}{1-g(N)\cdot \mathrm{e}^{-\mathrm{j}\omega N}} = \frac{\sum_{\xi=0}^{N-1}\left[\frac{1}{N}\sum_{\nu=0}^{N-1} h(N+\nu-\xi, N+\nu)\right]\cdot \mathrm{e}^{-\mathrm{j}\xi\omega}}{1-g(N)\cdot \mathrm{e}^{-\mathrm{j}\omega N}} \tag{4.26}$$

that is, the EFR is determined by mean value of the system's IR.

Example 4.2: First-Order Filter Impulse Response

Consider a parametric DS-1 with coefficient $a(n) = [1, 1, 0.75, 0.75]$ and $N = 4$. The IR of the system $h(0, m) = g(m)$ is shown in Fig. 4.4. From equation (4.26), Fig. 4.3 and Fig. 4.4, we can see that an LTI DS-1 with some equivalent coefficient *has an IR close to the averaged IR of* a PLTV DS-1.

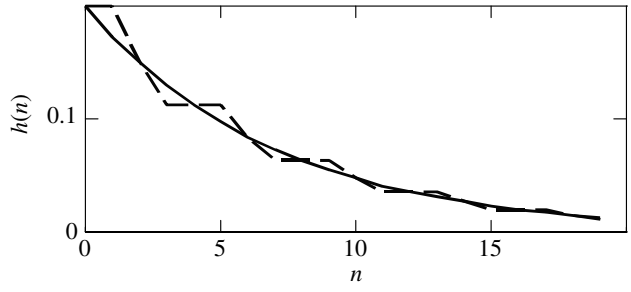

Figure 4.4 Impulse response of first-order systems

As a criterion for IR coincidence, we can use their equality at points corresponding to the integer number of periods, that is, $t = 0, N, 2N, \ldots$. For this case, the equivalent is

$$a = N\sqrt{\prod_{i=1}^{N} a(i)} \tag{4.27}$$

which is equal to the geometric mean of the time-varying coefficient over the period. It is obvious that the equivalent system is stable if the PLTV DS is stable.

Curve 1 in Fig. 4.4 represents an IR of the equivalent system and curve 2 represents the PF. One can see from the figure that both IR characteristics vary compatibly and incident values of the IR of the parametric system oscillate around the IR of the

time-invariant system. Equation (4.26) takes the form of a well-known formula for the time-invariant system impulse response if the coefficient value from equation (4.27) is used for the calculations:

$$H(\omega) = \frac{1}{1 - a \cdot e^{-j\omega}} \tag{4.28}$$

Figure 4.5 shows the EFR of a PLTV DS-1 (dashed line) and the EFR of an LTI filter (solid line) with a geometric mean value of the coefficient. The figure shows a very good coincidence of characteristic with no more than 0.1-dB difference between them. Thus, we can conclude that using the geometric mean of the coefficient is the correct approach for estimation of the IR and EFR of a first-order parametric filter.

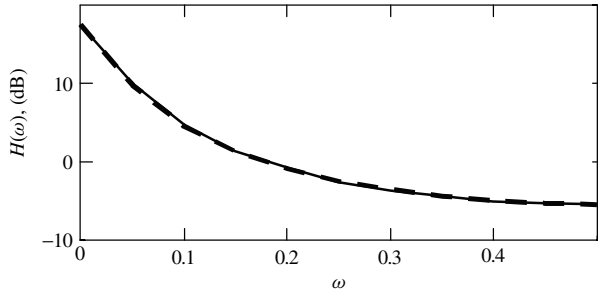

Figure 4.5 Frequency characteristics of the system from example 4.2

4.3 A RECURSIVE PARAMETRIC FILTER OF THE SECOND ORDER

A causal recursive PLTV DS of the second order (DS-2) is described by a difference equation:

$$y(n) = a_1(n)y(n-1) + a_2(n)y(n-2) + x(n) \tag{4.29}$$

where coefficients $a_1(n)$ and $a_2(n)$ are N-periodical:

$$a_1(n+N) = a_1(n), \quad a_2(n+N) = a_2(n) \tag{4.30}$$

The system's block diagram is shown in Fig. 4.6a.

4.3.1 Impulse Response

To find the characteristics of the second-order system, we will use the results obtained above for the PLTV DS-1, representing the PLTV DS-2 by cascade connection of the first-order system (Fig. 4.6b) [2, 4]. Firstly, we determine coefficients for the first-order system. The difference equations for the output signals are

$$u(n) = s_1(n) \cdot u(n-1) + x(n) \tag{4.31}$$

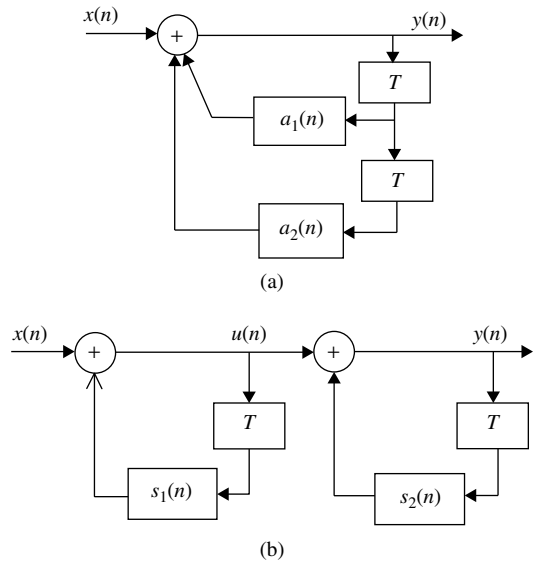

Figure 4.6 (a) Second-order recursive system block diagram and (b) its equivalent presentation

$$y(n) = s_2(n) \cdot y(n-1) + u(n) \tag{4.32}$$

where $u(n)$ is a signal at the output of the first system, and $s_1(n)$, $s_2(n)$ are coefficients of the equivalent cascaded system.

From equation (4.32), we obtain

$$u(n-1) = y(n-1) - s_2(n-1) \cdot y(n-2) \tag{4.33}$$

and from equation (4.31), it follows

$$u(n) = s_1(n) \cdot [y(n-1) - s_2(n-1) \cdot y(n-2)] + x(n) \tag{4.34}$$

Substituting (4.34) into equation (4.32), we obtain

$$y(n) = [s_1(n) + s_2(n)] \cdot y(n-1) - s_1(n) \cdot s_2(n-1) \cdot y(n-2) + x(n) \tag{4.35}$$

Comparison of equation (4.35) with (4.29) gives conditions for the equivalency of structures represented in Fig. 4.4:

$$\begin{cases} s_1(n) + s_2(n) = a_1(n) \\ \\ s_1(n) \cdot s_2(n-1) = -a_2(n) \end{cases} \quad \text{for } n = 1, 2, \ldots, N \tag{4.36}$$

If a solution of equation (4.36) exists, then it means that the second-order system can be represented by cascaded systems of the first order. In $2N$ equations (4.36), there

are $2N + 1$ variables. An additional condition for equivalency is the periodicity of coefficient $s_2(n)$:

$$s_2(n) = s_2(n + N) \tag{4.37}$$

Excluding $s_1(n)$ from equation (4.36), we obtain

$$s_2(n - 1) = -a_2(n)/[a_1(n) - s_2(n)] \tag{4.38}$$

for $n = 1, 2, \ldots, N$. Equation (4.38) forms systems of equations for different N that can be solved by sequential substitution:

$$s_1(n) = a_1(n) - s_2(n) = \frac{A_n + B_n \cdot s_2(0)}{C_n + D_n \cdot s_2(0)} \tag{4.39}$$

Rewriting (4.38) using equation (4.39), we obtain

$$s_2(n - 1) = \frac{-a_2(n) \cdot [C_n + D_n \cdot s_2(0)]}{A_n + B_n \cdot s_2(0)} = \frac{-a_2(n) \cdot C_n - a_2(n) \cdot D_n \cdot s_2(0)}{A_n + B_n \cdot s_2(0)} \tag{4.40}$$

At the same time, from equation (4.39), it follows that

$$\begin{aligned} s_2(n - 1) &= a_1(n - 1) - \frac{A_{n-1} + B_{n-1} \cdot s_2(0)}{C_{n-1} + D_{n-1} \cdot s_2(0)} \\ &= \frac{a_1(n - 1) \cdot C_{n-1} + a_1(n - 1) \cdot D_{n-1} \cdot s_2(0) - A_{n-1} - B_{n-1} \cdot s_2(0)}{C_{n-1} + D_{n-1} \cdot s_2(0)} \end{aligned} \tag{4.41}$$

Comparing the numerators and denominators of both equations, we note that they are identical for the following recurrent relations:

$$\begin{cases} A_{n-1} = a_1(n - 1) \cdot A_n + a_2(n) \cdot C_n \\ B_{n-1} = a_1(n - 1) \cdot B_n + a_2(n) \cdot D_n \\ C_{n-1} = A_n \\ D_{n-1} = B_n \end{cases} \tag{4.42}$$

The initial values of coefficients A_n, B_n, C_n and D_n are determined as follows: for $n = N$, according to equation (4.37), $s_2(0) = s_2(N)$, and equation (4.41) becomes identical for

$$A_N = a_1(N),\ B_N = -1,\ C_N = 1,\ D_N = 0 \tag{4.43}$$

A_1, B_1, C_1 and D_1 can be found by sequentially solving the recurrent equation (4.42) for the initial conditions specified in equation (4.43) for all $n = N, N - 1, \ldots, 2$. Then, by substituting them into equation (4.39), we obtain an expression for $s_1(1)$:

$$s_1(1) = \frac{A_1 + B_1 \cdot s_2(0)}{C_1 + D_1 \cdot s_2(0)} \tag{4.44}$$

Substituting this into the second equation of the system from equation (4.38), for $n = 1$, we obtain the square equation for $s_2(0)$:

$$B_1 \cdot s_2^2(0) + [A_1 + a_2(1) \cdot D_1] \cdot s_2(0) + a_2(1) \cdot C_1 = 0 \tag{4.45}$$

from which we obtain

$$s_2(0) = \frac{-[A_1 + a_2(1) \cdot D_1] \pm \sqrt{[A_1 + a_2(1) \cdot D_1]^2 - 4 \cdot a_2(1) \cdot B_1 \cdot C_1}}{2 \cdot B_1} \tag{4.46}$$

Two solutions for $s_2(0)$ indicate that there are two versions of cascaded representation for PLTV DFs. Other values for $s_2(n)$ for $n = N - 1, \ldots, 1$ can be derived from equation (4.38) for $s_2(N) = s_2(0)$, while values for $s_1(n)$ can be derived from the first equation of the system represented by equation (4.36).

Thus, the system described by equation (4.38) has a solution, and a PLTV DS of the second order can be represented by two cascaded first-order PLTV DSs. Coefficients of this equivalent system can be found using coefficients $a_1(n)$, $a_2(n)$ of an original system via algorithms (4.36) to (4.46). Coefficients $s_1(n)$, $s_2(n)$ of the equivalent representation are N-periodical and, in the general case, complex. There are two different sequences of coefficients $s_1(n)$, $s_2(n)$, which correspond to two different solutions of equation (4.30). Any of these sequences can be used for calculations, as the results will be the same.

The IR of the PLTV DS-2, represented by two cascaded equivalent first-order systems, is determined according to equation (1.69):

$$h(m, n) = \sum_{k=0}^{n} h_1(m, k) \cdot h_2(k, n) \tag{4.47}$$

where $h_1(m, k)$ and $h_2(k, n)$ are the IRs of the first and second systems, respectively, and can be derived from the known coefficients $s_1(n)$ and $s_2(n)$ using equation (4.12). Let us consider the following example.

Example 4.3: Second-Order Filter

Instant values of coefficients $a_1(n)$ and $a_2(n)$ of the DS-2 with period $N = 4$ are presented in Table 4.2. This table also contains two different sequences of coefficients $s_1'(n)$, $s_2'(n)$ and $s_1''(n)$, $s_2''(n)$ for an equivalent representation of the second-order system via cascaded connections of the first-order systems. Table 4.3 provides IR values $h(m, n)$ calculated directly from the difference equation (4.29) for the unit pulse input signals (1.2) applied at time $m = 3$, and also values of two IRs $h'(m, n)$ and $h''(m, n)$ for the equivalent representation, calculated from equations (4.36) to (4.46).

Table 4.2 Coefficients of the DS-2 and its equivalent representation DS-1

Initial system			Equivalent representation			
			The first variant		The second variant	
N	$a_1(n)$	$a_2(n)$	$s_1'(n)$	$s_2'(n)$	$s_1''(n)$	$s_2''(n)$
0	−0.75	−1	$-0.375 + j1.301$	$-0{,}375 - j1.301$	$-0{,}375 - j1.301$	$-0{,}375 + j1.301$
1	−0.5	−1	$-0.205 + j0.710$	$-0.295 - j0.710$	$-0.205 - j0.710$	$-0.295 + j0.710$
2	−0.75	−0.75	$-0.375 + j0.901$	$-0.375 - j0.901$	$-0.375 - j0.901$	$-0{,}375 + j0.901$
3	−0.5	−0.75	$-0.295 + j0.710$	$-0.205 - j0.710$	$-0.295 - j0.710$	$-0.205 + j0.710$

Table 4.3 IR of the DS-2 and its equivalent representation by the DS-1

	DS-2	Equivalent system	
$m = 3$		The first variant	The second variant
n	$h(3, n)$	$h'(3, n)$	$h''(3, n)$
0	0	0	0
1	0	0	0
2	0	0	0
3	1.0000000	0.9999999	0.9999999
4	−0.5000000	−0.5000000	−0.5000000
5	−0.6250000	−0.6249999	−0.6249999
6	0.8125000	0.8124999	0.8124999
4	−0.1406250	−0.1406251	−0.1406251
7	−0.5390625	−0.5390623	−0.5390623
8	0.5449219	0.5449218	0.5449218
9	0.2666016	0.2666014	0.2666014

The data from these tables show that the IR calculated from a difference equation coincides with the IR calculated using equivalent DS-2 representation by cascaded systems. Two different solutions of equation (4.46) correspond to the same equivalent systems. Note also that if $a_1(n)$ are real, coefficients of the first-order systems are complex conjugates.

If IR reduction is used as the criterion for PLTV systems, then for a stable DS-2, the following expressions should be correct:

$$|g_1(N)| < 1, |g_2(N)| < 1 \tag{4.48}$$

where $g_1(N)$ and $g_2(N)$ are determined from equation (4.13) using coefficients $s_1(n)$ and $s_2(n)$, respectively. In equation (4.31), absolute values have been adopted, since coefficients $s_1(n)$ and $s_2(n)$ are generally complex and, as a result, $g_1(N)$and $g_2(N)$ are also complex.

4.3.2 Generalized Transfer Function

We obtain an expression for the GTF of the second-order system using equation (1.70):

$$H(z,n)=\sum_{k=0}^{n}H_1(z,k)\cdot h_2(k,n)\cdot z^{k-n} \tag{4.49}$$

We will determine the GTF of the DS-2 following a procedure similar to first-order systems analysis:

$$H(z,n)=H(z,\mu N+\nu)=\sum_{\eta=0}^{\mu-1}\sum_{\xi=0}^{N-1}H_1(z,\eta N+\xi)\cdot h_2(\eta N+\xi,\mu N+\nu)$$
$$\cdot z^{\eta N+\xi-\mu N-\nu}+\sum_{\xi=0}^{\nu}H_1(z,\mu N+\xi)\cdot h_2(\eta N+\xi,\mu N+\nu)\cdot z^{\mu N+\xi-\mu N-\nu} \tag{4.50}$$

Equation (4.32) corresponds to the GTF of the stable DS-1 and was derived from equation (4.21):

$$H_1(z,k)=H_1(z,\eta N+\xi)=H_1(z,\xi)=\frac{\sum_{\chi=0}^{N-1}h_1(N+\xi-\chi,N+\xi)\cdot z^{-\chi}}{1-g_1(N)\cdot z^{-N}} \tag{4.51}$$

Using expression (4.15) for the IR of the second DS-1, from equation (4.32), we obtain

$$H(z,n)=H(z,\mu N+\nu)=\sum_{\eta=0}^{\mu-1}g_2^{\mu-\eta}(N)\cdot z^{(\eta-\mu)\cdot N}\sum_{\xi=0}^{N-1}H_1(z,\xi)$$
$$\cdot h_2(N+\xi,N+\nu)\cdot z^{\xi-\nu}+g_2^{\mu}(N)\cdot\sum_{\xi=0}^{\nu}H_1(z,\xi)\cdot h_2(\xi,\nu)\cdot z^{\xi-\nu} \tag{4.52}$$

The next step is to evaluate the steady-state GTF. We will have to consider equation (4.52) for $\mu\to\infty$, taking into account that for the stable DS-2 $g_2(N)<1$, the sum along η is a decreasing geometrical mean, converging to $\dfrac{1}{1-g_2(N)\cdot z^{-N}}$. The second half of equation (4.35), which corresponds to a transition process, tends to zero and can be disregarded. Finally, the GTF of a second-order PLTV system is described by

$$H(z,\nu)=\frac{1}{1-g_2(N)\cdot z^{-N}}\cdot\sum_{\xi=0}^{N-1}H_1(z,\xi)\cdot h_2(N+\xi,N+\nu)\cdot z^{\xi-\nu} \tag{4.53}$$

Summarizing what should be done to evaluate the integral characteristics of a PLTV of the second order, an algorithm for determination of characteristics of the DS-2 involves the following procedure:

1. DS-2 representation by two cascaded DS-1 coefficients $s_1(n)$ and $s_2(n)$.
2. Calculation of coefficients $s_1(n)$ and $s_2(n)$.
3. Determination of the stability of the first-order systems.
4. Calculation of the IR and GTF of the first cascaded system using equations (4.36) to (4.46), (4.12) and (4.52).
5. Calculation of the IR and GTF of the whole cascaded structure calculation using equations (1.69) and (4.53).
6. Substitution of $z = e^{j\omega}$ to determine characteristics in the frequency domain.
7. Evaluation of the signal and combinational components (CCs) of the GFR using equation (2.13).

In the next example, components of the GFR are introduced, calculated by the method described above. We will come back to these results later, during discussion of the approximate method of parameter evaluations.

Example 4.4: Evaluation of Signal and Combinational Components

Figure 4.7 [5] (solid lines) shows the signal (EFR) and CCs of the system GFR with coefficients from example 4.3 calculated using the algorithm described above.

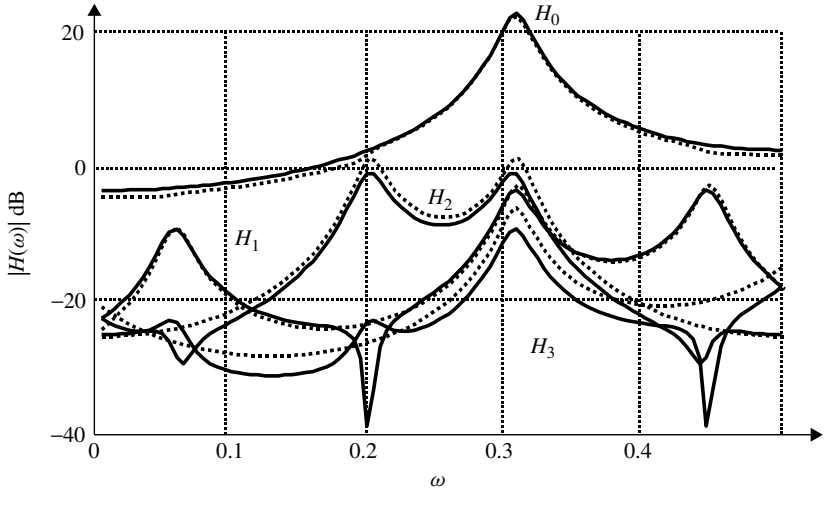

Figure 4.7 PLTV DS-2 GFR components

4.4 PARAMETRIC FILTERS OF AN ARBITRARY ORDER

In the previous sections, we introduced analytical methods for evaluating integral characteristics of first- and second-order recursive PLTV DSs. Let us now evaluate the GTF for an arbitrary-order PLTV DS. Any other system characteristics can be derived from this function if necessary. It is interesting to note that, in the general case, GTF cannot be presented in an analytically closed form for continuous periodically time-variant systems, except for the first-order case [6].

4.4.1 Direct Equation Solution

The difference equation (1.21) can be represented for all $0 \le n \le N-1$ as a system of linear equations:

$$\sum_{k=0}^{K_1} a_k(n) \cdot z^{-k} \cdot H(z, n-k) = \sum_{k=0}^{K_2} b_k(n) \cdot z^{-k} \tag{4.54}$$

This can be rewritten in the matrix form

$$[A_{mn}(z)] \cdot [H(z, n)] = [B_n(z)] \tag{4.55}$$

where values of the coefficient matrix are determined according to the following algorithm:

1. $A_{mn}(z) = 0$ is the matrix of initial coefficients.
2. An integer $i = n - k + pN$ has to be found for all $0 \le n \le N-1$ and $0 \le k \le K_1$, where another integer p is selected to satisfy the condition $0 \le i \le N-1$. Then, $a_k(n) \cdot z^{-k}$ is added to the previous value $A_{ni}(z)$. This is necessary to count a periodicity of $H(z, n) = H(z, n+N)$.
3. Values of the constant term column are determined as

$$B_n(z) = \sum_{k=0}^{K_2} b_k(z) \cdot z^{-k} \tag{4.56}$$

Having these values of the coefficients, the matrix form (4.55) corresponds to the difference equation (4.54). Solution of the system can be obtained by one of the known methods [5] for any given z. For example, using multiplication of the left and right parts of the equation (4.55) by reverse coefficient matrix, we obtain

$$[A_{mn}(z)]^{-1} \cdot [A_{mn}(z)] \cdot [H(z, n)] = [A_{mn}(z)]^{-1} \cdot [B_n(z)]$$

or

$$[H(z,n)] = [A_{mn}(z)]^{-1} \cdot [B_n(z)] \tag{4.57}$$

To calculate the GFR, $z = e^{j\omega}$ is substituted into equation (4.55) and GFR harmonics are determined using equation (2.13). The algorithm will be more easily understood if we consider the following example of calculations.

Example 4.5: **Direct Solution for $N = 4$**

For a PLTV DS-2 and the period $N = 4$, the coefficient matrix can be written as

$$[A_{mn}(z)] = \begin{bmatrix} a_0(0) & 0 & a_2(0)\cdot z^{-2} & a_1(0)\cdot z^{-1} \\ a_1(1)\cdot z^{-1} & a_0(1) & 0 & a_2(1)\cdot z^{-2} \\ a_2(2)\cdot z^{-2} & a_1(2)\cdot z^{-1} & a_0(2) & 0 \\ 0 & a_2(3)\cdot z^{-2} & a_1(3)\cdot z^{-1} & a_0(3) \end{bmatrix}$$

Consider a recursive PLTV DS-2 with coefficients from example 4.3. Since there are differences in the form of equations (4.27) and (4.54), in the coefficient matrix it is necessary to designate $a_0(n) = -1$ and $b_0(n) = 1$. Let us start calculations from direct current (DC) that correspond to $\omega = 0$ and, consequently, $z = 1$. In this case, we have $H(0, n) = 0{,}23;\ 0{,}48;\ 0{,}47;\ 0{,}405$, which coincide exactly with values calculated using the algorithm from Section 4.3. For the frequency $\omega = \pi/8$, the solution of equation (4.57) gives the following values: $H(\pi/8, 0) = 0.34 + 0.34j$; $H(\pi/8, 1) = 0{,}43 + 0.47j$; $H(\pi/8, 2) = 0.27 + 0.23j$; $H(\pi/8, 3) = 0.47 + 0.33j$. These results could also be obtained using the algorithm and calculations in Section 4.3.

Note that in the case when $a_k(n) = a_k = \text{const}$, which is the case for LTI systems, solution of equation (1.21) can be obtained by applying a discrete Fourier transform (DFT) to both parts of equation (4.54):

$$\sum_{k=0}^{K_1} a_k \cdot z^{-k} \cdot H_i(z) = \sum_{k=0}^{K_2} b_{ki} \cdot z^{-k} \tag{4.58}$$

where

$$b_{ki} = \frac{1}{N} \sum_{n=0}^{N-1} b_k(n) \cdot e^{-jni\Omega} \tag{4.59}$$

From this, it follows that

$$H_i(z) = \frac{\sum_{k=0}^{K_2} b_{ki} \cdot z^{-k}}{\sum_{k=0}^{K_1} a_k \cdot z^{-k}} \tag{4.60}$$

For a non-recursive PLTV DS, when $a_0 = 1$, $a_k = 0$ and $k > 0$, the obtained expression coincides with equation (4.9).

4.4.2 Equation Solution in a State Space

As discussed before, difference equations can be introduced in the state space [7]. In the time domain, the system can be described by

$$w[n+1] = Aw[n] + bx[n] \tag{4.61}$$

$$y[n] = C^T w[n] + Dx[n] \tag{4.62}$$

where matrix $\boldsymbol{A}$, vectors $\boldsymbol{b}$ and $\boldsymbol{c}$, and scalar D represent the system stricture and coefficients. For example, for the canonical second-order filter with coefficients b_1 and b_2 in the non-recursive part and $-a_1$ and $-a_2$ in the recursive part, the parameters under consideration will take the following forms:

$$A = \begin{bmatrix} -a_1 & -a_2 \\ 1 & 0 \end{bmatrix}, b = \begin{bmatrix} 1 \\ 0 \end{bmatrix}, C^T = [b_1 - a_1 \quad b_2 - a_2], D = [1] \tag{4.63}$$

A similar approach can be taken for time-variant systems where, obviously, coefficients a_i and b_i will be functions of time n. For periodically time-variant systems, this approach was developed in [8]. For the general case, the state equations (4.61) and (4.62) have the following time-dependent form:

$$w[n+1] = A[n]w[n] + b[n]x[n] \tag{4.64}$$

$$y[n] = C^T[n]w[n] + D[n]x[n] \tag{4.65}$$

In equations (4.64) and (4.65), the system matrixes are N-periodical for PLTV systems. In this case, as for previous cases, we can apply DFT for the parameter matrixes:

$$A[n] = \sum_{k=0}^{N-1} A_k \exp(\mathrm{j}\Omega nk) \tag{4.66}$$

$$b[n] = \sum_{k=0}^{N-1} b_k \exp(\mathrm{j}\Omega nk) \tag{4.67}$$

$$C[n] = \sum_{k=0}^{N-1} C_k \exp(\mathrm{j}\Omega nk) \tag{4.68}$$

$$D[n] = \sum_{k=0}^{N-1} D_k \exp(\mathrm{j}\Omega nk) \tag{4.69}$$

where $\Omega = 1/N$ is the main frequency in the Fourier presentation. Assuming that the order of the system is K, these matrixes have the following dimensions: $\boldsymbol{A}$ is a constant $K \times K$ matrix, $\boldsymbol{b_K}$ is a constant $K \times 1$ matrix, $\boldsymbol{C_k}$ is a $K \times 1$ matrix and D_k is a constant scalar.

As our goal is to determine the GFR, which is the system reaction to the complex sinusoidal signal, we should consider this signal as an input signal:

$$x[n] = \exp(\mathrm{j}\omega n) \tag{4.70}$$

Let the vector of transfer functions between the input signal $x[n]$ and the state vector $w[n]$ be $q(\exp(\mathrm{j}\Omega), n)$. This vector links the state vector and the input signal as follows:

$$w[n] = q[\exp(\mathrm{j}\omega), n]x[n]|_{x[n]=\exp(\mathrm{j}\omega n)} \tag{4.71}$$

Now we can introduce the GFR via system parameters and the transfer function:

$$H(\mathrm{e}^{\mathrm{j}\omega}, n) = C^T[n]q[\mathrm{e}^{\mathrm{j}\omega}, n] + D[n] \tag{4.72}$$

The transfer vector, like the system parameters, is periodical and can be represented via Fourier transform as

$$q[\mathrm{j}\omega, n] = \sum_{k=0}^{N-1} q_k(\mathrm{e}^{\mathrm{j}\omega}) \exp(\mathrm{j}\Omega nk) \tag{4.73}$$

Now we can replace all terms in the state–space equation in the Fourier notation (4.66) to (4.69) and (4.73) to obtain

$$\sum_{k=0}^{N-1} H_k(\mathrm{e}^{\mathrm{j}\omega}) \exp(\mathrm{j}\Omega nk) = \left(\sum_{\lambda=0}^{N-1} C_\lambda^T \exp(\mathrm{j}\Omega n\lambda)\right) \times \left(\sum_{\gamma}^{N-1} q_\gamma(\mathrm{e}^{\mathrm{j}\omega}) \exp(\mathrm{j}\Omega n\gamma)\right) + \sum_{k=0}^{N-1} D_k \exp(\mathrm{j}\Omega nk) \tag{4.74}$$

This equation is true for any n and, taking into account the periodicity of the complex exponential function equation (4.74), can be represented in the following matrix format:

$$\begin{vmatrix} H_0 \\ H_1 \\ \cdots \\ \cdots \\ H_{N-1} \end{vmatrix} = \begin{vmatrix} C_0^T & C_{N-1}^T \cdots \cdots \cdots C_1^T \\ C_1^T & C_0^T \cdots \cdots \cdots C_2^T \\ \cdots\cdots\cdots\cdots\cdots\cdots \\ \cdots\cdots\cdots\cdots\cdots\cdots \\ C_{N-1}^T & C_{N-2}^T \cdots \cdots \cdots C_0^T \end{vmatrix} \cdot \begin{vmatrix} q_0 \\ q_1 \\ \cdots \\ \cdots \\ q_{N-1} \end{vmatrix} + \begin{vmatrix} D_0 \\ D_1 \\ \cdots \\ \cdots \\ D_{N-1} \end{vmatrix} \tag{4.75}$$

This equation can be further rearranged to obtain the more compact matrix form

$$\boldsymbol{H = CQ + D} \tag{4.76}$$

where ***H, C, Q*** and ***D*** reflect components of equation (4.75). To find the GFR in the closed analytical form, we need to evaluate vector ***Q***. If we replace the components

in equation (4.61), with appropriate equations (4.66), (4.67) and (4.71), and take into account equation (4.73), we obtain the following relationships between q_i and the system parameters:

$$\left\{\sum_{k=0}^{N-1} q_k e^{j\omega} \exp(j\Omega(n+1)k)\right\} \exp(j\omega(N+1)) = \left\{\sum_{\lambda=0}^{N-1} A_\lambda e^{j\Omega n\lambda}\right\} \times \left\{\sum_{\gamma=0}^{N-1} q_\gamma e^{j\omega} \exp(j\Omega n\gamma)\right\} \exp(j\omega n) + \left\{\sum_{k=0}^{N-1} b_k e^{j\Omega nk}\right\} \exp(j\omega n) \tag{4.77}$$

Equation (4.77) is true for any n. Comparing both sides of this equation and taking into account the periodicity of complex exponent functions, we obtain

$$\begin{vmatrix} q_0 \exp j(\omega) \\ q_1 \exp j(\omega+\Omega) \\ \cdots\cdots\cdots \\ \cdots\cdots\cdots \\ q_{N-1} \exp j(\omega+\Omega(N-1)) \end{vmatrix} = \begin{vmatrix} A_0 & A_{N-1} \cdots\cdots A_1 \\ A_1 & A_0 \cdots\cdots A_2 \\ \cdots\cdots\cdots\cdots\cdots\cdots \\ \cdots\cdots\cdots\cdots\cdots\cdots \\ A_{N-1} & A_{N-2} \cdots\cdots A_0 \end{vmatrix} \times \begin{vmatrix} q_0 \\ q_1 \\ \cdots \\ \cdots \\ q_{N-1} \end{vmatrix} + \begin{vmatrix} b_0 \\ b_1 \\ \cdots \\ \cdots \\ b_{N-1} \end{vmatrix} \tag{4.78}$$

or

$$\begin{vmatrix} e^{j\omega}E - A_0 & -A_{N-1} \cdots\cdots\cdots\cdots -A_1 \\ -A_1 & e^{j(\omega+\Omega)}E - A_0 \cdots\cdots -A_2 \\ \cdots\cdots\cdots\cdots\cdots\cdots\cdots\cdots \\ \cdots\cdots\cdots\cdots\cdots\cdots\cdots\cdots \\ -A_{N-1} & -A_{N-2} \quad e^{j(\omega+\Omega(N-1))}E - A_0 \end{vmatrix} \times \begin{vmatrix} q_0 \\ q_1 \\ \cdots \\ \cdots \\ q_{N-1} \end{vmatrix} = \begin{vmatrix} b_0 \\ b_1 \\ \cdots \\ \cdots \\ b_{N-1} \end{vmatrix} \tag{4.79}$$

In a more compact matrix form, this equation takes the form

$$\hat{\boldsymbol{A}}\boldsymbol{Q} = \boldsymbol{B} \tag{4.80}$$

where $\hat{\boldsymbol{A}}$ is a $KN \times KN$ matrix, $\boldsymbol{Q}$ is a $KN \times 1$ column and $\boldsymbol{E}$ is the $K \times K$ unit matrix. In case of the stable PLTV DS, the rank of $\hat{\boldsymbol{A}}$ equals the order of the matrix $\hat{\boldsymbol{A}}$. Then, we can evaluate the sought Q as follows:

$$\boldsymbol{Q} = \hat{\boldsymbol{A}}^{-1}\boldsymbol{B} \tag{4.81}$$

Now we have all components of equation (4.75) to evaluate the GFR spectrum and the last step is to put the evaluated $H_i(\omega)$ into (2.13):

$$H(e^{j\omega}, n) = \sum_{k=0}^{N-1} H_k(e^{j\omega}) \exp(-j\Omega nk) \tag{4.82}$$

Let us apply this approach to first-order system analysis.

Example 4.6: First-Order Filter

Consider a stable parametric filter of the first order with a constant coefficient $b_1 = b$ in the non-recursive part and a periodically time-varying coefficient with the period $N = 2$ in the recursive part of the filter $a_1 = a(1 - cosn\pi)$ [8]. Taking into account (4.63) and assuming $a_2 = b_2 = 0$, we obtain a state equation for the canonical first-order filter:

$$\begin{vmatrix} w_1(n+1) \\ w_2(n+1) \end{vmatrix} = \begin{vmatrix} 0 & a(1-\cos n\pi) - b \\ b - a(1+\cos n\pi) & 0 \end{vmatrix} \times \begin{vmatrix} w_1(n) \\ w_2(n) \end{vmatrix} + \begin{vmatrix} 1 \\ 1 \end{vmatrix} x(n)$$

$$y(n) = [1, 1][w_1(n)w_2(n)]^T + x(n) \tag{4.83}$$

For instance, for a = $b = 0.5$, the equations in (4.63) become

$$A_0 = \begin{vmatrix} 0 & 0 \\ 0 & 0 \end{vmatrix}, A_1 = \begin{vmatrix} 0 & -0.5 \\ -0.5 & 0 \end{vmatrix}, b_0 = \begin{vmatrix} 1 \\ 1 \end{vmatrix}, b_1 = \begin{vmatrix} 0 \\ 0 \end{vmatrix} \tag{4.84}$$

$$C_0^T = [1 \quad 1], C_1^T = [0 \quad 0], D_0 = 1, D_1 = 0$$

Substituting components of equation (4.79) with (4.84) we obtain

$$\begin{vmatrix} e^{j\omega} & 0 & 0 & 0.5 \\ 0 & e^{j\omega} & 0.5 & 0 \\ 0 & 0.5 & -e^{j\omega} & 0 \\ 0.5 & 0 & 0 & -e^{j\omega} \end{vmatrix} \cdot \begin{vmatrix} q_0 \\ q_1 \end{vmatrix} = \begin{vmatrix} 1 \\ 1 \\ 0 \\ 0 \end{vmatrix} \tag{4.85}$$

The solution of this equation is

$$\begin{vmatrix} q_0 \\ q_1 \end{vmatrix} = \begin{vmatrix} \frac{4e^{j\omega}}{4e^{j2\omega}+1} & \frac{4e^{j\omega}}{4e^{j2\omega}+1} & \frac{2}{4e^{j2\omega}+1} & \frac{2}{4e^{j2\omega}+1} \end{vmatrix} \tag{4.86}$$

The GFR spectrum components can be evaluated from the following equation:

$$\begin{vmatrix} H_0 \\ H_1 \end{vmatrix} = \begin{vmatrix} 1 & 1 & 0 & 0 \\ 0 & 0 & 1 & 1 \end{vmatrix} \cdot \begin{vmatrix} q_0 \\ q_1 \end{vmatrix} + \begin{vmatrix} 1 \\ 0 \end{vmatrix} = \begin{vmatrix} \frac{4e^{j2\omega}+8e^{j\omega}+1}{4e^{j2\omega}+1} & \frac{4}{4e^{j2\omega}+1} \end{vmatrix} \tag{4.87}$$

From equation (2.12), which is for our case

$$H(e^{j\omega}, n) = \sum_{k=0}^{N-1} H_k(e^{j\omega}) \exp(-j\Omega nk) \tag{4.88}$$

we obtain

$$H(e^{j\omega}, n) = \frac{4e^{j2\omega} + 8e^{j\omega} + 1 + 4\cos n\pi}{4e^{j2\omega} + 1} \tag{4.89}$$

For frequency $\omega = 0$, we obtain $H(0, 0) = 3.4$; $H(0, 1) = 1.8$; $H(0, 2) = 3.4$; $H(0, 3) = 1.8$ and so on, and for frequency $\omega = \pi/8$, we obtain $H(\pi/8, 0) = 11.4 - j3.36$; $H(\pi/8, 1) = 1.07 - j3.36$ and so on.

4.5 APPROXIMATE METHOD FOR ANALYSIS OF PERIODICAL LINEAR TIME-VARIANT DISCRETE SYSTEMS

We have discussed two approaches to parametric system analysis: through the analytically calculated integral characteristics and through appropriate difference equations and computer simulations. These methods for GFR evaluation give an exact result, but require a large number of calculations. These calculations, in some instances, mask the physical sense behind the system analysis. In engineering practice, approximate methods of analysis have a very important role. They not only give reasonably accurate results but are also transparent for the physical processes occurring, which allows for a clearer understanding of the system. Let us consider one of these approximate methods.

In Section 4.2, we discussed an approximate method for analysis of a first-order discrete system, which was represented as an LTI system with a constant coefficient equal to the mean geometrical value of coefficient variation. For second- and higher-order systems, this approach is not directly applicable. Instead, we will consider an approximate method of calculation based on calculation of GFR harmonics.

Equation (4.54), for the recursive part of the system, can be written as

$$\sum_{k=0}^{K_1} a_k(n) \cdot z^{-k} \cdot H(z, n-k) = 1 \tag{4.90}$$

and applying a DFT, we obtain

$$\frac{1}{N} \sum_{n=0}^{N-1} \mathrm{e}^{-\mathrm{j}mn\Omega} \cdot \left[\sum_{k=0}^{K_1} a_k(n) \cdot z^{-k} \cdot H(z, n-k) \right] = \frac{1}{N} \sum_{n=0}^{N-1} \mathrm{e}^{-\mathrm{j}mn\Omega} \tag{4.91}$$

From (4.91), we can derive a system of equations for GFR harmonics using DFT properties for multiplication of functions [3]:

$$\sum_{i=0}^{N-1} H_i(z) \cdot \sum_{k=0}^{K_1} a_{k,m-i} \cdot z^{-k} \cdot \mathrm{e}^{-\mathrm{j}ki\Omega} = \delta(m) \tag{4.92}$$

where

$$a_{km} = \frac{1}{N} \sum_{n=0}^{N-1} a_k(n) \cdot \mathrm{e}^{-\mathrm{j}mn\Omega} \tag{4.93}$$

represents the coefficients via a Fourier series.

In the frequency domain, we obtain the following system of equations for GFR harmonics:

$$\sum_{i=0}^{N-1} H_i(\omega) \cdot \sum_{k=0}^{K_1} a_{k,m-i} \cdot \mathrm{e}^{-\mathrm{j}k(\omega+i\Omega)} = \delta(m), m = 0, \ldots, N-1 \tag{4.94}$$

The system of N linear equations represented by (4.94) can be solved by the computer for each particular frequency ω. In comparison with equation (4.55), more computer calculations are required to determine system coefficients, but the structure of the coefficient matrix has a regular nature regardless of the order of the system and the period N, and is, therefore, simpler for programming. The results of calculations using equations (4.55) and (4.94) are the same.

We can now simplify the solution for equation (4.94) by considering the physical implications of the appearance of combinational components (CCs). Figure 4.8 presents, as an example, a structure of the recursive second-order PLTV DS, where a feedback of the systems has been split into two branches: branch **A** has constant (averaged) coefficients a_{10} and a_{20}, and branch **B** has a variable part of the coefficient components. In this figure, elements of the unit delay have been replaced by $e^{j\Theta}$ multiplication. For the analysis of particular systems, Θ should be replaced by the actual frequency of the signal passing through the element.

Consider signal $x(n) = e^{j\omega n}$ passing through the system. According to equation (2.18), an output signal of the system is

$$y(n) = e^{j\omega n} \cdot H(\omega, n) = e^{j\omega n} \cdot \sum_{k=0}^{N-1} H_k(\omega) \cdot e^{j\Omega kn} = e^{j\omega n} \cdot H_0(\omega) + \sum_{k=1}^{N-1} H_k(\omega) \cdot e^{j(\omega + k\Omega)} \tag{4.95}$$

Through branch **A**, the following components pass to the system input:

1. The output signal component with frequency ω:

$$e^{j\omega n} \cdot H_0(\omega) \cdot (a_{10} \cdot e^{-j\omega} + a_{20} \cdot e^{-2j\omega}) \tag{4.96}$$

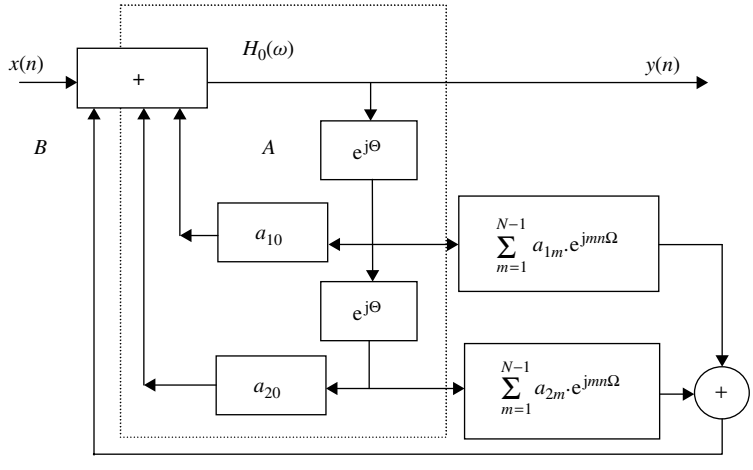

Figure 4.8 Generation of CCs in a recursive PLTV DS-2

2. The output combinational components with frequencies $\omega + k\Omega$:

$$\sum_{k=1}^{K_1} H_k(\omega) \cdot e^{j(\omega+k\Omega)n} \cdot \left[a_{10} \cdot e^{-j(\omega+k\Omega)} + a_{20} \cdot e^{-2j(\omega+k\Omega)}\right] \tag{4.97}$$

Through branch **B**, the following components pass to the input:

1. Combinational components that have been obtained as a result of modulation of the output signal component by the time-varying parts of coefficients:

$$e^{j\omega n} \cdot H_o(\omega) \cdot \sum_{m=1}^{N-1} (a_{1m} \cdot e^{-j\omega} + a_{2m} \cdot e^{-2j\omega}) \cdot e^{jmn\Omega} \tag{4.98}$$

2. Products of the secondary modulation of the output combinational components:

$$\sum_{k=1}^{N-1} H_k(\omega) \cdot e^{j(\omega+k\Omega)n} \cdot \sum_{m-1}^{N-1} \left[a_{1m} \cdot e^{-j(\omega+k\Omega)} + a_{2m} \cdot e^{-2j(\omega+k\Omega)}\right] \cdot e^{jmn\Omega} \tag{4.99}$$

We can now assume that the total power of GFR combinational components is small in comparison with the power of the signal component:

$$\sum_{i=1}^{N-1} |H_i(\omega)|^2 << |H_0(\omega)|^2 \tag{4.100}$$

We can also assume that for coefficients of the recursive part the following condition is satisfied:

$$\sum_{i-1}^{N-1} \sum_{k=0}^{K_1} |a_{ki}|^2 << \sum_{k=0}^{K_1} |a_{k0}|^2 \tag{4.101}$$

which corresponds to the smallness of variation of coefficient amplitudes in comparison with their mean value. As will be shown later in examples, these assumptions are mutually dependent. If the variation in coefficient amplitudes is reduced, the power of the CCs is also proportionally reduced. Conditions (4.100) and/or (4.101) are the limiting factors in applying the approximate method. Nevertheless, for the parametric filters considered in this book, the approximate method is fully applicable.

The conditions (4.100) and (4.101) mean secondary modulation components in the feedback have a second order of smallness and can be neglected. Returning to equation (4.94), we neglect all terms in double sum over i, k except terms for $i = 0$ and $i = m$. Then, for $m = 0$ in equation (4.94), we obtain

$$H_0(\omega) \approx \frac{1}{\sum_{k=0}^{K_1} a_{k0} \cdot e^{-jk\omega}} \tag{4.102}$$

and for $m \neq 0$ from equation (4.94), we obtain

$$H_0(\omega) \cdot \sum_{k=0}^{K_1} a_{km} \cdot \mathrm{e}^{-\mathrm{j}k(\omega+m\Omega)} + H_m(\omega) \cdot \sum_{k=0}^{K_1} a_{k0} \cdot \mathrm{e}^{-\mathrm{j}k(\omega+m\Omega)} \approx 0$$

or

$$\begin{aligned} H_m(\omega) &\approx -\frac{H_0(\omega) \cdot \sum_{k=0}^{K_1} a_{km} \cdot \mathrm{e}^{-\mathrm{j}k(\omega+m\Omega)}}{\sum_{k=0}^{K_1} a_{k0} \cdot \mathrm{e}^{-\mathrm{j}k(\omega+m\Omega)}} \\ &= -H_0(\omega) \cdot \sum_{k=0}^{K_1} a_{km} \cdot \mathrm{e}^{-\mathrm{j}k(\omega+m\Omega)} \cdot H_0(\omega + m\Omega) \end{aligned} \tag{4.103}$$

The obtained expressions have a clear physical meaning:

1. An EFR of the parametric filter corresponds approximately to the frequency response of an LTI system with constant coefficients equal to the time mean values of the time-varying coefficients (as shown in Fig. 4.5).
2. The input signal with frequency ω is amplified by the system according to its EFR at the frequency $H_0(\omega)$. This signal at the feedback is modulated by the harmonics of the time-varying coefficients, and the newly generated harmonic components with frequencies $\omega + k\Omega$ are filtered by the system according to its EFR at combinational frequencies $H_0(\omega + k\Omega)$.

Thus, the harmonics appearing at the recursive part of a PLTV DS are weakened by the system itself according to its equivalent frequency response. The narrower the pass band of the recursive part, the smaller will be the level of CCs at the system output.

Expressions (4.102) and (4.103) are considerably simpler than the accurate methods of analysis introduced earlier. They can be recommended for fast approximate estimation of PLTV DS characteristics. Let us confirm this by the following example.

Example 4.7: Evaluation of GFR Components

The GFR signal and CCs for a PLTV DS-2 with parameters from examples 4.4 and 4.3 were calculated by the approximate approach described above. The signal components (SCs) and CCs of the GFR are shown in Fig. 4.7 by dotted lines. Comparison of these components with those obtained by the exact analytical method, shown in Fig. 4.7 by solid lines, demonstrates a good qualitative and quantitative coincidence of the results, even for a relatively large coefficient amplitude. Strictly speaking, the assumption in equation (4.101) is not executed for the given case. However, at the maximums of pass bands, deviation of calculated data does not exceed 0.5 dB for all GFR components.

4.6 SUMMARY

In this chapter, the major characteristics of digital filters (DFs) with periodically time-varying coefficients were introduced. Impulse and frequency response of the first- and second-order systems were derived in an analytically closed form.

Only parametric systems with the period of coefficient variation being a multiple of the sampling period were considered. This restriction on the coefficient variation period does not reduce the analyses' generality but essentially helps to simplify an analytical description of these systems. This simplifies calculations and clarifies the system behaviour and the physical processes driving these relatively complex systems.

Eventually, it became possible to replace the systems under consideration with their approximate equivalent block diagram. These diagrams are convenient to use where PLTV DSs are a part of more complex systems. One of the interesting conclusions derived from our analysis is that PLTV systems can act very similar to LTI systems under some conditions discussed in the chapter. In this case, PLTV filters have averaged frequency response, when the variations in characteristic relevant to these average parameters can be viewed like some sort of noise with predictable parameters in terms of power and spectrum. It is also important to note that in the case of recursive parametric narrowband filtering, these noise components are effectively filtered out by the system itself to levels low enough for practical applications.

4.7 ABBREVIATIONS

CC	combinational component
DF	digital filter
DFT	discrete Fourier transform
DRS	digital recursive systems
DS	discrete system
DS-1	discrete system of the first order
DS-2	discrete system of the second order
EFR	equivalent frequency response
GFR	generalized frequency response
GTF	generalized transfer function
IR	impulse response
LTI DS	linear time-invariant digital system
PF	parametric filter
PLTV DRS	periodically time-variant digital recursive system
PLTV DS	periodically linear time-variant discrete system
SC	signal components

4.8 VARIABLES

$H_0(\omega)$	an equivalent frequency response
Ω	normalized frequency of system parameter variation

ω	normalized frequency of the signal
$s_1(n), \quad s_2(n)$	coefficients of the systems in the equivalent representation.
$a(n)$	time-varying coefficients of the recursive part of a difference equation
$b(n)$	time-varying coefficients of the non-recursive part of a difference equation
F	frequency
$g(m, n)$	impulse response of the recursive part
$G(z)$	GTF of the recursive part
$h(m, n)$	impulse response
$H(z, n)$	generalized transfer function
$u(n)$	signal at the output of the first system
$X(\omega), X(\psi)$	spectrum of the input signal
$X(n)$	input discrete random process
$x(n)$	input signal
$X(z)$	z-transform of the input signal
$Y(\omega)$	spectrum of the output signal
$Y(n)$	output discrete random process
$y(n)$	output signal
$Y(z, n)$	z-transform of the output signal

4.9 REFERENCES

[1] Cherniakov M, Sizov V (1985) Analysis of the first-order periodic non-stationary digital recursive filter. *Electron. Tech.*, **10**(4), 17–20.

[2] Cherniakov M, Kojuhov I, Sizov V (1985) Presentation of the periodically non-stationary second-order digital recursive filter by cascaded links of the first order. *Electron. Tech.*, **10**(6), 17–19.

[3] Peled A, Liu B (1976) *Digital Signal Processing*, New York: John Wiley.

[4] Cherniakov M, Sizov V, Kojuhov I (1989) Characteristics of periodic non-stationary digital recursive filters. *Radioelectronics*, **4**, 55–57.

[5] Cherniakov M, Sizov V, Donskoi L (2000) Synthesis of a periodically time-varying digital filter. *IEE Proc. Vision, Image Signal Process.*, **147**(5), 393–399.

[6] Erugin N (1966) *Linear Systems of Ordinary Differential Equations: With Periodic and Quasi-Periodic Coefficients*, New York: Academic Press.

[7] Haykin S, Van Veen B (1999) *Signal and Systems*, New York: John Wiley & Sons.

[8] Feng Z, He H, Unbehauen R (1992) The determination of the generalized frequency response for linear periodically shift-variant digital filters, *Proc. Midwest Symp. on Cas*, Washington, DC, USA, V.1, 591–593.

5

Design Studies for Parametric Filters

It has been discussed in previous chapters that a signal at an output of a periodically linear time-variant discrete system (PLTV DS) contains a number of spectral components for the harmonic input waveform. One of these spectral components coincides with the input signal frequency $\omega = \psi$ and is a signal component (SC). The others are combinational components (CC) with frequencies $\omega = \psi + k\Omega$, originated within the system itself. If the SC is considered to be desirable, then a PLTV DS behaves like a frequency filter. In the general case, characteristics of such a filter are determined not by the instantaneous filter coefficients, but by their time-averaged values. Such a system is called a PLTV digital filter (DF) or a parametric filter (PF). In a PF, CCs at the system output are considered as noise or interference. In the course of filter design, it is important not only to estimate their level but also to reduce their influence on system performance.

In contrast, if at the PLTV DS output one or more of the CCs are considered desirable, then the effect of the frequency components should be emphasized by an appropriate choice of system parameters. This could be the basis of design of digital functional elements, which provide functions of frequency converters, phase and synchronized detectors, correlators and other devices, similar to those used for analog techniques. For analysis of these functional elements, the approaches developed in previous chapters can be used, but their more detailed study is beyond the scope of this book.

The analysis of numerous publications dedicated to time-variant systems, and in particular PLTV DSs, shows that there is no theory or method of design of such systems similar to those we have for LTV systems [1]. Different elements of time-variant DS design can be found in [2–33]. A number of recent publications are dedicated to two-dimensional LTV filter analysis, which are outside the scope of this book, but are essentially dedicated to the same problems [34–38].

In this chapter, using examples, we discuss a number of peculiarities that distinguish PF design from linear time-invariant (LTI) digital filter (DF) analysis. We will

An Introduction to Parametric Digital Filters and Oscillators Mikhail Cherniakov
© 2003 John Wiley & Sons, Ltd ISBN: 0-470-85104-X

consider only PF design, using as criteria their approximate equivalent frequency response (EFR) and the CC level.

5.1 RECURSIVE PARAMETRIC FILTERS

5.1.1 Frequency Response Correction

Let us first consider how to improve frequency response approximation in DFs using the effect of coefficient variation or simply using a PF instead of an LTI DS. Coefficients of DFs are always represented by a finite word length that leads to appropriate limitations on the accuracy of the filter frequency response approximations. To design a DF with constant coefficients that satisfy a criterion to enhance the accuracy of approximation, it is necessary to increase the coefficient word length or, in other words, to reduce the coefficient quantization step q_s [1]. These requirements increase the system complexity, which can be unviable in some situations. For example, in a system that uses an 8-bit fixed-point microcontroller for signal processing, the coefficient lengths have already been predetermined. For modernization purposes, let an extra filtering algorithm be performed by the controller. Moreover, the desired frequency response can be approximated only by using, say, a 12-bit word length. Sometimes, the only solution is to replace the controller, but in some cases we can solve the problem at the software level by replacing an LTI algorithm by the use of a PF.

To replace an LTI filter by a PF, their frequency response and EFR should coincide. We have discussed that the EFR of a PLTV DS is obtained by time-averaging of the system coefficients. Now let us consider examples of EFR analysis.

Example 5.1: **EFR for a First-Order Recursive Filter**

Consider a PF of the first-order (PLTV DF-1 or PF-1 (parametric filter of the first order)) in which coefficient $a(n)$ can take only two values: 0.75 and 1 with period $N = 8$. The timing diagram is $a = 1$ over Tn_1 for the period TN $(0 \le n_1 < N)$ and at times it is equal to $a = 0.75$ over the period $T(N - n_1)$. For instance, the case when $n_1 = 0$ corresponds to the filter with constant coefficient $a = 0.75$ and the case when $n_1 = 8$ corresponds to the filter with constant coefficient $a = 1$. It is interesting to note that for $a = 1$ the filter does not satisfy stability requirements [2].

A set of EFRs for a PF-1, calculated using equation (4.26), is shown in Fig. 5.1. The narrowest frequency band corresponds to $n_1 = 7$. This figure shows that, in contrast to a filter with constant parameters and coefficients quantized with the step $q_s = 2^{-2}$, the PF can have eight different EFRs by changing the timing diagrams of the coefficient variation. This is equivalent to an increase in coefficient quantization word length by 3 bits or $q_s = 2^{-5}$.

So, by changing a duty cycle of the coefficient variation timing diagram we are tuning the filter cut-off frequency.

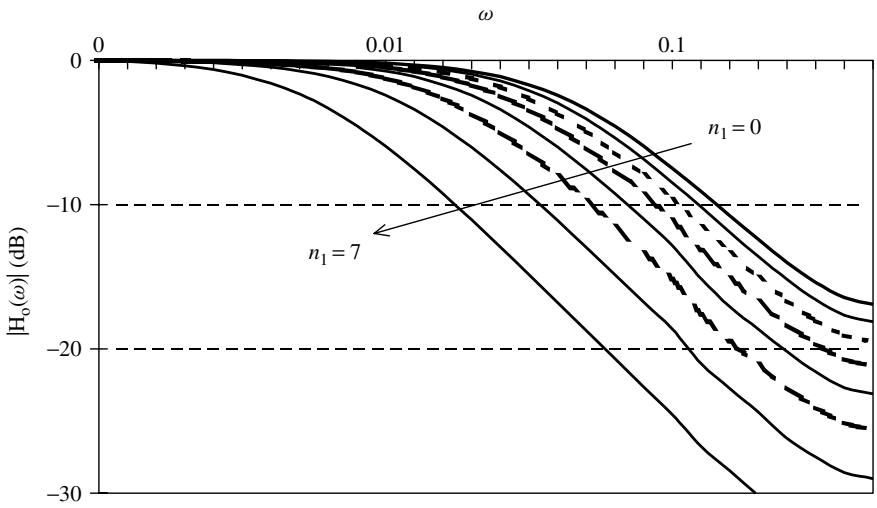

Figure 5.1 Normalized EFR of PF-1

Example 5.2: First-Order Narrowband Low-Pass Filter

Let us design a narrowband recursive DF-1 with a normalized cut-off frequency $\omega_c = 2 \cdot 10^{-4}$ at the -3-dB level. First, we will calculate the exact value of the filter coefficient that corresponds to this cut-off frequency [1], that is, $a = 0.9987442$. The filter gain at $\omega = 0$ is $G_{dc} = \dfrac{1}{1-a} = 58.02\,\text{dB}$ and we assume that the gain error should not exceed ± 0.25 dB. The minimum number of bits in the coefficient representation that still attains this level of accuracy is 12. If the coefficient $a_{q0} = 1 - 5 \cdot 2^{-12}$ is chosen, the filter gain is 58.27 dB. The nearest best 10-bit coefficient $a_{q1} = 1 - 2^{-10}$ corresponds to 60.02-dB gain and the 11-bit coefficient $a_{q2} = 1 - 3 \cdot 2^{-11}$ corresponds to 56.68-dB gain. In both cases, the gain deviation exceeds ± 0.25 dB.

Consider now a PF-1 with a coefficient that can take two values: $a(0) = a_{q1}$ and $a(1) = a_{q2}$ with period $N = 2$. Calculation of PF characteristics using the geometrical mean value gives $G_{dc} = 58.27$ dB, which corresponds to the filter specification but is obtained via a shorter word length. So, this is another example that demonstrates an increase in accuracy of approximation of characteristics within a given word length by using a PLTV DS.

Example 5.3: Second-Order Filter with Highly Quantized Coefficients

Consider a PLTV DF of the second order (PLTV DF-2 or PF-2 (parametric filter of the second order)), in which coefficients $a_1(n)$ and $a_2(n)$ are quantized with step $q = 2^{-2}$ and the coefficient variation period $N = 4$. Figure 5.2 demonstrates several amplitude effective frequency responses of such filters, with different coefficient values corresponding to different curves. Response (1) corresponds to a DF with constant coefficients: $a_1 = -0.5$ and $a_2 = -0.75$. The other responses correspond to PFs with the following timing diagrams of coefficient variation:

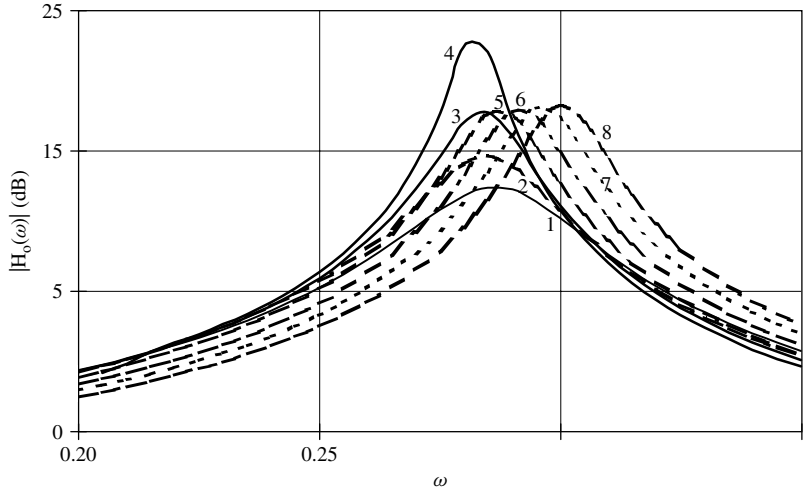

Figure 5.2 Amplitude EFR of the second-order PF

for $a_1 = -0.5$ we have

$$a_2 = \{-0.75; -0.75; -0.75; -1\} - (2)$$
$$a_2 = \{-0.75; -0.75; -1; -1\} - (3)$$
$$a_2 = \{-0.75; -1; -1; -1\} - (4)$$

for $a_2 = \{-0.75; -0.75; -1; -1\}$ we have

$$a_1 = \{-0.5; -0.5; -0.5; -0.75\} - (5)$$
$$a_1 = \{-0.5; -0.5; -0.75; -0.75\} - (6)$$
$$a_1 = \{-0.5; -0.75; -0.75; -0.75\} - (7)$$
$$a_1 = -0.75 - (8)$$

Similar to the PF-1 in example 5.1, coefficient variation in the PF-2 leads to the appearance of responses that occupy intermediate positions. These responses correspond to the frequency responses (FRs) of time-invariant filters with more bits in coefficient representations. In this case, for instance, between responses 3 and 8, there are three intermediate curves. So, these PFs have an efficient fourfold reduction in the quantization step.

Therefore, as discussed above, this effect can be used to improve approximation of filter responses. Consider the following example of a filter design.

Example 5.4: Second-Order Filter with Given Cut-Off Frequencies

Let us consider a second-order filter with specified cut-off frequencies $\omega_{c1} = 0.170$ and $\omega_{c2} = 0.172$ at the level of -3 dB [3]. The amplitude–frequency response of the filter

with constant coefficients is

$$|H(\omega)| = \left| \frac{1 - e^{-2j\omega}}{1 - a_1 e^{-j\omega} - a_2 e^{-2j\omega}} \right| \tag{5.1}$$

The coefficient values, which can be found through these cut-off frequencies, are $a_1 = 0.9465492$ and $a_2 = -0.9875119$. The FR of the filter with these constant coefficients is shown in Fig. 5.3a, curve 1.

The coefficients of DFs have limited word length. An example of the quantized coefficients grid with step $q_s = 2^{-7}$ is shown in Fig. 5.3b. The quantized coefficients $a_{11} = 1 - 3 \cdot 2^{-6}$, $a_{12} = 1 - 7 \cdot 2^{-6}$, $a_{21} = -1 + 2^{-6}$ and $a_{22} = -1 + 2^{-7}$ are closest to the exact values evaluated above for the idealized filter. The nodes of the grid (points 2–5) correspond to the different combinations of quantized coefficients and various displacements of the LTI DF frequency responses (shown in Fig. 5.3a). The indexes of curves and corresponding nodes in parts (a) and (b) of Fig. 5.3 coincide. As can be seen, the FR of the filter with quantized coefficients deviates considerably from the desired FR (curve 1).

Now let us study a PF-2 with coefficients having the timing diagram with period $N = 4$ and values $a_1(n) = \{a_{11}, a_{12}, a_{21}, a_{12}\}$ and $a_2(n) = \{a_{21}, a_{22}, a_{21}, a_{22}\}$. The EFR (curve 6 – the dotted line) of this PLTV filter almost coincides with the required characteristic (curve 1 – continuous line).

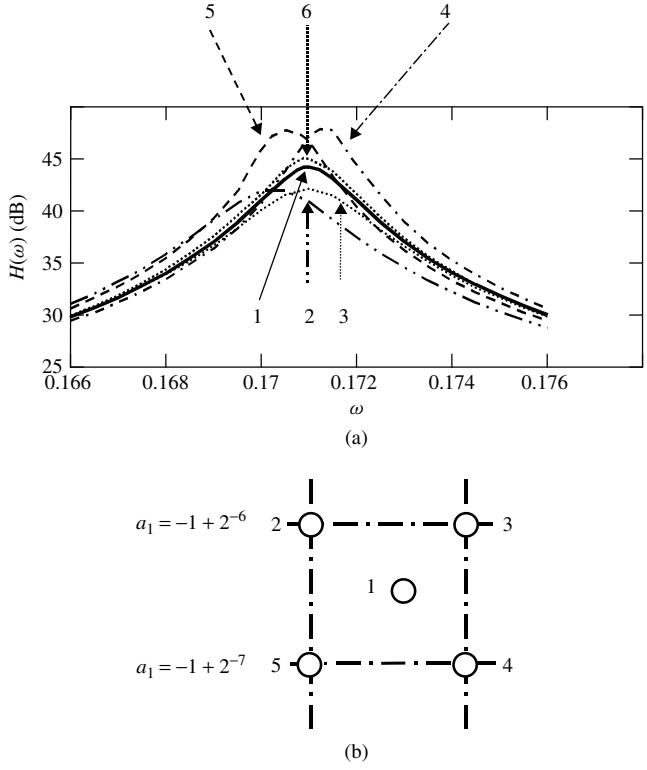

Figure 5.3 Amplitude–frequency response of PF-2

So, once again we have demonstrated that the use of a PF can increase the accuracy of DF approximation for given coefficient word lengths. It is definitely not necessary for all PF coefficients to be time-varying. Some coefficients can be constant. Consider another example of filter design.

Example 5.5: Low-Pass Filter with Given Flatness

In this example, we will design a low-pass filter (LPF) with the amplitude–frequency response deviating no more than 1 dB in the pass-band $\omega < 0.1$ and with attenuation of at least -32 dB in the stop-band $\omega \geq 0.15$. This filter was calculated by the known methods [1] and can be represented as two cascaded filters of the second order with the FR

$$H(\omega) = \frac{1 + b_{11} \cdot \mathrm{e}^{-\mathrm{j}\omega} + \mathrm{e}^{-2\mathrm{j}\omega}}{1 + a_{11} \cdot \mathrm{e}^{-\mathrm{j}\omega} + a_{12} \cdot \mathrm{e}^{-2\mathrm{j}\omega}} \cdot \frac{1 + b_{21} \cdot \mathrm{e}^{-\mathrm{j}\omega} + \mathrm{e}^{-2\mathrm{j}\omega}}{1 + a_{21} \cdot \mathrm{e}^{-\mathrm{j}\omega} + a_{22} \cdot \mathrm{e}^{-2\mathrm{j}\omega}} \tag{5.2}$$

with coefficients $a_{11} = -1.4686$, $a_{12} = 0.6006$, $b_{11} = -1.125$ and $a_{21} = -1.5$, $a_{22} = 0.875$, $b_{21} = 0.25$. Note that all coefficients except a_{11} and a_{12} are represented by binary numbers with quantization step $q_s = 2^{-3}$. So, it is a big challenge to replace coefficients a_{11} and a_{12} by 3-bit numbers. A normalized FR with coefficients in the pass-band is represented in Fig. 5.4 (curve 1). The other curves in the figure correspond to a_{11} and a_{12} representations by 10 bits (curve 2), 7 bits (curve 3), 4 bits (curve 4) and 3 bits (curve 5). We will now study these approximations in more detail.

Consider first the FR of the filter with quantized constant coefficients. For the step $q_s = 2^{-10}$, the filter FR almost coincides with the given exact FR (deviation is not more than 0.02 dB, curve 2). With bigger steps the deviation increases. Thus, for $q_s = 2^{-7}$ the deviation is 0.05 dB and the FR still remains within the given specification (curve 3). For $q_s = 2^{-4}$ the closest coefficient values are $a_{11} = -1.4375, a_{12} = 0.625$ and the FR (curve 4) within the pass-band has a 5-dB deviation. It is interesting to note that for $q = 2^{-3}$ and coefficients $a_{11} = -1.5$ and $a_{12} = 0.625$, the FR is closer to the

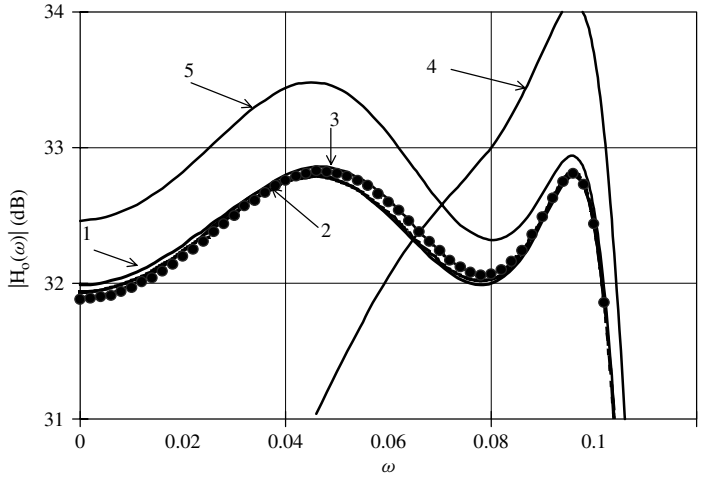

Figure 5.4 Characteristics of the fourth-order filter

specification and has a deviation in the pass-band of about 1.2 dB (curve 5). This can be explained by some mutual compensation in FRs of the two filter stages.

Now let us synthesize this filter using periodically varying coefficients with $q_s = 2^{-4}$ and period $N = 8$. The following timing diagram of coefficient variation

$$a_{11}(n) = \{-1.4375; -1.4375; -1.4375; -1.4375; -1.5; -1.5; -1.5; -1.5\}$$

and

$$a_{12}(n) = \{0.5625;\ 0.5625;\ 0.5625;\ 0.625;\ 0.625;\ 0.625;\ 0.625;\ 0.625\}$$

gives the required result (see dots near curve 3). The quantization step of the coefficient values under consideration is 2^{-4}, but the accuracy of equivalent coefficient representation corresponds to the quantization step 2^{-7}.

It is possible to further reduce the coefficient word length by up to 3 bits at the expense of the period of coefficient variation, which increases to $N = 16$. Thus, for $a_{11}(n)$ equal to -1.375 over $4T$ and -1.5 over $12T$, and for $a_{12}(n)$ equal to 0.5 over $3T$ and 0.625 over $13T$, the resulting FR also satisfies the filter specification.

5.1.2 Multiplier-Free Filters

In PF design, coefficients that do not require a multiplier and can be developed by a small number of shifts and summation components or logical procedures can be used. Such coefficients have a minimum number of units in binary code and in some literature are referred to as primitive coefficients. In the following examples, we will consider coefficients with no more than two units in a binary code representation, that is, $\pm 2^{-\nu} \pm 2^{-\xi}$, where $\nu, \xi = 0, 1 \ldots$.

Example 5.6: **First-Order Parametric Filter**

Consider the PF-1 from example 5.2, but having a coefficient with period $N = 4$ and timing diagram $a(n) = \{1 - 2^{-10}; 1 - 2^{-10}; 1 - 2^{-10}; 1 - 2^{-9}\}$. The time mean value of such a coefficient coincides with the value from example 5.2. The amplitude–frequency responses of this filter and its counterpart from example 5.2 are nearly equal to each other. However, coefficients in example 5.6 are primitive for the given word length and 2 bits less than their LTI DF equivalent.

Example 5.7: **Second-Order Parametric Filter**

The band-pass filter of the second order from example 5.4 can also be approximated with primitive coefficients if the period is increased until $N = 8$:

$$a_1 = \{a_{11}; a_{11}; a_{11}; a_{11}; a_{11}; a_{12}; a_{12}\}$$
$$a_{11} = 1 - 2^{-4}, a_{12} = 1 - 2^{-5}$$
$$a_2 = \{a_{21}; a_{21}; a_{21}; a_{21}; a_{22}; a_{22}; a_{22}\}$$
$$a_{21} = 1 - 2^{-6}, a_{22} = 1 - 2^{-7}$$

The amplitude–frequency response of such a filter satisfies the requirements given in example 5.4.

It is obvious that using primitive coefficients can have considerable design advantage compared to using filters that have multipliers. This advantage can be especially important for complex systems containing large numbers of filters or channels. As an example, we can consider a bank of filters (a comb filter).

Example 5.8: Bank of Filters

Consider a bank $M = 128$ second-order filters of equal pass-band, covering a frequency span from direct current (DC) to one-half of the sampling frequency. The bank forms a "comb" of overlapping filters. The FR of an individual time-invariant filter is described by equation (5.1). The resonance frequencies of each filter are $\omega_{0l} = \dfrac{(l-1)}{2(M-1)}$, where l is the sequence number of the filter. The pass-band of each filter is $\Delta\omega = \dfrac{1}{2(M-1)}$ for an amplitude–frequency response overlapping at the level of -3 dB. As an example, Table 5.1 shows coefficient values for filters 51 and 54 in two cases: time-invariant filters and parametric filters. All coefficients (constant and time-varying) are rounded off to primitive values. Figure 5.5 shows the normalized amplitude–frequency responses of these filters.

The required FRs corresponding to coefficient values are shown by continuous lines. The characteristics of time-invariant filters with rounded-off primitive coefficient values are shown by dashed lines and the PF-2 characteristics are depicted by dots. These graphs

Table 5.1 Comb filter coefficient values

Filter number l	Exact coefficients values	LTI DF with primitive coefficients	PF for $N = 8$
51	$a_1 = 0.64759$	$a_1^* = 2^{-1} + 2^{-3}$	$a_1' = 2^{-1} + 2^{-2}, n_{11} = 1$
	$a_2 = -0.97556$	$a_2^* = -1 + 2^{-5}$	$a_1'' = 2^{-1} + 2^{-3}, n_{12} = 7$
			$a_2' = -1 + 2^{-5}, n_{21} = 5$
			$a_2'' = -1 + 2^{-6}, n_{22} = 3$
52	$a_1 = 0.60123$	$a_1^* = 2^{-1} + 2^{-3}$	$a_1' = 2^{-1} + 2^{-3}, n_{11} = 5$
	$a_2 = -0.97556$	$a_2^* = -1 + 2^{-5}$	$a_1'' = 2^{-1} + 2^{-4}, n_{12} = 3$
			$a_2' = -1 + 2^{-5}, n_{21} = 5$
			$a_2'' = -1 + 2^{-6}, n_{22} = 3$
53	$a_1 = 0.55499$	$a_1^* = 2^{-1} + 2^{-4}$	$a_1' = 2^{-1} + 2^{-4}, n_{11} = 6$
	$a_2 = -0.97556$	$a_2^* = -1 + 2^{-5}$	$a_1'' = 2^{-1} + 2^{-5}, n_{12} = 2$
			$a_2' = -1 + 2^{-5}, n_{21} = 5$
			$a_2'' = -1 + 2^{-6}, n_{22} = 3$
54	$a_1 = 0.50781$	$a_1^* = 2^{-1} + 2^{-7}$	$a_1' = 2^{-1} + 2^{-7}, n_{11} = 7$
	$a_2 = -0.97556$	$a_2^* = -1 + 2^{-5}$	$a_1'' = 2^{-1} + 2^{-8}, n_{12} = 1$
			$a_2' = -1 + 2^{-5}, n_{21} = 5$
			$a_2'' = -1 + 2^{-6}, n_{22} = 3$

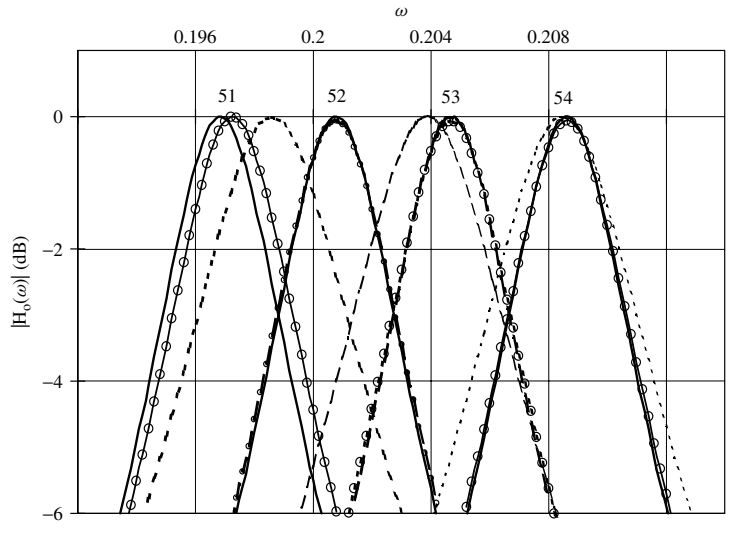

Figure 5.5 FR of the comb filter components

show that frequency responses of filters with constant primitive coefficients deviate considerably from the desired characteristics, while the PF-2 responses are very close to the specifications. The 51st PF-2 with a 2-bit word length for the most roughly approximated quantized coefficient a_1 has the maximum deviation. However, increasing the period to $N = 16$ results in the coincidence of its FR with the required characteristics. Thus, the example shows that an application of PFs with primitive coefficients provides a high level of approximation accuracy when the desired characteristics cannot be obtained by time-invariant filters with primitive coefficients.

Let us try to roughly estimate the number of mathematical operations required to develop a bank of filters using PFs, fast Fourier transform (FFT) and filter realization by time-invariant second-order sections. The generalized block diagram of this comb filter is shown in Fig. 5.6a. Figure 5.6b shows the sequence of calculations, in the form of a block diagram, in one of the PFs-2 with primitive coefficients $\pm 2^{-\nu} \pm 2^{-\xi}$.

From Fig. 5.6 it can be seen that a second-order filter with these coefficients requires four summations and four shifts. A full structure of the comb filter also includes a non-recursive part common to all channels. We can estimate that the whole comb filter requires $4M$ shifts and $4M$ summations. Note that the number of these components does not depend on coefficient word length.

Consider now the comb filter using M-points FFT algorithm [1]. The multiplication is obtained by a number of shifts and summations. The FFT algorithm is based on a uniform structure with two complex inputs and two complex outputs, called a *butterfly*. The butterfly requires four multiplications and six summations of real numbers. FFT coefficients, in general, are not primitive numbers. For L-bit coefficients, the multiplication requires L shifts and L summations. To calculate the M-points FFT, approximately $(M/2) \cdot \log_2 M$ base butterfly evaluations are required. Thus, for one frequency channel the FFT algorithm requires $2L \cdot \log_2 M$ shift operations and $3L \cdot \mathrm{Log}_2 M$ summation operations.

In contrast to the comb filters, the FFT algorithm is applied to blocks of M word input data and, consequently, the output spectrum appears M times fewer than sampling frequency. This is not suitable for a number of applications. The better algorithm for comparison is the sliding FFT, where the algorithm is repeated for each new sample of input signal. This sliding FFT requires approximately $(M/2) \cdot \log_2 M$ butterfly operations. Comb filter realization using the traditional LTI DF requires for each recursive system two summations and two multiplications (L shifts and summations) of real numbers. We can estimate the number of elementary operations required for such comb filter realization as $2M \cdot L$ shifts and $2M \cdot (L + 2)$ summations.

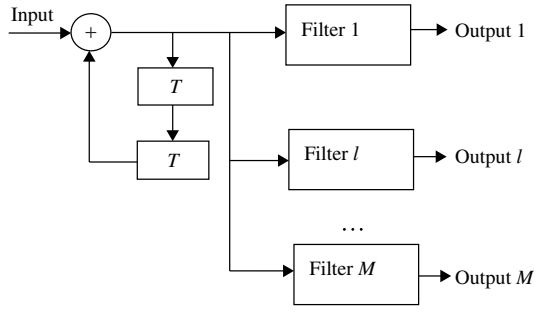

(a) General structure

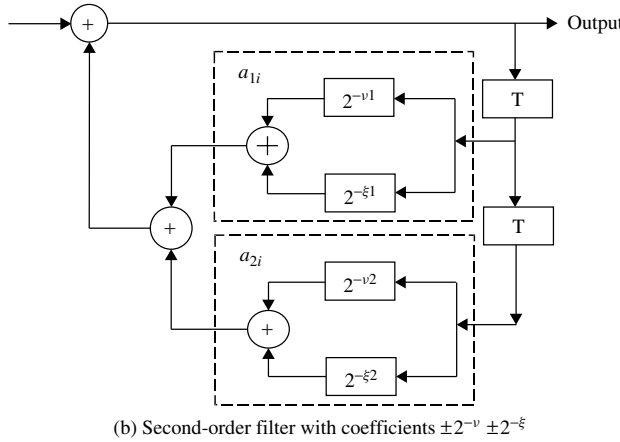

(b) Second-order filter with coefficients $\pm 2^{-\nu}$ $\pm 2^{-\xi}$

Figure 5.6 Block diagram of PF: (a) general structure and (b) second-order filter with coefficients $\pm 2^{-\nu} \pm 2^{-\xi}$

The number of mathematical operations required for comb filters with $M = 128$ channels and 8-bit coefficient word lengths are collected in Table 5.2 for the four algorithms discussed above. These numbers of operations should be performed for each new sample of an input signal. Of course, this is no more than the first and rather rough evaluation, but it shows the real potential offered by PF applications in comb filtering.

The limiting case for the use of primitive coefficients is for coefficients equal to -1, 0, 1, as discussed in [5–8]. This case, however, has more theoretical than practical importance because of the considerable level of output CCs, which is noted in [7].

Table 5.2 Number of operations in a comb filter with 128 channels

Variant of realization	Number of shifts	Number of summations
LTI DF-2	2 048	2 560
FFT without weighting window	112	168
Sliding FFT without weighting window	14 336	21 504
PF with "simple" coefficients	512	512

5.1.3 High-Efficiency Parametric Filters

Narrowband filters are often used for signal processing. If there are no special requirements, recursive systems of the first and second order are used for this purpose. Higher-order filtering systems are usually built as connections of these primary systems, with aims to unify system architecture, reduce round-off noise and minimize data word length. To obtain a narrow pass-band or narrow transition band between the pass- and stop-bands, the filtering systems have to include stages with a high efficiency factor Q.

There is a maximum limit for the value of Q in recursive filters with constant coefficients for a given word length.

Consider a first-order recursive filter with the frequency response

$$H(\omega) = \frac{1}{1 - a \cdot \mathrm{e}^{-\mathrm{j}\omega}} \tag{5.3}$$

A -3-dB cut-off frequency ω_0 for this filter is specified from

$$\frac{|H(\omega_0)|^2}{|H(0)|^2} = \frac{(1-a)^2}{(1 - 2a \cdot \cos\omega_0 + a^2)} = \frac{1}{2} \tag{5.4}$$

For small ω_0, $\cos\omega_0 \approx 1 - \dfrac{\omega_0^2}{2}$, and it is not difficult to show that

$$\omega_0 \approx \frac{1-a}{\sqrt{a}} \tag{5.5}$$

from which it can be seen that the filter bandwidth decreases when coefficient a approaches 1.

For a binary quantization of the coefficient with word length L, the coefficient closest to unity is $a = 1 - 2^{-L}$, and the minimum possible frequency band for this word length is

$$\omega_{0\,\min} \approx \frac{1 - (1 - 2^{-L})}{\sqrt{1 - 2^{-L}}} \approx 2^{-L} \tag{5.6}$$

It is possible to obtain a similar expression for second-order filters. In general, the recursive part of a second-order DF is a digital resonator [1, 39] with the efficiency factor Q increasing when $|a_2| \to 1$. So, the coefficient word length determines the maximum achievable Q.

Consider a recursive PF-1. This filter is stable if the product of coefficient values over the variation period is less than unity. So, unlike a first-order LTI DF, where stability of the system requires that the constant coefficient is always less than one, the instantaneous value of the PF-1 coefficient can exceed one. This provides new possibilities to develop high-Q filters. The equivalent value of the coefficient in the PF is approximately equal to the geometrical mean of the product of all instantaneous coefficient values. For instance, consider the filter with instantaneous coefficient values $a_1 = 1 - q$ and $a_2 = 1 + q, n = 0 \ldots N - 1$. For the timing diagram of these coefficients and $N = 2$, the filter is stable, since $g_N = a_1 \cdot a_2 = (1 - q) \cdot (1 + q) = 1 - q^2 < 1$. An equivalent coefficient $a = \sqrt{(1 - q^2)} \approx 1 - \dfrac{q^2}{2}$ is considerably closer to 1 than the coefficient for an LTI DF with the same quantization step. Now consider a few numerical examples.

Example 5.9: High-Q Filters

For the quantization step $q = 2^{-8}$, the LTI DF has the maximal coefficient value $a_{\max} = 1 - 2^{-8}$, while the PF has the equivalent coefficient value $a_{\max} = 1 - 2^{-15}$. So, for this case Q is 128 times higher for the PF than for the LTI filter. In the general case, for arbitrary N, an equivalent coefficient is equal to

$$a = \sqrt[N]{a_1^{n_1} \cdot a_2^{n_2}} \tag{5.7}$$

Taking the logarithm of this equation, we can find those n_1 and n_2 for which an equivalent coefficient maximally approaches the required coefficient a:

$$n_1 = \left\langle N \cdot \ln \frac{a}{a_2} \middle/ \ln \frac{a_1}{a_2} \right\rangle, n_2 = N - n_1 \tag{5.8}$$

Here $< x >$ denotes the function that rounds off the x to the closest integer.

Example 5.10: Quantization Step $q = 0.25$

Consider a case when $q = 0.25$. For the period $N = 16$, the coefficient $a(n)n_1 = 7$ takes the value $a_1 = 0.75$ and $n_2 = 9$ takes the value $a_2 = 1.25$. The equivalent coefficient of this filter is $a = \sqrt[16]{0.75^7 \cdot 1.25^9} = 0.999657$, that is, 1370 times closer to 1 than the equivalent coefficient for a time-variant filter with the same number of bits.

Example 5.11: High-Q Second-Order Filter

Consider a pass-band second-order filter with a constant coefficient $a_1 = -1$ and a time-varying coefficient $a_2(n)$ with the quantization step $q = 2^{-6}$ varying with period

$N = 16 : a_2' = 1 - 2^{-6}$ and $a_2'' = 1 + 2^{-6}$. A set of FRs corresponding to different n_1 is shown in Fig. 5.7.

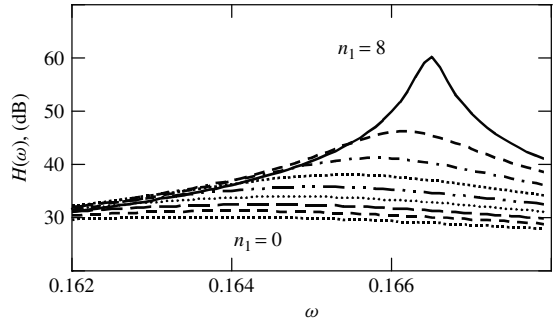

Figure 5.7 Amplitude–frequency responses of a PF-2

Figure 5.7 shows that increasing n_1 for the period increases Q to a maximum of 30 dB. The lowest FR in the figure corresponds to the filter with constant coefficients of given word length of 6 bits. The highest FR in the figure corresponds to the case when $n_1 = n_2 = 8$. It has to be noted that the approximate representation of an equivalent constant coefficient as a mean value for the period is not correct in this case, since this corresponds to an unstable LTI DF. For a high-Q filter, it is necessary to use accurate methods to evaluate PF characteristics.

For some coefficient combinations, Q can increase to infinity. In these cases, the stability of the filter is violated. Moreover, for some coefficients, when the resonance frequency of the filter is close to one of the harmonics appearing with the frequency of coefficient variation, generation can occur even if all instantaneous coefficient values correspond to a stable LTI DF. For some resonance frequencies, the system stability will not be violated even when all instantaneous coefficient values correspond to an unstable LTI DF. This effect has been described in [10–14] and is also the subject of Chapter 6.

The given examples show that the strong connection between coefficient word length and limited Q of the system that is typical for LTI systems is not true for filters with time-varying coefficients. Instantaneous values of PF coefficients can belong to the area where the relevant LTI filters are unstable. In this case, a considerably higher Q for the system can be achieved via coefficient variations. This is a unique peculiarity of PFs. Note also that the coefficients 1 ± 2^{-L} are primitive and, as was discussed, can have reasonably simple hardware implementation.

5.2 COMBINATIONAL COMPONENTS IN PARAMETRIC FILTERS

In previous sections, we considered how to provide filtering via PLTV DSs. This assumes that the only desired part of a generalized frequency response (GFR) is its EFR. Using periodically time-varying coefficients, it is possible to design filters with specified frequency responses by technically more effective ways; for example, by

using coefficients with low-bit word lengths or by using primitive coefficients. These options became possible because of the introduction of an extra degree of freedom in filter design, that is, coefficient variation. We can form a desired EFR by the choice of the period of coefficient variation N, the timing diagram within the period, as well as the value of the coefficients themselves. In return for this technical advantage, we have to be ready for possible complications in filter stability and the presence of CCs in the output signal spectrum, which act as interference. The magnitude and spectrum of CC interference directly depends on the filter EFR and the timing diagram of coefficient variation. We can view the CC interference as a penalty for the good and sometimes unique results of using PLTV DSs for filtering. When PFs are used for signal processing, the interference level should meet some criteria. These criteria can be quantitatively specified only relevant to a particular PF application. Nevertheless, it is obvious that under other equal conditions this interference level should be minimized.

For practical PF applications, it is important to compare the CC power with other possible noise and distortions. The main undesired process in DFs is the noise of data quantization and the round-off noise occurring during intermediate calculations. Moreover, the CC level has to be considered relevant to the given GFR of the filter. For example, there is no sense in decreasing the CC level to -60 dB if the filter damping at the stop-band requires -30 dB. Before we consider different approaches to reducing interference, let us consider the criteria for evaluating the CC level.

5.2.1 Evaluation of the Level of Combinational Components

In Chapter 3, a criterion for an integral level of CC interference was introduced – the level of integral interference can be determined as a ratio of the total CC power to the power of the useful signal over all frequency bands (equation 3.32). Application of this integral criterion for evaluation of the CC level requires a large amount of calculations and knowledge of the exact GFR of the filter. Let us consider here a simplified version of this parameter for evaluation.

From Section 4.5 it follows that in a recursive PF the maximal level of the GFR combinational harmonics is determined by its EFR. This is the result of CC filtering by the recursive filters themselves. This fact allows for simplification of the procedure for estimating the CC level [15].

Consider, in Fig. 5.8, the shapes of the EFR and GFR combinational harmonics of a PLTV DF with $N = 4$ from example 4.3 (Fig. 5.8 is similar to Fig. 4.7 and is repeated here for convenience). Characteristics are given for one-half of the frequency band $\omega/2\pi \in \{0, \ldots, 0.5\}$. In the second half, all characteristics are a mirror image of those in the first half.

It can be seen from Fig. 5.8 that the GFR has six maximums. Three of them are at frequency $\omega_0 \approx 0.31$, which coincides with the maximum of the EFR $H_0(\omega)$. Three others correspond to the combinational frequencies $\omega_0 + k\Omega$: 0.052, 0.19 and 0.44. The shape of the CC maximums in the EFR pass-band is the same as the EFR shape.

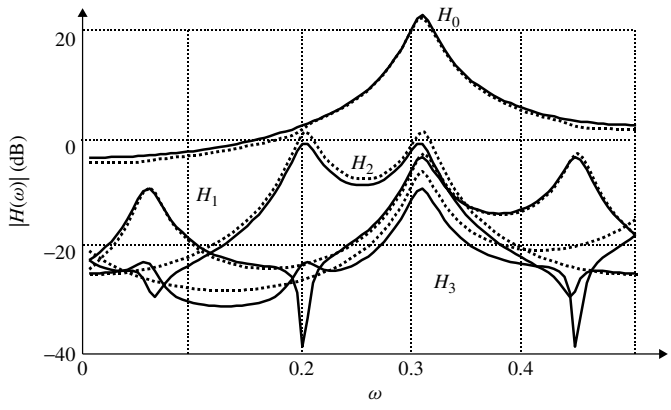

Figure 5.8 GFR components of a PLTV DS-2

According to equation (4.103), the bandwidth of GFR harmonics $H_i(\omega)$ is equal to the bandwidth of the $H_0(\omega)$. We can now approximate $H_0(\omega)$, assuming that within the pass-band $H_0(\omega)$ is constant and equal to its maximum, while outside the pass-band $H_0(\omega)$ is equal to zero (see Fig. 5.8). From this approximation, the normalized CC level can be evaluated using only GFR maximums:

$$\gamma = \frac{\sum_{m=1}^{N-1} \left\{ |H_m(\omega_0)|^2 + \sum_{i=1}^{N-1} |H_m(\omega_0 + i\Omega)|^2 \right\}}{2 \cdot |H_0(\omega_0)|^2} \tag{5.9}$$

The calculated CC level from equation (5.9) is close to results obtained from the more accurate equation (3.33). Let us refer to equation (5.9) as the *amplitude criterion* of the CC level. Taking into account the mirror symmetry of GFR, it is possible to halve the number of maximums in equation (5.9). Also, because the maximum levels are equal in pairs, the calculations can be made only at the resonant frequency of the filter (see Fig. 5.8), and equation (5.9) can be further simplified to

$$\gamma = \frac{2 \cdot \sum_{m=1}^{N-1} |H_m(\omega_0)|^2}{|H_0(\omega_0)|^2} \tag{5.10}$$

It is obvious that CC evaluation according to the amplitude criterion requires considerably fewer computations than calculation according to the integral criterion. To compare the accuracy of these approximate and exact methods, a number of calculations were made following these two criteria. The results are collected in Table 5.3.

The data in Table 5.3 confirm the correctness of the amplitude criterion and the appropriateness of introducing equation (5.9). These methods for evaluating the CC level cannot themselves reduce the interference level, but are simply an instrument

Table 4.3 CC levels for a PF-2

Criterion	Equations	ρ in (dB)
Integral criterion (calculations in 100 frequency points)	(3.32)	−14.61
Integral criterion (calculations in 1000 frequency points)	(3.32)	−14.61
Amplitude criterion (calculations in all GFR maximums)	(5.9)	−14.59
Amplitude criterion (calculations at the resonant ω_0)	(5.10)	−14.59

for PF performance analysis. In the next section, we will address the methods of reducing the CC level.

5.2.2 Methods of Reducing Combinational Components

I. *Optimization of the coefficient variation timing diagram*

Equation (4.103) specifies the level of CCs of the GFR $H_m(\omega), m \neq 0$. The EFR $H_0(\omega)$ of the filter is the factor for each evaluation of the GFR harmonics $H_m(\omega)$. Hence, dividing the numerator and the denominator of equation (5.9) by $H_0(\omega_0)$, after simple transformations we obtain

$$\gamma \approx 2 \cdot \sum_{m=1}^{N-1} |H_0(\omega_0 + m\Omega)|^2 \cdot \sum_{k=0}^{K_1} a_{km}^2 \tag{5.11}$$

From this equation a simple conclusion follows: the CC level is proportional to the total power of the alternative part of the PF coefficients. So, to obtain a minimum CC level, it is necessary to minimize the amplitude of coefficient variation. The emerging CCs are filtered by the EFR of the system, and the more distant they are relative to the resonance frequency ω_0, the greater is the attenuation of the combinational harmonics. This means that in the general case, the smaller the period of coefficient variation, the bigger is the reduction in CC level.

Example 5.12: **Dependence of Combinational Components on the Amplitude of Coefficient Variation**

Consider the narrowband LPF from example 5.2. Examples 5.2, 5.6 and 5.11 demonstrated that approximation of the desired EFR with a given accuracy could be obtained by using different periodically time-varying coefficients. There was no indication of any difference in the accuracy of EFR approximation using different timing diagrams of coefficient variations. However, the CC levels essentially depend on this timing. In Table 5.4 are the collected results of CC level evaluation for coefficients used in examples 5.2, 5.6 and 5.11. The table shows that the CC level increases as coefficient amplitude and period increase, which coincides with the general rule formulated above.

Table 5.4 CC levels in a PF-1

Example	Coefficient variations	Gain (dB)	CCs level (dB)
	$a_1 = 1 - 2^{-10}, a_2 = 1 - 3 \cdot 2^{-11}$	58.27	−75.25
5.2	$N = 2, n_1 = 1, n_2 = 1$		
5.6	$a_1 = 1 - 2^{-10}, a_2 = 1 - 2^{-9}$	58.27	−68.26
	$N = 4, n_1 = 3, n_2 = 1$		
5.11a	$a_2 = 1 - 2^{-8}, a_2 = 1 + 2^{-8}$	58.22	−29.71
	$N = 32, n_1 = 21, n_2 = 11$		(−49.94)
5.11b	$a_2 = 1 - 2^{-8}, a_2 = 1 + 2^{-8}$	57.66	−50.44
	$N = 3, n_1 = 2, n_2 = 1$		
5.11c	$a_1 = 1 - 2^{-8}, a_2 = 1$	57.70	−56.45
	$N = 3, n_1 = 1, n_2 = 2$		

Example 5.13: CC Level versus Coefficient Variation Timing Diagram

Consider the band-pass PF-2 from examples 5.4 and 5.7. Table 5.5 shows the calculated level of CCs for different timing diagrams.

Table 5.5 CC levels in a PF-2

Coefficient values	Timing diagrams of coefficient variations	Gain (dB)	CC level (dB)
Binary	$a_1(n) = \{a_{11}; a_{12}; a_{12}; a_{12}\}$	44.64	−47.37
$L = 7, N = 4$	$a_2(n) = \{a_{21}; a_{22}; a_{21}; a_{22}\}$		
$a_{11} = 1 - 3 \cdot 2^{-6}$	$a_1(n) = \{a_{21}; a_{11}; a_{12}; a_{12}\}$	44.64	−41.49
$a_{12} = 1 - 7 \cdot 2^{-6}$	$a_2(n) = \{a_{21}; a_{22}; a_{21}; a_{22}\}$		
$a_{21} = -1 + 2^{-6}$	$a_1(n) = \{a_{12}; a_{11}; a_{12}; a_{12}\}$	44.64	−41.85
$a_{22} = -1 + 2^{-7}$	$a_2(n) = \{a_{21}; a_{22}; a_{21}; a_{22}\}$		
Primitive	$a_1(n) = \{a_{11}; a_{11}; a_{11}; a_{11}; a_{11}; a_{11}; a_{12}; a_{12}\}$	43.90	−34.29
$L = 7, N = 8$	$a_2(n) = \{a_{21}; a_{21}; a_{21}; a_{21}; a_{21}; a_{22}; a_{22}; a_{22}\}$		
$a_{11} = 1 - 2^{-4}$	$a_1(n) = \{a_{11}; a_{11}; a_{11}; a_{11}; a_{11}; a_{11}; a_{12}; a_{12}\}$	43.90	−35.12
$a_{12} = 1 - 2^{-5}$	$a_2(n) = \{a_{21}; a_{22}; a_{21}; a_{21}; a_{22}; a_{21}; a_{21}; a_{22}\}$		
$a_{21} = -1 + 2^{-6}$	$a_1(n) = \{a_{11}; a_{11}; a_{11}; a_{12}; a_{11}; a_{11}; a_{11}; a_{12}\}$	43.90	−35.54
$a_{22} = -1 + 2^{-7}$	$a_2(n) = \{a_{21}; a_{22}; a_{21}; a_{21}; a_{22}; a_{21}; a_{21}; a_{22}\}$		

From the given data it can be seen that if the amplitude and period of coefficient variation increases, then the CC level rises; however, optimization of coefficient arrangement has less influence on the CC level than the amplitude of variation, especially for large N. In any case, the CC levels indicated in Table 5.5 are small and the extent of the problem of their further reduction depends on the particular PF application.

II. *Use of additional LTI filters*

It is obvious that a further reduction of CC levels can be obtained by means of additional LTI filters, narrowing the pass-band at the input or the output of the system. Of course, the frequency response of these filters can be taken into account when the frequency response of the final system is evaluated. As follows from the discussions in Chapter 3, these additional filters narrow the input and output signal band and reduce spectrum overlapping after sampling and reconstructing the signal (see Fig. 3.5). In this case, an extra reduction in the CC level is outside the PF pass-band. The contribution of additional filters can be taken into account as follows:

$$\rho = \frac{\displaystyle\int_0^{2\pi} \sum_{k=1}^{N-1} S_X(\omega + k\Omega) \cdot |H_{\text{in}}(\omega)|^2 \cdot |H_k(\omega + k\Omega)|^2 \cdot |H_{\text{out}}(\omega)|^2 \cdot \mathrm{d}\omega}{\displaystyle\int_0^{2\pi} S_X(\omega) \cdot |H_{\text{in}}(\omega)|^2 \cdot |H_0(\omega)|^2 \cdot |H_{\text{out}}(\omega)|^2 \cdot \mathrm{d}\omega} \tag{5.12}$$

where $H_{\text{in}}(\omega)$ and $H_{\text{out}}(\omega)$ are frequency responses of the input and the output filters, respectively. The effect of CC level reduction by using additional filters can be determined for each particular case.

III. *Grouping of non-stationary and stationary systems within complex systems*

An effect similar to the application of additional filters can be obtained in higher-order complex filtering systems if LTI as well as PLTV stages of a lower order are used. In this case, an optimal grouping of the stages can weaken spurious pass-bands at the input or reduce output CCs.

If there is a requirement to maximally reduce signal transformation from combinational bands into the desired band, then LTI stages have to be placed closer to the system input. If the requirement is to maximally suppress components of transformation from the desired band into combinational frequencies at the output, then the LTI stages have to be placed after the parametric stages. This problem has already been briefly discussed in Chapter 2.

IV. *Reduction of the output sampling rate*

Output sampling frequency can be reduced if the PF is a low-pass, narrowband filter. Let us consider the PF output signal $y(n)$ if the input signal is a harmonic waveform:

$$y(n) = \mathrm{e}^{\mathrm{j}\omega n} \cdot H(\omega, n) \tag{5.13}$$

We assume that the output signal is observed (sampled) at the time instants $n = \mu N$, where μ is an integer. Then,

$$y(\mu N) = \mathrm{e}^{\mathrm{j}\omega\mu N} \cdot H(\omega, \mu N) = \mathrm{e}^{\mathrm{j}\omega\mu N} \cdot H(\omega, 0) \tag{5.14}$$

Equation (5.14) shows that a PF behaves similarly to an LTI system with frequency response $H(\omega) = H(\omega, 0)$ if $n = \mu N + \nu$, where $\nu = 0, \ldots, N - 1$.

So, in the considered case a reduction of the sampling rate at the system output can fully remove CCs from PF output signals. Depending on the actual time moments of signal sampling relative to the timing diagram of coefficient variation, there is some uncertainty in the value of the transformation coefficient. However, when the CC level is low, this uncertainty is small and has the same order as the value of the CCs themselves.

5.2.3 Comparison of the Combinational Components and Noise Levels in Digital Filters

For some applications, it is not necessary to devote much effort to reducing CC levels as levels should be just less than the level of quantization and round-off noise of intermediate calculation results [1]. So, to formulate a requirement for CC levels there is good reason to firstly evaluate the noise level at the filter output. This depends on the particular filter architecture and GFR, which is demonstrated in the following typical examples showing how to compare CC levels and filter output noise levels. Consider the following two examples, which connect values of CC level, round-off noise and coefficient word length for a particular filter.

Example 5.14: **Variance Evaluation of Combinational Components**

For an LTI DF of the first order, the output round-off noise level of the intermediate calculations up to word length L is determined as follows [1]:

$$\sigma^2 = \frac{2^{-2L}}{12(1-a^2)} \tag{5.15}$$

Substitution of the filter coefficient $a = 0.9987442$ from example 5.2 results in different levels of round-off noise depending on the word length of the calculations. These results are shown in Table 5.6.

Table 5.6 Round-off noise and CC levels

Calculation word length L	DS-1 round-off noise (dB)	CC level in PF-1 (dB)	DS-2 round-off noise (dB)
8	−29.9	−56.5	−17.7
9	−36.0		−20.7
10	−42.0	−68.2	−23.7
11	−48.0		−26.7
12	−54.0		−29.7
13	−60.0		−32.8
14	−66.1	−66.1	−35.8
15	−72.1		−38.8
16	−78.1		−41.8

The values shown in Table 5.6 can be compared with the values of CC level for the equivalent GFR for a PF-1, shown in Table 5.4. From the comparison it follows that the CC level can be essentially less than the round-off noise.

However, this conclusion cannot be extrapolated to all filters and the levels of CCs and noise should be compared for each particular case.

Example 5.15: **Combinational Components and Round-Off Noise**

For a recursive system of the second order, the output round-off noise can be calculated using the following expression:

$$\sigma^2 = \frac{2^{-2L}}{12} \cdot \frac{1-\alpha^2}{1+\alpha^2} \cdot \frac{1}{\alpha^4 - 2\alpha^2 \cdot \cos(2\theta) + 1} \tag{5.16}$$

where $\alpha = \sqrt{a_2}$, $\cos\theta = -\dfrac{a_1}{2\alpha}$.

Table 5.6 shows values of round-off noise calculated by equation (5.16) for a DF-2 with coefficients $a_1 = 0.9465492$ and $a_2 = -0.9875119$ from example 5.4 for different calculation word lengths L.

We can compare the round-off noise with the CC levels for different variants of the PF-2, shown in Table 5.5. For the 7-bit calculation (example 5.4) with the best timing diagram, the CC level is -47.4 dB and remains considerably lower than the calculated round-off noise level with word length $L = 16$.

5.3 PARAMETRIC FILTER DESIGN – A CASE STUDY

Synthesis of complex filtering systems in the general case is a serious engineering problem. Utilization of PLTV algorithms gives an additional degree of freedom in terms of the filter parameters and choice of characteristics. This extra degree of freedom not only helps to design systems with given characteristics but also introduces new problems: more parameters need to be taken into account during filter design.

A number of papers discuss the problems of synthesis and technical realization of time-variant digital systems [16–18] and, in particular, periodically time-variant digital systems [5–8, 19–26]. In this book, we are not pretending to introduce a successive and universal method of LTV filter design. Instead, we are introducing a simplified algorithm or set of instructions for developing a PF with specified parameters. This algorithm is based on the PLTI DS analysis developed in the previous chapters of the book. It is based on the simple assumption that the EFR of a PF averaged over the period coefficients is the equivalent of an appropriate time-invariant filter.

One of the implications of such an approach is that for the given filter's specifications, determination of the coefficients of an equivalent LTI filter should be attempted first by known methods [1]. If the specification cannot be met by using a filter with constant coefficients, then the required characteristics can perhaps be obtained by using periodically time-varying coefficients. An equivalent LTI filter with averaged coefficient values can be used for the rough estimation of PF characteristics. These

characteristics are the first approximation, which, in some cases, can be defined more precisely by using approaches developed in Chapter 4.

At the same time, the CC level and its correspondence to the given specification have to be checked. If necessary, CC levels should be reduced via one of the methods discussed in this chapter. Some methods of CC level reduction could influence the desired EFR or the system structure. In some of these cases, requirements for the EFR of the PF have to be defined more precisely. Figure 5.9 shows a step-by-step diagram of the PF development according to the given requirements for the EFR. We will consider this algorithm using an example of a filter design.

Example 5.16: Filter Synthesis

Here, we present a more detailed consideration of the DF-1 from examples 5.1 and 5.2, applying the algorithm for PF development from Fig. 5.9. Assume that this filter should be designed using an 8-bit word length microcontroller without a hardware multiplier.

1. On the basis of the given requirements, our goal is to design a DF-1 with a cut-off frequency of $\omega_c = 0.0002$ at the level -3 dB and with the FR deviation less than ± 0.25 dB.
2. An exact value for the LTI DF coefficient [1] is $a = 0.9987442$ and the filter gain at DC equals 58.02 dB.

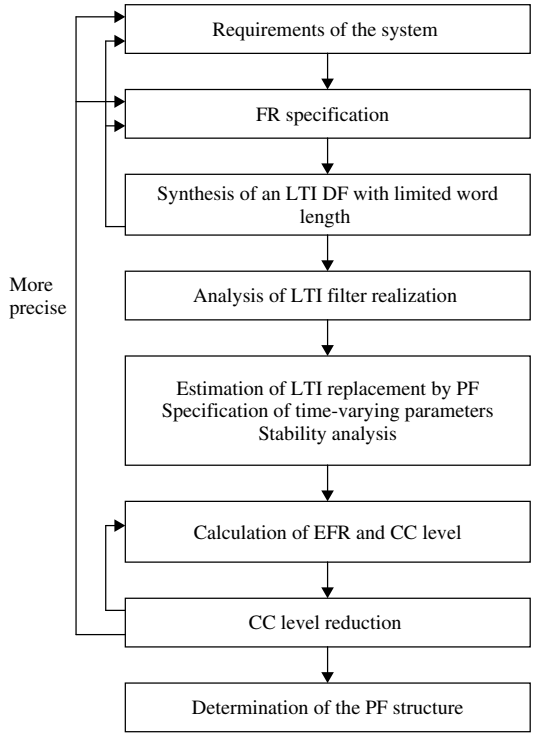

Figure 5.9 Step-by-step PF development

3. The coefficient values that provide FR deviation less than ± 0.25 dB are $a_{\min} = 0.99867$ and $a_{\max} = 0.998814$. A minimal word length and value for the LTI filter with quantized coefficients complying with the specifications is $a_{q0} = 1 - 5 \cdot 2^{-12}$ and the required gain is 58.27 dB.
4. In order to use the selected hardware, the determined word length has to be reduced. The coefficient value closest to one for the given word length is $1 - 2^{-8}$. For this word length, a required cut-off frequency cannot be obtained (see example 5.11). Possible solutions for this problem include amending requirements for the system or using periodically time-varying coefficients.
5. Use equation (5.3) to estimate the FR for different coefficient variation periods N. The following parameters of the PF provide sufficient FR approximation: $N = 32, n_1 = 11, a_1 = 1 - 2^{-8}$ and $n_2 = 21, a_2 = 1 + 2^{-8}$ (from example 5.11a from Table 5.4). To meet the given system specifications, the geometrical mean of the equivalent coefficient must be 0.998772 and the filter gain must be 58.22 dB. This PF also meets the stability criterion. For smaller valves of N, it is not possible to obtain the required accuracy from FR approximation.
6. Calculate the CC level. For the regular timing diagram of coefficient variation, when the same instant coefficient values are repeated in succession, the CC level is -29.7 dB. This value approximately corresponds to the round-off noise level for the 8-bit calculation introduced in Table 5.4. Optimization of the timing diagram (as in example 5.13) considerably reduces the CC level, down to -49.9 dB. These CC components are fully masked by the round-off noise.
7. Further simplification can be obtained using period $N = 3$. For this period (see examples 5.11b,c from Table 5.4), the EFR also meets the filter specifications. The resulting -56.5 dB CC level is even less than that considered in step 6.
8. Taking into account that the filter is low-pass and narrowband, it is possible to reduce sampling frequency in three times to overcome CC interference problem.

Thus, we obtain coefficient values $a_1 = 1 - 2^{-8}$, $a_2 = 1$; period $N = 3$; a timing diagram of coefficient variation $n_1 = 1$, $n_2 = 2$. This PF fully meets the specifications, can be developed by an 8-bit microcontroller and does not use directly the multiplication procedure.

5.4 SUMMARY

Various generic problems of time-variant linear discrete systems (DSs) were discussed in Chapters 2 to 4. In this chapter, the accumulated generic knowledge was applied for PF analysis. We specified functions of PFs to be, in some instances, a direct equivalent of LTI digital filters. Coefficient variations are used to add some flexibility or degree of freedom to filter characteristics, achieved by making some hardware/software simplifications. In this chapter, we proposed ways to reduce word length requirements, use of primitive coefficients that allow us to replace multiplications by more simple shifting operations and use of coefficients that correspond to a non-stable LTI.

Replacement of LTI by LTV systems is not a penalty-free procedure. Owing to variation of filter coefficients, multiplicative interferences appear at the filter output.

In this chapter, we discussed how to both evaluate the level of these interferences and reduce their negative effects. Using numerous examples, it was shown that for many practical applications the interference level can be minimized to an acceptable level.

Of course, nobody is proposing to replace traditional LTI DFs by parametric filters. The goal of the book is to supply professional designers with some extra flexibility for system design. The hope is that demonstrated examples of PFs representing applications of time-variant systems have persuaded the reader that PLTV DSs are serious weapons in an engineer's arsenal.

5.5 ABBREVIATIONS

CC	combinational component
DF	digital filter
DS	discrete system
EFR	equivalent frequency response
FFT	fast Fourier transform
GFR	generalized frequency response
LPF	low-pass filter
LTI	linear time-invariant
PF	parametric filter
PF-1	parametric filter of the first order
PF-2	parametric filter of the second order
PLTV	periodical linear time-variant

5.6 VARIABLES

$\Delta\omega_n$	noise frequency band
ψ	input frequency
ω	normalized output frequency
γ	amplitude criteria
Ω	normalized frequency of system parameter variation
$\delta(n, k)$	unit sample sequence
ω_0	resonant frequency
σ^2	level of round-off noise
ω_c	cut-off frequency
A	signal amplitude
$a(n)$	time-varying coefficients of the recursive part of a difference equation
$b(n)$	time-varying coefficients of non-recursive part of a difference equation
G	system gain
$g(m, n)$	impulse response of the recursive part
$H(\psi, \omega)$	bifrequency function
$h(m, n)$	impulse response

$H(z, n)$	generalized transfer function
$i, l, m, n, k, \nu, \xi, \eta$	integers
L	coefficient word length
M	number of filters in a comb
N	period
Q	quality factor
q	quantization step
T	sampling period
$X(\omega)$, $X(\psi)$	spectrum of the input signal
$X(n)$	input discrete random process
$x(n)$	input signal
$X(z)$	z-transform of the input signal
$Y(\omega)$	spectrum of the output signal
$Y(n)$	output discrete random process
$y(n)$	output signal
$Y(z, n)$	z-transform of the output signal

5.7 REFERENCES

[1] Ifeachor EC, Jervis BW (2002) *Digital Signal Processing. A Practical Approach*, UK: Prentice Hall.

[2] Cherniakov M, Sizov V (1985) Analysis of the first order periodic non-stationary digital recursive filter. *Electron. Tech.*, **10**(4), 17–20.

[3] Cherniakov M, Rogozkin IB, Sizov VI (1991) Digital non-stationary filters. *Electron. Tech.*, **10**(3), 26–32.

[4] Cherniakov M, Rogozkin IB (1990) Digital non-stationary systems, *Electron. Tech.*, **10**(6), 34–39.

[5] Kitson FL, Griffits LJ (1982) The design of time-varying digital filters which employ binary valued coefficients, *IEEE Int. Conf. on ASSP*, Vol. **1**, Paris, France, 302–305.

[6] Kitson FL, Griffits LJ (1981) Highly quantized, non-recursive digital filters, *Systems and Comp.: Annual Asilomar Conf. on Circuits*, 65–69.

[7] Park S, Aggarwal JK (1985) Recursive synthesis of linear time-variant digital filters via Chebyshev approximation. *IEEE Trans.*, **Cas-32**(3), 245–251.

[8] Kitson FL, Griffits LJ (1988) Design and analysis of recursive periodically time-varying digital filters with highly quantized coefficients. *IEEE Trans.*, **ASSP-36**(5), 674–685.

[9] Scoular S, Rogozkin I, Cherniakov M (1993) Review of Soviet research on linear time-variant discrete systems. *Signal Process.*, **30**(1), 85–101.

[10] Betz VP, Cherniakov M (1989) Algorithm of parametrical generation of digital signals. *Commun. Tech.*, **8**, 26–33.

[11] Cherniakov M (1989) Conditions of digital parametric frequency multiplier generation. *Radiotech. Electron.*, **5**, 1108–1110.

[12] Betz VP, Cherniakov M (1987) Application of the discrete transmission matrix method for amplitudes of the digital filter stability. *Radiotechnica*, **4**, 24–26.

[13] Betz VP, Cherniakov M (1987) Stability of the digital filters with random varying parameters. Izvestia Vuzov, *Radioelectronika*, **2**, 72–75.

[14] Subramanyan R, Radhakrishna RK (1986) Novel high-Q narrowband/notch digital filter. *Electron. Lett.*, **22**(16), 870–872.
[15] Cherniakov M, Sizov V, Donskoi L (2000) Combinational components at the output of periodically time-varying filters, *Proc. 5th Int. Conf. WCCC-ICSP-2000*, Vol. **1**, Beijing, China, August, 143–146.
[16] Feng Z, He H, Unbehauen R (1992) The determination of the generalized frequency response for linear periodically shift-variant digital filters, *Proc. Midwest Symp. on Cas*, Washington, DC, USA, V.1, 591–593.
[17] Yang X, Kawamata M, Higuchi T (1995) Approximations of IIR periodically time-varying digital filters. *IEE Proc. Circuits, Devices Syst.*, **142**(6), 387–393.
[18] Li D (1993) Finite-time-domain synthesis of recursive linear time-variant causal digital filters by separable sequences. *IEEE International Symposium on Cas*, May 1993, Singapore, 359–362.
[19] Ghanekar S, Tantaratana S, Frank L (1993) Design and architecture of multiplier-free filters using periodically time-varying ternary coefficients. *IEEE Trans.*, **Cas-I-40**(5), 365–370.
[20] Loefler CM, Burrus CS (1982) Design of periodically time-varying digital filters. *IEEE Int. Symp. Circuits Syst.*, 663–665.
[21] Loefler CM, Burrus CS (1984) Optimal design of periodically time varying and multirate digital filters. *IEEE Trans.*, **ASSP-32**(6), 991–997.
[22] Ferrara ER (1985) Frequency-domain implementation of periodically time-varying filters. *IEEE Trans.*, **ASSP-32**(4), 883–892.
[23] Prater JS, Loefler CM (1992) Analysis and design of periodically time-varying IIR filters, with applications to transmultiplexing. *IEEE Trans.*, **ASSP-40**(11), 2715–2725.
[24] Min XW, Ishii R (1990) Equivalent structures of a periodically time varying digital filter. *Trans. IEICE*, **E73**(6), 893–900.
[25] Yang X, Kawamata M, Higuchi T (1996) Balanced realization and model reduction of periodically time-varying state-space digital filters. *IEE Proc. Vis., Image Signal Process.*, **143**(6), 370–376.
[26] Nikolaidis SS, Mourjopoulos JN, Goutis CE (1993) A dedicated processor for time-varying digital audio filters. *IEEE Trans.*, **Cas-II-40**(7), 452–455.
[27] Dubiner Z, Porat M (1997) Time-variant filtering in the time-frequency space: performance analysis and filter design, *Conference Record of the Thirty-First Asilomar Conference on Signals, Systems & Computers*, Vol. **2**, 1471–1473.
[28] King CW, Lin CA (1995) A unified approach to scrambling filter design. *IEEE Trans.*, **SP-43**, 1753–1765.
[29] Wang S, Zhang C (1999) Minimum order input-output equation for LTV digital filters with time-varying state dimension. *Signal Process.*, **76**(3), 301–309.
[30] Wang S, Zhang C (2000) Invertibility and inverses of linear time-varying digital filters. *IEEE Trans.*, **Cas-II-47**(10), 1126–1131.
[31] Zhang C, Liao Y (1997) A sequentially operated periodic FIR filter for perfect construction. *IEEE Trans.*, **Cas-II-16**(4), 475–486.
[32] Zhang C, Wang S, Zheng Y (1998) Minimum order input-output equation for linear time-varying digital filters. *IEEE Signal Process. Lett.*, **5**(7), 171–173.
[33] Zhang H, Dejung W, Zhao Z (1990) On the design of nearest optimal recursive linear shift-variant digital filters, *IEEE Int. Symp. on Cas*, Vol. **1**, 141–143.
[34] Joo KS, Bose T (1996) Two-dimensional periodically shift variant digital filters. *IEEE Trans. Cas Video Technol.*, **6**(1), 97–107.
[35] McLernon DC (1994) On periodically time varying two-dimensional state-space filters, *Proc. Int. Symp. on Cas*, May, 221–224.

[36] McLernon DC (1996) On finite word effects in two-dimensional multirate periodically time-varying filters, *Proc. 38th Midwest Symp. on Cas*, Vol. **1**, 486–489.
[37] Rajan S, Joo KS, Bose T (1996) Analysis of 2-D state-space periodically shift variant digital filters. *IEEE Trans.*, **Cas–II-15**(3), 395–413.
[38] Bellanger M (1989) *Digital Processing of Signals: Theory and Practice*, New York: John Wiley & Sons.

Part Three
Digital Parametric Oscillators

6
Digital Parametric Oscillators

In Chapters 2 to 4, we discussed generic aspects of linear time-variant digital systems and, in particular, those with periodically varying parameters. Using this theory in Chapter 5, we investigated parametric filters (PFs) that are based on periodically linear time-variant discrete systems (PLTV DSs). The major function of a PF is similar to that of linear time-invariant (LTI) digital systems, that is, signal filtering. In some instances, introduction of a PF is one example of practical applications of PLTV DSs.

In this chapter, another more "exotic" tool based on PLTV DSs – the digital parametric oscillator (DPO) – will be introduced. It can also be regarded as a practical output from the introduced theory.

Analysis of second-order recursive systems (Chapter 3) with high quality factor (Q) and periodically varying coefficients showed a rather sophisticated dependence between the law of coefficient variation and the system stability. For convenience, we referred to the law of coefficients variation as some external control signals (CSs). In particular, we found that instability occurred at frequencies integer to the half of CS main harmonics $\Omega_C : S\Omega_C/2$, where $S = 1, 2, 3 \ldots$. In these instability regions, parametric generation occurs in a process similar to that for a well-known capacitor, an inductor (LC) resonance circuit with a periodically varying capacitor. Consequently, this periodically time-varying digital resonator (DR) becomes a digital parametric oscillator. So, the goal of this chapter is to introduce the theory behind DPOs, another useful tool for signal processing based on PLTV systems. It is very important to recall that the word "linear" in these systems refers only to the input signals. Relative to the CSs, the parametric systems are essentially non-linear and the superposition principle is not applicable when CSs are considered.

These or similar digital parametric generators have not been described in the literature apart from the author's work [1–19]. The method of investigating these systems used in this book is based on the classical Liapunov theory. Introduction to the Liapunov theory for continuous parametric systems can be found in [20].

An Introduction to Parametric Digital Filters and Oscillators Mikhail Cherniakov
© 2003 John Wiley & Sons, Ltd ISBN: 0-470-85104-X

6.1 REGIONS OF PARAMETRIC OSCILLATIONS

Let us consider a high Q, recursive second-order DR with periodically varying coefficient(s) or, in other words, a periodically varying digital resonator (PVDR). This system is, in some instances, an equivalent of resonance LC circuits with periodically varying capacitor and/or inductor. From the mathematical point of view, the condition for the origin of oscillations in PVDRs is an increase in "generalized" energy introduced by the square of the state vector norm (SVN). From the physical point of view, this instability means that at the resonator the output process will increase in time even in the absence of any signal at the input. In the general case, this output process may or may not be coherent with the CS parameters.

In Chapter 3, we investigated the stability of a second-order PLTV system. This study identified special instability enclaves within the stability area of a PF. We assume now and will prove later that the areas of instability correspond to parametric instability zones (PIZ). Coherent narrowband oscillations with central frequency $S\Omega_{ci}/2 (S = 1, 2, 3 \ldots)$ occur at the output of the system even in the absence of any input signals when PLTV parameters correspond to these instability regions. Consider the behaviour of a PVDR in the instability areas discussed above and relations between the CS and a process at the system output. Assume that any signal at the DR input is absent, but initial conditions (words stored in the internal registers) are non-zero.

The analysis of PVDR stability has revealed regions where there is unlimited increase in "generalized" system energy, which is a necessary (but not sufficient) condition for generation of parametric oscillation. To determine regions of parametrical generation (RPG) in the overall system's instability area, we rely on the fact that when parametrical generation is initialized, quasi-harmonic (narrowband) oscillations coherent with the CS appear at the system output. It is important to note that the presence of CS sub-harmonics is the fundamental feature of parametric generation processes [21].

Note also that one of the conditions for parametric generation is an increase in the SVN module value or, simply, the magnitude of the output signal. Eventually, the magnitude rise in digital systems leads to internal registers overfilling and the system operates in the saturated mode. So, in the general case these parametric generators should be investigated in two modes: non-limited (quasi-linear) and saturated (steady-state).

It is interesting to note that there is one unique combination of CS and PVDR parameters where parametric oscillations occur, but have a constant average magnitude over time. This mode corresponds to the case where the DPO operates exactly at the boundary of the parametric instability zones. Perhaps this is not a practical mode of operation, but it makes theoretical sense and will be used for the analysis.

Let us first analyse the system behaviour at the PIZ boundary, where the solution is assumed to be periodic with a constant envelope. This will be a good introduction for readers into the DPO.

The system is described by a uniform linear difference equation:

$$y(n) + a_1(n)y(n-1) + a_2(n)y(n-2) = 0 \tag{6.1}$$

and from this equation we will derive the major features of an output (generating) signal, assuming, as mentioned before, non-zero initial conditions. Let us represent periodically time-varying coefficients $a_1(n) = a_1(n+N)$ and $a_2(n) = a_2(n+N)$ by a quadrature Fourier series:

$$\begin{cases} a_1(n) = a_1 + \sum_{m=1}^{M} \alpha_{1m} \cos(m2\pi n/N) \\ a_2(n) = a_2 + \sum_{m=1}^{M} \alpha_{2m} \cos(m2\pi n/N) \end{cases} \tag{6.2}$$

where α_{1m}, α_{2m} are the Fourier coefficients and a_1, a_2 are average values of the coefficients.

To determine spectral characteristics of the output signal $y(n)$, we first apply a discrete Fourier transform (DFT) to equation (6.1). Let us select a DFT sampling interval in frequency domain equal to $\Omega_c/2 = \pi/N$, since the output signal spectrum contains components proportional to the sub-harmonic frequencies of the CS. Substituting for $a_1(n)$ and $a_2(n)$ by representation of their Fourier series expansion, we obtain

$$\begin{aligned} &\sum_{n=0}^{N-1} y(n)\mathrm{e}^{-\mathrm{j}S\pi n/N} + a_1 \sum_{n=0}^{N-1} y(n-1)\mathrm{e}^{-\mathrm{j}S\pi i/N} \\ &\quad + \left[\sum_{m=1}^{M} \alpha_{1m} \sum_{i=0}^{N-1} (\mathrm{e}^{\mathrm{j}2\pi mn/N} + \mathrm{e}^{-\mathrm{j}2\pi mn/N}) y(n-1)\mathrm{e}^{-\mathrm{j}S\pi n/N} \right] \Big/ 2 \\ &\quad + a_2 \sum_{n=0}^{N-1} y(n-2)\mathrm{e}^{-\mathrm{j}S\pi n/N} \\ &\quad + \left[\sum_{m=1}^{M} \alpha_{2m} \sum_{n=0}^{N-1} (\mathrm{e}^{\mathrm{j}2\pi mn/N} + \mathrm{e}^{-\mathrm{j}2\pi mn/N}) y(n-2)\mathrm{e}^{-\mathrm{j}S\pi n/N} \right] \Big/ 2 = 0 \end{aligned} \tag{6.3}$$

Denoting the Sth spectral component as $\hat{y}_S = \sum_{n=0}^{N-1} y(n)\mathrm{e}^{-\mathrm{j}S\pi n/N}$ and taking into account the DFT property in the time and frequency domains, we obtain the following expression for the additives of equation (6.3):

$$\sum_{n=0}^{N-1} y(n-1)\mathrm{e}^{-\mathrm{j}S\pi n/N} = \hat{y}_S \mathrm{e}^{-\mathrm{j}S\pi/N} \tag{6.4}$$

$$\sum_{n=0}^{N-1} y(n-2)\mathrm{e}^{-\mathrm{j}S\pi n/N} = \hat{y}_S \mathrm{e}^{-\mathrm{j}2S\pi/N} \tag{6.5}$$

$$\sum_{n=0}^{N-1} y(n-1)\mathrm{e}^{-\mathrm{j}S\pi n/N_\mathrm{e} \pm \mathrm{j}2\pi mn/N} = \hat{y}_{S\pm 2m} \mathrm{e}^{-\mathrm{j}(S\pm 2m)\pi/N} \tag{6.6}$$

$$\sum_{n=0}^{N-1} y(n-2)\mathrm{e}^{-\mathrm{j}S\pi n/N_\mathrm{e} \pm \mathrm{j}2\pi mn/N} = \hat{y}_{S\pm 2m} \mathrm{e}^{-\mathrm{j}(S\pm 2m)\pi/N} \tag{6.7}$$

It is possible to find a formula connecting the S and $S \pm 2m$ components of the parametric oscillator output signal. Taking into account equations (6.4) to (6.7) and the expression describing the Sth and $(S \pm 2m)$th spectrum components from equation (6.3), we obtain

$$\begin{aligned}
\hat{y}_S = & \frac{-\sum_{m=1}^{M} \alpha_{1m}[\mathrm{e}^{-\mathrm{j}\pi(S-2m)/N}\hat{y}_{S-2m} + \mathrm{e}^{-\mathrm{j}\pi(S+2m)/N}\hat{y}_{S+2m}]}{2(1 + a_1\mathrm{e}^{-\mathrm{j}S\pi/N} + a_2\mathrm{e}^{-\mathrm{j}2S\pi/N})} \\
& - \frac{\sum_{m=1}^{M} \alpha_{2m}[\mathrm{e}^{-\mathrm{j}2\pi(S-2m)/N}\hat{y}_{S-2m} + \mathrm{e}^{-\mathrm{j}2\pi(S+2m)/N}\hat{y}_{S+2m}]}{2(1 + a_1\mathrm{e}^{-\mathrm{j}S\pi/N} + a_2\mathrm{e}^{-\mathrm{j}2S\pi/N})} \\
= & \frac{\sum_{m=1}^{M} \hat{y}_{S-2m}[\alpha_{1m}\mathrm{e}^{-\mathrm{j}\pi(S-2m)/N} + \alpha_{2m}\mathrm{e}^{-\mathrm{j}2\pi(S+2m)/N}]}{2(1 + a_1\mathrm{e}^{-\mathrm{j}S\pi/N} + a_2\mathrm{e}^{-\mathrm{j}2S\pi/N})} \\
& - \frac{\sum_{m=1}^{M} \hat{y}_{S+2m}[\alpha_{1m}\mathrm{e}^{-\mathrm{j}\pi(S+2m)/N} + \alpha_{2m}\mathrm{e}^{-\mathrm{j}2\pi(S+2m)/N}]}{2(1 + a_1\mathrm{e}^{-\mathrm{j}S\pi/N} + a_2\mathrm{e}^{-\mathrm{j}2S\pi/N})}
\end{aligned} \tag{6.8}$$

It was specified above that the sufficient condition for parametric oscillation is the presence of a dominant component in the output signal $y(n)$ spectrum at one of the frequencies $S\Omega_c/2$. In other words, the DPO generates a narrowband signal coherent with the CS. Analysis of equation (6.8) shows that this criteria corresponds to the denominator of (6.8) approaching zero:

$$1 + a_1\mathrm{e}^{-\mathrm{j}S\pi/N} + a_2\mathrm{e}^{-\mathrm{j}S2\pi/N} = 0 \tag{6.9}$$

Equation (6.9), in the general case, represents a complex value and it should be first separated into imaginary (Im) and real (Re) parts:

$$\begin{aligned}
\mathrm{Im}\{z\} &= a_1 \sin(S\pi/N) + a_2 \sin(2S\pi/N) \\
\mathrm{Re}\{z\} &= a_1 \cos(S\pi/N) + a_2 \cos(2S\pi/N)
\end{aligned} \tag{6.10}$$

Then, two conditions for the existence of a dominant component in the output signal spectrum can be found. The first one follows from the condition that the Im part of equation (6.9) is equal to zero:

$$a_1 \sin(S\pi/N) + a_2 \sin(2S\pi/N) \approx 0 \tag{6.11}$$

or

$$a_1 \approx -2a_2 \cos(S\pi/N) \tag{6.12}$$

from which

$$S\pi/N \approx \cos^{-1}(-a_1/2a_2) \tag{6.13}$$

The next step is to transform equation (6.10) into

$$1 - 2a_2 \cos^2(S\pi/N) + a_2 \cos^2(S\pi/N) - a_2 \sin^2(S\pi/N) \approx 0 \tag{6.14}$$

and we thus obtain the second condition:

$$a_2 \approx 1 \tag{6.15}$$

From equations (6.12) and (6.15) it follows that the sufficient conditions for parametric generation in a PVDR are as follows:

1. The DR has to have a high Q.
2. The DR has to have the resonance frequency at $\omega_{\text{res}} \cong S\Omega_c/2$, which is the Sth CS sub-harmonic frequency. This has an easy explanation. When $a_2 \approx 1$ (high Q), the condition described by equation (6.13) becomes similar to the known equation for the resonance frequency of the second-order DR $\omega_{\text{res}} = \cos^{-1}(-a_1/2\sqrt{a_2})$ [22].

Hence, for these conditions there is a dominant component in the output signal $y(n)$ spectrum, that is, generated parametric oscillations are quasi-harmonic. From equation (6.8), it also follows that modulation components $\hat{y}_{S\pm 2m}$ appearing in the output signal spectrum are caused by the mth (including $m = 1$) CS harmonics. Thus, the DR and CS parameters fully determine the output signal spectrum.

To confirm the effect of parametric oscillations in the PVDR and determine the characteristics of an output signal spectrum, let us consider results of system modelling. For particular values of $a_1(n)$, $a_2(n)$ and initial conditions, the modelling allows us to obtain an exact solution for equation (6.1). The output signal spectrum $\hat{y}(\omega/\Omega_c)$ can be calculated via DFT of the output signal $y(n)$ periodic component $\tilde{y}(n)$.

It is necessary to underline the following peculiarity of the modelling. Analytical description of the output signal was obtained for PIZ boundaries, where the solution is periodic. For practical modelling it is, in some instances, impossible to operate directly at these boundaries, as they are infinitely thin lines, a mathematical abstraction. When the PVDR parameters correspond to any internal area restricted by this PIZ boundary, an average magnitude of the output signal $y(n)$ is an exponentially increasing function. This will be studied later in detail. The following example illustrates what has just been discussed.

Example 6.1: Spectrum of an Output Signal

Consider the modelling results for a harmonic CS: $a_2(n) = 0.988 + 0.125\cos(2\pi n/6)$, and constant coefficient $a_1 = -1.414$. For parametric generation at the first CS sub-harmonic $S = 1$, the DR resonance frequency should be $\omega_{\text{res}} \approx 2\pi/12$, which approximately corresponds to the coefficient a_2 value. The CS spectrum for this case is shown in Fig. 6.1 by dashed lines and the output signal spectrum is shown in Fig. 6.1 by solid lines. The modelling result confirms that there is a narrowband output signal for the given DR and CS parameters. The main spectral harmonic is approximately 15 dB above the side components and the position of the main harmonic corresponds to the first CS's sub-harmonic.

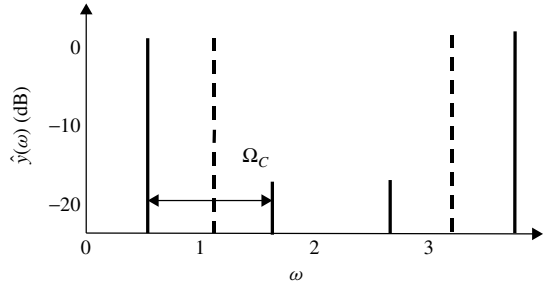

Figure 6.1 Signals spectrum in a DPO

Thus, if the regions of parametric instability satisfy conditions (6.13) and (6.15), then the output signal has a dominant component at one of the frequencies integer to CS spectrum sub-harmonics, that is, there are parametric oscillations in the system. Such regions, illustrated in Fig. 6.2, are called *regions of parametric generation* (RPGs).

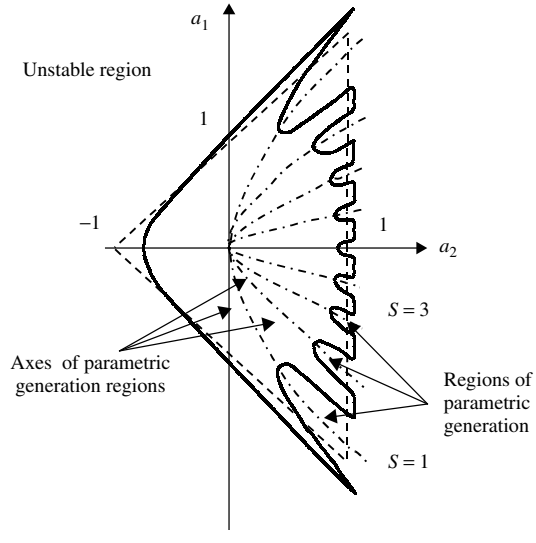

Figure 6.2 Regions of parametric generation

6.2 PARAMETRIC RESONANCE IN DIGITAL RESONATORS

We identified regions of parametric generation using the similarity between continuous and discrete parametric systems as well as common sense. In this section, we will study a parametric resonance phenomenon in digital systems using a more solid mathematical approach. Let us analyse characteristics of an output signal, assuming that parameters of the PVDR correspond to the internal regions of PIZs and parametric oscillations occur.

As detailed above, increasing quasi-harmonic oscillations present at the DPO output for non-zero initial conditions. According to [23], a general solution of the second-order parametric differential equation can be represented as a linear combination of two normal components: increasing and decreasing components. The time period when the decreasing component has sufficient value in comparison with the increasing component corresponds to the transient. At the end of this time, the decreasing component becomes small enough to be neglected and monotonically increasing quasi-harmonic oscillations are established. These oscillations are coherent with the CS. Eventually, the increasing magnitude of oscillations leads to an overflow of the register's capacity during arithmetical operations and to limitation of the output signal. This saturated mode will be analysed later. Here, the non-limited mode will be studied.

The non-limited regime of a digital parameter occurs in two cases. In the first case, it exists for a relatively short transient between oscillation excitation and the moment of register overflow. The second case involves the use of DRs specifically designed to maximize the transient period. This can be achieved by scaling internal words, used, for example, in digital filters based on fixed-point arithmetic [22].

Solutions for equation 6.1 that describe signals at the oscillator output in the non-limited mode depend on initial conditions and eigenvalues of the appropriate monodromy matrix (MM). In the non-limited mode, the parametric oscillator operation is determined by two time constants – τ_1 for an increasing oscillation component and τ_2 for a decreasing component – spectral characteristics of the periodical component $\hat{y}(\omega)$ and phase relations between the CS and the signal at the output of the DPO. The time constant for the decreasing component specifies the length of the transient period. So, all characteristics are determined by the DR parameters, CS and initial conditions. The aim of the following material is to establish an accurate dependence between these parameters and characteristics of generating signals.

The homogeneous difference equation (6.1), which describes a DPO, has two linear independent non-zero fundamental solutions: $[Y_1(i)]$ and $[Y_2(i)]$. Any other solution is just a linear combination of these fundamental solutions [24]:

$$[Y(i)] = g_1[Y_1(i)] + g_2[Y_2(i)] \tag{6.16}$$

where $g_{1,2}$ are constants. In order to form a fundamental system for $[Y_1(i)]$ and $[Y_2(i)]$, it is necessary and sufficient that the Kazoratty determinant

$$\Delta(i) = \det \begin{bmatrix} y_1(i) & y_2(i) \\ y_1(i-1) & y_2(i-1) \end{bmatrix} \tag{6.17}$$

is not equal to zero.

In the general case, in regions of parametric generation, the solutions of equation (6.1) are not periodic. However, among them there are solutions that are multiplied by a constant value λ when n increases by the period of the CS variation $T = N$:

$$[Y(n+N)] = [C(N+n, n)][Y(n)] = [C(N, 0)][Y(n)] = \lambda[Y(n)] \tag{6.18}$$

Such solutions are called normal and will be used hereon. Physically, this condition means that the state vector at the moments separated by the interval T has the same position in space, but its module differs in λ times. To find these normal solutions, we use the right side of equation (6.18):

$$[C(N, 0)][Y(n)] = \lambda[Y(n)] \tag{6.19}$$

or

$$[[C(N, 0)] - \lambda[I_2]] = 0 \tag{6.20}$$

This system has a non-trivial solution only in the case when

$$\det[[C(N, 0)] - \lambda[I_2]] = 0 \tag{6.21}$$

The characteristic equation (6.21) has two solutions, λ_1 and λ_2:

$$\lambda_{1,2} = -\frac{C_{11} + C_{22}}{2} \pm \sqrt{\left(\frac{C_{11} + C_{22}}{2}\right)^2 - \prod_{n=1}^{N} a_2(n)} \tag{6.22}$$

For each of $\lambda_{1,2}$, such $[Y_1(0)]$ and $[Y_2(0)]$ can be found where solutions of the equation are normal and, hence, can be represented as

$$[Y_1(n + mN)] = \lambda_1^m [Y_1(1)] \tag{6.23}$$

or

$$[Y_2(n + mN)] = \lambda_2^m [Y_2(1)] \tag{6.24}$$

As was shown in Chapter 3, $\lambda_{1,2}$ must be real. Only in this case are $[Y_1(n)]$ and $[Y_2(n)]$ normal.

To determine $[Y_1(n)]$ and $[Y_2(n)]$, the next set of equations has to be substituted into equation (6.21):

$$\begin{cases}(C_{11}-\lambda_{1,2})y_{1,2}(n)+C_{12}y_{1,2}(n-1)=0\\ C_{21}y_{1,2}(n)+(C_{22}-\lambda_{1,2})y_{1,2}(n-1)=0\end{cases} \tag{6.25}$$

From equation (6.25), we can obtain the following expression, which connects output signals $y_{1,2}(n)$ and $y_{1,2}(n-1)$ at the consecutive sampling intervals (n) and $(n-1)$:

$$y_{1,2}(n)=-\frac{C_{12}-C_{22}+\lambda_{1,2}}{C_{21}+C_{11}-\lambda_{1,2}}y_{1,2}(n-1) \tag{6.26}$$

or in matrix notation:

$$[Y_{1,2}(n)]=\begin{bmatrix}y_{1,2}(n)\\ y_{1,2}(n-1)\end{bmatrix}=\begin{bmatrix}-\dfrac{C_{12}-C_{22}+\lambda_{1,2}}{C_{21}+C_{11}-\lambda_{1,2}}\\ 1\end{bmatrix} \tag{6.27}$$

Note that equation (6.17)

$$\begin{aligned}\Delta(n)&=\det\begin{bmatrix}y_1(n) & y_2(n)\\ y_1(n-1) & y_2(n-1)\end{bmatrix}=\det\begin{bmatrix}-\dfrac{C_{12}-C_{22}+\lambda_1}{C_{21}+C_{11}-\lambda_1} & -\dfrac{C_{12}-C_{22}+\lambda_2}{C_{21}+C_{11}-\lambda_2}\\ 1 & 1\end{bmatrix}\\ &=-\frac{C_{12}-C_{22}+\lambda_1}{C_{21}+C_{11}-\lambda_1}+\frac{C_{12}-C_{22}+\lambda_2}{C_{21}+C_{11}-\lambda_2}\end{aligned} \tag{6.28}$$

is equal to zero only for $\lambda_1=\lambda_2=0$. In the considered case, we obtain $\lambda_1\lambda_2=\prod_{n=1}^{N}a_2(n)\approx 1$, that is, the requirement for a high Q in RPGs. This is a necessary and sufficient condition for $[Y_1(n)]$ and $[Y_2(n)]$ to form a fundamental system for solutions of equation (6.1).

Thus, a general solution of equation (6.1) in RPGs can be represented as a linear combination of two normal components:

$$[Y(n)]=g_1[Y_1(n)]+g_2[Y_2(n)] \tag{6.29}$$

A solution through the system period N can be found using eigenvalues of MM as follows:

$$[Y(n+N)]=g_1[Y_1(n+N)]+g_2[Y_2(n+N)]=\lambda_1 g_1[Y_1(n)]+\lambda_2 g_2[Y_2(n)] \tag{6.30}$$

and by analogy,

$$[Y(n+mN)]=\lambda_1^m g_1[Y_1(n)]+\lambda_2^m g_2[Y_2(n)] \tag{6.31}$$

Thus, depending on the value of $\lambda_{1,2}$, different solutions can be obtained, as summarized below (see also Fig. 6.2):

1. *Stable region:* If $|\lambda_{1,2}| < 1$, then both fundamental solutions decrease, equation (6.1) is stable and the system possesses filtering properties.
2. *Region of parametric generation:* Roots $\lambda_{1,2}$, are real, an absolute value of one of them is larger than 1 and the second root is less than 1. Such a situation corresponds to the system operation within RPGs. According to equation (6.22),

$$\lambda_1 \lambda_2 = \prod_{n=1}^{N} a_2(n) \approx 1 \tag{6.32}$$

since a necessary condition for quasi-harmonic oscillations is high Q, that is, $a_2 \sim 1$ (as specified by equation 6.15). At the boundary of RPGs, the condition $|\lambda_1| = |\lambda_2| = 1$ is true.
3. *Unstable region:* If $|\lambda_{1,2}| > 1$, then non-parametrical instability occurs. Moreover, if λ_1 and λ_2 are real and outside the stability area determined as

$$\left(\frac{C_{11} + C_{22}}{2}\right)^2 - \prod_{n=1}^{N} a_2(n) < 0$$

then the output process will have a divergent non-periodic character. If λ_1 and λ_2 are complex conjugates, there will be increasing oscillations, non-coherent with the CS.

Thus, the process of excitation of parametrical oscillations can be divided into two stages:

1. *Solution normalization transient:* At this stage, both the increasing components $g_1\lambda_1^m[Y_1(n)]$ and the decreasing components $g_2\lambda_2^m[Y_2(n)]$ should be taken into account and the output oscillations are not fully coherent with the CS. There is a transient process in the DPO that is the cause of amplitudes and phase disturbance.

2. *A normal solution:* At this stage, the decreasing component can be neglected and the solution converges to only the normal increasing component:

$$[Y(n + mN)] \approx \lambda_1^m[Y(n)] \tag{6.33}$$

or

$$y(n + mN) \approx \lambda_1^m y(n) \tag{6.34}$$

Thus, using equation (6.22) it is possible to determine the relation between equation (6.1) coefficients and solutions (6.33) that describe the digital parametrical generator (DPG) output process in the non-limited mode. Let us illustrate these using computer modelling.

Example 6.2: Oscillation Initiated via a Fast Sinusoidal Control Signal

Oscillations have been excited by the sinusoidal CS: $a_2(n) = 1.0 \pm 0.25\sin(\pi n/2)$ in an RPG. The output waveform for two values of the constant coefficient, $a_1 = -1.25$ (continuous line) and -1.41 (dashed line), are sketched in Fig. 6.3. Both values for a_1 provide parametrical generation at the frequency of the first CS sub-harmonic; however, eigenvalues for these two cases differ considerably. Thus, for $a_1 = -1.25$ eigenvalues approach 1: $\lambda_1 = -1.031$ and $\lambda_2 = -0.970$.

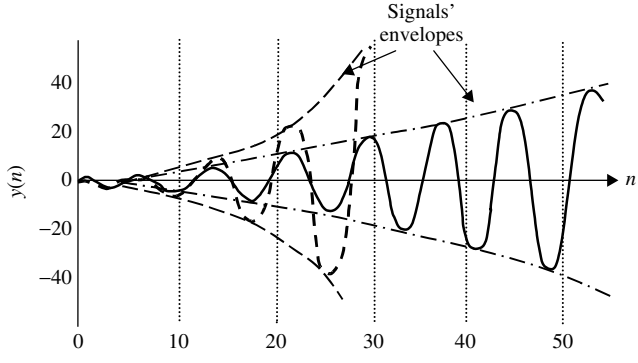

Figure 6.3 Parametric oscillation excitation

For the coefficient $a_1 = -1.41$, the oscillation excitation occurs when CS parameters correspond to the RPG axis that is described by $a_1^2 = 4a_2\cos^2(\pi/4) = 2a_2$. In this case, the eigenvalues are considerably different from 1: $\lambda_1 = -1.637$, $\lambda_2 = -0.611$.

The output process in both cases has an increasing component. The larger the absolute value of λ_1, the faster is the increase in the magnitude of oscillations. The solution normalization occurs at the beginning, but it is difficult to separate it from the background of the fast increasing component $\lambda_1^m g_1 y_1(n)$. Figure 6.3 clearly shows the interdependencies between the DPO parameters and the rate of increase of the magnitude of the output signal.

The next example shows the process of normalization of the output oscillation.

Example 6.3: Solutions Normalization

Consider a stage of solution normalization using a sinusoidal CS that is transient. For better visualization, only periodic components of $\tilde{y}(n)$ of the transitional process are shown in Figs. 6.4a, b. The periodical component $\tilde{y}(n)$ of the output process can be found from $y(n)$ by

$$\tilde{y}(n) = y(n)/\lambda_1^{n/N} \tag{6.35}$$

The modelling results are sketched in Fig. 6.4. Oscillations in the DPG have been generated by sinusoidal variation of the coefficient: $a_2(n) = 1.0 \pm 0.1\sin(\pi n/2)$. The periodic component $\tilde{y}(n)$ is shown in Fig. 6.4 for $a_1 = -1.41$, where corresponding eigenvalues $\lambda_1 = -1.1$ and $\lambda_2 = -0.92$ (Fig. 6.4a) and -1.39 (Fig. 6.4b) are represented by a solid line, and corresponding eigenvalues $\lambda_1 = -1.04$ and $\lambda_2 = -0.95$ are

represented by a dashed line. To provide a sense of scale, a periodic component of the output process is shown in these figures by a solid line after 500 periods of CS. Similar to the previous example, comparison of these results shows that the duration of the transitional process in terms of the phase normalization period is less for value $a_1 = -1.41$ than for the value $a_1 = -1.39$. It is also important to highlight that the transient refers to both amplitude and phase of normalization of the output process, when in many situations only amplitude variations are easily visible.

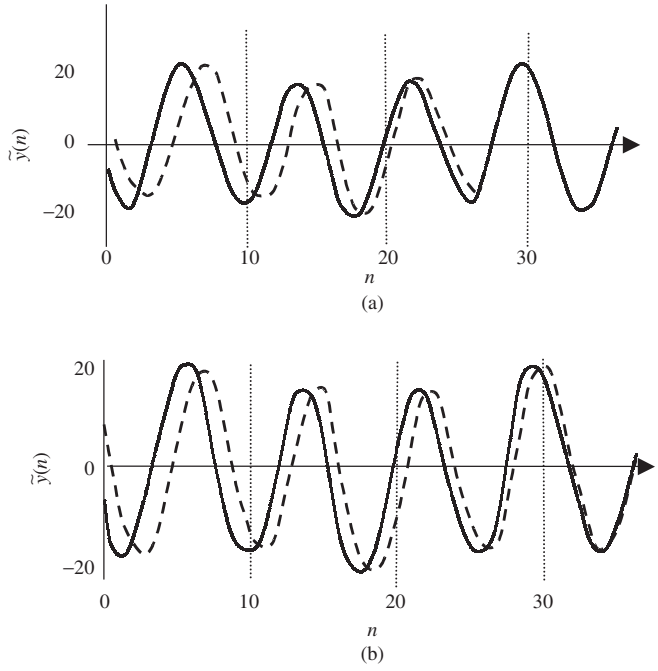

Figure 6.4 Solution normalization

Example 6.4: Comparison of Increasing and Decreasing Components

Increasing and decreasing components of a DPO output signal are sketched in Fig. 6.5a, b. In this PVDR, coefficient $a_2(n)$ varies by a sinusoidal law with $a_2(n) = 0.95 \pm 0.08 \sin(\pi n/2)$, and constant coefficient $a_1 = -1.34$ provides parametrical oscillation at the first CS sub-harmonic. Normal components $y_1(n)$ (Fig. 6.5a) and $y_2(n)$ (Fig. 6.5b) were selected from the output process. For the specified CS and DR parameters, eigenvalues are equal to $\lambda_1 = -1.01$ and $\lambda_2 = -0.85$.

To select the increasing component, the initial conditions are set at $y(0) = 1.00$ and $y(-1) = 0.578$. These ICs exclude the decreasing component. Similarly, to exclude the increasing component, ICs are set at $y(0) = 1.00$ and $y(-1) = 1.8227$. An explanation for why we can exclude one of the signal components $y_{1,2}$ by choosing particular initial conditions will be provided later. This effect is true for both continuous and digital systems, but we can easily control these values and thus exclude the transient, if necessary, only in digital systems.

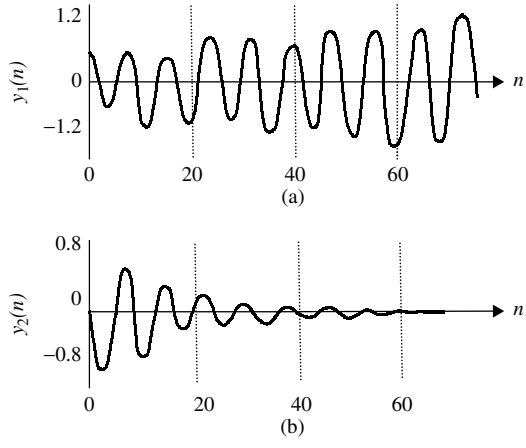

Figure 6.5 Solution components

Thus, analysis of equation (6.1) and the above examples shows that during excitation of parametrical oscillations, a DPO output process can be represented as a linear combination of the two normal increasing and decreasing components. In the general case, there is a transitional process in DPO when the mode of operation changes. After the transient, the output signal corresponds to a normal increasing component coherent with CS. The rates of component increase or decrease are determined by MM eigenvalues and the ratio between these components is specified by the initial conditions $y(0)$ and $y(-1)$.

6.3 APPROXIMATE METHOD OF EVALUATING A REGION OF PARAMETRICAL GENERATION

Stability analysis and the effect of excitation of parametric generation in PVDRs were discussed above. Basically, this is the essence of DPO operations. However, the rather tedious mathematical representations shown above sometimes mask the physical sense of a system's operation. So, let us introduce here an approximate method to determine the boundaries of regions of parametric generation. Using this approach, we can clearly demonstrate the dependence between the RPG and CS parameters. To develop the proposed approximation, we rely on the fact that the DPO output signal has an essential asymmetry in its spectrum relative to the dominating central frequency. This spectrum asymmetry is the consequence of the output signal having both amplitude and frequency (phase) modulation (AFM). The proposed method is based on the analysis of the signal spectrum.

Let us consider the sinusoidal CSs:

$$a_1(n) = a_1 + \gamma_1 \cos(2\pi n/N)$$

and

$$a_2(n) = a_2 + \gamma_2 \cos(2\pi n/N)$$

Output signal spectral components $\hat{y}_{S+2}$ and $\hat{y}_{S-2}$ are symmetrical relative to the main spectral component $\hat{y}_S$. Assuming that an output signal has AFM, we can write that

$$|\hat{y}_{S+2}| \gg |\hat{y}_{S-2}| \text{ or } |\hat{y}_{S+2}| \ll |\hat{y}_{S-2}|$$

For this case, equation (6.8) takes the form

$$\hat{y}_S = -\frac{\gamma_1 e^{-j\pi(S-2)/N} + \gamma_2 e^{-j\pi(S-2)/N}}{2(1 + a_1 e^{-j\pi S/N} + a_2 e^{-j\pi S/N})} \hat{y}_{S-2} = \delta^{(S)} \hat{y}_{S-2} \tag{6.36}$$

where $\delta^{(S)}$ is a factor connecting arbitrary spectrum components, separated by two frequency references, which are the main CS frequencies $\Omega_C = 2\pi/N$. Similar to equation (6.36), for $\hat{y}_{S-2}$ and $\hat{y}_{S-4}$ we can write

$$\hat{y}_{S-2} = \delta^{(S-2)} \hat{y}_{S-4}, \ldots, \hat{y}_{S-2n} = \delta^{(S-2n)} \hat{y}_{S-2n-2} \tag{6.37}$$

From these equations a recurrent relation can be obtained, which connects any two spectrum components separated by $2n$ frequency references:

$$\hat{y}_S = \prod_{k=0}^{n-1} \delta^{S-2k} \hat{y}_{S-2n} \tag{6.38}$$

Similarly, we can obtain relations connecting mirror spectrum components $\hat{y}_S$ and $\hat{y}_{-S}$, which will be used hereon in

$$\hat{y}_S = \prod_{k=0}^{S-1} \delta^{S-2k} \hat{y}_{-S} \tag{6.39}$$

Taking into account the property of DFT for periodic spectrums $|\hat{y}_S| = |\hat{y}_{-S}|$, we obtain the condition under which the PVDR generates periodic AFM oscillations:

$$\left| \prod_{k=0}^{S-1} \delta^{(S-2k)} \right| = 1 \tag{6.40}$$

Using equation (6.40), a boundary for the RPG could be determined. Factor δ contains all DR-CS parameters necessary for boundary determination: a_1, a_2, γ_1, γ_2 and N that corresponds to the RPG. Following are examples of such calculations.

Example 6.5: Sinusoidal Control Signal

Determine boundaries of the RPG using the approximate method for a sinusoidal CS with $a_2(n) = a_2 + 0.125 \sin(2\pi n/16)$, and constant coefficient $(\gamma_1 = 0) a_1 = -1.85$.

Figure 6.6 shows the RPG calculated using the precise method of MM root analysis (solid line) and using the approximate method (dashed line). The coincidence of these RPG boundaries demonstrates that the proposed approximation method has high accuracy, at least for system analysis at a qualitative level.

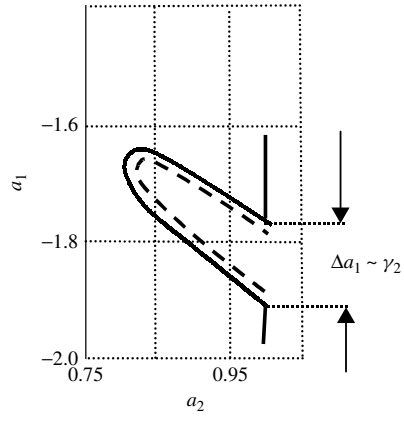

Figure 6.6 RPG for $S = 1$ and sinusoidal CS

Consider now in more detail how to use the proposed method in practice. For a parametric oscillator, it is important to estimate RPG sizes for excitation of different sub-harmonics S versus CS parameters. Let us apply the method described above to a DPO where oscillations are generated by sinusoidal variation of $a_2(n)$ with an amplitude γ_2 and period $N = 4$. Note that selection of these parameters does not limit generalization from the results obtained below.

Condition (6.40) for $S = 1$ takes the form

$$\begin{aligned} |\delta^{(1)}| &= |-\gamma_2/[2(1 + a_1 e^{-j\pi 4} + a_2 e^{-j2\pi/4})]| \\ &= \gamma_2/\{2[(1 + a_1/\sqrt{2})^2 + (a_2 + a_1/\sqrt{2})^2]^{1/2}\} = 1 \end{aligned} \tag{6.41}$$

or

$$\gamma_2^2/4 = (1 + a_1/\sqrt{2})^2 + (a_2 + a_1/\sqrt{2})^2 \tag{6.42}$$

Equation (6.42) has the solution $a_1 = -\sqrt{2} \pm \gamma_2/2$ when the average coefficient $a_2 \approx 1$, that is, the width of the RPG cross section (the size of the RPG along the a_1 axis) is $\Delta a_1 \approx \gamma_2$ (see Fig. 6.6).

This result has a very explicit physical interpretation: the size of the RPG along the a_1 axis is proportional to the magnitude of CS variation. It is also important to recall that in the discussed case, the a_1 axis, in some instances, corresponds to the frequency domain.

Consider the same method for $S = 2$ assuming the same CS-DR parameters:

$$|\delta^{(2)}||\delta^{(0)}| = \left| \frac{\gamma_2 e^{-j\pi}}{2(1 + a_1 e^{-j\pi/2} + a_2 e^{-j\pi})} \right| \cdot \left| \frac{\gamma_2}{2(1 - a_1 + a_2)} \right| = 1 \tag{6.43}$$

or

$$\frac{\gamma_2^2}{4[(1-a_2)^2+a_1^2]^{1/2}(1+a_1+a_2)}=1 \tag{6.44}$$

In the region of high Q ($a_2 \approx 1$) $a_1 = -1 \pm (1+\gamma_2^2/4)^{1/2}$, that is, the width of the region cross section is proportional to $\Delta a_1 \approx \gamma_2^2/4$ for $S = 2$.

Analysis of equation (6.40) shows that the number of factors in the product is equal to the order number of sub-harmonic S at which oscillations are generated. Each of the factors is proportional to $\gamma/2$, that is, each is directly related to the variation in CS amplitude. For the sinusoidal CS, condition (6.40) for generation of parametric oscillations takes the form

$$\left|\prod_{k=0}^{S-1}\delta^{(S-2k)}\right| = \left|B\left(\frac{\gamma}{2}\right)^S\right| = 1 \tag{6.45}$$

where factor B is determined by the system parameters and the condition $|\gamma| < 1$ is true.

Hence, as the order of the generating sub-harmonic S increases, the sizes of the appropriate RPGs exponentially decrease.

Example 6.6: Second Sub-Harmonic Generation

For a harmonic CS with $a_2(n) = a_2 + 0.125\sin(2\pi n/16)$, RPGs have been calculated for the first and second sub-harmonics (Fig. 6.7) using the approximate method (solid line) and the exact method of MM root analysis (dashed line). Similar to the previous example, comparison of these data shows relatively high (specifically for $a_2 \sim 1$) coincidence of regions and confirms the conclusion that RPG size decreases proportional to $\sim(\gamma/2)^S$.

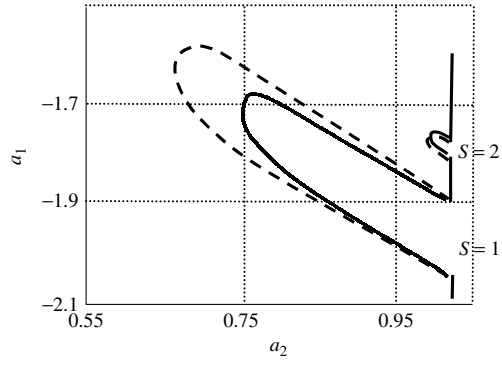

Figure 6.7 RPG for $S = 1$, 2 and sinusoidal CS

The results of approximate DPG analysis can be summarized as follows:

1. At the resonator output, quasi-harmonic oscillations coherent with the CS appear at the central frequency $\Omega_C S/2$.
2. These oscillations are modulated by phase and amplitude with the CS.

3. The size of the RPG is directly related to the amplitude of CS variation $\gamma/2$.
4. When S increases, the RPG size along a_1 in a high Q DR decreases and can be roughly estimated as $\Delta a_{1S} \approx 2(\gamma/2)^S$ for $|\gamma| < 1$.
5. Taking into account the coherent nature of the output signal, the parametric oscillator can be viewed as a frequency multiplier by the factor $S/2$ or a phase lock loop.

The RPG size along the a_1 axis is closely related to another practical parameter, the digital parametric generator synchronization band $\Delta\omega_s$. The meaning of this newly introduced parameter follows from some similarity between the phase lock loop and the parametric oscillator. Assume that the DPO is a "black box" where the CS is an input signal with central frequency ω_{in} and the output is another quasi-harmonic signal with central frequency $\omega_{\text{out}} = \omega_{\text{in}} S/2$. This is true if all the DR and CS parameters correspond to the RPG and variation of the input signal frequency $\Delta\omega_{\text{s}}$ occurs within the RPG. Outside this synchronization frequency band, the "black box" no longer generates a coherent signal. So, in some instances this synchronization band is equivalent to a pull-in range in a phase lock loop.

In the first approximation, the synchronization band of the DPO can be estimated using the RPG width Δa_{1S} as follows:

$$\begin{aligned}\Delta\omega_s &= \omega_{\max} - \omega_{\min} \\ &= 2\{\cos^{-1}[-(a_1 + \Delta a_{1S}/2)/2\sqrt{a_2}] - \cos^{-1}[-(a_1 - \Delta a_{1S}/2)/2\sqrt{a_2}]\}/S\end{aligned}$$

For the high Q DR, this equation can be simplified to

$$\Delta\omega_s = 2\{\cos^{-1}[-(a_1 + \Delta a_{1S}/2)/2] - \cos^{-1}[-(a_1 - \Delta a_{1S}/2)/2]\}/S$$

6.4 ANALYSIS OF NON-PERIODIC COMPONENTS

Now let us return to the accurate solution for equations that describe DPOs and analyse non-periodic components of the output signal. Consider the process of oscillation excitation at the stage of solution normalization. There are two comparable components in the output signal at this stage: increasing $y_1(n) = g_1\lambda_1^m \tilde{y}_1(n)$ and decreasing $y_2(n) = g_2\lambda_2^m \tilde{y}_2(n)$. They have non-periodic exponential parts as well as periodic $\tilde{y}_1(n)$ and $\tilde{y}_2(n)$ parts oscillating with the central frequency $S\Omega_C/2$. The rate of magnitude increase or decrease of these components depends on the non-periodic multipliers $g_1\lambda_1^m$ and $g_2\lambda_2^m$. These multipliers determine the duration of the transient in the DPO.

Following the traditional approach, the rate of increase in the output process $g_1\lambda_1^m$ can be characterized by a time constant $\tau_1 = l_1 T$, where T is the sampling period. The rate of increase is determined as the time interval during which its amplitude increases (or decreases) e times, that is,

$$y_1(n + l_1) = \lambda_1^{l_1/N} y_1(n) = \text{e}y(n) \tag{6.46}$$

or

$$\lambda_1^{l_1/N} = \text{e} \tag{6.47}$$

So, the time constant τ_1 of the increasing component is determined as

$$\tau_1 = l_1 T = NT/\ln|\lambda_1| \tag{6.48}$$

and the decreasing component of the output signal has the time constant

$$\tau_2 = -NT/\ln|\lambda_2| = NT/\ln|\lambda_2^{-1}| \tag{6.49}$$

For a PVDR, one of the conditions to excite oscillations is a high Q ($a_2 \to 1$), and according to equation (6.36), $\lambda_1\lambda_2 \approx 1$ or $\lambda_1 \approx 1/\lambda_2$. From comparison of equations (6.48) and (6.49) in the first approximation, we obtain

$$\tau \approx \tau_1 \approx \tau_2 = NT/\ln|\lambda_1| \approx NT/\ln|\lambda_2^{-1}| \tag{6.50}$$

The next examples illustrate the qualitative dependence of the time constant τ on DPO parameters.

Example 6.7: Region of Parametric Generation versus Control Signal Amplitude

Consider a DPO where the sinusoidal CS excites oscillations

$$a_2(n) = a_2 + \gamma_2 \cos(2\pi n/8)$$

The RPGs calculated for three values of γ_2, corresponding to $S = 1$, are shown in Fig. 6.8, where the solid line corresponds to $\gamma_2 = 0.25$, the dashed line corresponds to $\gamma_2 = 0.125$, and the dashed-dotted line corresponds to $\gamma_2 = 0.0625$.

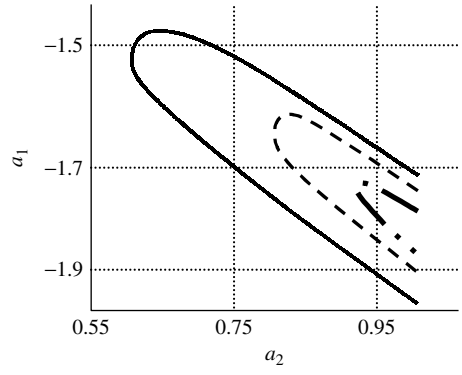

Figure 6.8 RPG for $S = 1$ and sinusoidal CS

Using equations (6.48) and (6.49), the time constants $\tau_{1,2}$ have been calculated inside these regions for different combinations of parameters a_1, a_2, γ_2 and shown in Fig. 6.9. The key to this figure is shown in Table 6.1.

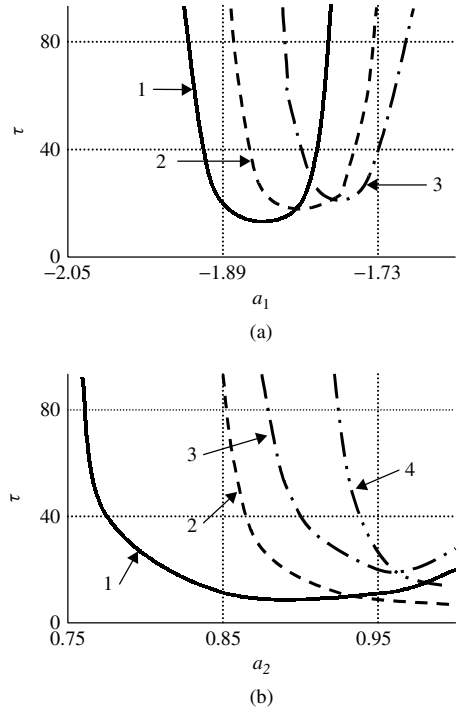

Figure 6.9 Time constant dependence on DPG parameters

Table 6.1 DPO Parameters for Fig. 6.9

Curve nos.	a_1	a_2	γ_2	Figure nos.
1	–	1.0	0.125	–
2	–	0.96	0.125	6.9a
3	–	0.92	0.125	–
1	−1.76	–	0.25	–
2	−1.86	–	0.25	6.9b
3	−1.8	–	0.125	–
4	−1.83	–	0.125	–

Figure 6.9a illustrates that τ depends to a large extent on DPO parameters. This is a predictable result as the time constants depend on the eigenvalues $\lambda_{1,2}$, which are specified by the same parameters of the system. The time constant has a minimum value at the axis of the RPG, where there are best conditions for oscillation excitation. The time constant sharply increases when the parameters approach the RPG boundary, where modules of the eigenvalues are close to 1.

Dependence of τ on a_2 is shown in Fig. 6.9b. Curve 2 corresponds to the monotone τ decreasing while a_2 increases, which does not contradict results given above. Curve 1 has an extreme corresponding to the location of the RPG axis $S = 1$ for its cross section

$a_1 = -1.76$. Curve 3 has an extreme where it crosses the RPG axis, while curve 4 does not have an extreme, since the cross section $a_1 = -1.83$ is below this axis (Fig. 6.8).

Time constants τ_1 and τ_2 determine the duration of the transient in a DPO. One of the possible criteria for determination of the transient period is that the difference between the increasing and decreasing components is much more than 1 and the decreasing component can be neglected.

Denote $h_{TP}(n)$ as the ratio of the magnitude of the increasing component to the magnitude of the decreasing component and introduce the following parameter:

$$h_{TP}(n) = \frac{g_1 \exp(n/\tau_1)}{g_2 \exp(-n/\tau_2)} = g_1 g_2^{-1} \exp[(\tau_1 + \tau_2)n/\tau_1\tau_2] \approx$$
$$\text{or} \quad h_{TP}(n) \approx g_1 g_2 \exp(2n/\tau) \quad \text{for} \quad a_2 \to 1 \tag{6.51}$$

Let the criterion for completion of a transient period be that one component exceeds the other by the given ratio h_{TPO}. Then, for known $g_{1,2}$, it is possible to determine the time of completion of the transient period $T_{tr} = l_{tr}T$:

$$l_{tr} = \ln(h_{TP0}\, g_2/g_1)\tau_1\tau_2/(\tau_1 + \tau_2) \tag{6.52}$$

The absolute value for h_{TP0} can be specified for any particular application. As an example, consider a digital system operating with L bits fixed-point arithmetic. The criterion for completion of the transient period can be reduction of the decreasing component $g_2 \exp(-n/\tau_2)$ below the level of the lowest bit 2^{-L}, which means that the condition of the completion of the transient period is

$$|g_2 \exp(-n/\tau_2)| \le 2^{-L} \tag{6.53}$$

The time of completion can be determined as

$$l_{tr} = -\tau_2 \ln(2^{-L}/|g_2|) \tag{6.54}$$

Equations (6.52) and (6.54) show that the duration of the transient period depends not only on time constant τ but also on the relation between components $y_1(n)$ and $y_2(n)$ at the moment $n = 0$. This relation is determined by the initial conditions.

Thus, the behaviour of non-periodic oscillation components can be described using two time constants $\tau_{1,2}$. The value of τ depends on its location within the RPG, reaching a minimum at its axis and increasing as it approaches the RPG boundaries.

6.5 ANALYSIS OF THE PERIODIC COMPONENTS

In the previous section, the non-periodic increasing and decreasing components $g_1\lambda_1^m$ and $g_2\lambda_2^m$ were investigated. They determine the output signal envelope and its dynamic in a DPO operating in the non-limited mode. Let us now consider the spectrum of the periodic components $\tilde{y}_1(n)$ and $\tilde{y}_2(n)$ of this signal.

First, we will study the behaviour of the output periodical component during the transient period. It is important to recall that the transient affects not only the signal

envelope but also the signal phase. We defined the transient period as the time when the decreasing solution component cannot be neglected. In the non-limiting mode of DPO operation, equation (6.1) has non-periodic solutions, which does not allow the use of the DFT algorithm directly to determine spectrum characteristics of the output signal $y(n)$. However, DFT can be used for analysis of the periodic components of this process. For the increasing component $g_1 \exp(n/\tau)\tilde{y}_1(n)$, an appropriate equation to describe the DPO has the form

$$g_1 e^{n/\tau}\tilde{y}_1(n) + a_1(n) g_1 e^{(n-1)/\tau}\tilde{y}_1(n-1) + a_2(n) g_1 e^{(n-2)/\tau}\tilde{y}_1(n-2) = 0 \qquad (6.55)$$

or

$$\tilde{y}_1(n) + a_1(n) e^{-1/\tau}\tilde{y}_1(n-1) + a_2(n) e^{-2/\tau}\tilde{y}_1(n-2) = 0 \qquad (6.56)$$

Denoting

$$\begin{cases} a_1'(n) = a_1(n) e^{-1/\tau} \\ a_2'(n) = a_2(n) e^{-2/\tau} \end{cases} \qquad (6.57)$$

we obtain a difference equation of the second order relative to the periodic component $\tilde{y}_1(n)$:

$$\tilde{y}_1(n) + a_1'(n)\tilde{y}_1(n-1) + a_2'(n)\tilde{y}_1(n-2) = 0 \qquad (6.58)$$

To determine the spectrum of $\tilde{y}_1(n)$, we use the results of DFT application to a similar equation (6.1). So, for the harmonic CS variation,

$$\begin{cases} a_1'(n) = a_1' + \gamma_1' \cos(2\pi n/N) \\ a_2'(n) = a_2' + \gamma_2' \cos(2\pi n/N) \end{cases} \qquad (6.59)$$

we obtain relations between spectrum components for the output signal, which is an amplitude–frequency modulated narrowband process:

$$\hat{y}_{1(S)} = -\frac{\gamma_1' e^{-j\pi(S\pm 2)/N} + \gamma_2' e^{-j\pi 2(S\pm 2)/N}}{2(1 + a_1' e^{-j\pi S/N} + a_2' e^{-j2\pi S/N})}\hat{y}_{1(S\pm 2)} \qquad (6.60)$$

Note that condition (6.9) for excitation of quasi-harmonic parametric oscillations is that the resonance frequency of the DR approximately equals $\omega_{\text{res}} \approx S\Omega_C/2$. This provides the condition $|\hat{y}_S| \gg |\hat{y}_{S+2}|$ because the denominator is approaching zero. Although in equation (6.60) $a_1' \neq a_1$ and $a_2' \neq a_2$, the condition $|\hat{y}_S| \gg |\hat{y}_{S+2}|$ is still satisfied, as

$$\omega_{\text{res}}' = \omega_{\text{res}}$$

and

$$\omega_{\text{res}}' = \cos^{-1}\left(-a_1'/2\sqrt{a_2'}\right) = \cos^{-1}(-a_1 \exp(-1/\tau)/\{2[a_2 \exp(-2/\tau)]^{1/2}\})$$
$$= \cos^{-1}(-a_1/2\sqrt{a_2})$$

Division of the frequency by a factor 2 is feasible for the harmonic CS in the RPG corresponding to $S = 1$ where condition $|\hat{y}_S| = |\hat{y}_{S+2}|$ is true. The reason for this is that these spectral components are the mirror constituents. Hence, the spectrum is determined by the ratio of harmonic $\hat{y}_{1(S+2)} = \hat{y}_{13}$ to the main harmonic $\hat{y}_{1S} = \hat{y}_{11}$:

$$\hat{y}_{11} = -\frac{\gamma_1' e^{-j3\pi/N} + \gamma_2' e^{-j6\pi/N}}{2(1 + a_1' e^{-j\pi/N} + a_2' e^{-j2\pi/N})} \hat{y}_{13} \tag{6.61}$$

From this equation the level of the modulation component $\hat{y}_{13}$ can be evaluated:

$$|\hat{y}_{11}| = -\left| \frac{\gamma_1' e^{-j3\pi/N} + \gamma_2' e^{-j6\pi/N}}{2(1 + a_1' e^{-j\pi/N} + a_2' e^{-j2\pi/N})} \right| \cdot |\hat{y}_{13}| \tag{6.62}$$

Using the same approach, we can obtain an expression for the spectrum of the periodic decreasing component $\tilde{y}_2(n)$:

$$|\hat{y}_{21}| = -\left| \frac{\gamma_1'' e^{-j3\pi/N} + \gamma_2' e^{-j6\pi/N}}{2(1 + a_1' e^{-j\pi/N} + a_2' e^{-j2\pi/N})} \right| \cdot |\hat{y}_{23}| \tag{6.63}$$

where $\gamma_1'' = \gamma_1 e^{1/\tau_2}$, $\gamma_2'' = \gamma_2 e^{2/\tau_2}$, $a_1'' = a_1 e^{1/\tau_2}$, $a_2'' = a_2 e^{2/\tau_2}$. So, the equations introduced above specify the spectrum components of the periodical constituent of the DPO output signal.

It is also helpful to know the phase relations between the CS and the output oscillations $y(n)$. After completion of the transient period, $y(n)$ contains only a normal increasing component $y_1(n) = g_1 \lambda_1^m \tilde{y}_1(n)$, with the main spectrum components of the periodical signal $\tilde{y}_{CP}(n) \approx A \sin(S\overline{\Omega}_C n/2 + \varphi)$. From here,

$$y(n) \approx g_1 A \lambda_1^{n/N} \sin(S\overline{\Omega}_C n/2 + \varphi) \tag{6.64}$$

Taking into account equation (6.26), which connects two adjacent references of the normal increasing component, we obtain

$$g_1 A \lambda_1^{n/N} \sin(S\overline{\Omega}_C n/2 + \varphi) = -g_1 \lambda_1^{(n-1)/N} \sin(S\overline{\Omega}_C n/2 + \varphi) \frac{C_{12} - C_{22} + \lambda_1}{C_{21} + C_{11} - \lambda_1} \tag{6.65}$$

or

$$\begin{aligned} \sin(S\overline{\Omega}_C n/2)\cos\varphi + \cos(S\overline{\Omega}_C n/2)\sin\varphi = -\frac{C_{12} - C_{22} + \lambda_1}{C_{21} + C_{11} - \lambda_1} \lambda_1^{-1/N} \\ \times \{\sin[S\overline{\Omega}_C (n-1)/2]\cos\varphi + \cos[S\overline{\Omega}_C (n-1)/2]\sin\varphi\} \end{aligned} \tag{6.66}$$

From this equation, an initial phase φ of the output periodic component relative to the CS can be determined:

$$\varphi = \tan^{-1}\left\{\frac{\sin(S\overline{\Omega}_C n/2) + \lambda_1^{-1/N}\sin[S\overline{\Omega}_C(n-1)/2]\dfrac{C_{12}-C_{22}+\lambda_1}{C_{21}+C_{11}-\lambda_1}}{\cos(S\overline{\Omega}_C n/2) + \lambda_1^{-1/N}\cos[S\overline{\Omega}_C(n-1)/2]\dfrac{C_{12}-C_{22}+\lambda_1}{C_{21}+C_{11}-\lambda_1}}\right\} \tag{6.67}$$

Expression (6.67) is correct for any time moment n. For simplicity, assume that $n = 0$:

$$\begin{aligned}\varphi &= \tan^{-1}\left\{\frac{\lambda_1^{-1/N}\sin[S\overline{\Omega}_C(n-1)/2]\dfrac{C_{12}-C_{22}+\lambda_1}{C_{21}+C_{11}-\lambda_1}}{1+\lambda_1^{-1/N}\cos[S\overline{\Omega}_C(n-1)/2]\dfrac{C_{12}-C_{22}+\lambda_1}{C_{21}+C_{11}-\lambda_1}}\right\} \\ &= \tan^{-1}\left\{\frac{-\lambda_1^{-1/N}\sin[S\overline{\Omega}_C/2](C_{12}-C_{22}+\lambda_1)}{C_{21}+C_{11}-\lambda_1+\lambda_2^{-1/N}(C_{12}-C_{22}+\lambda_1)\cos[S\overline{\Omega}_C/2]}\right\}\end{aligned} \tag{6.68}$$

Thus, the initial phase of the output process in a non-limiting mode is determined by the CS and the DR. Note that equation (6.1) accepts two opposite phase solutions for one CS. This is consistent with the conclusion above that the main source of oscillations is a halving of the CS frequency.

We can now study the generating signal spectrum by applying the analytical approach developed above in some examples.

Example 6.8: Spectrum of the Output Signal of a Digital Parametric Oscillator

Let us study the output signal spectrum for the case of the sinusoidal CS $a_2(n) = 0.96 + \gamma_2\cos(2\pi n/N)$. Consider the relation between dominant output spectral component (y_{11}) and side (modulation) components (y_{13}) of this signal for different values a_1 and γ_2. The results calculated according to equation (6.63) and obtained by computer modelling of the ratios y_{13}/y_{11} are shown in Fig. 6.10. The calculated results are introduced by dashed

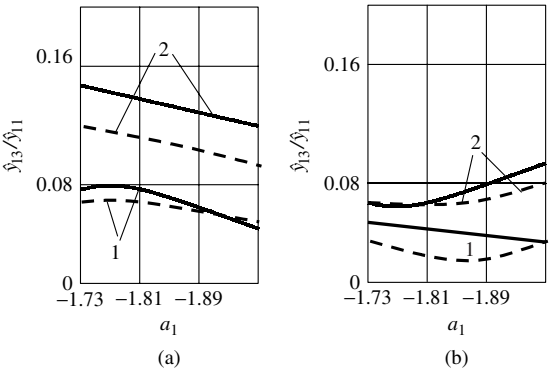

Figure 6.10 Level of modulation components

lines in Fig. 6.10a for $N = 4$ and Fig. 6.10b for $N = 8$, where $\gamma_2 = 0.125$ is represented by curve 1 and $\gamma_2 = 0.25$ by curve 2. In the same figures, the solid line shows the level of the modulation components obtained by computer modelling. Analysis of these graphs confirms the consistency between the analytical estimation and the modelling.

Example 6.9: Relative Phase of the Output Signal

Consider now the phase relationships in a DPO. Appropriate values of the phase φ have been calculated using equation (6.68) and by computer modelling for the RPG when $S = 1$ and the harmonic CS $a_2(n) = 0.96 + 0.125\sin(2\pi n/8)$. The dependence of the calculated value (dashed line) and the computer-modelled value (solid line) on a_1 is shown in Fig. 6.11.

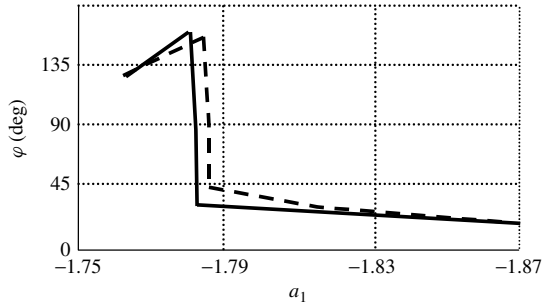

Figure 6.11 Relative phase of the output signal

A sharp variation in the initial phase can be seen near the centre of the RPG ($a_1 \approx -1.78$), which is the resonance frequency. This coincides with the behaviour of the phase characteristic of the DR.

6.6 WIDEBAND CONTROL SIGNAL

In the previous section, we discussed DPOs with sinusoidal control signal. Let us now consider the case when a CS spectrum has more than one harmonic and, in particular, the case of a DPO with binary variation of coefficients. This has both theoretical and practical significance. A DPO with a sinusoidal CS could, theoretically, generate signals with any central frequency $S\Omega_C/2$. But the condition for excitation of oscillations becomes tougher with the increase of the sub-harmonic number S. In some instances, the sub-harmonic number has a practical limit that can be estimated as $S = 3 - 6$. Actually, this figure is no more than a rule of thumb. When the DPO is used for frequency synthesis, instead of using a sinusoidal CS with high S, one of the binary CS harmonics can be used for signal excitation. Before we study this problem it is important to recall once again that relative to the CS, a parametric oscillator is an essentially non-linear system. This introduces a limitation to the use of non-sinusoidal CSs in a DPO: regions of parametric generation determined by different CS spectral components should not overlap. The situation when two or more spectral harmonics initiate parametric oscillations at the same time is outside the scope of this book.

Consider the excitation of parametric oscillations by binary variation of the coefficients, which can be represented via the Fourier series expansion (6.2). Assume that the system operates at the RPG boundary and, consequently, the output signal has a constant envelope. For this case, the equation connecting output signal spectrum (6.7) in a matrix form is

$$\begin{bmatrix} \hat{y}_S \\ \hat{y}_{S-2} \\ \dots \\ \hat{y}_{S-2M} \end{bmatrix} = \begin{bmatrix} \delta_1(S) & \delta_2(S) & \dots & \delta_M(S) \\ 1 & 0 & \dots & 0 \\ \dots & \dots & \dots & \dots \\ 0 & 0 & \dots & 0 \end{bmatrix} \cdot \begin{bmatrix} \hat{y}_{S-2} \\ \hat{y}_{S-4} \\ \dots \\ \hat{y}_{S-2M-2} \end{bmatrix} \tag{6.69}$$

where

$$\delta_m^{(S)} = \frac{-\gamma_1\alpha_{1m}\mathrm{e}^{-\mathrm{j}\pi(S-2m)/N} - \gamma_2\alpha_{2m}\mathrm{e}^{-\mathrm{j}2\pi(S-2m)/N}}{2(1 + a_1\mathrm{e}^{-\mathrm{j}\pi S/N} + a_2\mathrm{e}^{-\mathrm{j}2\pi S/N})}\hat{y}_{13} \tag{6.70}$$

are coefficients connecting components $\hat{y}_S$ and $\hat{y}_{S\pm2m}$ for an AFM output signal. Or,

$$[\hat{Y}^{(S)}] = [A^{(S)}][\hat{Y}^{(S-2)}] \tag{6.71}$$

where $[\hat{Y}^{(S)}]$ is a column matrix containing M frequency samples, $y(n)$; $[\hat{Y}^{(S-2)}]$ is a column matrix, shifted on two frequency samples relative to the matrix $[\hat{Y}^{(S)}]$; and $[A^{(S)}]$ is a square $M \times M$ matrix, connecting column matrixes $[\hat{Y}^{(S)}]$, separated by two frequency samples. In addition, similar to the sinusoidal CS ($M = 1$) case, we obtain the recurrent relation

$$[\hat{Y}^{(S)}] = \prod_{k=0}^{S-n}[A^{(S-2k)}][\hat{Y}^{(S)}] = [C(S, -S][\hat{Y}^{(-S)}] \tag{6.72}$$

Now, we should take into account the periodicity of the DFT ($|\hat{Y}_S| = |\hat{Y}_{-S}|$) and the quasi-harmonic (narrowband) nature of excited oscillations ($|\hat{Y}_S| \gg |\hat{Y}_{S\pm2m}|$). For these obvious conditions, it is sufficient to consider only the first elements in vectors and we can write the following approximate equation:

$$|C_{11}(S_1, -S)| \approx 1 \tag{6.73}$$

where $|C_{11}(S_1, -S)|$ is the first element of the matrix $[C(S, -S)] = \prod_{k=0}^{S-1}[A^{(S-2k)}]$.

Let us study the results in the next example.

Example 6.10: **Bi-Frequency Control Signal**

Let us determine the conditions for excitation of parametric oscillations for a CS that contains only the first $\Omega_1 = 2\pi n/N$ and the third $\Omega_3 = 3\Omega_1 = 6\pi n/N$ harmonics in its spectrum: $a_2(n) = a_2 + \alpha_{21}\cos(2\pi n/N) + \alpha_{23}\cos(6\pi n/N)$

1. To excite oscillations at the frequency of the first CS sub-harmonic π/N ($S_1 = 1$), determine the matrix

$$[C(1,-1)] = [A^{(1)}] = \begin{bmatrix} \delta_1^{(1)} & 0 & \delta_3^{(1)} \\ 1 & 0 & 0 \\ 0 & 1 & 0 \end{bmatrix} \tag{6.74}$$

Condition (6.73) in this case takes the form

$$|C(1,-1)| = |A^{(1)}||\delta_1^{(1)}| = 1 \tag{6.75}$$

that is, parametrical generation at the first sub-harmonic is a result of the halving of the first harmonic frequency $2\pi/N$.

2. Similarly, for RPG $S_1 = 2$, we obtain

$$[C(2,-2)] = [A^{(2)}][A^{(0)}] = \begin{bmatrix} \delta_1^{(2)} & 0 & \delta_3^{(2)} \\ 1 & 0 & 0 \\ 0 & 1 & 0 \end{bmatrix} \begin{bmatrix} \delta_1^{(0)} & 0 & \delta_3^{(0)} \\ 1 & 0 & 0 \\ 0 & 1 & 0 \end{bmatrix}$$
$$= \begin{bmatrix} \delta_1^{(2)}\delta_1^{(0)} & \delta_3^{(0)} & \delta_3^{(2)}\delta_3^{(0)} \\ \delta_1^{(0)} & 0 & \delta_3^{(0)} \\ 1 & 0 & 0 \end{bmatrix} \tag{6.76}$$

Condition (6.73) $|C_{11}(\lambda,-\lambda)| = |\delta_1^{(2)}\delta_1^{(0)}| = 1$ shows that oscillations at the CS frequency are determined by the first harmonic, and the size of the RPG is proportional to $\alpha_{21}^2/4$. A similar result was obtained when harmonic CSs were discussed.

3. The conditions for oscillation excitation at the third sub-harmonic can be determined using the same method. We should take into account that two mechanisms of oscillation excitation are competing at the third sub-harmonic ($3/2N$): the third sub-harmonic of Ω_1 or $S_1 = 3$ and the first sub-harmonic of Ω_3 or $S_3 = 1$, as they are equal to each other. Thus,

$$[C(3,-3)] = \begin{bmatrix} \delta_1^{(3)}\delta_1^{(1)}\delta_1^{(-1)} + \delta_3^{(3)} & \delta_3^{(1)}\delta_1^{(3)} & \delta_1^{(3)}\delta_1^{(-1)}\delta_3^{(-1)} \\ \delta_1^{(1)}\delta_1^{(-1)} & \delta_3^{(1)} & \delta_1^{(1)}\delta_3^{(-1)} \\ \delta_1^{(-1)} & 0 & \delta_3^{(-1)} \end{bmatrix} \tag{6.77}$$

and

$$|C_{11}(3,-3)| = |\delta_1^{(3)}\delta_1^{(1)}\delta_1^{(-1)} + \delta_3^{(3)}| = 1 \tag{6.78}$$

In equation (6.78), the term $\delta_1^{(3)}\delta_1^{(1)}\delta_1^{(-1)}$ reflects the multiplication of the first harmonic while $\delta_3^{(3)}$ reflects the division of the third harmonic. For the case under consideration here, when $|\gamma_2| < 1$ it is obvious that $|\delta_1^{(3)}\delta_1^{(1)}\delta_1^{(-1)}| \ll |\delta_3^{(3)}|$, and condition (6.78) takes the form $|\delta_3^{(3)}| = 1$, that is, in this case dominates halving of the third harmonic frequency or $S_3 = 1$. This result is easily predictable from our previous study.

From the example, we can draw this important conclusion: in the general case, the *main* mechanism of oscillation excitation is a halving of the corresponding harmonic in the broadband (multi-frequency) CS spectrum.

The dependence between the amplitude of the CS spectral components and the size of RPGs is sketched in Fig. 6.12.

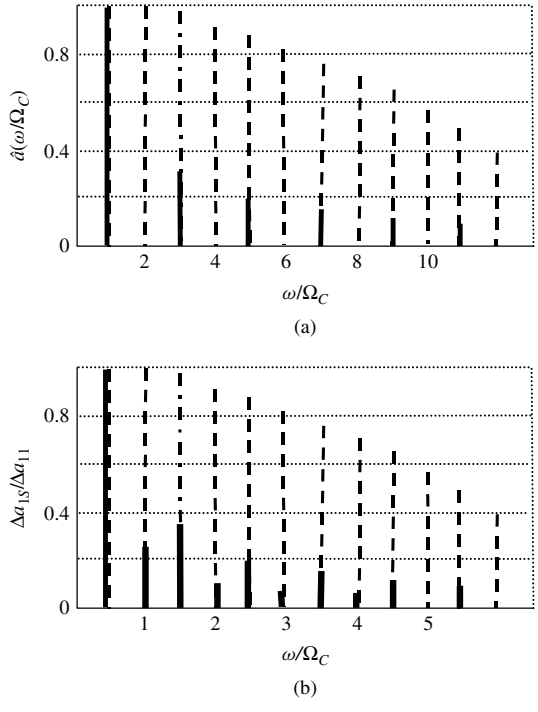

Figure 6.12 Relations between CS and RPG

The solid line in Fig. 6.12a shows an amplitude spectrum $\hat{a}(\omega/\Omega_C)$ of a binary CS with $N = 32$ and $q = 2$, containing only odd harmonics, which decrease with the harmonic number. The dashed line in Fig. 6.12a shows a spectrum of the CS with $N = 32$ and $q = 16$, which contains both odd and even harmonics. The spectrum components for narrowband ($q = 2$) and wideband ($q = 16$) CSs are normalized according to the level of the first frequency component of the spectrum.

Figure 6.12b shows the results of RPG calculations using the method of MM eigenvalues analysis. The vertical axis corresponds to the width of the RPG cross section Δa_{1S} along a_1 (for a given a_2), normalized relative to the widest region of parametric generation Δa_{11} that corresponds to $S_1 = 1$. So, Fig. 6.12b introduces parameter $\Delta a_{1S}/\Delta a_{11}$ depending on the sub-harmonic order number at which oscillations occur. For a narrowband CS (solid line), the RPGs are considerably larger for odd S than for even S. For a wideband CS (dashed line), the dependence of the size of RPGs on sub-harmonic number repeats the case for the CS spectrum. There is parametric resonance for both odd and even sub-harmonic numbers S.

These data support the conclusions drawn from the approximate method of boundary estimation: the basic mechanism of oscillation excitation is halving of the harmonic frequency of the CS and the size of the parametric generation region is proportional to the amplitude of these harmonics.

Thus, the approximate method outlined above yields boundary estimations that correspond to physically observed results, which once again highlights the parametric nature of the output oscillations. These parametric oscillations occur in two cases: (i) when one of the CS frequency components is halved ($S_i = 1$) and (ii) when CS spectrum components are multiplied ($S_i > 1$). However, the dominating factor is the mechanism of the halving of the harmonic components in the broadband CS spectrum. The size of RPGs in terms of CS main frequency $\Delta\omega_C$ for high Q resonators, that is, $a_2 \approx 1$ can be approximately estimated using an amplitude of the corresponding CS spectrum harmonic.

6.7 PERIODIC COMPONENTS SPECTRUM

As discussed above, in the general case a sinusoidal CS with frequency Ω_C can initiate parametric oscillations with a central frequency $\Omega_C S_1/2$. At the same time, parametric oscillations with the same central frequency $\Omega_C S_1/2$ could be initiated by the ith harmonic of a binary CS or $\Omega_C S_i/2 = \Omega_C S_1/2$. What will be the main difference in the output signal spectrum for these two cases? In this section, we will show that the difference is in the spectrum of the output signal. When a sinusoidal CS is used, the output process is modulated by only one CS harmonic. For the non-sinusoidal CS, in particular the binary CS, the output process is modulated by the multi-harmonic CS's spectrum.

Expressions for the periodical component of the DPO output spectrum were obtained earlier for a harmonic CS. These results can be expanded to describe output signal spectrums for the non-harmonic CS case. The most practically interesting case is when the CS is a binary (pulse) signal. Such a waveform can be represented as a Fourier series expansion. Applying DFT to equation (6.58), we obtain an expression in the matrix form, connecting the spectrum components $\hat{y}_{1S}$ of the output signal periodical components:

$$\begin{bmatrix} \hat{y}_S \\ \hat{y}_{S-2} \\ \dots \\ \hat{y}_{S-2M} \end{bmatrix} = \begin{bmatrix} \delta'_1(S) & \delta'_2(S) & \dots & \delta'_M(S) \\ 1 & 0 & \dots & 0 \\ \dots & \dots & \dots & \dots \\ 0 & 0 & \dots & 0 \end{bmatrix} \cdot \begin{bmatrix} \hat{y}_{S-2} \\ \hat{y}_{S-4} \\ \dots \\ \hat{y}_{S-2M-2} \end{bmatrix} \tag{6.79}$$

where

$$\delta_m^{(S)} = -\frac{\gamma'_1 \alpha_{1m} \mathrm{e}^{-\mathrm{j}\pi(S-2m)/N} - \gamma'_2 \alpha_{2m} \mathrm{e}^{-\mathrm{j}2\pi(S-2m)/N}}{2(1 + a'_1 \mathrm{e}^{-\mathrm{j}\pi S/N} + a'_2 \mathrm{e}^{-\mathrm{j}2\pi S/N})} \tag{6.80}$$

are coefficients, connecting components $\hat{y}_{1(S)}$ and $\hat{y}_{1(S+2M)}$ of the AFM output signal spectrum. In equation (6.80), the following notations are used: $a'_1 = a_1 e^{-1/\tau}$, $a'_2 = a_2 e^{-2/\tau}$, $\gamma'_1 = \gamma_1 e^{-1/\tau}$ and $\gamma'_2 = \gamma_2 e^{-2/\tau}$. Similar results can be obtained for a spectrum of the periodic decreasing component.

From equation (6.80), it follows that the spectrum of the output periodical component for a binary CS contains not only the main component at the frequency of generation $S\Omega_C/2$ but also the modulation components. Levels of these spectral

components are determined by the CS-DR parameters. The time constant does not essentially influence the spectrum qualitatively, and leads only to some quantitative changes.

Results of this small section on periodic components qualitatively fully coincide with those obtained earlier. This confirms that for any CS waveform the DPO output process contains the main central spectral component and any CS spectral components up-converted to this central frequency.

6.8 THE TRANSIENT IN DIGITAL PARAMETRIC OSCILLATORS

We considered output signal spectrums in DPOs with multi-frequency CSs and indicated that this mode is prospective when a DPO is used for a frequency multiplication. The other important parameter is the duration of the transient period, as any variations of CS and/or DR parameters cause a transient to occur.

The time constant of the decreasing component specifies the transient in a DPO. When higher-order sub-harmonics are generated, the physical mechanism behind the process remains the same and differs mainly at a qualitative level. So, using the accurate mathematical analysis and modelling introduced in this chapter, we will investigate the transient for a DPO operating in a frequency multiplying mode by the following set of examples. You will see that the example results are consistent with the theory that the major mechanism of excitation of parametric oscillations is the halving of one of the CS spectrum harmonics. The time constant depends on this particular harmonic amplitude and the DPO parameters that specify the RPG.

Example 6.11: Frequency Multiplier, $S_3 = 1$

Time constants $\tau_{1,2}$ were calculated for the DPO governed by the binary CS with $N = 16$ and $q = 2$ in a sub-harmonic generation mode ($S_3 = 1$). Results of the calculations are sketched in Fig. 6.13 and the keys to the figure are mentioned in Table 6.2.

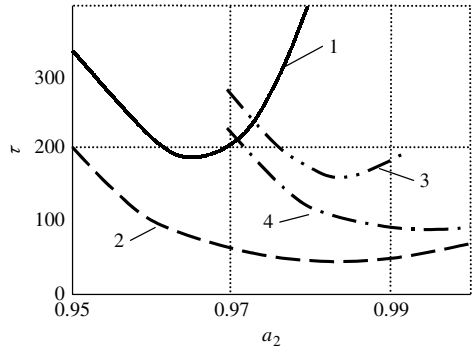

Figure 6.13 The time constant versus DPO parameters

Table 6.2 DPO Parameters for Fig. 6.13

Curve nos.	a_1	γ_2
1	−1.34	0.25
2	−1.36	0.25
3	−1.38	0.125
4	−1.39	0.125

Curves 1 and 2 show the dependence of $\tau_{1,2}$ on coefficient a_2 for $\gamma_2 = 0.25$ and $a_1 = -1.34$ and -1.36 respectively. The time constant dependence on DPO parameters a_1 and a_2 in RPG $S_3 = 1$ is similar to the curve for $S_1 = 1$ (see Fig. 6.9), but the values of $\tau_{1,2}$ are considerably higher.

Example 6.12: High Multiple Harmonic Generations

Figure 6.14 shows the dependence of the DPO's time constant on the sub-harmonic i number (assuming that $S_i = 1$). It was considered for a binary CS $a_2 = 1 \pm 0.25$ with $N = 512$ and $q = 256$ for $i = 8 - 128$, where these time constants have the minimum values within appropriate RPGs. The results reflect the fact that the time constants, with other conditions equal, are inversely proportional to the CS amplitude. Higher generating sub-harmonics i are excited by the CS harmonics with smaller amplitudes.

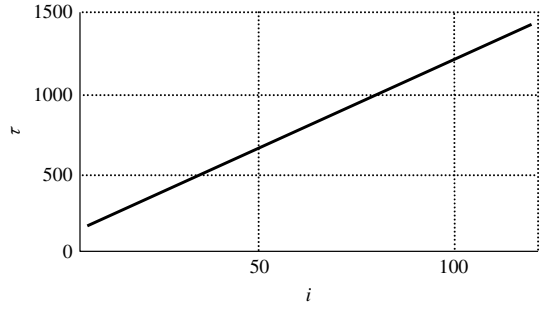

Figure 6.14 The time constant versus the sub-harmonic number

The absolute duration of the transient period depends on the time constant τ itself and also on the DPO's initial conditions regardless of the cause of the appearance of the transient. Examples of causes of a transient include switching the system on, a phase shift in the CS, and the DPO switching to another sub-harmonic generation mode.

Example 6.13: Transient versus Initial Conditions

Oscillations were excited in a DPO with different ICs at the third sub-harmonic $S_3 = 1$ by a binary coefficient variation $a_2(n) = 1.03 \pm 0.125$ with $q = 2$ and $N = 12$. The phase delay relevant to the steady-state oscillations versus the time instants n is shown in Fig. 6.15.

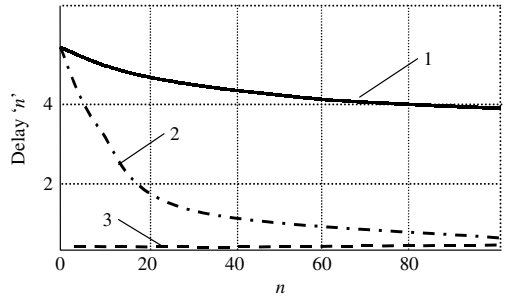

Figure 6.15 Phase delay due to the transient

The delay of the output oscillations is shown in Fig. 6.15 by curve 1 for ICs $y(0) = 2.936$, and $y(-1) = 2.234$, by curve 2 for $y(0) = -0.252$, $y(-1) = -1.657$, and by curve 3 for $y(0) = -1.657$, $y(-1) = -2.292$. These three curves clearly show that the duration of the transient essentially depends on the ICs.

The absence of the transient for case 3 can be easily explained by the fact that ICs $y(0) = -1.657$, $y(-1) = -2.292$ correspond to the system engine vector. In the general case, to reduce or exclude the transient in a DPO we can exploit the fact discussed above that the duration of the transient depends not only on the time constant but also on the initial conditions. This is clearly seen from equation (6.16). The relation between increasing and decreasing components depends not only on eigenvalues of MM (equation (6.1)) but also on the constants g_1 and g_2 (equation (6.16)), which are determined by the ICs $y(0)$ and $y(-1)$. In contrast with ICs for analog parametric circuits, the ICs in this case can be easily corrected, if necessary, by writing appropriate words in the DR registers.

The transient can be fully prevented if the eigenvector of the MM is chosen as the ICs. From matrix theory it is known that the eigenvector is mapped by the matrix onto another vector, which takes the same (or opposite) position in the space but is λ times longer [24]. Thus, if the MM eigenvector is selected as the ICs, then one of the solutions is equal to zero (g_1 or g_2 is equal to zero).

Thus, to prevent the transient, the second term in equation (6.16) should equal zero. In this case, $y(n) = y_1(n)$, when $y(0)$ and $y(-1)$ are determined from equation (6.26):

$$y(0) = [-(C_{12} - C_{22} + \lambda_1)/(C_{21} + C_{11} - \lambda_1)]y(-1) \tag{6.81}$$

From the technical point of view, the structure of an oscillator with controllable ICs has to contain a subsystem that simultaneously provides DPO parameter variation and writes down values for $y(n)$ and $y(n-1)$ equal to the MM eigenvector in the oscillator registers. This is a technically feasible way to develop, for example, a frequency synthesizer without a transient during frequency hopping.

6.9 SUMMARY

Analysis of periodically linear time-varying digital systems identified some specific instability areas in the parameter domain of high Q digital resonators, which

are known as regions of parametric generation. In terms of frequency, these areas correspond to the sub-harmonics of the CS spectral components. The system behaviour in these instability areas corresponds to parametric oscillation generation mode. A digital PF in this mode can be viewed as a DPO, which can be used for signal generation and processing in various systems.

Relative to the input signal, which is the CS in our case, a DPO can operate, in some instances, similar to a phase lock loop, frequency multiplier, or frequency–amplitude converter.

A DPO can filter out and/or multiply one of the CS spectrum component frequencies by $S/2$ as well as track this frequency over easily predictable frequency bands. The DPO time constant under otherwise equal conditions has strict dependence on the CS period. The oscillator in the described non-limiting mode can be used as a precise time-amplitude converter. Using the theory introduced in this chapter many other practical and "exotic" DPO applications can be proposed.

6.10 ABBREVIATIONS

CS	control signal
DFT	discrete Fourier transform
DPG	digital parametrical generator
DPO	digital parametric oscillator
DR	digital resonator
IC	initial condition
MM	monodromy matrix
PF	parametric filter
PIZ	parametrical instability zone
PLTV DS	periodically linear time-variant discrete system
PVDR	periodically varying digital resonator
RPG	region of parametrical generation
SVN	state vector norm

6.11 VARIABLES

$H_0(\omega)$	an equivalent frequency response
$\hat{y}_S$	dominant component
$\tilde{y}(n)$	periodic component of a signal
Ω	normalized frequency of system parameter variation
ω	normalized frequency of the signal
λ_1, λ_2	eigenvalues
$s_1(n), s_2(n)$	coefficients of the systems in the equivalent representation
$a(n)$	time-varying coefficients of the recursive part of a difference equation

$b(n)$	time-varying coefficients of the non-recursive part of a difference equation
f	frequency
$g(m, n)$	impulse response of the recursive part
$G(z)$	GTF of the recursive part
$h(m, n)$	impulse response
$H(z, n)$	generalized transfer function
Q	on/off factor
Q	quality factor
S	order number of the sub-harmonic
S_i	order of the sub-harmonic excited by the ith harmonic of a CS
$u(n)$	signal at the output of the first system
$X(\omega)$, $X(\psi)$	spectrum of the input signal
$X(n)$	input discrete random process
$x(n)$	input signal
$X(z)$	z-transform of the input signal
$Y(\omega)$	spectrum of the output signal
$Y(n)$	output discrete random process
$y(n)$	output signal
$Y(z, n)$	z-transform of the output signal
$\Delta\omega_s$	synchronization frequency band

6.12 REFERENCES

[1] Scoular SA, Cherniakov M, Rogozkin I (1993) Review of Soviet research on linear time-variant discrete systems. *Signal Process.*, **30**(1), 85–101.

[2] Cherniakov M, Bets V (1989) Characteristics of digital parametric generator in regime of oscillation exiting. *Radioelectronica*, **12**, 55–57.

[3] Cherniakov M, Bets V (1989) Algorithm of parametric generation of digital signals. *Commun. Tech. Ser. Radiocommun. Tech.*, **8**, 26–33.

[4] Cherniakov M (1989) Conditions of digital parametric frequency multiplier generation. *Radiotech. Electron.*, **5**, 1108–1110.

[5] Cherniakov M, Bets V, Mashonkin A, Seregin A (1988) Experimental investigation of the digital parametric frequency multiples, *Electron. Tech.*, Ser. 10, **5**(71), 18–20.

[6] Cherniakov M (1988) Passing of the harmonic signal and amplitude noise through digital parametric oscillator. *Radiotechnika*, **3**, 24, 25.

[7] Cherniakov M, Bets V (1987) Stability of digital filters with randomly changing parameters. Izvestia Vuzov, Proc., *Radioelectronika*, **2**, 72–75.

[8] Cherniakov M, Bets V (1987) Discrete transform matrix method application for the amplitude stability of digital filters. *Radiotechnika*, **4**, 24–26.

[9] Cherniakov M, Bets V (1990) *A Digital Frequency Multiplier*, Patent of the USSR, No. 1518863.

[10] Cherniakov M, Donskoi L (1999) Signal processing via digital dynamic systems in parametric instability mode, *IEEE Int. Conf. TENCON*, Korea, September, 165–168.

[11] Cherniakov M, Tomarov P (1991) A discrete parametric oscillator for frequency measurement, *Proc. Conf. on Digital Signal Processing in Communication and Control*, Rostov, USSR, 16–20 September, 98–102.

[12] Cherniakov M, Tomarov P (1991) Digital parametric oscillator as a device for frequency measurement, *Russian Workshop on Digital Signal Processing in Systems of Communication and Control*, Rostov, USSR, 54–56.

[13] Cherniakov M, Bets V, Tomarov P (1990) Oscillations failure in digital parametric tracing filter, *Proc. Conf. on Transmission, Reception and Signal Processing in Radio Communication Systems*, Rostov, USSR, 17–24.

[14] Cherniakov M, Bets V (1989) Estimation of excitement boundaries of the digital parametric oscillator, *Proc. Conf. on Methods and Means of the Digital Signal Processing and Transformation*, Riga, USSR, 274–277.

[15] Cherniakov M, Bets V (1988) Fast algorithm of oscillation of the periodical sequence, *Proc. Conf. on Problems of Design of Measure Devices with Inner Intellect and its Perspective*, Kaunas, USSR, 41–44.

[16] Cherniakov M, Sizov V, Shirokov A (1988) The use of a microprocessor in the loop of FAPF frequency synthesiser, *Proc. Conf. on the Problems of Measure Systems Design with Inner Intellect and Perspective of their Development*, Kaunas, USSR, 56, 57.

[17] Cherniakov M, Bets V, Seregin A (1986) Influence of the noise component of the parameter change on stability of periodically non-stationary digital filters, *Proc. Conf. on Methods and Microelectronic Means of Digital Signal Processing and Transform*, Riga, USSR, 406–409.

[18] Cherniakov M, Bets V, Mudrik D (1985) Investigation of stability of periodic non-stationary algorithms of digital filters, *Proc. Conf. on Microprocessors '85*, MIET, Moscow, USSR, 27, 28.

[19] Cherniakov M (1985) Digital periodically non-stationary systems in signal processing technique, *Proc. Conf. on Microprocessors '85*, MIET, Moscow, USSR, 23, 24.

[20] Merkin DR (1977) *Introduction to the Theory of Stability*, New York: Springer.

[21] Kharkevich A (1962) *Nonlinear and Parametric Phenomena in Radio Engineering*, New York: John F. Rider Publishing.

[22] Ifeachor EC, Jervis BW (2002) *Digital Signal Processing: A Practical Approach*, UK: Prentice Hall.

[23] D'Angelo H (1976) *Linear Time-Varying Systems: Analysis and Synthesis*, Boston: Allyn & Bacon.

[24] Herstein I, Winter D (1988) *Matrix Theory and Linear Algebra*, New York, London: Macmillan Publishing.

7

Parametric Oscillator in Steady-State Mode

Chapter 6 introduced the generic problems of digital parametric oscillators (DPOs) in non-limiting mode. In this chapter, we will consider a number of problems associated with DPO analysis as well as with their practical application for signal processing and generation. As a case study, we will consider results of DPO modelling using MATLAB.

The non-limiting mode can be viewed as an independent regime of DPO operation as well as a temporal period, which exists from the moment of oscillation excitation till the moment of overflow of the internal registers. Register overflow is typical for many or even for most applications; it is called a steady-state (SS) mode of DPO operation.

The conditions for excitation and the characteristics of the output signal were determined in Chapter 6 for the non-limiting mode of parametric digital resonators (DRs). Using the difference equation analysis, it was shown that the solution has two components: the decreasing component, which specifies the transient, and the increasing component, which is the essence of the DPO operation. Sooner or later, with an increase in the magnitude of the output signal the system reaches saturation owing to the limited capacity of registers and enters a steady-state mode. The generator in the SS mode can be described by a non-linear difference equation with time-varying coefficients:

$$y(n) = \Phi\{F[-a_1(n)y(n-1)] + F[-a_2(n)y(n-2)]\} \tag{7.1}$$

where Φ is a non-linearity, occurring during the sum operation, and F is a non-linearity, occurring during the multiplication operation.

It is not possible to obtain an exact analytical solution for equation (7.1) in the general case. Hence, the major instrument for system analysis is computer modelling. Analysis of DPOs shows that the main difference between the SS and non-limiting modes is with the amplitude limitation of the output process in the SS mode, when

An Introduction to Parametric Digital Filters and Oscillators Mikhail Cherniakov
© 2003 John Wiley & Sons, Ltd ISBN: 0-470-85104-X

all processes of oscillation excitation remain similar. This is partly the consequence of a special type of non-linearity, which has an essentially linear locality.

The second important practical issue is the possible presence of noise components in the control signal (CS) spectrum. As discussed earlier, a DPO is essentially a non-linear system relative to the CSs, which limits analytical approaches to the study. We will consider one important case of a small (relative to CS magnitude) noise presence in the control channel using a simplified analytical approach and modelling.

7.1 LIMITING MODE OF PARAMETRIC OSCILLATORS

In the non-limiting mode, when a transition process is completed, a DPO output signal can be represented by a normal increasing component. As soon as the amplitude of the oscillations reaches the maximum possible value for the given number of bits in the processor, the amplitude saturates and the oscillator starts to operate in the SS or limiting mode. This mode is described by equation (7.1). When fixed-point arithmetic is used, the non-linearity (F) of the multiplication is practically absent. Since during a scaling all numbers are selected to have an absolute value less than 1, there is no overflow during multiplication calculations. To further ease our task, but without a loss of generality, we can analyse a simplified equation with only one non-linearity:

$$y(n) = \Phi[-a_1(n)y(n-1) - a_2(n)y(n-2)] \tag{7.2}$$

Consider the non-linear characteristic of an adder Φ. If numbers with fixed points are presented in an inverse or complementary code, then the characteristic of the adder Φ looks as shown in Fig. 7.1a. The largest positive number is adjacent to the largest absolute value of the negative number.

Adder overflow leads to strong modulation of $y(n)$ (sign variation from the maximally possible positive value to the maximally possible negative value and vice versa) and the oscillator is constantly in a transition mode of parametric oscillations. To provide a steady-state limiting mode of parametric generation, the adder's characteristics have to look like a "saturating adder" or a "soft limiter" (Fig. 7.1b):

$$\Phi(y) = \begin{cases} y & \text{for} \quad |y| \le C \\ C & \text{for} \quad |y| > C,\ y > 0 \\ -C & \text{for} \quad |y| > C,\ y < 0 \end{cases} \tag{7.3}$$

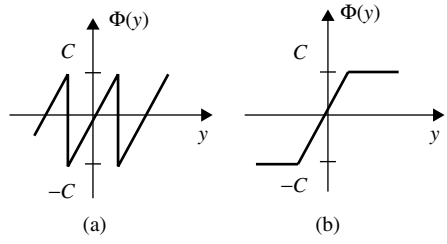

Figure 7.1 Adder characteristics

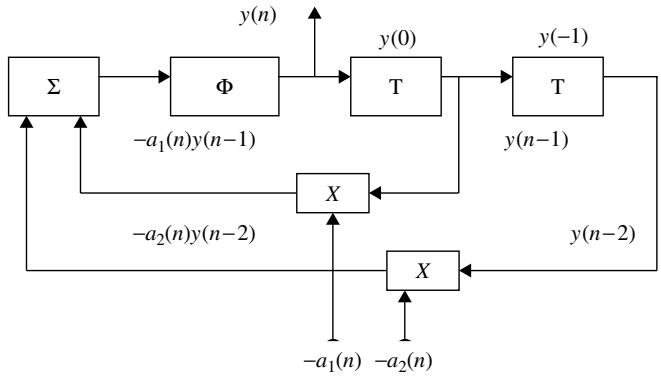

Figure 7.2 DPO equivalent structure

which is widely used for digital recursive filters with constant coefficients to prevent oscillations caused by overflows [1].

The resulting new equivalent diagram of the parametric digital oscillator corresponding to the steady-state limiting mode is shown in Fig. 7.2.

The main peculiarity of the SS mode is the presence of the non-linear stage Φ. We will study this mode by considering some computer simulation results.

Example 7.1: Comparison of the Steady-State and Non-Limiting Modes

To evaluate the characteristics of the output process affected by the non-linearity Φ, let us compare the output waveforms generated via equation (6.1) during oscillation excitation and equation (7.2), which corresponds to the SS mode under the same CS and initial conditions (ICs). These waveforms are sketched in Fig. 7.3.

The DR and CS parameters in this example are as follows: the CS is a square wave $a_1 \pm \gamma_1$ with amplitude $\gamma_1 = 0.125$, period $N = 8$ and $q = 2$ (see Fig. 7.3a), and constant second coefficient $a_2 = 0.99$. Consider two cases:

1. The DPO generates a first CS sub-harmonic, that is, the region of parametrical generation (RPG) $S_1 = 1$, and the appropriate average value of the first coefficient is $a_1 = -0.84$.
2. The DPO generates a third CS sub-harmonic, that is, $S_3 = 1$ and $a_1 = -0.74$.

The steady-state output waveform is shown in Fig. 7.3b by a solid line for $S_1 = 1$ and a dashed line shows the periodical component of non-limiting oscillations scaled to the same amplitude. Similar waveforms for the $S_3 = 1$ case are shown in Fig. 7.3c.

Comparison of the results demonstrates that introducing the non-linearity Φ leads to some limitation of the output signal amplitude and a shift in signal phase variation. The amplitude limitation is bigger and better seen in Fig. 7.3b, where the DPO has a smaller time constant (broader band). For this case, spectral components, occurring because of the harmonic signal limitation, are not fully filtered out. The mutual phase shift can be explained as an effect of amplitude–phase conversion in the hard limiter.

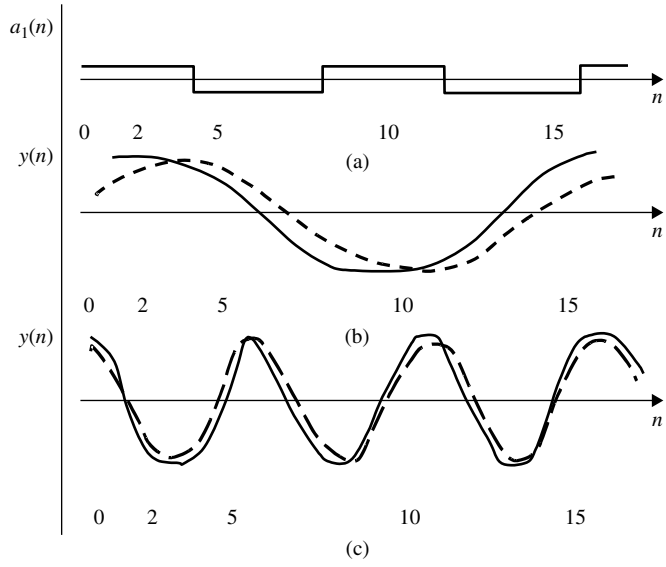

Figure 7.3 Waveforms of the output process in a DPO

When the DPO time constant is bigger (narrower band), which is the case with $S_3 = 1$, these two waveforms become closer to each other and to a harmonic function. This tendency was confirmed in many other examples and corresponds to common sense. Any spectral components of the generating signal are filtered by the DR itself; hence, the narrower the DR frequency response, the smaller will be the levels of side spectral components. This effect is similar to the case of the parametric filter, where combinational components were filtered out by the recursive filter itself.

Now let us study the size and the positions of RPGs in a steady-state mode in the $a_1 - a_2$ plane. It is not difficult to suppose that the conditions of oscillation excitation are precisely the same as they are in the linear mode. This is a consequence of the specific character of the non-linearity Φ: it has only a soft limitation, with a linear part about the zero-crossing point. Since generation starts at a low-bit data circulation (assuming that the ICs correspond to a linear part of Φ), the physical conditions for oscillation excitation in both circuits are the same. Nevertheless, let us confirm this using the next example [2].

Example 7.2: Evaluation of Regions of Parametrical Generation for Digital Parametric Oscillators in a Steady-State Mode

RPGs for the non-limiting mode for $S_1 = 1$ and $S_3 = 1$ are shown in Fig. 7.4a, b. Oscillations were excited by binary coefficient $a_1(n)$ variations for two amplitudes: $\gamma_1 = 0.25$ (solid line), 0.125 (dashed-dotted line) and $N = 8, q = 2$, when constant second coefficient $a_2 = 0.99$. These RPGs were evaluated by an exact method of monodromy matrix (MM) eigenvalues analysis. For the same conditions, RPGs were evaluated by computer modelling, the results of which are shown in Fig. 7.4 for both the non-limiting and the steady-state modes. All three sets of results fully coincide and verify the placement of

excitation region boundaries. This comparison shows that oscillation initiation processes are identical in both modes.

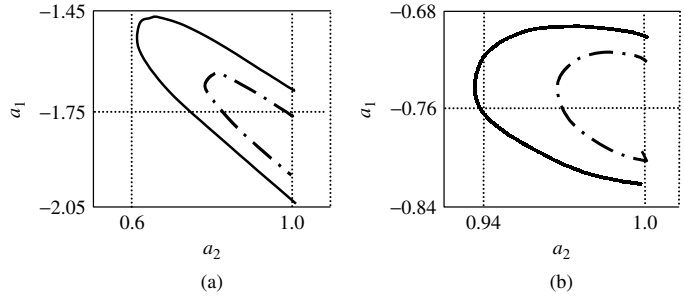

Figure 7.4 RPG for non-limiting and steady-state modes

As was discussed, the accurate analytical investigation of DPOs in the SS mode is a complicated task, since there is no general solution of non-linear parametric difference equations. A more practical method for investigation of such systems is modelling. This method has been discussed repeatedly in this book and its high quality performance has been demonstrated. In the general case, computer modelling of digital systems may correspond to an exact solution for particular selected systems and signal parameters.

Analysis of the modelling results yields the following main characteristics of DPOs in SS mode, which are, fundamentally, very close to those obtained for the non-limiting mode, except items 5 and 6:

1. Output signals are quasi-harmonic (with the dominant spectral component at the frequency of the Sth CS sub-harmonic).
2. Output and CSs are coherent.
3. The output signal spectrum $y(n)$ contains modulation components due to the alternative constituents of the CS.
4. The CS and DR parameters fully determine the characteristics of the output signal.
5. Average amplitude of the output signal is constant, which is the result of the amplitude limitation.
6. The output signal spectrum always contains harmonics of the main signal frequency, which is also the result of amplitude limitation.

Let us illustrate these statements with examples of DPO modelling in the steady-state mode. The quasi-harmonic nature of the output process during oscillation excitation was shown analytically in Chapter 6 for the non-limiting case and verified by modelling for the steady-state mode (see Fig. 7.3) for different parameters of the generator and CS. Consider the spectrum of the DPO output signal in SS mode using the following example.

Example 7.3: Output Signal Spectrum Components in Steady-State Mode

Consider Fig. 7.5, where the output signal spectrum $y(n)$ has been obtained for the SS mode in a DPO with the following parameters: the CS is the binary sequence $a_2(n) =$

1.08 ± 0.625 with $N = 32$, $q = 16$ and $a_1 = -1.41$. In this spectrum, a central frequency component at $S_8 = 1$ is 13 dB higher than the level of the closest (and largest) side components at frequencies $\omega_{\text{side}} = 4\,\Omega_C \pm \Omega_C$.

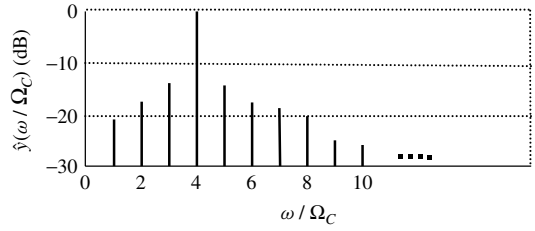

Figure 7.5 Spectrum of the output process

So, the output signal is a quasi-harmonic with the central frequency component dominating relative to side components. In spite of the amplitude limitation, the side spectrum components are relatively small as a result of the DR's filtering properties.

A strong dependence between the initial phases of the CS and the periodical component of the output process at the stage of oscillation excitation has been determined analytically (equation (6.68)) and verified by computer modelling (Figs. 6.11–6.15). In the steady-state mode, the output signal also remains coherent with the CSs, but an additional phase shift appears because of amplitude–phase conversion at the DR's non-linearity [2]. Consider the following example.

Example 7.4: Phase Relationships between the Control Signal and the Output Signal

Quasi-harmonic oscillations were excited at the first sub-harmonic ($S_1 = 1$) of the CS in a DPO with binary varying coefficients $a_1(n) = -1.38 \pm 0.125$ ($N = 4$, $q = 2$) and $a_2 = 0.96$. The CS waveform and output DPO signals in SS mode and non-limiting mode are shown in Fig. 7.6.

The output signal of the SS mode (solid line) and the periodic component of the oscillation excitation stage (dashed line) are shown in Fig. 7.6b, c. The transient process was removed by selecting ICs equal to the MM eigenvector: $y(0) = 1$, $y(-1) = 0.43$ (Fig. 7.6b) and $y(0) = -1$, $y(-1) = -0.43$ (Fig. 7.6c). The initial phases of oscillations for the non-limiting and SS modes are similar.

The output signal has some amplitude modulation despite the presence of a limiter in a DPO operating in SS mode. The reason is that in this case the limiter is not a memory-less network. Amplitude normalization requires some averaging time specified by the system time constant. Consequently, the output signal has some amplitude and phase modulations. As discussed earlier, the indicator of amplitude and phase (frequency) modulations is an asymmetry in the output signal spectrum relative to the central (dominant) component. Consider this effect for the SS mode in the following examples.

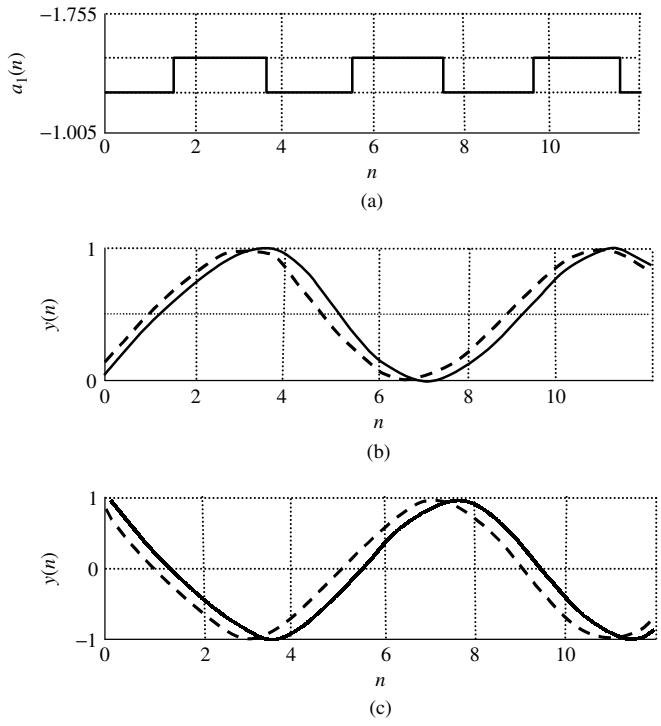

Figure 7.6 DPO output signal

Example 7.5: Modulation of the Output Signal

The existence of amplitude–phase modulation in the output spectrum is illustrated in Fig. 7.7, which shows spectrums of the output signal for SS oscillations (solid line) and for the periodic component of the oscillation excitation mode (dashed line) evaluated by Fourier transform.

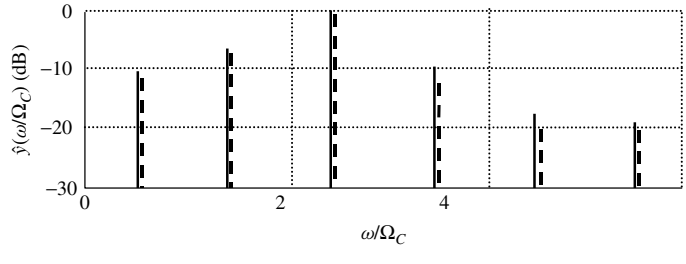

Figure 7.7 Spectrum of the DPO output signal

Oscillations at the fifth CS sub-harmonic have been excited by binary variation of coefficient $a_1(n) = -1.41 \pm 0.125$ with $q = 2$, $N = 20$ at the resonance frequency $\omega_{\text{res}} \approx \pi/4$. There are non-symmetrical spectrum components at frequencies $(S \pm 2m)\Omega_C/2$,

where $m = 1, 2, 3 \ldots$ in the output spectrums at both the excitation (dashed line) and SS (solid line) stage of oscillations.

So, even in the limiting case, the output signal contains small amplitude modulation as a consequence of DR inertia. The cause of modulation is variations of DR parameters by the CS. The relationship between the CS and output signal spectrums can be seen from the next example.

Example 7.6: Output Signal Modulation Components versus Control Signal Spectrum

Oscillations were excited by a binary variation of coefficient $a_2(n) = 0.96 \pm 0.0625$ ($N = 12$, $q = 2$). The CS spectrum (dashed line) and output DPO signal spectrum (solid line) initiated by this CS are shown in Fig. 7.8. The figure clearly shows that the CS spectrum contains only odd harmonics. In the output signal spectrum, these harmonic ($m = 1, 3, 5, 7 \ldots$) components are strongly expressed.

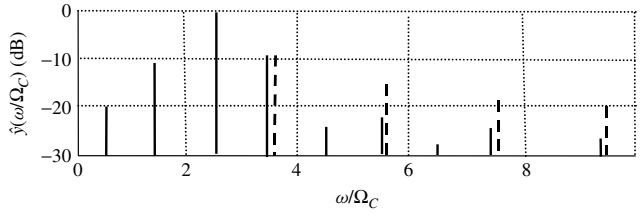

Figure 7.8 DPO output signal and CS spectrums

From Fig. 7.8 it follows that the output signal is modulated by CS components in the DPO operating in SS mode. The following example illustrates this even more clearly. This example demonstrates that the magnitude of these modulation components is proportional to the CS magnitude.

Example 7.7: Dependence of Modulation Components

The DPO was modelled to demonstrate the dependence between CS amplitude and the level of the output signal modulation components. The DPO was in the SS mode of signal generation by a CS with variable amplitude γ_2. The relationship between the normalized levels of the nearest modulation spectral components in the output process versus γ_2 is shown in Fig. 7.9 for different RPGs.

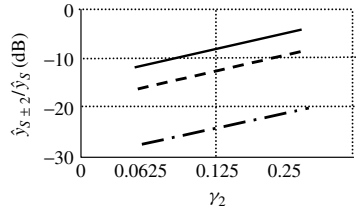

Figure 7.9 Modulation components versus CS magnitude

The modelling results were obtained during oscillation excitation by binary variation of coefficient $a_2(n)$ with $N = 12$ and $q = 2$ at the third (solid line) and the fifth (dashed line) CS sub-harmonics. Oscillation excitation at the sub-harmonic of high multiplicity $S = 128$ by a wideband binary CS with $q = 256$ and $N = 512$ is shown in the same figure by the dashed-dotted line. From Fig. 7.9 we conclude that the level of $y(n)$ spectrum modulation components proportionally depends on the CS magnitude.

The next subject for study is the influence of the average DR coefficients a_1, a_2 on the spectrum of the output processes. In the first approximation for high Q resonators, coefficient a_2 is responsible for the generator's filtering properties, that is, the time constant, when a_1 specifies the DR resonance frequency. Using the next example, we will study this dependence.

Example 7.8: The Influence of Digital Resonator Parameters on the Output Process

Consider a dependence between the DR-CS parameters and the output signal spectrum using the $S = 1$ generation region (see Fig. 7.10) obtained by a binary CS: $a_1(n) = a_1 \pm \gamma_1$ with $N = 16$, $q = 2$ and $\gamma_1 = 0.125$ (Fig. 7.11a). Inside this RPG, two pairs of parameters, those at points 1, 2 and 3, 4, have been chosen for investigations:

1. Points 1 and 2 correspond to $a_2 = 0.98$ and $a_1 = -1.99$ and $a_1 = -1.92$. A DPO with these parameters has different time constants: $\tau = 5.93$ for point 1 and $\tau = 10.09$ for point 2.
2. Points 3 and 4 correspond to $a_1 = -1.92$ and $a_2 = 0.92$ ($\tau = 7.29$) and 0.87 ($\tau = 17.92$).

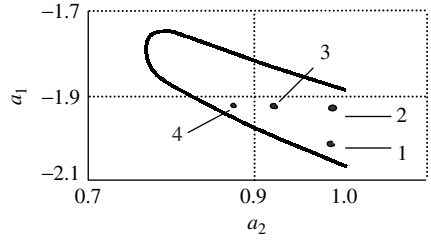

Figure 7.10 DR-CS parameters

The output waveform $y(n)$ in the SS mode (solid line) and normalized output waveform $\tilde{y}(n)$ for the non-limiting mode (dashed line) are sketched in parts b, c, d, e of Fig. 7.11, corresponding to the parameters of points 1, 2, 3 and 4 (Fig. 7.10), respectively.

Comparing $y(n)$ and $\tilde{y}(n)$, note that the existence of the non-linearity makes the shape of oscillations "more rectangular". This is obviously because the amplitude limiter is present. It is better seen in DPOs with smaller τ, as the resonator introduces weaker harmonic filtering. The bigger the time constant τ (narrower band), the better is the output signal approximation to the sinusoidal waveform.

This once again confirms the fact that a DR with higher Q (bigger τ, narrower band) provides better filtering of the output spectrum modulation components.

Consider this effect once again in the following example.

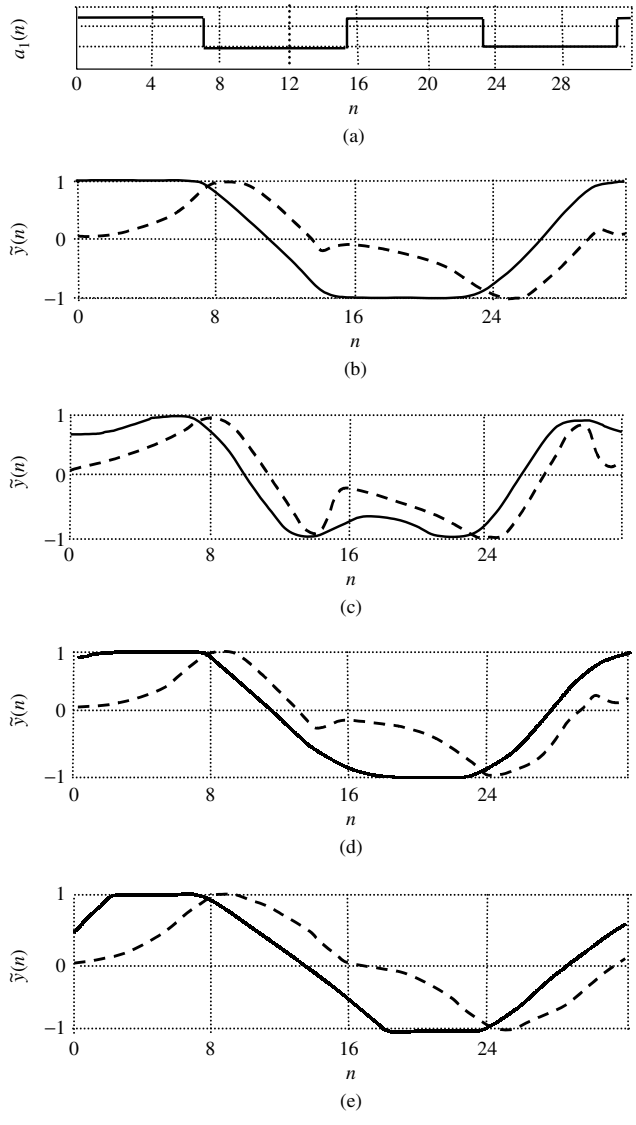

Figure 7.11 DPO output waveforms

Example 7.9: Output Processes in High Q Oscillator

Let us consider the influence of the DPO time constant on the output waveform. A DPO similar to that in example 7.8 is used, but it operates in the $S_3 = 1$ oscillation

mode (see Fig. 7.12). Results of this DPO modelling are shown in Fig. 7.13: $y(n)$ for the SS mode (solid line) and $\tilde{y}(n)$ for the non-limiting mode (dashed line) are shown in Fig. 7.13b for $a_1 = -1.63$, $a_2 = 0.99$, $\tau = 283.8$ (point 1, Fig. 7.12) and in Fig. 7.13c for $a_1 = -1.645$, $a_2 = 0.99$, $\tau = 91.9$ (point 2, Fig. 7.12). Since the time constant values τ for $S_3 = 1$ are considerably larger than for $S = 1$ under the same conditions, the shape of the oscillations in the case $S_3 = 1$ is much closer to a harmonic waveform.

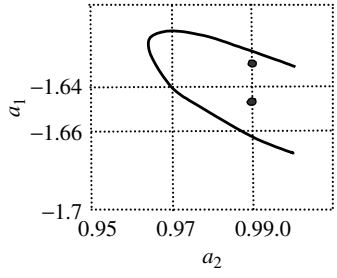

Figure 7.12 Region of parametric generation $S_3 = 1$

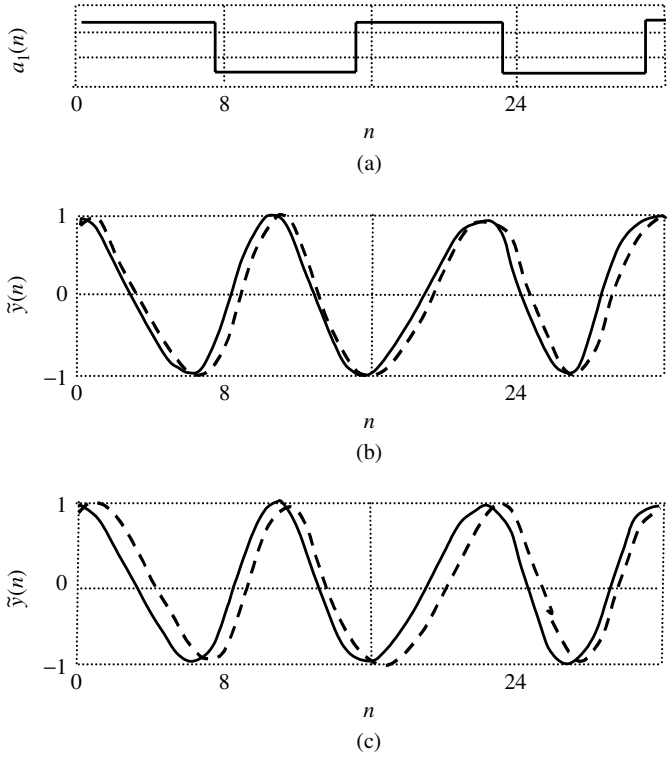

Figure 7.13 Output processes for different DPO parameters ($S_3 = 1$)

Analysis of the modelling results for a DPO in SS mode yields the following conclusions:

1. The existence of the adder non-linearity does not essentially change the main character of the output process in comparison with the non-limiting operating generation mode.
2. The magnitude of the increasing component is restricted by the limited capacity of the internal DPO registers. The limiter itself translates the increasing oscillations to an almost rectangular shape, but the DPO essentially filters out side harmonics of the generating signal. For a bigger time constant, the filtering effect is stronger and the output process becomes closer to the sinusoidal waveform.
3. The output process is coherent with the CS and the dominant frequency $S\Omega_C/2$ component is accompanied by the modulation components. The constituents and location of these harmonics are determined by the CS spectrum. Their amplitudes are proportional to the coefficient variations (that is, the CS) as well as dependent on the resonator parameters a_1, a_2 and, consequently, the time constant τ.

7.2 DPO ANALYSIS IN THE PRESENCE OF NOISE

As discussed above, a DPO can be used as some sort of frequency multiplier, that is, a narrowband filtering system. In this section, we will discuss a very interesting practical case in which the deterministic CS is accompanied by a random process, which creates system noise. Unfortunately, no one has yet carried out a detailed analysis of this problem, either analytically or by modelling; this would be a good topic for future research.

In Chapter 3, the stability of second-order digital parametric systems was discussed for the case in which the CS contains not only deterministic but also random components. When noise is present, an appropriate system can be described by stochastic difference equations. Analysis of these equations is very complicated from the mathematical point of view and there are no solutions for the general case.

It is important to recall here once again that relative to control signals, DPOs are not linear systems and the superposition principle is not applicable. Nevertheless, for DPO applications we can consider one practically interesting case of a system with only a small level of noise. We assume that the CS is corrupted by additive noise, but its standard deviation is essentially less than the magnitude of the CS variations. In this case, the behaviour of the DPO can be evaluated at least in the first approximation. Representing signals and systems as row expansion series and using only first terms, some *equivalent* of the superposition principle can be used [3]. Now let us study the influence of interference on parametric oscillators in both non-limiting and SS modes.

Operation of the DPO at the stage of oscillation excitation is described by the difference equation (6.1). In the presence of noise, coefficients in this equation can be represented as a sum of the signal $a^0(n)$ (which is the CS in this case) and the centred noise component $\eta(n)$ [4]:

$$a(n) = a^{\circ}(n) + \eta(n) \tag{7.4}$$

Similar to equation (7.4), an output process $y(n)$ in the first approximation can be represented as the sum of two components: the signal $y^{\circ}(n)$ (due to the CS) and the noise $\xi(n)$ (due to the presence of noise component $\eta(n)$ at the input). This representation is possible if and only if

1. the noise components are small relative to the CS;
2. interaction between the CS and input noise produces components of second-order smallness;
3. the presence of noise does not collapse the parametric oscillations;
4. the presence of noise does not disturb the mode of quasi-harmonic parametric generation, for example, by changing the RPGs.

It is important to note that these conditions are not always applicable even for a "small" noise. But introduction of this analysis is still useful for the understanding of DPO operations.

Thus,

$$y(n) = y^{\circ}(n) + \xi(n) \tag{7.5}$$

and equation (6.1) takes the form

$$\begin{aligned}[y^{\circ}(n) + \xi(n)] + [a_1{}^{\circ}(n) + \eta_1(n)][y^{\circ}(n-1) \\ + \xi(n-1)] + [a_2{}^{\circ}(n) + \eta_2(n)][y^{\circ}(n-2) + \xi(n-2)] = 0\end{aligned} \tag{7.6}$$

or

$$\begin{aligned}y^{\circ}(n) + a_1{}^{\circ}(n)y^{\circ}(n-1) + a_2{}^{\circ}(n)y^{\circ}(n-2) + \xi(n) + a_1{}^{\circ}(n)\xi(n-1) + a_2{}^{\circ}(n)\xi(n-2) \\ + \eta_1(n)y^{\circ}(n-1) + \eta_2(n)y^{\circ}(n-2) + \eta_1(n)\xi(n-1) + \eta_2(n)\xi(n-2) = 0\end{aligned} \tag{7.7}$$

Taking into account that

$$y^{\circ}(n) + a_1{}^{\circ}(n)y^{\circ}(n-1) + a_2{}^{\circ}(n)y^{\circ}(n-2) = 0 \tag{7.8}$$

consider only the first order of smallness in equation (7.7). This equation, with respect to the random component of the output process, can be written as

$$\xi(n) + a_1{}^{\circ}(n)\xi(n-1) + a_2{}^{\circ}(n)\xi(n-2) + \eta_1(n)y^{\circ}(n-1) + \eta_2(n)y^{\circ}(n-2) = 0 \tag{7.9}$$

or

$$\xi(n) + a_1{}^{\circ}(n)\xi(n-1) + a_2{}^{\circ}(n)\xi(n-2) = -\eta_1(n)y^{\circ}(n-1) - \eta_2(n)y^{\circ}(n-2) \tag{7.10}$$

The non-uniform difference equation (7.9) has a general solution relative to $\xi(n)$, which is a sum of solutions for the uniform part and solutions due to the existence of constant terms. The solutions for the uniform part of equation (7.9) were determined

earlier. The right part of equation (7.10) also represents oscillations at frequency $S\Omega_C/2$, modulated by CS components, which includes noise components. The spectrum of the output process contains signals at frequencies $(S\Omega_C/2) \pm \omega_N$, where the dominant component at frequency $S\Omega_C/2$ is surrounded by modulation components.

Let us describe this solution in technical terms. If a deterministic periodical CS causing excitation of parametric oscillations is accompanied by a small noise, the DPO will convert this random process at the output central frequency $S\Omega_C/2$ [4]. This conclusion is important from a practical point of view. It specifies that relative to the input process, which is a sum of the deterministic CS and random noise, a DPO acts as a narrowband frequency converter or a chain of a memory-less frequency multiplier with the multiplication coefficient $S/2$ and a narrowband filter. Parameters of the DPO specify not only a central output frequency (multiplication coefficient S) but also the filtering property of this system. For a better understanding, consider the next example, where noise is a narrowband harmonic-like process. Here, for the sake of simplicity of presentation, we introduce the interference component at the discrete frequency ω_N and later will study the noise component with a broader spectrum.

Example 7.10: Control Signal Accompanied by Narrowband Interference

Oscillations in the GPO are excited by the sinusoidal CS $a_1 = a_{10} + \gamma_1 \sin \Omega_C n = a_{10} + 0.125 \sin(\pi n/4)$. Coefficient $a_2 = 0.96$ is chosen to provide oscillations in the RPG $S = 1$. Narrowband interference at the frequency $(1 + 0.1)\,\Omega_C$ (sketched in Fig. 7.14a) with a magnitude -16 dB lower than the γ_1 is added to the CS.

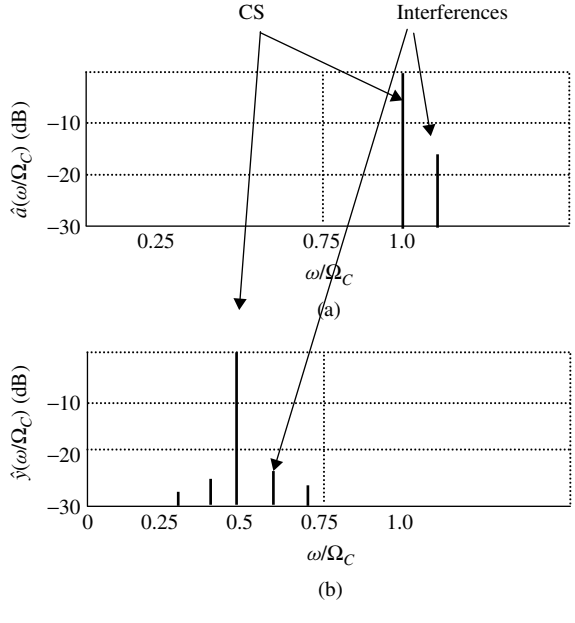

Figure 7.14 DPO with narrowband interference

An output signal spectrum is shown in Fig. 7.14b. At the output, besides the central spectrum component at frequency $S\Omega_C/2$, the signal contains interference components at frequencies $\Omega_C/2 \pm 0.1n\Omega_C$. Its maximum level is equal to -24 dB at frequency $0.5\,\Omega_C + 0.1\,\Omega_C$. This well illustrates the conclusion drawn above that interference (noise) is heterodyned (up- or down-converted) to the output frequencies and processed according to the equivalent frequency response of the parametric oscillator.

In spite of the clear physical sense of this conclusion, it is only true in the case of "small" noise. As a result of the essential non-linearity of the process behind the DPO operation, the boundary of this "smallness" is not defined. It is also important to recall here that non-linearity is the fundamental property of the parametric difference equation relative to the law of coefficient variation or the CS in the discussed case.

The existence of random noise in the CS leads not only to output signal parameters but also to the location, size and even shape of RPGs, depending on this random process. A strict determination of conditions for excitation of parametric oscillations by a signal with random components has not been introduced in the literature. This is mainly due to mathematical difficulties [5]. Random matrixes describe trajectories of motion of such systems in a vector space. The theory of such matrixes is rather sophisticated and no one study has specified exact conditions for oscillation excitation in closed analytical form. So, this problem can be introduced here via computer modelling. Consider the influence of a small noise component on the conditions for excitation of parametric oscillations. We will use oscillations occurring in RPG $S = 1$, which was investigated in Chapter 6 (Fig. 6.7).

Example 7.11: Influence of Noise on Boundaries of Regions of Parametrical Generation

An RPG for the harmonic law of CSs $a_2(n) = \gamma_2 \sin(2\pi n/16)$, with amplitude $\gamma_2 = 0.125$, is shown by the solid line in Fig. 7.15. In the same figure, a boundary of the appropriate RPG is shown when a white Gaussian random process accompanies the deterministic sinusoidal CS (dashed line). The following algorithm was used to obtain this result: calculate the MM for a CS with period N at the point with coordinates a_1, a_2; determine if oscillations are occurring by applying criteria (3.27) and analysing

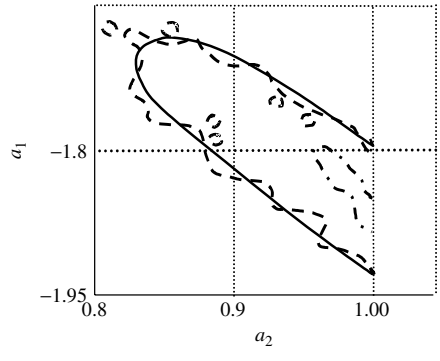

Figure 7.15 RPG deformation by noise

MM eigenvalues. Depending on the values of deterministic parameters a_1 and $a_2 + \gamma_2 \sin(\Omega_C n)$, as well as random components $\eta_1(n)$ and $\eta_2(n)$, different RPG boundaries are obtained.

In Fig. 7.15, the dashed line represents the case when $a_2(n)$ is corrupted by white noise with variance $\sigma_2^2 = 0.01$, when $\gamma_2 = 0.125$. For comparison, RPG boundaries for oscillations excited by only two independent white noise components with variances $\sigma_1^2 = \sigma_2^2 = 0.01 (\gamma_1 = \gamma_2 = 0)$ are represented by a dashed-dotted line.

Example 7.10 shows that the boundaries of RPGs now also have random components. Their statistical parameters – probability density function of boundary variation, a mean value and variance – can be evaluated by data collection and processing via computer simulation. The following explicit algorithm was used to calculate the parameters:

1. For a given deterministic sinusoidal CS, specify the RPG boundary by analysis of the eigenvalues $\lambda_{1,2}$.
2. Choose arbitrary points a_{1b} and a_{2b} at this boundary.
3. Add low-level white noise to the deterministic CS and again calculate the RPG boundary in the vicinity of a_{1b} and a_{2b}. To do this, calculate eigenvalues $\lambda_{1,2}$ successively for 100 independent samples to collect appropriate statistics.
4. Calculate histograms of the RPG boundary distribution for the given point a_{2b} and for 10 values of a_1 with equal steps between $a_{1b} - 0.05$ and $a_{1b} + 0.05$. For each calculation, evaluate the values of $|\lambda_1|$ to determine if excitation of parametric oscillation has occurred.

From the obtained data, we found a distribution for the location of RPG boundaries, which is close to the normal law. The Gaussian-like distribution of the boundary is easily predictable as we are dealing with a narrowband system. Using the next example, let us study the parameters of this distribution with the mean value $M(a_1)$ and variance σ_a^2.

Example 7.12: Parameters of Boundary Variation for Regions of Parametrical Generation

Approximated probability density functions of RPG boundary distribution relative to the boundaries for only deterministic CSs are shown in Fig. 7.16 for three different

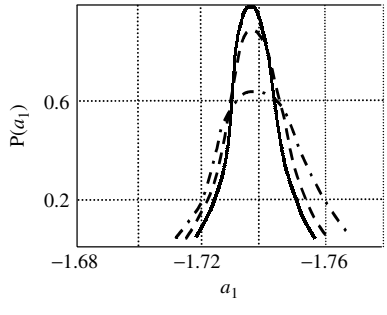

Figure 7.16 RPG boundary distribution

variances of the noise. These distributions were calculated for $a_{1b} = -1.735$ and $a_{2b} = 0.95$. For the noise with variance $\sigma_2^2 = 4 \cdot 10^{-4}$, the boundary distribution along a_1 has the mean value $M(a_1) = -1.736$ and variance $\sigma_a^2 = 5.85 \cdot 10^{-4}$ (solid line); for $\sigma_2^2 = 8 \cdot 10^{-4}$, the mean value $M(a_1) = -1.737$ and variance $\sigma_a^2 = 7.93 \cdot 10^{-4}$ (dashed line); and for $\sigma_2^2 = 2 \cdot 10^{-3}$, the mean value $M(a_1) = -1.738$ and the variance $\sigma_a^2 = 1.54 \cdot 10^{-3}$ (dotted-dashed line). So, when the variance of the boundary distribution directly depends on the power of the CS's noise component, the mean value does not change.

The dependencies of σ_a^2 on the CS's noise variance is shown in Fig. 7.17 for $a_2 = 0.95$, $a_1 = -1.735$ (solid line) and $a_2 = 0.91$, $a_1 = -1.705$ (dashed line) at the RPG boundary. Simulations have been provided for the white noise.

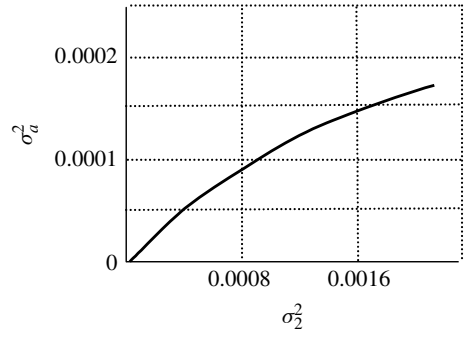

Figure 7.17 RPG boundary variance versus the noise power

Analysis of example 7.12, shown in Fig. 7.17, confirms that variation of the RPG boundary directly depends on the power of the CS's random components.

The influence of broadband noise on the output signal spectrum will be discussed in the next example.

Example 7.13: Control Signal Accompanied by White Noise

Consider a DPO with a sinusoidal CS corrupted by small additive white noise. The CS-to-noise ratio is 35 dB. Spectrum $\hat{y}(\omega/\Omega_C)$ of the periodic component of the output process for $a_2 = 0.99$ (solid line) and $a_2 = 0.96$ (dashed line), $a_1 = -1.81$ and CS amplitude $\gamma_2 = 0.125$ is shown in Fig. 7.18.

We can see that the noise components also present in the output signal spectrum. When the input noise has a broad uniform spectrum, the output signal spectrum is narrowband, which is the consequence of the DPO's filtering properties as well as strong system non-linearity relative to the CS.

The analysis here of the influence of CS noise components on DPO operation has been very brief and does not give essential information for quantitative analysis. Perhaps this is one direction for future research. However, at least two conclusions should be derived: the additive noise causes random variations of RPG boundaries as well as stochastic modulation of the output signal.

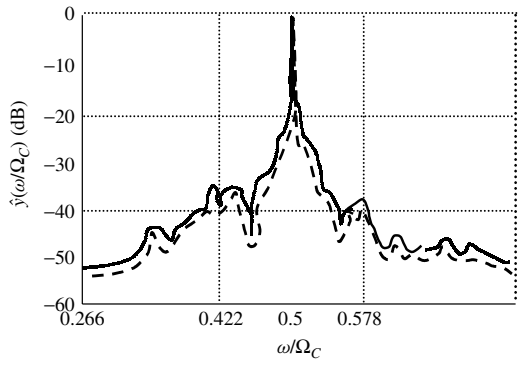

Figure 7.18 Output signal spectrum in the presence of input noise

7.3 MODELLING OF A DIGITAL PARAMETRIC OSCILLATOR USING MATLAB – A CASE STUDY

In Chapters 6 and 7 we introduced digital parametric oscillators, which can be viewed as periodically time-varying systems for signal generation and processing. We analysed DPO characteristics and considered a number of examples. In these examples, the parameters used provided good results for visualization, but were not useful for practical applications. In this section, results of DPO modelling using Matlab will be presented, which will give readers a better understanding of the operation and practical applications of DPOs.

7.3.1 Non-Limiting Oscillation Mode

Example 7.14: **Sinusoidal Control Signal Representation**

Let us consider a DPO with a sinusoidal control signal:

$$CS(n) = a_1 + \gamma_1 \sin(n\Omega)$$

The spectrum and waveform of this CS are shown in Fig. 7.19a, b, respectively, for $\Omega = 0.5$ and $\gamma_1 = 0.01$. For the coefficient $a_2 = 0.999$, this CS causes parametric oscillation in the region $S = 1$. The spectrum and waveform of the output signal are shown in Fig. 7.19b, c, respectively.

As shown in Fig. 7.19, the output spectrum has two harmonics: one at the relative frequency 0.25, which is the main component, and the second at frequency 0.75, the first CS sub-harmonic, which is the modulating component. As a result of high DR efficiency ($a_2 = 0.999$ and $\gamma_1 = 0.01$), the modulation harmonic is -70 dB relative to the main harmonic.

We have already discussed that the DPO output signal spectrum and waveform depend on the system parameters, even when the oscillator operates within the same RPG and the CSs have the same period. Parameters such as a_1, a_2, γ_1 and γ_2 influence the DPO time constant τ. Let us consider this effect in the following example.

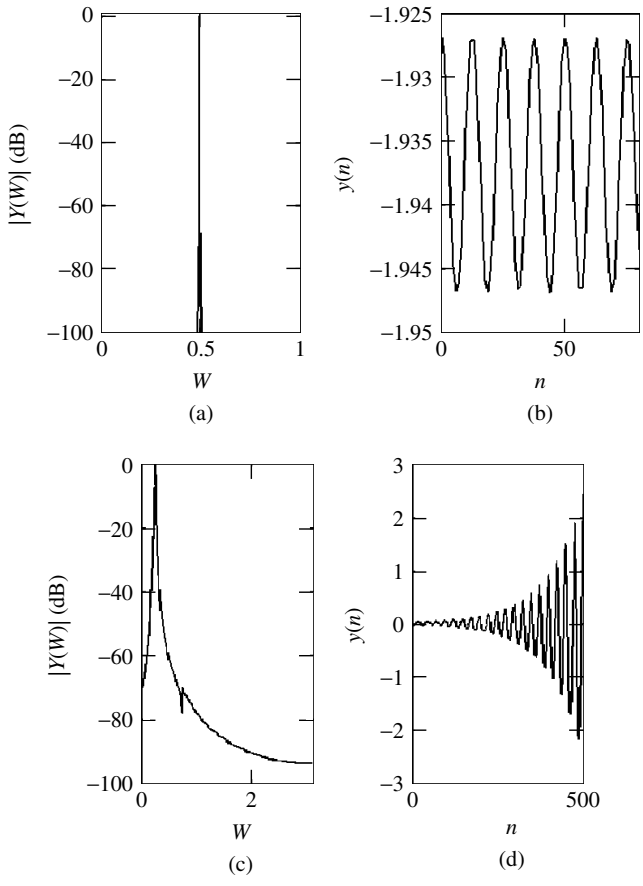

Figure 7.19 CS and DPO output signal spectrum and waveform

Example 7.15: Time Constant Influence on the Output Signal of a Digital Parametric Oscillator

Let Ω, S and a_2 have fixed values. We will study the influence of the parameter γ_1 on the output waveform and spectrum. When we change γ_1, we are changing the DPO time constant, which is the rate of increase in the signal amplitude. The parameters are fixed at the following values:

$$\begin{cases} \Omega = 0.5 \\ s = 1 \\ a_2 = 0.999 \\ a_1 = -1.9369 \end{cases}$$

and for $\gamma_1 = 0.005$ the time constant $\tau = 8$; for $\gamma_1 = 0.01$, $\tau = 4$; for $\gamma_1 = 0.02$, $\tau = 2$; and for $\gamma_1 = 0.05$, $\tau = 1$. The output signal spectrums and waveforms are shown in Fig. 7.20a, b, c, d, respectively. It is clear that with reduction of the time constant, the

rate of increase of the signal envelope rises and the signal spectrum becomes broader as it contains stronger modulation components.

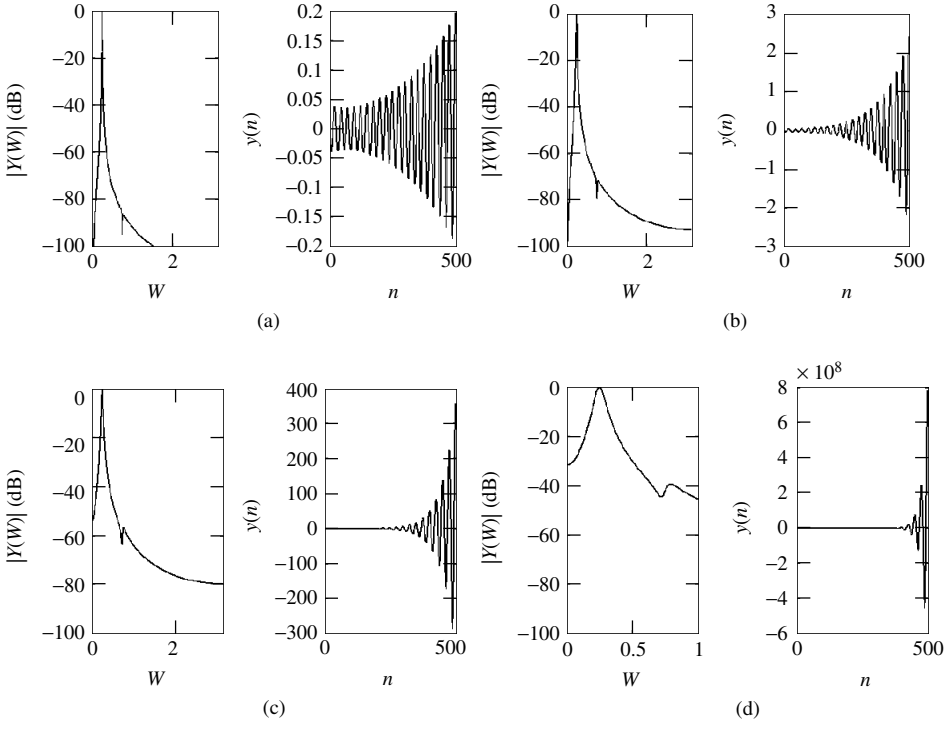

Figure 7.20 Signal and spectrum variation for different DPO time constants

For a sinusoidal CS it is rather difficult to initiate parametric oscillation in a mode $S > 1$ because of rapid reduction of RPG size. Nevertheless, it is possible and the next example will demonstrate the output signal spectrums for $S = 2$ and $S = 3$ oscillation modes.

Example 7.16: Signal Generation in $S > 1$ Mode in a Digital Parametric Oscillator

In order to generate sub-harmonics higher than $S = 1$, we fix all DPO and CS parameters except a_1, which is varied in order to excite oscillations in RPGs for $S = 2$ and $S = 3$. So, let $\Omega = 0.5$, $a_2 = 0.999$ and $\gamma_2 = 0.05$. Then, the following values of a_1 should apply: for signal generation in $S = 1$ or $\frac{\Omega}{2} = 0.25$, $a_1 = -1.9369$; for $S = 2$ or $\Omega = 0.5$, $a_1 = -1.7543$; and for $S = 3$ or $\frac{3\Omega}{2} = 0.75$, $a_1 = -1.4626$. Spectrums of the relevant signals are shown in Fig. 7.21a–c, respectively. With all other conditions equal, the DPO time constant increases as S increases. As a consequence of this, as Fig. 7.21 clearly shows, the spectrum narrows as S increases.

It is important to recall that the size of the region of parametric oscillations decreases proportional to $\left(\frac{\gamma}{2}\right)^S$. In this example, $\gamma = 0.05$; therefore, the RPG sizes are $\left(\frac{\gamma}{2}\right)^S_1 = 0.025$; $\left(\frac{\gamma}{2}\right)^S_2 = 6.25 \cdot 10^{-4}$ and $\left(\frac{\gamma}{2}\right)^S_3 = 1.56 \cdot 10^{-6}$ for $S = 1$, $S = 2$ and $S = 3$, respectively.

A DPO can operate like a phase lock loop tracing the frequency of an input signal. In the DPO case, an input signal is the control signal. Let us demonstrate this effect in the next example.

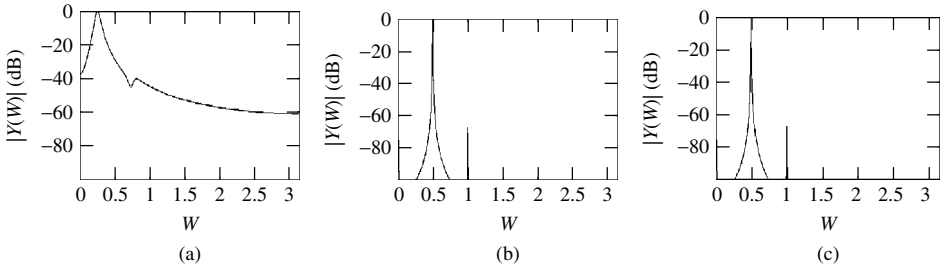

Figure 7.21 Output signal spectrum for different S

Example 7.17: Variation of the Control Signal Central Frequency

In this example, all oscillators are fixed, but the CS frequency is shifted relative to some central frequency Ω_{centre}. It is assumed that at this frequency, parametric oscillations are present at the DPO output. Now, let the CS frequency be described as $\Omega = \Omega_{\text{centre}}(1 + \alpha)$, where $\alpha \ll 1$ is a real number. We will investigate the spectrums of output signals for different values of α. The system parameters are $\Omega_{\text{centre}} = 0.5$, $S = 1$, $a_2 = 0.999$, $\gamma = 0.05$, $a_1 = -1.9369$. Output signal spectrums and waveforms for $\alpha = 0$ ($\Omega = 0.5$), $\alpha = 0.06$ ($\Omega = 0.53$), $\alpha = -0.06$ ($\Omega = 0.47$), $\alpha = 0.16$ ($\Omega = 0.58$) and $\alpha = 0.24$ ($\Omega = 0.62$) are shown in Fig. 7.22a, b, c, d, e, f, respectively. The latter frequency $\Omega = 0.62$ is slightly outside the DPO synchronization band. For this signal, it is clear that there is more than one dominating harmonic in its spectrum and the waveform is strongly modulated as well as having a decreasing envelope.

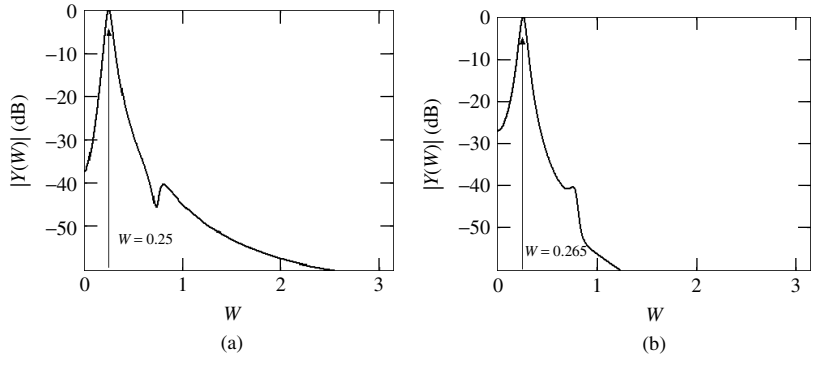

Figure 7.22 Frequency tracking in a DPO

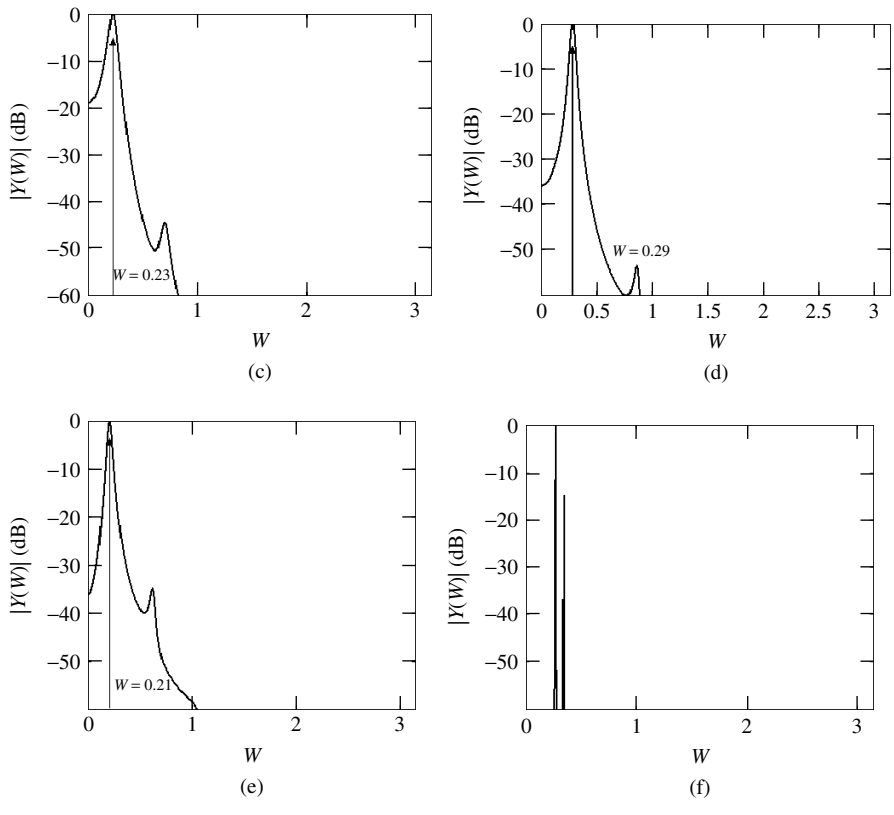

Figure 7.22 (*continued*)

7.3.2 Steady-State Oscillation Mode

In the previous sections, the output signal was considered to be in a non-limiting mode. However, when the amplitude of the output signal is increasing, the system eventually reaches saturation due to overflow of the DPO internal registers. For this mode, the system is described by the difference equation

$$y(i) = \Phi[[a_1(i)y(i-1)] + [-a_2(i)y(i-2)]]$$

In the preceding equation, $\Phi(*)$ is a non-linearity with the following characteristics:

$$\Phi(y) = \begin{cases} y & \text{for } |y| < M \\ M & \text{for } \quad y > M \\ -M & \text{for } y < -M \end{cases}$$

Let us consider the signal spectrum and waveform for the steady-state mode as a function of the CS amplitude γ in the next example.

Example 7.18: Digital Parametric Oscillator with a Sinusoidal Control Signal in the Steady-State Mode

A signal waveform at the transient between non-limiting and steady-state mode is shown in Fig. 7.23a for the following DPO parameters: $\Omega = 0.5$, $S = 1$, $a_2 = 0.999$, $\gamma = 0.01$, $M = 1$, $a_1 = -1.9369$. The signal waveform and its spectrum are shown in Fig. 7.23b, c, respectively, for the same parameters, but for the steady-state mode.

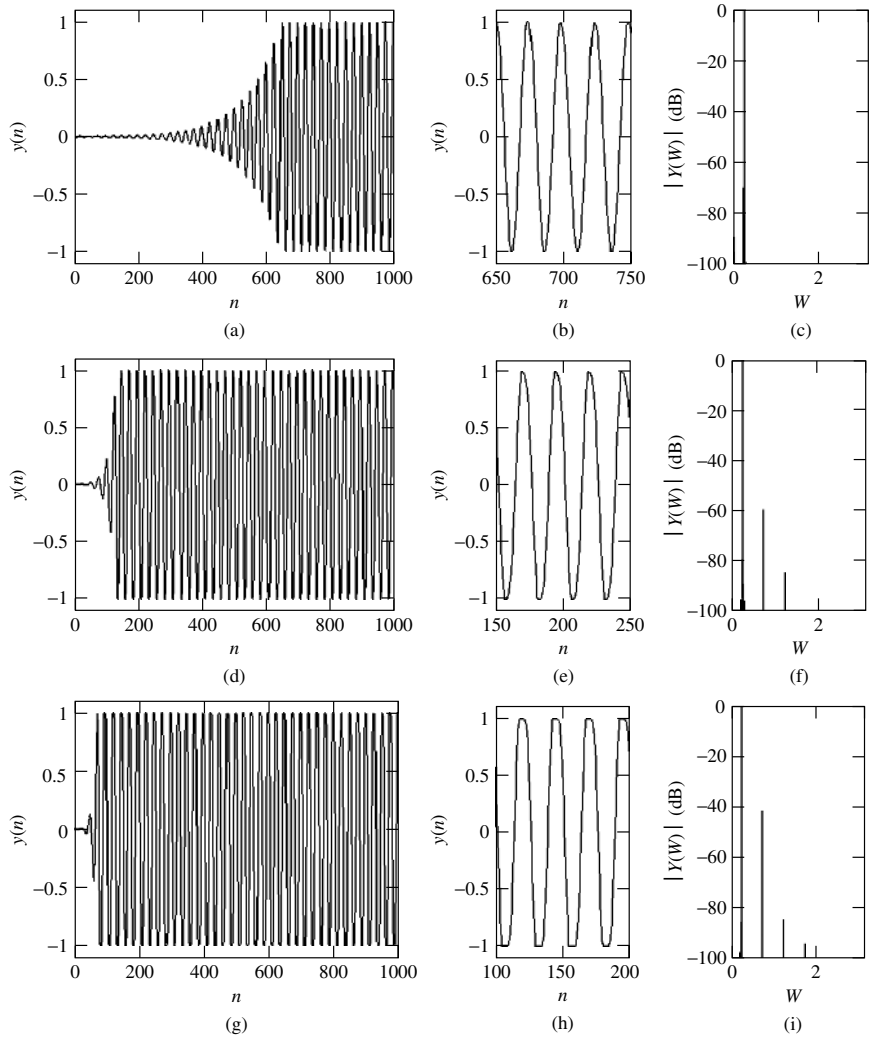

Figure 7.23 Transient from non-limiting and steady-state mode

It is interesting to note that the signal spectrum in the steady-state mode is rather pure, and this can be explained by the suppression of the amplitude modulation in the limiter. When this amplitude is increased, stronger modulation components are present in the spectrum. This is shown in Fig. 7.23d–i, which correspond to the case of $\gamma = 0.05$

and $\gamma = 0.1$, respectively. Moreover, as follows from a previous discussion the DPO time constant decreases as the CS amplitude increases. We can clearly see this with the analysis of the rate of amplitude increase in the non-limiting cases (Fig. 7.23a, d, g). In Fig. 7.23h, the output waveform is almost a square wave, which is the consequence of the poor auto-filtering property of DPOs for large values of γ.

7.3.3 A Digital Parametric Oscillator with Non-Sinusoidal Control Signal

To provide DPO operation in the $S > 1$ mode [6, 7], it is convenient to use a non-sinusoidal CS. This signal contains a number of harmonics of the main frequency $m\Omega$. So, instead of generating a signal at the Sth sub-harmonic $S\Omega/2$ using the Ω component in the CS spectrum, it is easier to generate the first sub-harmonic from the mth harmonic of CS, $m\Omega/2$. We have already notated this sub-harmonic as $S_m = 1$. Consider now examples of such oscillation generation using a rectangular CS. This rectangular CS has the period $N = \frac{2\pi}{\Omega}$, amplitude variation $\pm\lambda$ and the parameter a_1, which is an average value of the CS and can be derived from $a_1 = -\frac{4a_2}{1+a_2}\cos(\omega_R)$, depending on the desired angular frequency ω_R.

Example 7.19: **Rectangular Control Signal**

In this example, we use a CS with the following parameters: $\Omega = \frac{2\pi}{12}$, $\gamma = 0.1$, $a_2 = 0.99$. The waveform and spectrum of this CS are shown in Fig. 7.24a, b, respectively.

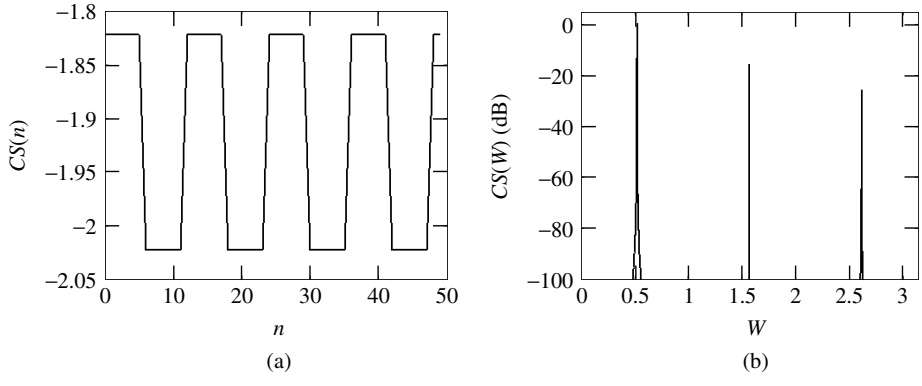

Figure 7.24 Rectangular signal waveform and spectrum

As Fig. 7.24 shows, the main component of the signal spectrum corresponds to $\Omega = 0.524$ when the third and fifth harmonics have relative amplitude of -15 and -25 dB, respectively.

To generate signals with the central frequencies $\omega_R = \frac{s\Omega}{2} = \frac{\pi}{12}, \frac{3\pi}{12}, \frac{5\pi}{12}, \frac{7\pi}{12}, \frac{9\pi}{12}$ and $\frac{11\pi}{12}$, we should evaluate appropriate values of a_1. These a_1 values, respectively, are

−1.9221, −1.4071, −0.515, 0.515, 1.4071 and 1.9221, and the relevant output signal spectrums are shown in Fig. 7.25a, b, c, d, e, f, respectively. In these examples, a steady-state mode of DPO is used.

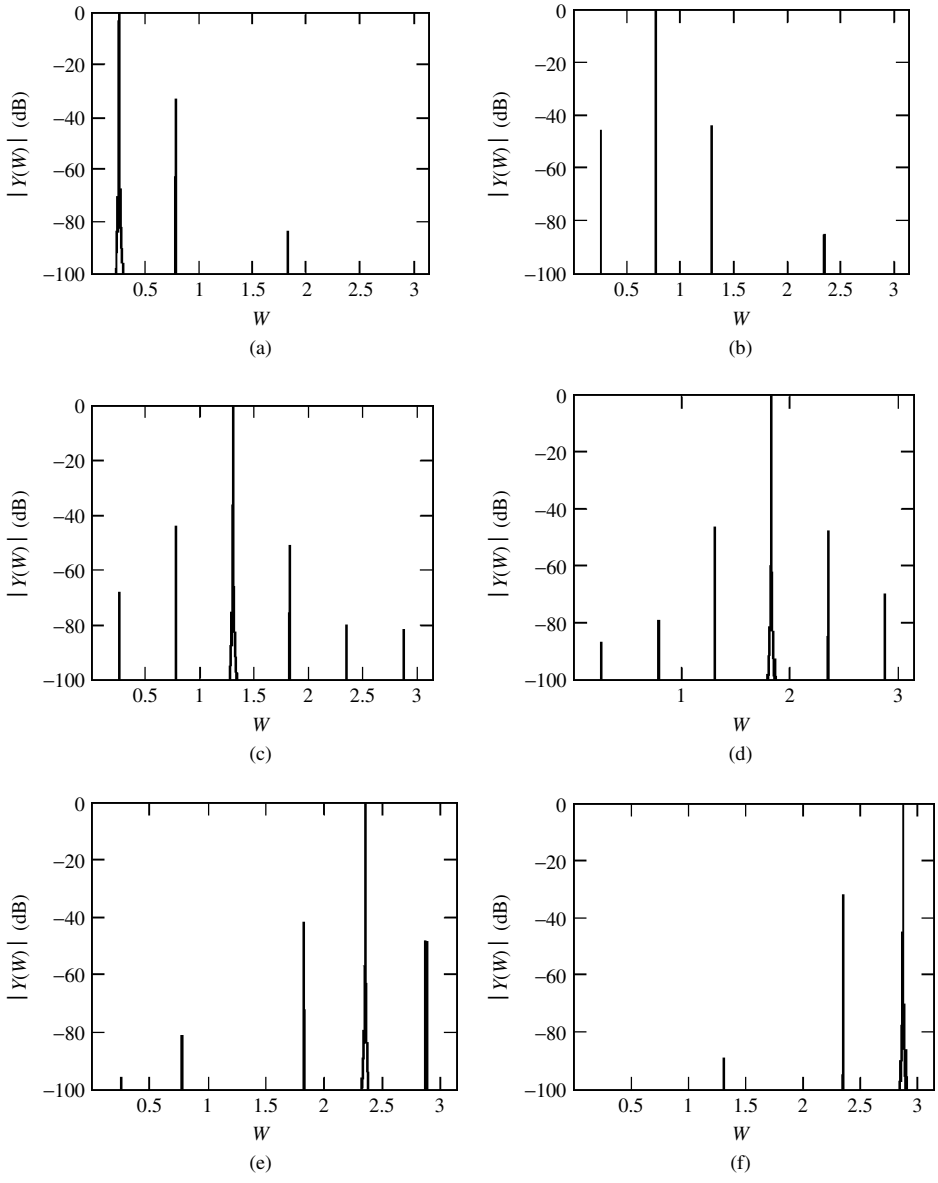

Figure 7.25 Signals generation by DPO with rectangle CS

Thus, using a rectangular CS we can generate sub-harmonics of higher order than we can using a sinusoidal CS.

7.3.4 Frequency Synthesizer

The examples considered above show that a DPO with a non-sinusoidal CS can be effectively used as a frequency synthesizer. This will be demonstrated using appropriate examples, but first it is important to recall that any changes in the DR or CS parameters lead to a transient period. During this transient period, the quality of the generating signal can deteriorate. The following example shows how the presence of a transient in a DPO can be visualized.

Example 7.20: **Phase Shift in a Sinusoidal Control Signal**

A sinusoidal CS with the parameters $\Omega = \frac{2\pi}{12}$, $S = 1$, $a_2 = 0.999$, $\gamma = 0.01$ initiated parametric oscillations in a DPO. Initial conditions correspond to the non-limiting operation mode at the beginning. The DPO output waveform is shown in Fig. 7.26a. Using the same ICs and DPO parameters, oscillations were initiated by a sinusoidal CS with 180° phase shift (see Fig. 7.26b) at a time moment corresponding to the non-limiting DPO mode. Figure 7.26c shows the transient period in the DPO output signal waveform.

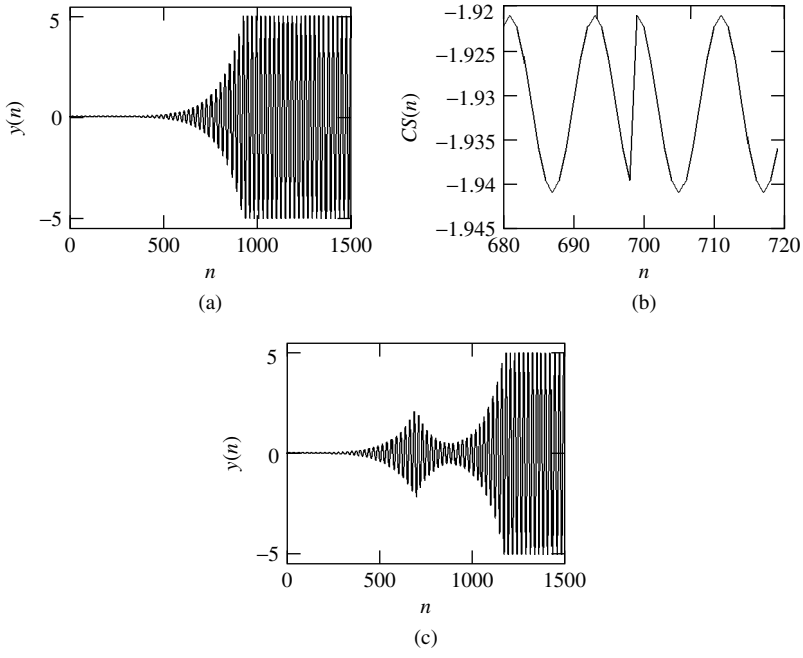

Figure 7.26 Transient in the DPO operating in non-limiting mode

When a DPO is operating in a steady-state mode, the transient is not very visible as it is buried in the phase modulation. However, this transient presents unless the ICs will not be selected that way to be an eigenvector of the corresponding difference equation.

Example 7.21: Frequency Synthesizer

For frequency synthesis, we will use a rectangular CS with the central frequency $\Omega = \frac{2\pi}{12}$ and amplitude $\pm\gamma = 0.1$. Coefficient a_2 is constant and equals 0.999, while coefficient a_1 is tuned to provide oscillations at frequencies $\frac{\Omega}{2}$ to -1.9309, $\frac{3\Omega}{2}$ to -1.4135 and $\frac{5\Omega}{2}$ to -0.5174. Each frequency occupies 1500 n time slots. The CS waveform is introduced in Fig. 7.27a and shown enlarged in Fig. 7.27b, c.

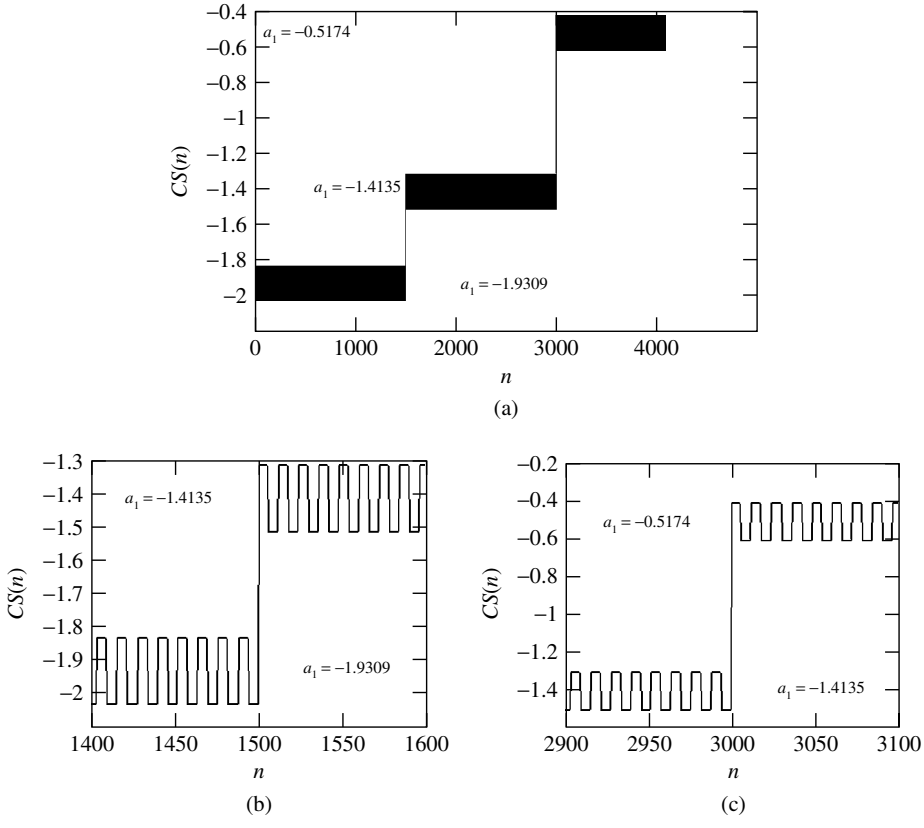

Figure 7.27 CS in the frequency synthesizer

With this CS, the DPO output signal changes its central frequency and relevant waveforms around the transition from $\frac{\Omega}{2}$ to $\frac{3\Omega}{2}$ (shown in Fig. 7.28a) and from $\frac{3\Omega}{2}$ to $\frac{5\Omega}{2}$ (shown in Fig. 7.28b).

From these figures we see that the output waveform is different for the different frequency bands. This can be easily explained by the fact that the DPO time constant directly depends on the CS magnitude. In our case, generation of sub-harmonics is initiated by the different harmonics of the CS, which have different amplitudes. With other conditions being equal, the smaller the amplitude, the larger is the time constant. This is why the waveform with frequency $\Omega/2$ is almost rectangular (due to poor filtering

by the DR), while the waveform with frequency $3\,\Omega/2$ is about sinusoidal (due to better filtering by the DR). Of course, for practical designing purposes, all this should be taken into account and mitigated by appropriate choice of DPO parameters. The spectrums of each of the three signals are shown in Fig. 7.29a–c.

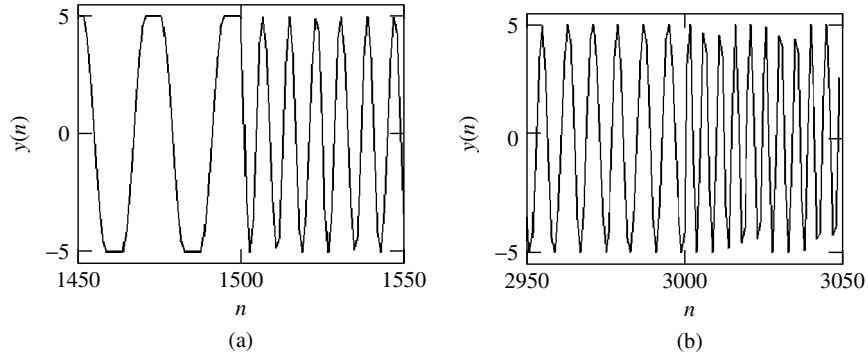

Figure 7.28 Frequency synthesizer output waveforms

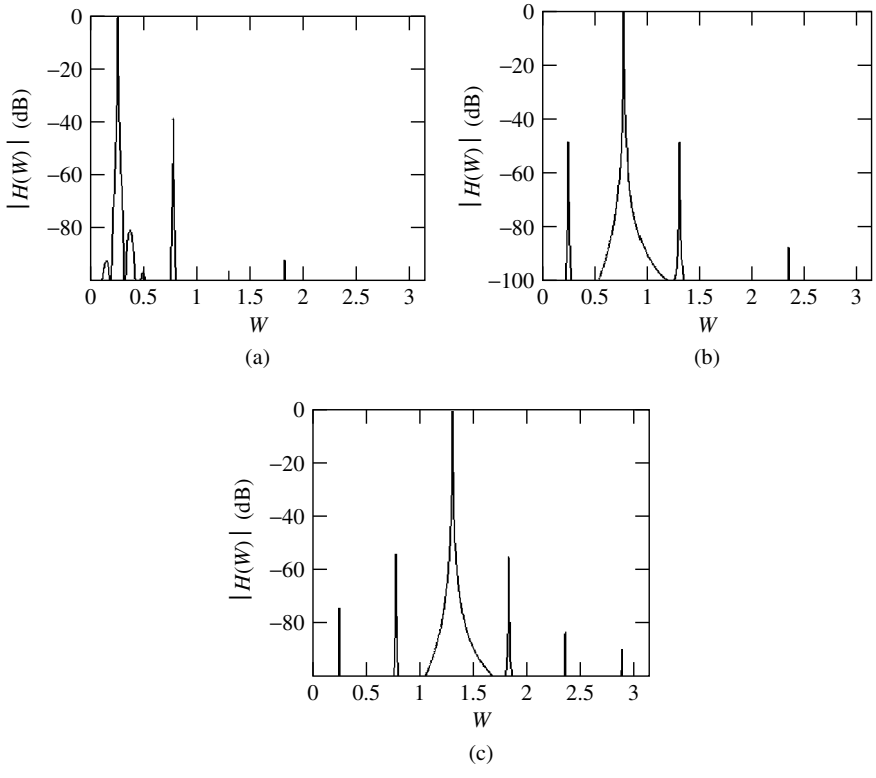

Figure 7.29 Spectrums of the generated signals

7.4 SUMMARY

This chapter has introduced practical aspects of digital parametric oscillator analysis. In particular, we examined the steady-state mode of DPOs, which is the most technically applicable case. In many aspects, the DPO behaves similarly in the SS and the non-limiting modes. The major difference is probably with the constant average amplitude of the output signal, which still has some amplitude modulation. Of course, the signal also has a phase modulation specified by the control signal and the oscillator parameters.

Another important practical parameter is the ability of the DPO to operate in the presence of random components in the CS. Unfortunately, an accurate analytical analysis for this case is not possible due to mathematical difficulties. Nevertheless, we were able to investigate the influence of small random interference on system performance.

The case study of DPO modelling using MATLAB can be viewed as the section that provides better understanding of DPO theory as well as demonstrating the potential characteristics of the oscillators. It is important to note that with appropriate choice of parameters, the purity of the signal spectrum can be in the order of 80 dB. Using the system eigenvector as the IC in the DPO registers allows for variation of the output signal without transient modulation. This makes the DPO prospective for use in frequency synthesizers, modems and other signal processing algorithms.

7.5 ABBREVIATIONS

CS	control signal
DPO	digital parametric oscillator
DR	digital resonator
IC	initial condition
MM	monodromy matrix
RPG	region of parametrical generation
SS	steady state

7.6 VARIABLES

Φ	a non-linearity, occurring during sum operation
γ_{N}	amplitude of the noise component
$H_0(\omega)$	an equivalent frequency response
ω_{N}	circular frequency of the noise component
$\hat{y}_S$	dominant component
$\tilde{y}(n)$	periodic component of a signal
$\overline{\tau}$	time constant

Ω	normalized frequency of system parameter variation
ω	normalized frequency of the signal
λ_1, λ_2	eigenvalues
γ_1, γ_2	amplitudes of the oscillations excited by variation of coefficients a_1 and a_2, respectively
$\sigma_X^2(n)$	deviation
$s_1(n)$, $s_2(n)$	coefficients of systems in the equivalent representation
$a(n)$	time-varying coefficients of the recursive part of a difference equation
$b(n)$-	time-varying coefficients of the non-recursive part of a difference equation
F	a non-linearity, occurring during multiplication operation
f	frequency
$g(m, n)$	impulse response of the recursive part
$G(z)$	generalized transfer function of the recursive part
$h(m, n)$	impulse response
$H(z, n)$-	generalized transfer function
$M(n)$	mean value
Q	quality factor
S	order number of the sub-harmonic
$S(\omega)$	spectral density
$u(n)$	signal at the output of the first system
$X(\omega)$, $X(\psi)$	spectrum of the input signal
$X(n)$	input discrete random process
$x(n)$	input signal
$X(z)$	z-transform of the input signal
$Y(\omega)$	spectrum of the output signal
$Y(n)$	output discrete random process
$y(n)$	output signal
$Y(z, n)$	z-transform of the output signal

7.7 REFERENCES

[1] Rabiner L, Gold B (1975) *Theory and Application of Digital Signal Processing*, New Jersey: Prentice Hall.

[2] Cherniakov M, Bets B (1989) Algorithm of parametric generation of digital signals, *Commun. Tech., Ser. Radiocommun. Tech.*, **8**, 26–33.

[3] Gonorovsky IS (1986) *Radiotechnical Systems and Signals*, Moscow: Radio and Svias.
[4] Cherniakov M (1989) Passing of the harmonic signal and amplitude noise through digital parametric oscillator, *Radiotechnica*, **3**, 24, 25.
[5] Hasminskiy PE (1969) *System Stability of the Differential Equations for Random Perturbations of its Parameters*, Moscow: Nauka.
[6] Cherniakov M (1989) Conditions of digital parametric frequency multiplier generation. *Radiotech. Electron.*, **5**, 1108–1110.
[7] Cherniakov M, Bets V, Tamarov P (1990) Oscillation failure in digital parametric tracing filters, *Proc. Conf. on Transmission, Reception and Signal Processing in Radio Communication Systems*, Rostov, USSR, 17–24.

Index

Aliasing regions, 60
Amplitude criterion, 163
Amplitude modulation, 216, 218, 233
Amplitude quantization, 41, 47
Amplitude spectrum, 7, 9, 42
Amplitude–frequency response, 24, 30, 35, 38, 39–41, 152–156, 161
Analog waveform, 1, 41
Autocorrelation function, 61, 77, 109
Average magnitude, 178, 181

Bifrequency function, 70, 71, 73, 86, 114

Canonic filters structure, 21, 22
Cascade connections, 22, 32, 63, 64, 129
Cascade filters structure, 21, 22
Causality of discrete systems, 22
Characteristic equation, 100, 102, 108, 109
Clock period, 48, 70
Comb filter, 156–159
Combinational component, 73, 88, 91, 93, 95, 135, 143, 144, 149, 161, 162, 164, 167, 168
Combined filter, 37, 40, 41
Continuous parametric system, 53, 177, 183
Control signal, 95, 99, 102–105, 177–194, 200, 212–239
Convolution, 8, 17, 19, 24, 50, 64, 77
Correlation interval, 107, 109

Decreasing component, 183, 186, 188, 189, 194, 196–198, 204, 205, 207
Degrees of freedom, 162, 168, 170
Deterministic signal, 61, 68, 86
Difference equation, 17, 18, 27, 31, 37, 41, 48, 49, 51, 54, 55, 57, 68, 70, 71, 83, 84, 95, 96, 121, 123, 125, 129, 132, 133, 136, 138
Digital parametric oscillator, 177–197
Digital resonators, 33–37, 105, 106, 177, 183, 207, 211
Digital signal processing, 1, 11
Discrete Fourier transform, 4, 9, 137, 179
Discrete linear system, 16, 17, 23, 25, 41, 47
Discrete signal, 1–13, 41, 60, 73
Dominant component, 180–182, 199, 215, 216, 224

Efficiency factor, 159, 160
Eigenvalues, 99, 100, 108, 110, 183, 185, 187, 188, 195, 207, 226
Eigenvalues analysis, 203, 214, 226
Eigenvector, 207, 216, 236, 239
Equivalent frequency response, 88, 128, 129, 135, 145, 150–153, 161–170, 225

Finite impulse response, 20
Fixed-point arithmetic, 183, 196, 212
Fourier series, 86, 122, 142, 179, 201, 204
Fourier transform, 4, 14, 24, 25, 41, 62, 76, 114
Frequency conversion, 58, 91
Frequency domain, 4, 25, 41, 52, 55–57, 77, 89, 91, 179, 191
Frequency modulation, 74, 189, 204

An Introduction to Parametric Digital Filters and Oscillators Mikhail Cherniakov

© 2003 John Wiley & Sons, Ltd

ISBN: 0-470-85104-X

Frequency response, 20, 23, 25, 49, 52, 55, 60, 70, 151–157, 161, 166, 169, 170
Frequency synthesis, 200, 237
Frequency synthesizer, 236–238
Fundamental system, 184, 185

General solution, 183, 185, 215, 223
Generalised transfer function, 52, 53, 55, 83, 85, 126, 127, 134

Homogeneous difference equation, 183

Impulse response, 2, 17, 19, 20, 22–28, 31, 33, 38, 39, 41, 49–53, 63, 64, 66–68, 77, 121–125, 128, 129, 132–135
Increasing component, 186–189, 194, 212, 222
Infinite impulse response, 1, 20, 48
Initial conditions, 96, 101, 113, 179, 181, 183, 188, 189, 206
Initial phase, 199, 200, 216
Instability region, 177, 178, 182
Integrated circuits, 177, 178

Laplace transform, 11, 14, 41
Limiting mode, 212, 213

Main harmonics, 182, 198
Modulation index, 72, 74, 77
Monodromy matrix, 95, 99, 100, 102, 107

Non-limited mode, 183, 186, 196
Non-linear difference equation, 211, 215
Non-periodic component, 193, 196
Non-trivial solution, 184
Non-uniform sampling, 70–72
Normal solution, 184, 186
Nyquist criteria, 2, 10, 60, 93

Oscillation excitation, 183, 187, 193, 195, 202, 203, 211–216, 219, 222

Parallel connections, 63, 64
Parametric filter, 121, 123, 129, 136, 141, 144, 145, 149–151, 155, 156, 159, 161, 168
Parametric oscillation, 178, 180–183, 186, 189, 192, 197, 200, 201, 203–205, 212, 223–226, 228, 230, 231, 236
Parametric recursive system, 99
Parametrical instability zone, 105, 178, 181, 183
Periodic component, 181, 183, 187, 188, 196, 213, 216, 217, 227
Periodical sequence, 4
Periodically linear time-variant system, 83, 84, 86–93, 103
Phase modulation, 216, 217, 236, 239
Phase spectrum, 7
Phase–frequency response, 24, 25, 30, 39
Pole of function, 11, 23, 33, 53
Power spectrum density, 75, 77
Primitive coefficient, 155–158, 170

Quantization step, 150, 152, 154, 155, 160
Quantized coefficient, 151, 153, 154, 157, 170
Quasi-harmonic oscillations, 178, 183, 186, 192, 197, 201

Random signal, 61, 63, 69, 89, 91
Recursive filter, 20, 27, 31, 32, 34, 40, 60, 123, 129, 146, 150, 159, 162
Regions of parametric oscillations, 178
Resonator efficiency, 105, 160
Round-off noise, 159, 162, 167, 168, 170

Sampling frequency, 1, 2, 8, 41, 59, 60, 83, 90, 91, 93, 114
Sampling interval, 1, 9, 70, 71, 75, 77, 179, 185, 193
Saturated mode, 178, 183
Second-order system, 100–102, 104, 106, 109–111, 114, 129, 130, 132, 134, 177, 178
Signal components, 88, 94, 143–145, 149
Spectral characteristics, 179, 183
Spectrum conversion, 59, 88
Stability area, 33, 103–106, 109–111, 178, 186
Stability criteria, 23, 29, 96, 125
Stability of discrete systems, 22, 95, 99
State space, 96, 138
State vector, 95, 96
State vector norm, 96, 113, 178
Steady-state oscillation, 215, 232
Stochastic sampling, 75
Stochastic system, 97, 107, 109, 114

Systems with feedback, 66, 95

Time constant, 28, 29, 31, 36, 183, 193–196, 205–208, 213, 214, 219, 229, 230, 234, 237
Time-amplitude converter, 208
Time-domain representation, 3
Time-invariant discrete linear system, 125
Time-variant discrete system, 47, 48, 50, 59, 61, 70, 77, 83, 90, 95
Time-varying coefficient, 48, 50, 70, 71, 84, 95, 160, 161, 164, 168, 170, 179, 211
Timing diagram, 150, 151, 153, 155, 162, 164, 165, 167, 168, 170
Trace of the matrix, 100
Transfer function, 20, 21, 23, 25–27, 31, 32
Transient period, 183, 196–198, 205, 206
Transient state matrix, 95
Transversal filter, 20, 37, 39, 40

Uniform linear difference equation, 179

Word length, 37, 150, 151, 153–155, 157–162, 167–170

z-transform, 1, 11–16, 18, 19, 25, 26, 31, 41, 52, 53, 64